

**Synthesis, Characterization and Application of Nanostructured
ZnO for the Photocatalytic Degradation of Malachite Green,
Methylene Green, Direct Blue-1, Orange-II, Acridine Orange and
Neutral Red Dyes in the Presence of Visible Light**

A thesis submitted for the degree of

Doctor of Philosophy

in

CHEMISTRY

By

Veer Singh Barde

Under the Supervision of

Dr. Brijesh Pare

DEPARTMENT OF CHEMISTRY

GOVT. MADHAV SCIENCE POST GRADUATE COLLEGE

(af. Vikram University) UJJAIN (M. P.)-456010 (India)

2018

Certificate of the Supervisor [Para-26(c)]

CERTIFICATE

This is to certify that the work entitled “**Synthesis, Characterization and Application of Nanostructured ZnO for the Photocatalytic Degradation of Malachite Green, Methylene Green, Direct Blue-1, Orange-II, Acridine Orange and Neutral Red Dyes in the presence of Visible Light**” is a piece of research work done by **Shri Veer Singh Barde** under my guidance and supervision for the degree of **Doctor of Philosophy in Chemistry, Vikram University Ujjain (M. P.) India**. That the candidate have put in as attendance of more than 200 days in the institute concerned or with the supervisor.

To the best of my knowledge and belief the thesis:

- i. embodies the work of the candidate himself;
- ii. has duly been completed;
- iii. fulfills the requirements of the Ordinance related to the Ph. D. degree of the University; and
- iv. is up to the standard both in respect of contents and language for being referred to the examiner.

Dr. Brijesh Pare
Supervisor

Dr. A. M. Chaturvedi
Head

Dr. Arpan Bhardwaj
Principal

Declaration by the Candidate (Para-26(b))

I declare that the thesis entitled “**Synthesis, Characterization and Application of Nanostructured ZnO for the Photocatalytic Degradation of Malachite Green, Methylene Green, Direct Blue-1, Orange-II, Acridine Orange and Neutral Red Dyes in the presence of Visible Light**” is my own work conducted under the supervision of **Dr. Brijesh Pare** at **Department of Chemistry, Govt. Madhav Science P. G. College, Ujjain (M. P.) India** approved by Research Degree Committee. I have put in more than 200 days of attendance in the institute concerned or with the supervisor.

I further declare that to the best of my knowledge the thesis does not contain any part of any work which has been submitted for award of any degree either in this University or in any other University/Deemed University without proper citation.

Dr. Brijesh Pare
Supervisor

Veer Singh Barde
Research Scholar

Dr. A. M. Chaturvedi
Head

Dr. Arpan Bhardwaj
Principal

Date: -

Acknowledgements

I would like to extend my most sincere acknowledgement and gratitude to a number of people and organizations. Without them, the quest towards my Ph. D. degree would be less rewarding, interesting and challenging.

My first debt of gratitude goes to my supervisor, **Dr. Brijesh Pare**, Professor, Department of Chemistry, Govt. Madhav Science P.G. College, Ujjain (M. P.) who has immensely inspired and encouraged at each and every stage of this work. His acceptance and faith in my ideas and his enormous support made this research work an enjoyable experience. I especially thank him for his prompt reading and careful critique of this work.

I am highly indebted to **Dr. (Mrs.) Usha Shrivastava**, former Principal, Govt. Madhav Science P.G. College, Ujjain (M. P.), **Dr. Arpan Bhardwaj** Principal I/C and **Dr. Ajay M. Chaturvedi**, Professor and Head, Department of Chemistry, Govt. Madhav Science P.G. College, Ujjain (M. P.) for giving me the opportunity to work in the laboratory and for providing me the required technical facilities.

I am very thankful to honorable teachers **Dr. B. K. Mehta**, **Dr. Uma Sharma** and **Dr. Shubha Jain**, School of studies in Chemistry and Biochemistry, Vikram University, Ujjain (M. P.) for their valuable suggestions during my research work.

I gratefully acknowledge the **University Grants Commission**, New Delhi and **Ministry of Tribal Affairs**, Government of India, which awarded me the Rajiv Gandhi National Fellowship during the Ph. D. degree under the RGNF scheme.

I am sincerely thankful to all the honorable teachers **Dr. (Mrs.) Neelam Kapil**, **Dr. Shakuntala Pandey**, **Dr. M. Makkad**, **Dr. Kalpana Singh**, **Dr. Arpan Bhardwaj**,

Mrs. Pratibha Namdeo, Dr. D. S. Raghuvanshi, Dr. Rekha Nagvanshi and Dr. J. S. Solanki, Dr. H. S. Dwivedi, Dr. I. K. Mangal and Dr. Anurag Titov, from Govt. Madhav Science P.G. College, Ujjain (M. P.) for their kind help, valuable suggestion and inspiration throughout this work.

I am thankful to **Mrs. Priya Pare** for her rare assistance and she has always been a source of inspiration to me advice during the tenure of research work.

I feel wordless to appreciate the selfless support, love, care and ever encouraging words of my father **Mr. Basariya Barde** and my mother **Mrs. Saybi Bai Barde**, uncle **Mr. Ganpat Barde**, brother **Mr. Gopal Barde**, brother-in-law **Mrs. Riyali Barde**, **Mrs. Usha, Mrs. Kavita** and **Ms. Sapna Barde**, niece **Pratibha, Sakshi, Priyanshi** and **Divya**, nephew **Yashwant** and **Rishabh**, my Brother-in-law **Mr. Sakharam Singoriya** and **Mr. Sunil Patel** and all the family members. My family is to direct me in the correct path and their helping hands for all my ventures and appreciations.

I would like to thank dear seniors **Dr. Pardeep Singh, Dr. Parkash More, Dr. Bhawna Sarwan, Dr. David Swami, Dr. Vijendra S. Solanki, Dr. Laveena Chouhan, Dr. Tripti A. Dwivedi, Dr. Jaya Parekh, Dr. Tehmina Qureshi and Dr. Varsha Sharma** for their great support during my research work. I specially thank **Dr. Pradeep Paliwal** and **Ashish K. Awasthi** for their guidance and support.

I would also like to thanks my coworkers **Mrs. Sunaina Chouhan, Mr. Satish Piplode, Ms. Vaishali Joshi, Mr. Amar J. Solanki** and **Ms. Garima Nagraj** for their adorable support and friendly contributions. I would also like to thank **Dr. Nayma Siddiqui, Mrs. Komal Chelaramani** and **Mr. Rakesh Porwal** for supporting as well as for their valued contributions.

I am also thankful to technical staff and office staff members **Mr. Mukesh Mittal, Mr. Virendra Sonparat, Mr. Nemichand Gupta, Mr. Rajveer Bhadoriya** and

Mr. Shivnarayan Sen, Mr. Kamal Sharma for their invaluable cooperation and help during the entire studies in this institute.

I would also like to thank **Mr. Meharban Barde, Dr. Ravindra Barde, Dr. Kaniya Meda, Dr. Vinod Thakur, Mr. Bhimsingh Barde, Mr. Lalsingh Barde, Subhash Khedkar, Mrs. Aarti Lohare, Dr. Veena Barde, Mr. Vinod Barde, Udaysingh Chouhan** and **Mr. Pannalal Dawar** for their supporting as well as valued contributions.

I thank all my friends **Sunil Barde, Parkash Thakur, L. S. Senani, Ravin Chouhan, Rakesh Jadhav, Pawan Dawar, Ajay Barde, Rakesh Barde, Brijesh Patel, Methu Dawar, Gangram Barde, Parkash Dodwe, Ms. Rina Sastiya, Ms. Sangita Vaskale, Ms. Radha** and **Ms. Sonam Dawar** who have supported me in every possible way during my work.

Finally, I devote this work as an offering to **Lord Mahakaleshwar** and pray to them to continue showering their blessings. I thanks them for wisdom, confidence and strength that has been bestowed upon me during this research work and indeed, throughout my life.

Veer Singh Barde

**This thesis is dedicated
to my beloved parents**

TABLE OF CONTENTS

CONTENTS	Page No
Certificates	
Declaration by candidate	
Acknowledgements	
CHAPTER – I: INTRODUCTION	1-27
1.1 Dyes under investigation with their classification	2
1.2 Water pollution by industrial effluents	9
1.3 Photo-catalytic degradation and Advanced Oxidation Processes	9
1.4 Nanotechnology applied for remediation of organic dyes from wastewater	14
1.5 Photocatalysis	15
1.6 Photo-catalytic activity of ZnO NPs	16
1.7 Environmental aspects of present research work	20
References	22
CHAPTER – II: LITERATURE REVIEW	28-45
2.1 Literature Review	28
References	42
CHAPTER – III: EXPERIMENTAL APPROACHES	46-57
3.1 List of required chemical	46
3.2 Preparation of solution required	46
3.3 Synthesis of nanostructured ZnO	47
3.4 Characterization techniques for nanostructured ZnO	48

3.5	Photo-reactor design and experimental conditions	51
3.6	Methods for identification of mineralized products	53
	References	57
CHAPTER – IV: RESULTS AND DISCUSSION		58-225
4.1	Characterization techniques for ZnO NPs catalyst	58
4.2	Effect of various experimental parameters on the degradation rate of Malachite Green dye	61
4.3	Effect of various experimental parameters on the degradation rate of Methylene Green dye	87
4.4	Effect of various experimental parameters for the degradation rate of Direct Blue-1 dye	115
4.5	Effect of various experimental parameters on the degradation rate of Orange –II dye	141
4.6	Effect of various experimental parameters on the degradation rate of Acridine Orange dye	167
4.7	Effect of various experimental parameters on the degradation rate of Neutral Red dye	193
	References	218
CHAPTER – V: CONCLUSION AND RECOMMENDATIONS		226-229
Summarized Tabulated Results		230-232
List of Publications		
Seminars, Conferences, Workshops and Trainings		

CHAPTER-I

Introduction

Introduction:

Nowadays environment is severely affected by hazardous water soluble organic dyes present in water effluents from textile and dyeing industries. Stability of these dyes causes severe ecological problems such as depleting of dissolved oxygen content of water and releasing toxic compounds in water bodies endangered the aquatic life. Several physical, chemical and biological methods have been used to remove dyes from contaminated water [1]. Among them, physical adsorption and degradation is considered as a competitive method because of high efficiency, economic suitability and easy to design and for operation. Photo-catalytic degradation is one of the best methods used for removal of toxic chemicals produced by dyes and degraded via redox reactions in the presence of photo-catalyst [2]. Photo-catalytic degradation for organic dyes are quite popular due to high efficiency, low cost method, less hazardous intermediate products, low reaction time and mild reaction conditions [3]. The most important reason for selecting ZnO NPs in present study as photo-catalyst is its ability to show photo catalytic efficiency in both UV and visible range of light. The present work deals with synthesis of ZnO nanoparticles and its used in the photo-catalytic degradation of dyes taken for present study using visible light irradiation [4-6]. In order to make the maximum use of visible light ZnO nanoparticles were used as photo-catalyst for the degradation of dyes. In the present work photo-catalytic degradation of dyes and decolorization of water under visible light has been investigated using ZnO nanoparticles as photo-catalyst. ZnO nanoparticles have especially been used as effective, nontoxic and cost-effective photo-catalyst for the degradation of a wide range of dyes. We investigated this degradation process under different reaction condition to assess the feasibility and optimization of process for industrial dyes effluents [7].

1.1: Dyes under investigation with their classification:

1.1.1: Dyes as pollutants:

Dyes are widely used in cellulosic fabrics, including textiles, paper making, wool, silk and tannin-mordant cotton and spirit ink manufacture and other coloring agents in many industries [8]. Dyes are carcinogenic and potential pollutants and hence attention has been paid toward the removal of harmful and hazardous contaminants from wastewater. Dyes are chemicals which on binding with material will give color to the material. The color of a dye is provided by the presence of chromophore group. Most of the synthetic dyes are organic compounds with multiple aromatic rings, either fused or connected by covalent bonds, and modified by various hydrophilic functional groups, such as amine, carbonyl, carboxylic acid, and hydroxyl groups to produce desired colors, increase the affinity to the materials being dyed and improve the solubility in solvents, such as water, during dyeing processes. Being synthetic organics, those dyes are often resistant to biodegradation in engineered treatment processes such as activated sludge, as well as in the natural aquatic environment. Azo dyes are very stable and carcinogenic in nature [9-11]. The ordinary light consists of electromagnetic radiations of varying wavelength which can be categorized as ultraviolet light (100-400 nm) and visible part (400-750 nm) shown in figure 1.1. When visible light falls on a substrate, depending upon the substance, some of it is absorbed, and some reflected. White surfaces reflect all the light whereas black surfaces absorb light over the entire range of visible light. In the case of dye, however, there is a selective absorption in visible region and reflection the rest of this region. This is a definite relationship between the color absorbed and color visualized with respect to a given range of the wavelength [12].

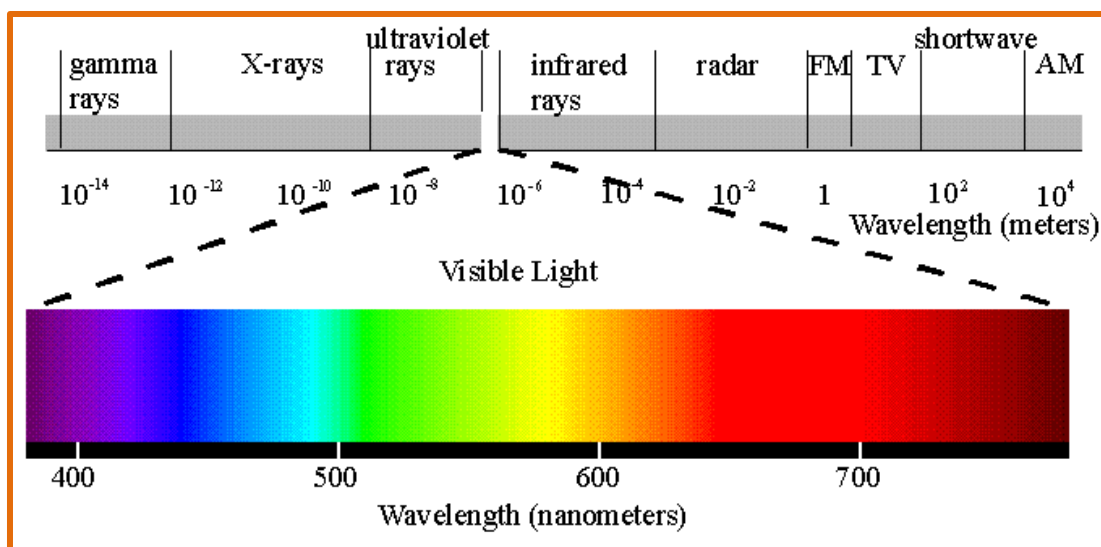


Fig. 1.1: electromagnetic radiations of varying wavelength

A Dye is made up of two parts, chromophores and auxochromes and there exists a relation between color and chemical constitution of a compound. The color usually appears in an organic compound if it contains unsaturated groups is called as chromophore (Greek *Chroma*—color, and *Phoros*— bearing) e.g. nitroso ($-\text{N}=\text{O}$), azo ($-\text{N}=\text{N}-$), azoamino ($-\text{N}=\text{N}-\text{NH}$) etc. Auxochrome is made up of *auxien* means to increase and *chroma* means colour i.e. the group which enhance like amino ($-\text{NH}_2$), sulphonic acid ($-\text{SO}_3\text{H}$), methyl ($-\text{CH}_3$) etc. Structural change in dye brings about a change in the absorption of dye molecule. If the absorption shifts towards higher wavelengths, the color deepens in the sequence: Yellow – Orange – Red – Purple – Violet – Blue – Green.

Any group or factor that produces the deepening of the color is known as bathochromic and the effect as bathochromic shift. If the absorption shifts towards lower wavelengths, the color lightens in accordance to the following sequence: Green – Blue – Violet – Purple – Red – Orange – Yellow, shown in Table 1.1 [13].

Table 1.1: Relationship of colors observed to wavelength of light absorbed

Light absorbed		Complementary color seen
Wavelength ($m\mu$)	Color	
400-435	Violet	Green – Yellow
435-480	Blue	Yellow
480-490	Green – Blue	Orange
490-500	Blue – Green	Red
500-560	Green	Purple
560-580	Yellow – Green	Violet
580-595	Yellow	Blue
595-605	Orange	Green – Blue
605-750	Red	Blue - Green

1.1.2: Classification of dyes:

There are several ways for classification of dyes. It should be noted that each class of dye has a very unique chemistry and particular way of bonding. While some dyes can react chemically with substrate forming strong bonds. Dyes are also classified by their chemical composition, the types of fibers to which they can be applied by the method of application. Dye molecules may attach to the surface of the fiber, be absorbed by the fiber or interact with the fiber molecules. The Society of Dyers and Colorists (SDC) and the American Association of Textile Chemists and Colorists (AATCC) classify dyes by their chemical composition. In the publication, the color index international dyes are listed by their generic name, which indicates the application class and a color index constitution number (CI number) indicates the chemical structure [14, 15].

1. Classification of dyes according to application

• Acid dyes	• Ingrain dyes
• Basic	• Vat dyes
• Direct dyes	• Sulphur dyes
• Mordant	• Disperse dyes
• Azoic dyes	• Reactive dyes
• Oxidation dyes	• Solvent dyes
• Food dyes	• Pigment dyes

2. Classification of dyes to their chemical constitution

• Nitro dyes	• Xanthene dyes
• Nitroso dyes	• Heterocyclic dyes
• Azo dyes	• Indogi dyes
• Triphenylmethane dyes	• Anthraquinone dyes
• Phathalein dyes	• Sulphur dyes
• Phenazine dyes	• Pathalocyanine dyes

The selected dyes for present study as sample contaminants for the present study belong to the following Classes [16, 17]

Triphenylmethane Class:

This group of dyes is the oldest known synthetic groups. They are of brilliant color due to resonance of unsymmetrical triphenylcarbonium ions and cover a range of shades from red to blue, including violet and green. Most basic dyes of this series are beautiful,

crystalline compounds with a reflex, the color of which is often complementary to the color in solution. However, the color fades rapidly in light and due to this reason they find less uses in textiles but are used for coloring papers, typewriter ribbons and are specially valued for in calico printing and other articles where fastness to light is not of much significance. These dyes have the quinonoid groups as their chromophores. The dye selected from this class is Malachite Green.

Phenothiazine Class:

Phenothiazine groups dyes are analogues to the oxazines dyes an atom of sulphur replacing oxygen in the heterocyclic ring. These dyes have phenazonium nucleus as chromophore with amino group's para to the ring nitrogen as auxochromes. Phenothiazine dyes have a colour range from green to blue and have been used for colouring paper, tannin mordanted cotton and silk. Fastness to light is usually only fair. We have selected Methylene Green dye to be investigated from this class [18].

Azo class:

Azo dyes have a chromophoric system containing azo group $-N=N-$, in association with one or more aromatic system. There may be more than one or more than one azo group present in dye. Most (60-70%) of the more than 10,000 dyes applied in textile – processing industries are azo compounds. Dyes belonging to this class are used to dye natural fibres like wool, cotton and silk as well as so synthetics like polyesters, acrylic and rayon. Azo dyes are the main contributors for water pollution caused by dyes because majority of azo dyes are water soluble and therefore easy for the body to absorb. We have selected Direct Blue-1 and Orange II dyes to be investigated in this class [19].

Acridine Class:

These dyes are derivatives of the basic compound acridine. This structure provides the chromophore and an amino or alkyl amino group is usually present in a para position with respect their methane carbon atom. Textile applications are chiefly in the printing and dyeing of silk and cellulosic fibers. These are largely used on leather and in spirit ink manufacture. Several acridine dyes are in use as antiseptic or medicinal. From acridine class of dyes we have selected Acridine Orange dye.

Phenazinium:

Phenazinium dyes are widely used as mordant to cotton silk and wool because of their stability, brilliant colors and fastness to light. These dyes are widely used as general biological stains. Phenazinium dyes can be used in determination of membrane potential changes. This dye has been widely used in many staining methods, but its commonest use is probably as a simple red nuclear counter stain. We have chosen Neutral Red dye to be investigated from this class [20].

The molecular structures of dyes under investigation are as follow:

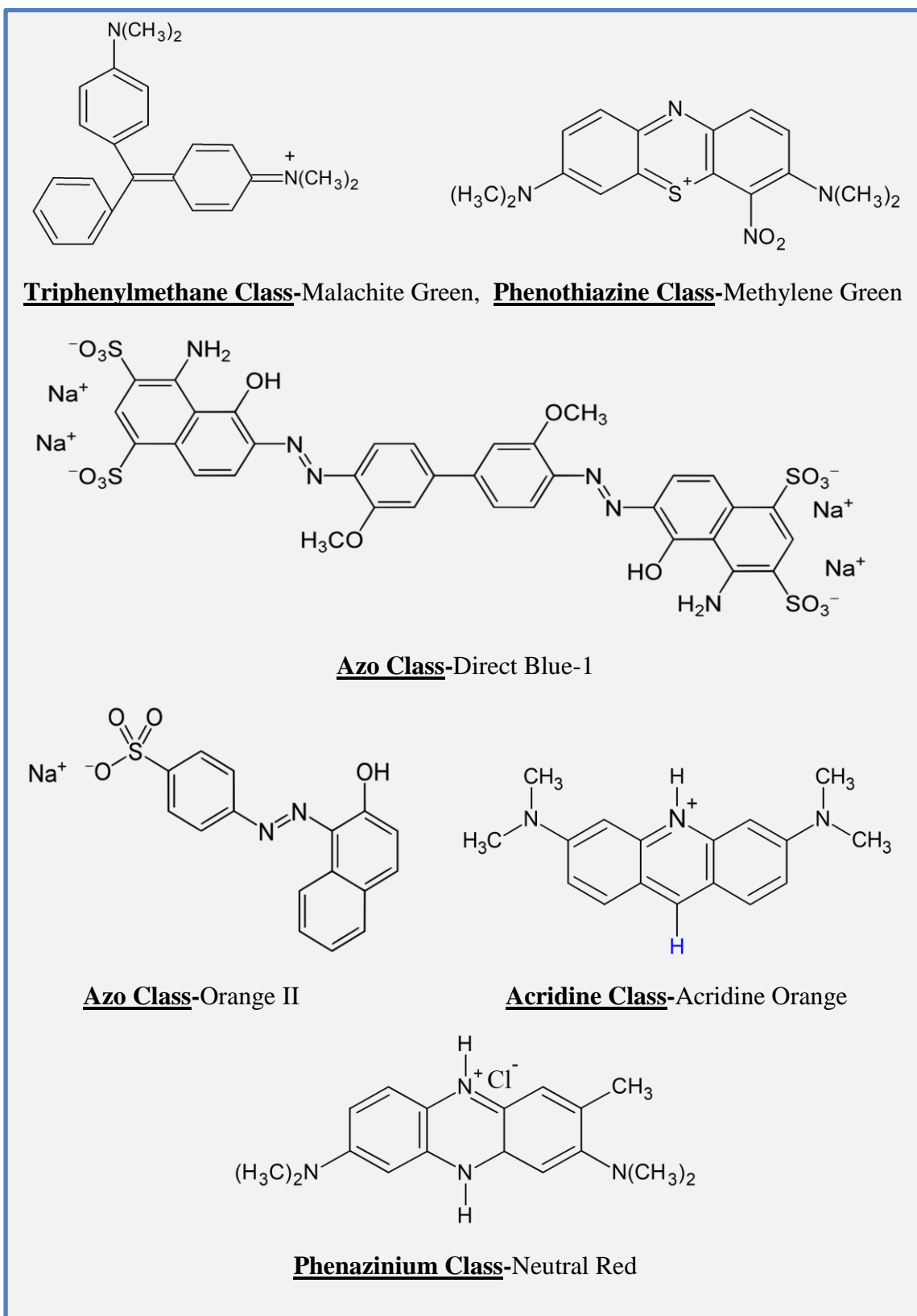


Fig. 1.2: Molecular structure of selected dyes

1.2: Water pollution by industrial effluents:

Industrialization is vital to a nation's economy because it assists as a vehicle for the development. Speedy industrialization has provided much comfort to human beings; however, it also has some adverse effects on environments. During the last fifty years, the number of industries especially textile in India has grown rapidly and this is a serious threat to human health and economy as well [21, 22].

By domestic sewage and industrial effluent discharge from large scale sugar industries, distilleries, tanneries, oil refineries, textile plants and the food, pharmaceutical, paint and coal processing industries which includes wastes like metals, detergents, acids alkalis, sulfates, chlorides, nitrites, color, dissolved and suspended solids, organic and microbial impurities. Such chemicals when discharged to environment have crucial impact on the aquatic life and health of human beings as well as animals [23]. The mineralization of dyes and other organic contaminants from wastewater effluents has now become the subject of considerable environmental concern. Dyes are carcinogenic and potential pollutants and hence attention has been paid toward the removal of harmful and hazardous contaminants from wastewater [24].

1.3: Photo-catalytic degradation and Advanced Oxidation Processes (AOPs):

Advance oxidation processes rely on the efficient generation of reactive radical species and are gradually attractive choices for water remediation from a wide range of organic pollutants of human health and environmental concern. AOPs are defined as a set of chemical treatment processes which are specially designed to remove organic compounds from wastewater [25]. For the treatment of wastewater containing dye residues advanced

oxidation processes (AOPs) have been considered as a promising alternative. Advanced oxidation processes, based on production of highly reactive radicals which promote the target pollutant destruction until production of minerals. AOPs generate extremely reactive hydroxide radicals which are responsible for the degradation of pollutants in the wastewater and $\cdot\text{OH}$ radicals attack the organic molecules rapidly and non-selectively. AOPs are known as versatile technologies because production of hydroxyl radicals by various alternative pathways. Additionally, AOPs can generate less toxic intermediates during the degradation of organic pollutants [26, 27]. Heterogeneous photo-catalysis is one of the advanced oxidation process, used as an efficient wastewater treatment technique for the total mineralization of organic materials [28, 29]. The ability of oxidants to initiate chemical reactions is measured by its oxidation potential [30]. The $\cdot\text{OH}$ radical has the second largest redox potential (2.80 eV at 25 °C) with the most potent being fluorine (3.06 eV at 25°C) and over the second choice for oxidation [31]. Relative oxidation potentials of several chemical oxidizers are shown in Table 1.2.

Table 1.2: Oxidizing potential for conventional oxidizing agents

Oxidizing agent	Electrochemical oxidation potential (EOP), eV	EOP relative to chlorine
Fluorine	3.06	2.25
Hydroxyl radical	2.80	2.05
Oxygen (atomic)	2.42	1.78
Ozone	2.08	1.52
Hydrogen peroxide	1.78	1.30
Hydrochloride	1.49	1.10
Chlorine	1.36	1.00
Chlorine Dioxide	1.27	0.93
Oxygen	1.23	0.90

$\cdot\text{OH}$ radicals are very reactive and non-selective and can react without any other additives with a wide range of contaminants rate usually in the order of 10^6 - 10^9 mol. $\text{L}^{-1}\text{S}^{-1}$ [32, 33].

AOPs can be classified by the phase where the process takes place like homogenous and heterogeneous. Non-photochemical and photochemical classifications are based on the methods for generating $\cdot\text{OH}$ radicals production. The versatility of AOPs is also enhanced by the fact that they offer different possible ways for $\cdot\text{OH}$ radicals. A list of the different possibilities offered by AOP is given in Fig.1.3 Generation of $\cdot\text{OH}$ is commonly accelerated by combining O_3 , H_2O_2 , UV radiation, electron-beam irradiation etc. out these, $\text{O}_3/\text{H}_2\text{O}_2$, O_3/UV and $\text{H}_2\text{O}_2/\text{UV}$ hold the greatest promise to oxidize textile wastewater [34].

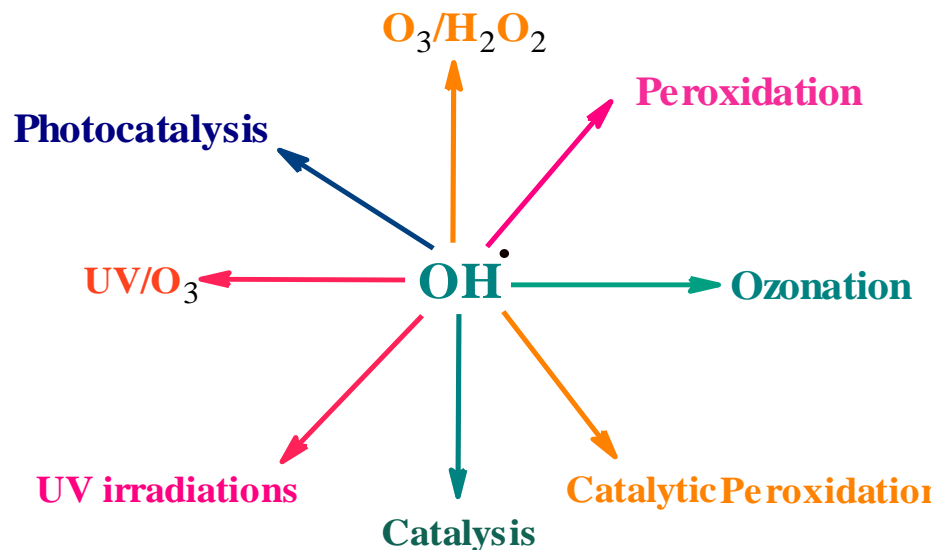


Fig.1.3: AOPs generate $\cdot\text{OH}$ Radical

AOPs methods exploit the high reactivity of hydroxyl radicals in driving oxidation processes, ultimately resulting in the mineralization of a variety of environmental contaminants. In this field of research, UV/visible-induced photo-catalytic degradation assisted by semiconductors represents a very appealing tool to implement low cost purification of waste waters on large scale [35, 36].

Non-photochemical and Photochemical AOPs:

On the basis of the advanced oxidation methods for generating $\cdot\text{OH}$ radicals, AOPs can also be classified as photochemical and non-photochemical processes. Photochemical advanced oxidation processes refers both to AOPs that need photons to initiate oxidation process and non-photochemical AOPs that increase their efficiency when working with artificial as well as natural radiations. But in several cases, conventional ozone or hydrogen peroxide oxidation of organic compounds does not completely oxidize organic substances into CO_2 and H_2O [37, 38]. Efficiency of these processes can be increased by supplementing the reaction with UV radiation. These processes have categorized as Table 1.3 [39]:

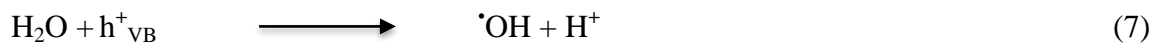
Table 1.3: Classification of Non-photochemical and Photochemical AOPs

Non-photochemical AOPs	Photochemical AOPs
Ozonation at elevated pH (> 8.5)	Ozone –UV radiation (O_3/UV)
Ozone + hydrogen peroxide ($\text{O}_3/\text{H}_2\text{O}_2$)	Hydrogen peroxide- UV radiation ($\text{H}_2\text{O}_2/\text{UV}$).
Ozone + catalyst (O_3/CAT)	Ozone-hydrogen peroxide- UV radiation ($\text{O}_3/\text{H}_2\text{O}_2/\text{UV}$).
Fenton system ($\text{H}_2\text{O}_2/\text{Fe}^{2+}$)	Photo-Fenton and Fenton-like systems.
	Heterogeneous photo-catalytic oxidation involving semiconductors and UV/visible irradiation.

The basis of heterogeneous photo-catalysis is the photo-excitation of a solid semiconductor as a result of the absorption of electromagnetic radiation in the near UV/visible spectrum. Under near UV/visible irradiation, a suitable semiconductor material may be excited by photons possessing energies of sufficient magnitude to produce conduction band electrons and valence band holes. These charge carriers are able to induce reduction or oxidation respectively. At the surface of the semiconductor particles these may react with absorbed species [40]



Holes possess an extremely positive oxidation potential and should thus be able to oxidize almost all chemicals. Even the one-electron oxidation of water resulting in the formation of hydroxyl radicals is energetically feasible.



Nowadays, the photo-catalytic degradation process is gaining importance in the area of wastewater treatment especially for wastewater containing small amounts of refractory organic substances [41, 42]. Additionally, heterogeneous photo-catalysis has several advantages over competing AOPs. These are complete mineralization, no waste disposal problem, low cost and only mild temperature and pressure conditions are necessary [43].

1.4: Nanotechnology applied for remediation of organic dyes from wastewater:

1.4.1: Nanotechnology:

Nanotechnology can be defined as the synthesis, characterization and applications of material science and engineering and device whose smallest functional organization in at least one dimension is on the nanometer scale [44]. In the year 1857, Faraday's reported systematic synthesis of gold sols [45] and introduce nano-science as a discipline and it started to swell further. In 1914, the first observation and size measurements of nanoparticles were performed by R. A. Zsigmondy, who reported a detailed study of gold sols and other nano-materials having size below 10nm [46]. Zsigmondy also introduced "nanometer" first time which is used scale clearly to measure particle size. In 1974, the term "nanotechnology" was first coined by Norio Taniguchi, a professor of Tokyo Science University [47].

The field of nanotechnology is one of the most active research areas in modern material science. Nanoparticles exhibit improved properties based on specific characteristics such as size, distribution and morphology. Hence, there have been impressive developments in the field of nanotechnology in the recent past year, with numerous methodologies developed to synthesis nanoparticles of particular shape and size depending on specific requirements. The recent advancement of nanotechnology has raised the possibility of environmental decontamination through several nano-materials, and tools [48, 49].

1.4.2: ZnO Nanostructured in wastewater treatment:

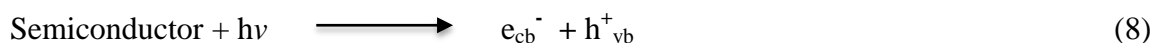
Several nanotechnologies are emerging as sustainable and economical process elements for remediation wastewater and nanotechnology encompasses a wide variety of processes that employ nano-sized materials as catalysts, oxidants, or to create nano-sized filters for

physical separation. For example, nano-sized particles of ZnO and TiO₂ can be used as photo-catalysts to produce reactive oxygen species that can either photo-catalytic degrade contaminants [50].

1.5: Photocatalysis:

The word photo-catalysis is composed of two parts: The prefix photo means "light" and catalysis is the process where a substance participates in modifying the rate of a chemical transformation of the reactants without being altered in the end. The term photo-catalysis implies the combination of photochemistry with catalysis. Both light and catalyst are necessary to achieve or to accelerate a chemical reaction. Photo-catalysis may be defined as the "acceleration of a photo-reaction by the presence of a catalyst". Hence, photo-catalysis is a reaction which uses light to activate a substance which modifies the rate of a chemical reaction without being involved itself. Photo-catalysis has been established as an efficient process for the mineralization of toxic organic compounds and has attracted much interest due to energy and environmental issues. The discovery of photo-catalysis suggested a large number of potential applications, such as photovoltaic cell, degradation of pollutants and photolysis of water. Since then, photo-catalysis has been a subject of attentive research [51, 52]. Further, semiconductor photo-catalysis is an attractive remediation of industrial wastewater. In recent years, nanostructured semiconductors have been actively studied for their fundamental scientific significance and potential technologic applications [53].

Mostly, ZnO is the utmost effective photo-catalyst for photo catalysis. In a heterogeneous photo-catalytic process, photo-induced chemical reactions or molecular transformations occur on the surface of the catalyst.



Where, e_{cb}^- and h_{vb}^+ are the electrons in the conduction band and the electron vacancy in the valence band respectively. Both these entities can migrate to the catalyst surface, where they can enter in a redox reaction with other species present on the surface. In most of the cases h_{vb}^+ can react easily with surface bound H_2O to produce $\cdot OH$ radicals, whereas, e_{cb}^- can react with O_2 to produce superoxide radical anion of oxygen [54].

1.6: Photo-catalytic activity of ZnO NPs

Over the years, many semiconductors such as Si, TiO_2 , WO_3 , ZnS, SnO_2 , Fe_2O_3 , ZnO, CdS, $SrTiO_2$, WO_2 , $\alpha\text{-}Fe_2O_3$, etc. have been used for photo-catalysts (Table 1.4) [55]. In the past two decades, ZnO has attracted much attention with respect to the degradation of various organic pollutants due to its high photosensitivity, stability and wide band gap. It usually appears as a white powder and is nearly insoluble in water. ZnO is present in the earth crust as zincate; however, most ZnO used commercially is produced synthetically [56]. In order for the semiconductors to be photochemically active as sensitizers the redox potential of the photo generated valence band hole must be sufficiently positive to generate hydroxyl radical which subsequently oxidizes the organic pollutants [57].

Table 1.4: Band gap energy of semiconductors

Semiconductors	Bandgap energy(eV)	Semiconductors	Bandgap energy (eV)
SiO_2	1.1	ZnO	3.2
TiO_2 (rutile)	3.0	TiO_2 (anatase)	3.0
WO_3	2.7	CdS	2.4
ZnS	3.7	$SrTiO_3$	3.4
SnO_2	3.5	WSe ₂	1.2
Fe_2O_3	2.2	$\alpha\text{-}Fe_2O_3$	3.1
Nb_2O_5	3.6	$BaCrO_4$	2.3

Recently, environmental engineers and researchers have shown interest in ZnO NPs as an alternative for UV-active TiO₂. Zinc oxide is a potential non-toxic photo-catalyst and also has a variety of technical applications including porcelain enamels, heat-resisting glass, and pigments in paint with UV-protective properties, healing ointment, and many more [58]. ZnO acts as a semiconductor due to its electronic structure, characterized by filled valence band and an empty conduction band [59]. Zinc oxide exists in mainly in two forms: wurtzite and zinc-blende. The wurtzite structure is most stable and thus most common at ambient conditions.

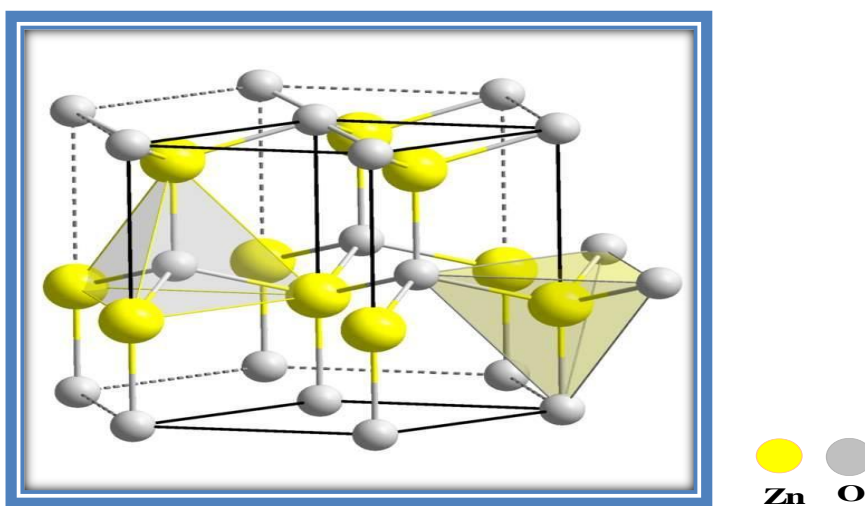


Fig. 1.4: Wurtzite structure of ZnO

1.6.1: Mechanism of ZnO NPs photo-catalysis:

With a large number of active sites, ZnO NPs exhibit very high surface reactivity, rendering it an efficient visible light photo-catalyst as compared to other photo-catalysts. Semiconductor ZnO NPs is a powerful photo-catalyst in the presence of visible light and used effectively in various photo-catalytic reactions. It is well known that semiconductor having a large band gap acts as a good photo-catalyst. The main advantage of using ZnO NPs photo-catalyst is its photo-activity in visible region. Studies also reveals that photo-

reactivity of ZnO NPs is independent of the particle size which is a huge advantage from the point of view of practical application of the ZnO NPs system in large-scale decontamination of polluted water [60, 61]. It is well established that valence band holes (h_{vb}^+) and conduction band electrons (e_{cb}^-) are generated when aqueous ZnO NPs suspension is irradiated with visible light energy greater than the its band gap energy ($E_g = 3.2$ eV). These electron-hole pairs interact separately with other molecule as shown in Fig. 1.5.

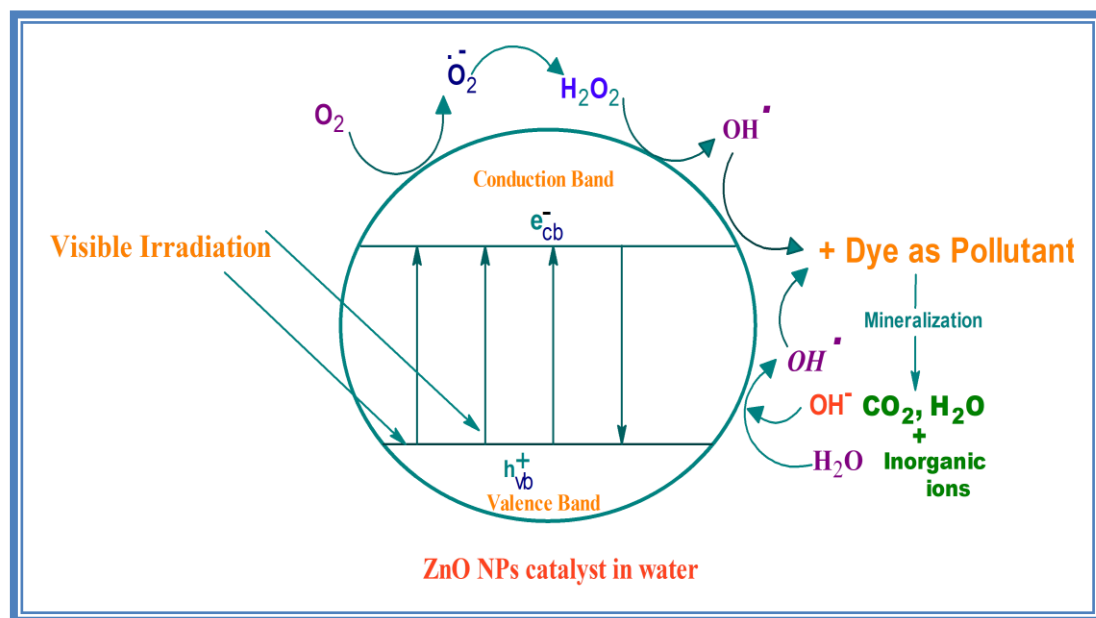
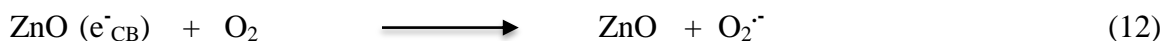


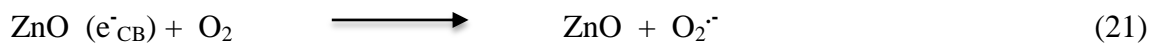
Fig.1.5: Photo-catalytic degradation mechanism using ZnO NPs

Valence band holes (h_{vb}^+) react with surface bound H_2O or OH^- to produce hydroxyl radical (OH^{\bullet}). Conduction band electrons (e_{cb}^-) reduce molecular oxygen to generate superoxide radicals, as shown in Eq. (9) to Eq. (18) [62, 63].





Secondly, sensitization of dye molecule by visible light leads to excitation of dye molecule in singlet or triplet state, subsequently followed by electron injection from excited dye molecule onto conduction band of semiconductor particles. The mechanism of dye sensitization is summarized in Eq. (19) to Eq. (27) [64, 67].



The mechanism of semiconductor photo-catalysis is of very complex nature. Dye molecules interact with $\text{O}_2^{\cdot-}$, $\cdot\text{OH}_2$, or $\cdot\text{OH}$ species to generate intermediates ultimately lead to degradation products. Hydroxyl radical ($\cdot\text{OH}$) being very strong oxidizing agent (oxidation potential 3.2 eV) mineralizes dye to various end products. The role of

reductive pathways in heterogeneous photo-catalysis has been found to be in minor extent as compared to oxidation [68-70].

1.7: Environmental aspects of present research work

Elimination of dyes and other commercial colorants from continual wastewater effluents of textile, paper mills and other colorant manufactures is now became the subject of considerable environmental concern. Since ancient times, fabrics have been dyed with extracts from minerals, animals, plants or plant products. In fact, things began to change around 1856 when inventors discovered how to make synthetic dyes. The synthetic dyes are cheaper to produce, brighter, more color-fast, and easy to apply to the fabric and other materials. In India, production of dyestuff and pigments is near about 80,000 tones and the textile industry accounts for the largest consumption of dyestuffs [71, 72]. About 20% of total dyes produced are lost in industrial effluents during the production and other industrial processes. Most of the effluents particularly those used in textile manufacturing processes are highly coloured. This is due to the stability of various modern dyes like azo, triarylmethane, reactive, acidic, basic, naphthol, vat dyes etc. which will have deleterious effect also in wastewater for a long time [73, 74]. Reports indicated that annually more than 50,000 tons are lost through effluents during industrial application and production processes [75]. During dye production and textile manufacturing processes a huge amount of wastewater containing dyestuffs with intensive color and toxicity introduced into aquatic systems, therefore, dyes are common industrial pollutants [76]. Azo dyes represent the largest class of organic colorants listed in the colour index and their relative share among reactive dyes, acid dyes and direct dyes is even higher and anthraquinone dyes are second largest class of the entries in the colour index, followed by triarylmethanes and phthalocyanines [77]. Textile mills are major consumers of water and

consequently one of the largest groups of industries causing intense water pollution. Textile processing employs a variety of chemical, depending on the nature of the raw material and products. The extensive use of chemicals results in generation of large quantities of highly polluted wastewater. Dyes are quite stable and therefore, conventional biological treatment methods for industrial wastewater are ineffective, resulting often in an intensively colored discharge from the treatment facilities. Additionally, they are readily reduced under anaerobic conditions to potentially hazardous aromatic amines etc. Thus, there is a need for developing treatment methods that are more effective in eliminating dyes from waste stream at its source [78].

The most problematic industries in terms of dye release to the environment in the form of wastewater are the production of dyes and the dyeing industry. The uncontrolled release of these compounds in the environment causes severe problems. They are designed to be chemical and photolytic stable and they are also highly persistent in natural environments. In addition, reactive dyes are highly water soluble and non-degradable under the typical aerobic conditions found in conventional, biological treatment system. In the present work photo-catalytic degradation, of dyes and decolorization of water under visible light has been investigated using ZnO nanoparticles as photo-catalyst. We investigated this degradation process under different reaction condition to assess the feasibility and optimization of process for industrial dyes effluents. The degradation of dyes under investigation was monitored by measuring chemical oxygen demand (COD). Increase in estimated CO_2 and detection of NO_3^- ions supported the mineralization process of the dyes taken for investigation. The UV-Visible spectral analysis further confirms the mineralization of dyes.

References:

1. Ahmad A., Setapar S. H. M., Chuong C. S., Khatoon A., Wani W. A. and Kumar M. R., *RSC Adv.* 5 (2015) 30801.
2. Kuriakose S., Satpati B. and Mohapatra S., *Advanced Material Lett.* 6 (2015) 1104.
3. Jain A. K., Gupta V. K., Bhatnagar A. and Suhas, *Journal Hazard. Mater.*, B101, (2003) 31.
4. Pare B., Tomar H., Singh P., Ayachit M. and Bhagwat V W., *Sci-fronts*, 1 (2007) 69.
5. Anpo M, *Pure Appl Chem*, 72 (2000) 1787.
6. Islam A. S. M. A., Ferdous T., Das A. K., Karim M. M. and Masum S. M., *Bangladesh J. Sci. Ind. Res.* 50 (2015) 1.
7. Dhatshanamurthi P., Santhi M. and Swaminathan M., *Journal of Water Process Engineering*, 16 (2017) 28.
8. Zaharia C. and Suteu D., *Environmental and Analytical Update. Rijeka, Croatia, In Tech*, (2012) 85.
9. Anjaneyulu Y., Sreedhara N., Chary, and Suman Raji D. S., *Decolourization of industrial effluents – Available methods and emerging technologies – A review. Rev. Environ. Sci. Biotechnol.*, (2005) 245.
10. Bisschops I. A. E. and Sanjers H, Literature review on textile wastewater characterization. *Environ. Technol.*, 24 (2003) 1399.
11. Cisncros R L, Espinoza A G, Litter M A, *Chemosphere* 49: (2002) 393.
12. Abrahart E. N., *Dyes and their intermediates*, Chem. Pub. Co., New York. (1997) 1.
13. Gomes R. J., *Estrutura e propriedades dos corantes. Barbosa e Xavier Lda., Braga, Portugal*, (2002) 12.
14. [http:// angelasancartier.net/dyes](http://angelasancartier.net/dyes) – Chemical and Synthetic.

15. Raval N. P., Shah P. U. and Shah N. K., *Appl Water Sci.*, (2016).
16. Christie R. M., *Royal Soci. Chem., Cambridge, UK*, (2001).
17. Hunger K., *Industrial Dyes: Chemistry, Properties, Applications*, Wiley VCH, Weinheim, (2003).
18. Sarwan B., *Ph. D. Thesis*, Department of Chemistry, Vikram University, Ujjain (M.P.) India (2011).
19. More P., *Ph. D. Thesis*, Department of Chemistry, Vikram University, Ujjain (M.P.) India (2012).
20. Singh P., *Ph. D. Thesis*, Department of Chemistry, Vikram University, Ujjain (M.P.) India (2009).
21. Cao M., Wang F., Zhu J., Zhang X., Quin Y. and Wang L., *Materials Letters*, 192 (2017) 1.
22. Rajasthan State Pollution Control Board, *Environ. Guidance Manual Textiles Projects*, Administrative Staff College of India, Hyderabad, (2011).
23. Gunvant H. S. and Vinod S. S., *Archives Appl. Sci., Res.*, 2 (2010) 126.
24. Jayanth Sarathi N., Karthik R., Logesh S., Srinivas Rao K. and Vijayanand K. *2nd Int. Conf. on Environ. Sci. and Devel.* 4 (2011) 120.
25. Munter R., *Proc. Estonian Acad. Sci. Chem.*, 50 (2001) 59.
26. Bethi B., Sonawane S. H., Bhanvase B. A. and Gumfekar S., *Chemical Engineering and Processing*, (2016) 1016.
27. Dewil R., Mantzavinos D., Poullos I. and Rodrigo M. A., *J. of Environ. Management*, 195 (2017) 93.

28. Mills A., Lee S. K., A web-based overview of semiconductor photochemistry-based current commercial applications, *J. Photochem. Photobiol. A: Chem.*, 152 (2002) 233.
29. Hoffmann M. R., Martin S. T., Choi W. and Behnemann D. W., *Environmental applications of semiconductor photocatalysis*, *Chem. Rev.* 95 (1995) 69.
30. Dorfman L. M. and Adams G. E., Reactivity of the Hydroxyl Radical, *National Bureau of Standards*, Report No. NSRDS-NBS-46, (1973).
31. Domencech X., Garden W. F. and Litter M. I., *Avanzados oxidation Processes for La eliminacion contaminants*, In: *Contaminants Eliminacion. La Plata: Network CYTED*, (2001).
32. Ball B. R., Brix K. V., Brancato M. S., Allison M. P. and Vail S. M., *Environ. Prog.*, 16 (1997) 121.
33. Kang J. W. and Hoffmann M. R., *Environ. Sci. Technol.*, 32 (1998) 3194.
34. Kdasi A. L., Idris A., Saed K. and Guan C. T., *Glob. Nest. Int. J.*, 6 (2004) 222.
35. Chen J. and Zhu L., *J. Photochem. Photobiol. A: Chem.*, 188 (2007) 56.
36. Jozwiak W. K., Mitros M., Czaplinska J. K. and Tosik R., *Dyes and Pigments*, 74 (2007) 9.
37. Sukanchan P., *Res. J. Chem. Environ.*, 16 (2012) 83.
38. Litter M., *Handbook Env. Chem.*, 2 (2005) 325.
39. Munter R., *Proc. Estonian Acad. Sci. Chem.*, 50 (2001) 59.
40. Silva D. C. and Faria J., *J. Photochem. Photobiol., A: Chem.*, 153 (2002) 1.
41. Konstantinous I. K. and Albanis T. A., *Appl. Cata., B: Environ.*, 49 (2004).
42. Ollis D. F., Pellizetti E. and Serpone N., *Environ. Sci. Technol.*, 25 (1991) 1523.
43. Yoon J., Lee Y. and Kim S., *Water Sci. Technol.*, 44 (2001) 1.

44. Matsudai M. and Hunt G., *Nippon Koshu Eisei Zasshi*, 52 (2005) 923.
45. Faraday M., *Philosophy Trans*, 147 (1857) 145.
46. Zsigmondy R., “*Colloids and the Ultramicroscope*”, *J. Wiley and sons*, NY (1914).
47. Taniguchi N., On the basic concept of ‘Nano-Technology’, *In: Proceedings of the Int. Conf. on Production Engi., Tokyo, Part II, Japan society precision Engi., Tokyo: JSPE (1974) 18.*
48. Ashby M. F., Ferreira P. J. and Schodek D. L., *Nanomaterial’s, Nanotechnologies and Design*, (2009) 467.
49. Qureshi T., *Ph. D. Thesis*, Department of Chemistry, Vikram University, Ujjain (M.P.) India (2013).
50. Zhang Y., Ram M. K., Stefanakos E. K. and Goswami D. Y., *Journal of Nanomaterial’s*, (2012) 1.
51. Serpone N., *Photocatalysis: Fundamentals and Application. Canada: John Wiley and Sons. Inc., (1989).*
52. Fujishima A. and Honda K., *Nature*, 238 (1972) 37.
53. Hung Q. L., Wang M., Zhong H. X., Chen X. T., Xue Z. L. and You X. Z., *Cryst. Growth Des.*, 8 (2008) 1412.
54. Mahmoodi N. M., Arami M., Limaee N. Y. and Tabrizi N. S., *J. Coll. Inter. Sci.*, 295 (2006) 159.
55. Mills A., Davies R. H. and Worslery D., *Chem. Soc. Hevs.*, 22 (1993) 417
56. Akir S., Barras A., Coffinier Y., Bououdina M., Boukherroub R. and Omrani A. D., *Ceramics International*, (2016) 1.
57. Morasae S., Mohammed Z., Amene N., Elhan K. and Alireza Z. M., *Thin Solid Films*, (2015) 1.

58. Kuriakose S., Satpati B. and Mohapatra S., *Adv. Mater. Lett.*, 6 (2015) 1104.
59. Chakrabarti S. and Dutta B. K., *J. Hazard. Mater.*, 112 (2004) 269.
60. Dinar B. and Icli S., *J. Photochem. Photobiol. A Chem.*, 140 (2001) 263.
61. Perillo P. M. and Atia M. N., *Chemical Technol.*, 11 (2016) 1.
62. Curri M. L., Comparelli R., Cozzoli P. D., Mascolo G., and Agostiano A., *Mater. Sci. Eng. C*, 23 (2003) 5.
63. Poullos I., Micropoulou E., Panou R. and Kostopoulou E., *Appld. Catal. B Environ.*, 41 (2003) 345.
64. Akyol A. and Bayramoglu M., *J. Hazard. Mater. B*, 124 (2005) 241.
65. Dhatshanamurthi P., Santhi M. and Swaminathan M., *Journal of Water Process Engineering*, 16 (2017) 28.
66. Galidino C., Jacqueus P. and Kalt A., *J. Photochem. Photobiol. A Chem.*, 141 (2001) 47.
67. Sarwan B., Pare B. and Acharya A. D., *Applied surface Science*, 301 (2014) 99.
68. Alton I. A., Balciogolu I. A. and Bahnmen D., *Wat. Res.*, 31 (1997) 1728.
69. Feng W. Nansheng D. and Helin H., *Chemosphere*, 41 (2000) 1233.
70. Pare B., Jonnalgadda S. B., Tomar H., Singh P. and Bhagwat V. W., *Desalination*, 232 (2008) 80.
71. http://en.wikipedia.org/wiki/Neutral_red.
72. http://www.ecology.kee.hu/pdf/0401_111118.pdf.
73. Chacon J. M., Leal Ma T., Sanchez M. and Bandala E. R., *Dyes and Pigments* 69 (2006) 144.
74. Konstantinou I. K. and Albanis T. A., *Appld. Catal. B Environ.*, 49 (2004) 1.
75. Mansilla H., Guttra L. C. and Merchant R., *Editorail CYTED*, (2001) 285.

76. Khezami L., Taha K. K., Ghiloufi I. and Mir L. El., *Water Sci. and Technology*, 73.4, (2016) 881.
77. Pare B., Solanki V. S., Gupta P. and Jonnalagadda S. B., *Indian Journal of Chemical Technology*, 23 (2016) 513.
78. Zhao J. and Liu G. J., *New J. Chem.*, 24 (2000) 411.

CHAPTER-II

Literature Review

2.1: LITERATURE REVIEW:

Textile dye and other dye stuff is being the major problem since long time and dangerous to environment and human health. Therefore degradation of these wastes has been gaining much attention of the researchers working in this field. In the last two decades, a fast evolution of research is carried out devoted to environment protection and conservation has been reported. In order to get knowledge of this field a detailed literature survey has been carried out related to nature and characterization of various photo-catalysts, photo-degradation methods, degradation of various dyes has been reviewed and summed up in this chapter. We focused particularly on some selected dyes, Malachite green, Methylene green, Direct Blue-1, Orange-II, Acridine Orange and Neutral red dyes degradation and ZnO NPs as photo-catalyst taken for present study. As we come to know that AOPs are quite efficient and removal of organic pollutants particularly from waste water, sufficient literature regarding this study is available.

In order to know the overall status of the present research problem taken under study a detailed and careful and detailed literature survey has been carried out. Exhaustive literature survey has been done using SCOPUS, a search engine of Elsevier etc.

In the year 2005, Akyol A. and Bayramoglu M., [1] studied the photo-catalytic degradation of Remazol Red F₃B using ZnO catalyst. They investigated the photo-catalytic degradation of Remazol Red F₃B dye in batch slurry reactor using 254nm and 365nm UV light sources in presence of ZnO catalyst. They concluded from results that decolorization and total organic carbon removal is affected by solution pH. They also mentioned that decolorization is faster at 365nm light and total organic carbon is not affected by wavelength of light used. They also noted that catalyst loading affected the efficiency of degradation and found to be optimum at 2g/litre of ZnO. They also studied

the effects of various parameters like intensity of light, wavelength of light, catalyst concentration, solution pH and initial dye concentration on photo-catalytic degradation of dye taken for study.

In the year 2006, Modarishalla N. and Behnajadi M. A., [2] reported photo-oxidative degradation of malachite green under the influence of UV light in H_2O_2 . They reported influence of parameters under which reaction was carried out. They studied that H_2O_2 and UV light independently showed negligible effect on degradation. They also proposed a simple kinetic model by which it is confirmed that the order of reaction is pseudo first order. They also noted spectral changes of malachite green during photo-oxidation and effect of UV light intensity and found that as the intensity of light increases decolorization rate increased because of greater product of hydroxyl radicals which are directly responsible for decolorization. Their findings are in good agreement with kinetic model.

In the year 2006, Jang Y. J. et al, [3] reported a comparative study of ZnO nanoparticles and its nano-crystalline particles on photo-catalytic degradation of methylene blue. They reported flame spray pyrolysis and spray pyrolysis assisted with electrical furnace were used for the preparation of the ZnO NPs and its nano-crystallites by using aqueous zinc nitrate solution as precursor materials. The prepared ZnO NPs and its nano-crystallites both are of 20nm diameter for composition of photo-catalytic activity. They observed that the photo-catalytic degradation capacity of ZnO NPs is greater than the capacity of the ZnO nanoparticles. They observed that as the concentration of ZnO NPs increased from 0.25mol to 1.5mol, the efficiency of photo-catalytic degradation increases which is higher than the earlier reports.

In the year 2007, Kanade K. G. et al, [4] reported the synthesis of prismatic Cu doped ZnO NPs in both aqueous and organic phases. The prepared NPs are of 40-85nm range in average. The structural study reveals that ZnO phase have wurtzite structure. The data obtained by decomposition of H₂S showed that Cu doped ZnO is active photo-catalyst under UV light as maximum hydrogen production rate achieved that is 1932micro mol per hr. They also studied that the Cu concentration as dopant on the catalytic activity of Cu-ZnO NPs as they found ZnO catalytic activity is lower than Cu-ZnO under UV-Visible light irradiation. They found that ZnO mediated in organic layer has higher degree of crystallinity as compared to that of water.

In the year 2007, Ghaly M. Y. et al, [5] investigated that the photo-catalytic oxidation of Morloin Navy 2 RM, a basic dye by TiO₂ in solar light. This decolorization follows the pseudo-first order kinetics and showed that as the concentration of H₂O₂ increases the decolorization. 99% dye decoloriaztion and 75% total organic carbon were completed under the condition of 1g/L TiO₂, 1.5ml/L H₂O₂ and pH 5.

In the year 2008, Akyol A. and Bayramoglu M., [6] studied the impact of catalyst type and UV wavelength on photo-catalytic degradation of the azo dyes in addition to known factors, such as such as waste water characteristics and process conditions. They also compared the photo-catalytic activity of ZnO and TiO₂ and tow wavelength of UV light (254nm and 365nm) on degradation of Remazol Red F-3B an azo dye. They observed from the results obtained that ZnO has better decolorization and total organic carbon removal efficiencies under 365nm UV light which is better than the TiO₂ under similar conditions, but TiO₂ decolorization performance is better than ZnO at 254nm UV light. Additionally they mentioned that TiO₂ has better TOC removal capacity than ZnO.

In the year 2008, Ullah R. and Dutta J., [7] synthesized undoped and Mn-doped ZnO by wet chemical co-precipitation method. They synthesized Mn doped ZnO NPs first time using wet chemical precipitation method which showed promising degradation activity. The aim of Mn-doped ZnO NPs synthesis was intended to create tail states, which can be used as effective photo-catalyst for the degradation of organic contaminants under visible light. They found that Mn-doped ZnO has better photo-catalytic degradation property than undoped ZnO NPs and also better than conventional metal oxide like titanium oxide for the degradation of methylene blue as a contaminant.

In the year 2009, Pare B. et al, [8] carried out photo-catalytic degradation of Lissamine fast yellow dye using ZnO under artificial light. They studied the process parameters like catalyst loading, H_2O_2 , $FeCl_3$ on degradation and found that ZnO effectively degrades the dye under solar and artificial light both. They mentioned that pH significantly affects the reaction rate while N_2 played a detrimental effect.

In the year 2010, Barick K. C. et al, [9] synthesized highly mesoporous self-cumulated nanoclusters of pure and magnesium cobalt and nickel doped ZnO by refluxing metal acetate precursors in diethylene glycol medium. They found that the prepared porous spherical shaped nano-crystals were made up of nano-crystals that are stable to some extent, well defined and having hexagonal wurtzite structure. They successfully doped Mn, Co and Ni into ZnO nanostructure which is evenly distributed in the sample. Pores are irregular in shape and randomly distributed in nanoclusters as shown by TEM images. Additionally, they studied the photo-catalytic activity of mesoporous pure or doped ZnO nanostructure on methylene blue dye and ZnO NPs showed better photo-catalytic activity. **In the year 2010**, Punjabi P. B. et al, [10] investigated the photochemical degradation of neutral red using potassium tri-oxalatoferate(III) and the rate of photo-

degradation was observed using spectrophotometer. They also studied the effect of pH, dye concentration, amount of light intensity on rate of photo-degradation. They prepared potassium trioxalato ferrate by stirring ferrous ammonium sulphate and H_2SO_4 and oxalic acid. The crystals of potassium trioxalato ferrete formed are extremely photosensitive and were preserved in dark to avoid exposure of light. They also found that optical density of Neutral red decreases with increasing time of exposure, oxidant concentration, is directly proportional to the rate of bleaching of dye but after obtaining an optimum rate at a particular concentration of dye, rate of reaction again started to downward.

In the year 2010, Jhiang Z. et al, [11] prepared flake like BiOBr semiconductor by using hydrothermal synthesis and used for methyl orange dye degradation. To study the synthesis of BiOBr materials XRD, SEM and UV-Visible characterization techniques have been carried out. They observed that morphology and crystallite size of the synthesized BiOBr material depends on temp and reaction duration. They found excellent activity and photo stability reveals that BiOBr have promising UV-Visible light responsive catalyst and can be used as alternate of existing photo-catalyst that are generally used for photochemical degradation of dyes.

In the year 2011, Pare B. et al, [12] used BaCrO_4 to degrade Azur B photo-catalytically in presence of visible light. They studied the disappearance of dye by spectrophotometer followed by pseudo-first order kinetics. They tested the degradation of dye testing COD. They also studied the effect of amount of semiconductors, pH, light intensity, dye concentration, oxidant on the rate of photo-degradation. They observed that NaCl and Na_2CO_3 retarded the rate of photochemical degradation while H_2O_2 and $\text{K}_2\text{S}_2\text{O}_8$ increase

the degradation rate. Neutral pH gives better degradation results. Moreover they proposed mechanism of photo-catalytic degradation.

In the year 2011, Chen C. et al, [13] prepared nano-sized ZnO by precipitation method using zinc nitrate, ammonium carbonate, ethanol and de-ionized water and calcination at 550 °C for 2 hrs. They found that, thus synthesis NPs shown good photo-catalytic activity. They determined the specific surface area by Brunauer-Enett-Teller (BET) method and structural properties were investigated by X-RD and morphology and particle size by SEM. They study the photo-chemical activity of the prepared ZnO NPs on Methyl orange dye. They also studied the effect various reaction parameters on degradation of dyes and reported that ZnO has better photo-catalytic activity.

In the year 2011, Sarwan B. et al, [14] prepared BiOCl catalyst by hydrolysis method and characterized by advanced characterization method and found that the size in the range of 6-13 nm. They studied the effect of toxicity reduction textile dye i.e. neutral red (NR) and photo-catalytic activity of BiOCl was investigated. They monitored the photo-catalytic degradation by HPLC photodiode-array-electrospray ionization mass spectrometry technology by intermediate and final products. They concluded photo-degradation of dye by observing decrease in COD and dye absorbance as well which shown complete mineralization of into CO₂ and organic ions. They also carried out catalyst recycling experiment which confirmed the stability of catalyst. They also carried out toxicity study, prior and after photo-catalytic treatment.

In the year 2012, Zhong J. B. et al, [15] prepared and Bi⁺³ doped ZnO synthesized ZnO photo-catalysis by a parallel flow precipitation method using different molar concentration of Bismuth and Zinc, then prepared photo-catalyst were characterized by spectral, structural and morphological techniques. BET results showed that BET area

increase when doping of Bi is carried out on ZnO. Doping of Bi^{+3} into ZnO affected the response to the light and photo induced charge separation rate and charge in ZnO morphology. Bi^{+3} doped ZnO possessed better photo-catalytic activity than ZnO and 5% Bi^{+3} doped ZnO gave the best results among all the concentration tested.

In the year 2012, Nihalani S. et al, [16] studied Barium strontium titanate semiconductor for the photo-chemical degradation of Malachite green and crystal violet dyes which are toxic for the human health. They established the maximum degradation conditions by varying various parameters like pH, light intensity, dye concentration, amount of semiconductor photo-catalyst and irradiation time. They concluded that degraded products are NO_2 , CO_2 , H_2O etc. and are nontoxic in nature, hence photo-degradation of toxic dyes into nontoxic materials. By the use of scavenger they confirmed the mechanism to be free radical.

In the year 2012, Ebrahimi H. R. et al, [17] studied the photo-catalytic degradation of direct yellow 86 by using nano-sized ZnO deposited on glass beads. They found the photo-decomposition rates to be different when they applied different atmospheres. The effect of four type atmospheres including air, nitrogen, oxygen and argon was investigated. They also studied the kinetics of decolorization and found the pseudo-first order kinetics under oxygen and argon atmosphere. They concluded that photodecomposition using ZnO nano-sized layered on glass was a novel alternative pathway for efficient wastewater treatment.

In the year 2012, Kant S. and Kumar A., [18] prepared ZnO and Ni- ZnO nanoparticles by sol-gel method, and then characterized the prepared NPs by various advance characterization techniques like SEM, HRTEM, X-RD and UV-Visible spectroscopy. They observed that between of doping the absorption increases in UV. They studied

doped both undoped ZnO NPs for the photo-catalytic degradation of Methylene blue. Both doped and undoped ZnO catalyst degraded Methylene blue effectively and it confirmed that the prepared catalysts have potential application for the removal of from wastewater and drinking water. The doping enhanced the photo-catalytic activity.

In the year 2013, Kansal S. K. and Prerna, [19] synthesized ZnO and Mn- doped ZnO NPs by using simple hydrothermal method and characterized and morphological techniques. They found that prepared NPs have wurtzite phase and hexagonal phase. They also studied the effect of doping agent Mn on the photo-catalytic activity of ZnO on direct blue 15 dye degradation. They found that doping of Mn on ZnO NPs reduced the photo-catalytic activity and suggested that pure ZnO showed better photo-catalytic degradation activity than Mn-doped ZnO for direct blue 15 dye degradation.

In the year 2014, Sarwan B. et al, [20] used hydrolysis method for the synthesized and several analytical tools were used to characterized the sample and found that BiOCl has average 7-10 pore diameter and $40 \text{ m}^2\text{g}^{-1}$ surface area. They confirmed the formation of OH radical by fluorescence technique. They used HPLC-ESI-DAD-MS spectroscopy technology for the detection of intermediate and final degradation products. They also study the recyclability of catalyst and reported that even after three recycle these is no less in catalytic, which confirmed that catalyst is essentially stable. This photo-catalyst completely mineralized the Nile blue dye as the formation of final products are nitrate ion and CO_2 .

In the year 2014, Beena B. et al, [21] prepared microwave assisted ZnO nano rod and confirmed by XRD using Scherrer's formula. They studied the surface morphology of prepared NPs by SEM and TEM. They used the ZnO rod as photo-catalyst in presence of UV light against Malachite Green dye. They found that ZnO NPs are efficient low cost

photo-catalyst and low degraded Malachite Green dye in presence of UV in shorted period of time.

In the year 2014, Shanthi S. et al, [22] applied solar photo-catalytic oxidation technique using ZnO NPs for the treatment of waste water for the removed of organics and dye staffs. They reported that when ZnO NPs were used instead of ZnO photo-catalytic activity enhanced. They used co-precipitation method for the synthesis of ZnO NPs. They used different energy source for photo-catalytic degradation.

In the year 2015, Ferdous T. et al, [23] prepared ZnO NPs using zinc nitrate hexahydrate and sodium hydroxide under optimum reaction condition. They studied the photo-catalytic activity of prepared ZnO NPs on Direct Brown R N dye in sunlight irradiation and found that ZnO NPs showed substantial capability of destroying Direct Brown R N dye from solution. The used catalyst gives better results than commonly used catalyst.

In the year 2015, Gupta S. et al, [24] carried out photo-catalytic degradation of Azure A, in presence of semiconductor barium chromate. They observed dye degradation rate using UV-Visible spectrophotometer at regular time interval and studied the effect of pH, concentration of dye, amount of photo-catalyst, of light intensity on dye degradation rate. They found that the optimum pH found to be 9.0 and amount of $\text{BaCrO}_4=0.06\text{g}$.

In the year 2015, Abdel-Khalek A. A. et al, [25] developed hygienically advance water treatment technique of environmental pollution and industrialization as the existing methods are costly, and requires well equipped laboratories. They presented a method for wastewater treatment, deterioration and decolorization of Methylene green using both pure ZnO and Ag^+ doped ZnO under UV-visible light. They studied the propagation of photo-degradation process by UV-Visible spectrophotometry. They also compared ZnO

with Ag^+ doped ZnO and found that doped ZnO was more efficient for photo-catalytic degradation.

In the year 2015, Josephine G. A. S. et al, [26] reported the photo-catalytic degradation of toxic dye Malachite green using a ZnO doped Dy_2O_3 photo-catalyst under visible light irradiation. They prepared nano-crystalline photo-catalyst by precipitation method using zinc nitrate, Dysprosium nitrate and sodium carbonate as processors and then characterized the prepared NPs by advance structural and spectral technique. The prepared NPs were crystalline, Nano sized and highly active in visible region as per the experimental results. They also studied the photo-degradation efficiency of Malachite green by various experimental parameters to set the optimum degradation by ZnO doped Dy_2O_3 photo-catalyst.

In the year 2015, Janani L. et al, [27] studied the photo-catalytic degradation of reactive blue with ZnO as photo-catalyst. They used 10 mg/lit dye solution with various concentration of photo-catalyst under UV light and also studied various reaction parameters like contact time, catalyst dose. They concluded that 5.0 g/lit photo-catalyst, at pH=7 for 180 minute gives best results for dye degradation.

In the year 2015, Malakar B. et al, [28] prepared ZnO NPs by feasible modified chemical route and studied it for removal of as photo-catalyst basic methylene blue from aqueous solution. They also characterized the prepared ZnO NPs by Thermogravimetry, XRD, FTIR, UV-Visible spectroscopy and TEM analysis. The prepare ZnO NPs was of 20nm particle size and show good activity against degradation of basic methylene blue dye.

In the year 2015, Kaneva N. et al, [29] prepared ZnO thin films sol-gel method using dip coating technique. They investigated the photo-catalytic activity of ZnO thin films for the

degradation of Malachite green and Methylene blue under UV-light illumination. From the results they conclude that thickest films on glass showed highest efficiency under UV-light.

In the year 2016, Pare B. et al, [30] reported photo-catalyst degradation of hazardous methylene blue dye using BaCrO_4 catalyst. They also investigated the effect of catalyst loading, initial dye, concentration and concentration of H_2O_2 , $\text{K}_2\text{S}_2\text{O}_8$, Na_2CO_3 and NaCl and intensity of light on decolorization. They studied the dye degradation by COD determination.

In the year 2016, Balcha A. et al, [31] synthesized ZnO by precipitation and sol-gel methods to understand how different synthetic methods can affect the photo-catalytic degradation. They evaluated photo-catalytic activity by photo-catalytic degradation of Methylene blue under photo-catalytic degradation. The effects of operational parameters such as photo-catalyst load and initial concentration of the dye on photo-catalytic degradation of the dye were also investigated. From results, they observed that sol-gel method is preferred over precipitation method in order to achieve higher photo-catalytic activity of ZnO nanostructure.

In the year 2016, Alam U. et al, [32] synthesized a series of Y and Co doped ZnO(YVZ) nanoparticles by surfactant assisted sol-gel technique to enhance photo-catalytic activity for degradation of organic pollutants under visible light. They tested photo-catalytic degradation of Rhodamine B, Methylene blue, 4-nitrophenol dyes under UV-light irradiation or other light.

In the year 2016, Khezami L. et al, [33] investigated V-doped ZnO Nano-powder for the degradation of Malachite green dye in aqueous medium. They confirmed the pore volume and specific area, of Nano-powder by N_2 adsorption method and adsorption and photo-

catalytic degradation of dye was done by batch experimental process. They also studied the kinetics of dye degradation by initial and final concentration. They reported that V-doped ZnO nano-powder is effective for Malachite green dye removal from waste water.

In the year 2016, Hussein A. S. and Fairouz N. Y., [34] studied naked Niobium oxide as a photo-catalyst for the industrial degradation of Malachite green dye. They used Nb_2O_5 as an application of advanced oxidation processes for photo-catalytic degradation of industrial waste i.e. Malachite green dye. They studied various parameters and found that optimum weight of catalyst was 0.1 g, dye concentration was 5 ppm, temperature was 25 °C and effective pH was 6.

In the year 2016, Lavand A. B. and Malghe Y. S., [35] Prepared Nano sized base, C and N doped as well Carbon, Nitrogen Co-doped ZnO Nano powder using micro-emulsion technique and characterized by morphological, structured and spectral techniques and found that these have wurtzite structure. They used this catalyst for the degradation of Malachite green dye and found that Carbon, Nitrogen co-doped ZnO showed better activity as compared to other catalyst used for under similar reaction conditions. They also studied that the prepared catalyst was stable and can be reused several times.

In the year 2016, Mohammad A. et al, [36] reported one pot room temperature synthesis of ZnO nano-flowers (ZnO-NFs) using asymmetric Zinc dimeric complex as a single molecular precursor. They used these nano-flowers for the photo-catalytic degradation of different dyes like Methyl orange, Chicago sky blue, Congo red and Eosin blue which are major river pollutant and industrial wastes. They found that it has better activity against Methyl orange compare to other dyes used under similar condition.

In the year 2017, Sarwan B. et al, [37] synthesized nano-scale zero valent Iron particles and BiOCl particles by borohydride reduction method and hydrolysis method

respectively. They used both the catalyst synthesized for the degradation of Nile blue dye decolorization under UV- light and compared the results indicated that nano-scaled zero valent Iron particles was more effective than BiOCl.

In the year 2017, Frunza L. et al, [38] studied different amount of TiO₂ and ZnO NPs on photo-catalytic degradation of Malachite green dye. They deposited these NPs upon wool fabrics which are not studied much. They found that photo-catalytic degradation of methylene blue dye followed simple apparently first order kinetics and demonstrated that methylene blue decolorization can serve at-least for self-clearing of fabrics.

In the year 2017, Shinde D. R. et al, [39] comparatively studied analytical reagent grade photo-catalysis like SnO₂, TiO₂ and ZnO and compared with Degussa P-25(TiO₂) photo-catalyst. They characterized all the received metal oxide by different physiochemical methods of analysis. They also studied the photo-chemical activity of all three AR grade oxides and mentioned that ZnO exhibited highest photo-catalytic activity.

In the year 2017, Kong J. Z. et al, [40] prepared Nitrogen doped ZnO g-C₃N₄ composite by facile and cost effective sol-gel method. From the results obtained N-doped/ZnO g-C₃N₄ exhibited enhanced photo-catalytic activity than other catalyst used under same reaction conditions for the photo-catalytic degradation of Methylene blue and Phenol under visible light irradiation. They also proposed degradation mechanism.

In the year 2017, Pirsahab M. et al, [41] synthesized Cr-doped ZnO NPs under mild hydrothermal conditions using chromium oxide and n-butyle amine as dopant and surface modifier respectively. They use this nearly prepared Cr-doped ZnO NPs for the photo-catalytic degradation of aniline in continuous reactor. They also investigated photo-degradation operational parameters and applying optimum conditions 93% of aniline can be degraded.

In the year 2017, Hitkari G. et al, [42] synthesized ZnO/ γ -Fe₃O₄ nano composites by simple co-precipitation method and BET analysis confirmed the mesoporous behavior of nano composites. They applied prepared nano composites for the photo-catalytic degradation Methylene blue and Rhodamine B organic dyes and found that it has better activity against Rhodamine B degradation in aqueous solution in compare with Methylene blue.

In the year 2017, Dhatshanamurthi P. et al, [43] investigated treatment of dye industry effluent by ZnO, a heterogeneous catalyst, in falling film photo-reactor under natural solar light. They prepared fevicol-ZnO coated on acrylic sheet by brush coating and coating of ZnO with 10 wt. % fevicol was found to be more adherent and efficiency for dye degradation. This is more efficient than commercial catalyst like ZnO and TiO₂-P25. They also studied various reaction parameters for dye degradation.

In the year 2017, Elmorsi T. M. et al, [44] reported Na-doped ZnO NPs by co-precipitation method using NaOH as a precipitating and doping agent as well. They reported Na-doped ZnO as high efficient photo-catalyst as it showed 98.9% of degradation of Congo red dye in 70 minutes under direct sun light. They also reported that as the initial dye concentration increased rate of degradation decrease as availability of ·OH radicals are constant. They also concluded that this Na-doped ZnO catalyst can be used as commercial photo-catalyst.

References:

1. Akyol A. and Bayramoglu M., *J. Hazard Materials B*, 124 (2005) 241.
2. Modirshahla N. and Behnajady M. A., *Dyes and Pigments*, 70 (2006)54.
3. Jang Y. J., Simer C. and Ohm T., *Materials Research Bulletin*, 41 (2006) 67.
4. Kanade K. G., Kale B. B., Baeg J. O., Lee S. M., Lee C. W., moon S. J. and Chang H., *Materials Chemistry & Phys.*, 102 (2007) 98.
5. Ghaly M. Y., Farah J. Y. and Fathy A. M., *Desalination*, 217 (2007) 74.
6. Akyol A. and Bayramoglu M., *Chemical Engi. & Processing*, 47 (2008) 2150.
7. Ullah R. and Dutta J., of *Hazardous materials*, 156 (2008) 194.
8. Pare B., Singh P. and Jonnalagadda S. B., *Indian Journal of Chem.*, 48 (2009) 1364.
9. Barick K. C., Singh S., Aslam M. and Bahadur D., *Microporous and Mesoporous materials*, 134 (2010) 195.
10. Jhala Y., Chittora A. K., Ameta K. L. and Punjabi P. B., *International J. Chem. Sci.:* 8 (2010) 1389.
11. Jiang Z., Yang F., Yang G., Kong L., Jones M. O., Xiao T. and Edwards P. P., *Journal of Photochemistry and Photobiology A: Chemistry*, 212 (2010) 8.
12. Pare B., Solanki V. S. and Jonnalagadda S. B., *Indian Journal of Chemistry*, 50 A, (2011) 1061.
13. Chen C., Liu J., Liu P. and Yu B., *Advance in Chemical Engi. & Sci.*, 1 (2011) 9.
14. Pare B., Sarwan B. and Jonnalagadda S. B., *Applied Surface Sci.*, 258 (2011) 247.
15. Zhong J. B., Li J. Z., Lu Y., He X. Y., Zeng J., Hu W. and Shen Y. C., *Applied Surface Sci.*, 258 (2012) 4929.
16. Nihalani S., Vijay A., Tripathi N. and Bhardwaj S., *ISOR J. of Applied Chemistry (IOSR-JAC)*, 2 (2012) 20.

17. Ebrahimi H. R., Modrek M. and Joohari S., *Indian Journal of Sci. Technol.*, 5 (2012) 1828.
18. Kant S. and Kumar A., *Adv. Mat. Letters*, 3 (2012) 350.
19. Kansal S. K. and Prerna, *Energy and Environment Focus*, 2 (2013) 203.
20. Sarwan B., Pare B. and Acharya A. D., *Applied Surface Sci.*, 301 (2014) 99.
21. Rejani P., Radhakrishnan A. and Beena B., *Iranica J. of Energy and Environment*, 5 (2014) 233.
22. Santhi S., Manjula R., Vinulakshmi M. and Rathina B. R., *Int. Journal of Research in Pharmacy and Chemistry*, 4 (2014) 571.
23. Islam A. S. M. A., Ferdous T., Das A. K., Karim M. M. and Masum S. M., *Bangladesh J. Sci. Ind. Res.*, 50 (2015) 1.
24. Gupata S., Tak P., Ameta R. and Benjamin S., *Journal of Adv. Chemical Science*, 1 (2015) 38.
25. Abdel-Khalek A. A., Nassar H. F., Gawad F. Kh. A. and Hashem A., *Der Pharma Chemica*, 7 (2015) 264.
26. Josephine G. A. S., Ramchandran S. and Sivasamy A., *Journal of Saudi Chemical Society*, (2015) 1.
27. Janani L., Henry K. and Edwine K., *International Journal of Research and Review*, 2 (2015) 343.
28. Malakar B., Miah A. T., Kalita C. and Saikia P., *Chemical Sci. Transactions*, 4 (2015) 788.
29. Kaneva N., Bojinova A., Papazova K., Dimitrov D., Svinyarov I. and Bodanov M., *Bulgarian Chemical Communications*, 47 (2015) 395.

30. Pare B., Solanki V. S., Gupta P. and Jonnalagadda S. B., *Indian Journal of chemical Technology*, 23 (2016) 513.
31. Balcha A., Yadav O. P. and Dey T., *Environ Sci. Pollut Res.*, (2016) 7750.
32. Alam U., Khan A., Raza W., Khan A., Bahnemann D. and Muneer M., *Catalysis Today*, (2016) 1.
33. Khezami L., Taha K. K., Ghiloufi I. and Mir L. El., *Water Sci. and Technology*, 73.4, (2016) 881.
34. Hussein A. S. and Fairouz N. Y., *Journal of Babylon University/Pure and Applied Sci.*, 24 (2016) 2510.
35. Lavand A. B. and Malghe Y. S., *Adv. Mater. Lett.*, 7 (2016) 181.
36. Mohammad A., Kappor K. and Mobin S. M., *Chemistry Select*, (2016) 3483.
37. Sarwan B., Pare B. and Acharya A. D., *Journal of Physics: Conf. Series*, 836 (2017) 1.
38. Frunza L., Diamadescu L., Zgura I., Frunza S., Ganea C. P., Negrila C. C., Enculescu M. and Birzu M., *Catalysis Today*, (2017) 1.
39. Shinde D. R., Tambade P. S., Chaskar M. G. and Gadave K. M., *Journal Drink. Water Eng. Sci.*, (2017) 20.
40. Kong J. Z., Zhai H. F., Zhang W., Wang S. S., Zhao X. R., Li M., Li A. D. and Wu D., *Nanoscale research Letters*, (2017) 12:526.
41. Pirsahab M., Shahmoradi B., Beikmohammadi M., Azizi E., Hossini H. and Ashraf G. M., *Scientific Reports*, (2017) 7:1473.
42. Hitkari G., Singh S. and Pandey G., *Int. Journal of Advance Research in Sci., Engi. And Technology*, (2017) 3960.

43. Dhatshanamurthi P., Santhi M. and Swaminathan M., *Journal of Water Process Engineering*, 16 (2017) 28.
44. Elmorsi T. M., Elsayed M. H. and Bakr M. F., *American Journal of Chemistry*, 7 (2017) 48.



CHAPTER-III

Experimental Approaches



Experimental Approaches:**3.1: List of required chemical**

Chemicals	Company/ Grade
Dyes	Sigma, Aldrich, LOBA Chemie
Zn(NO ₃) ₂ , NaOH,	SD Fine, AR
Sulphuric acid (H ₂ SO ₄), Oxalic acid, Hydrogen peroxide, Potassium dichromate, Ferrous ammonium sulphate and Mercuric sulphate.	SD Fine, AR
Sodium carbonate, Sodium chloride, Ferric chloride, Ferrous sulphate (FeSO ₄), Potassium persulphate, Phenolphthalein indicator solution and Barium chloride.	BDH, AR
Silver nitrate, Potassium nitrate, Ethyl alcohol (95%), Chloroform, Ferroin indicator, Magnesium chloride and Sodium sulphate.	BDH, AR

3.2: Preparation of solution required:

1. Malachite Green solution: Stock solution of Malachite green $1.0 \times 10^{-3} \text{ mol dm}^{-3}$ was prepared by dissolving 0.046 g Malachite green in 100 ml double distilled water.

2. Methylene Green solution: Stock solution of Methylene green $1.0 \times 10^{-3} \text{ mol dm}^{-3}$ was prepared by dissolving 0.0364 g Methylene green in 100 ml double distilled water.

3. Direct Blue-1 solution: Stock solution of Direct Blue-1 $1.0 \times 10^{-3} \text{ mol dm}^{-3}$ was prepared by dissolving 0.0992 g Direct Blue-1 in 100 ml double distilled water.

4. Orange-II solution: Stock solution of Orange-II $1.0 \times 10^{-3} \text{ mol dm}^{-3}$ was prepared by dissolving 0.0350 g Orange-II in 100 ml double distilled water.

5. Acridine Orange solution: Stock solution of Acridine Orange $1.0 \times 10^{-3} \text{ mol dm}^{-3}$ was prepared by dissolving 0.0265 g Acridine Orange in 100 ml double distilled water.

6. Neutral Red solution: Stock solution of Neutral Red $1.0 \times 10^{-3} \text{ mol dm}^{-3}$ was prepared by dissolving 0.0288g Neutral Red in 100 ml double distilled water.

7. Sulphuric acid solution: Stock solution of H_2SO_4 was prepared by diluting the calculated volume of acid with double distilled water and finally determined its concentration by titrating it against standard NaOH solution using phenolphthalein indicator.

8. Potassium persulphate solution: Stock solution of $\text{K}_2\text{S}_2\text{O}_8$ $1.0 \times 10^{-2} \text{ mol dm}^{-3}$ was prepared by dissolving 0.27 g $\text{K}_2\text{S}_2\text{O}_8$ in 100 ml distilled water.

Sodium carbonate solution: Stock Solution of Na_2CO_3 $1.0 \times 10^{-2} \text{ mol dm}^{-3}$ was prepared by dissolving 0.106 g Na_2CO_3 in 100 ml distilled water.

9. Sodium chloride solution: Stock Solution of NaCl $1.0 \times 10^{-2} \text{ mol dm}^{-3}$ was prepared by dissolving 0.058 g NaCl in 100 ml distilled water.

10. Hydrogen peroxide solution: The aqueous solution of H_2O_2 $1.0 \times 10^{-1} \text{ mol dm}^{-3}$ was prepared by adding 1.02 mL of H_2O_2 in 100 ml distilled water.

11. Ferric Chloride solution: Stock solution of FeCl_3 $1.0 \times 10^{-2} \text{ mol dm}^{-3}$ was prepared by dissolving 0.162 g FeCl_3 in 100 ml distilled water.

3.3: Synthesis of nanostructured ZnO

Precipitation method was used to prepare ZnO nanoparticles. For this, 0.45 mol dm^{-3} aqueous solution of zinc nitrate [$\text{Zn}(\text{NO}_3)_2 \cdot 4\text{H}_2\text{O}$] and 0.9 mol dm^{-3} aqueous solution of sodium hydroxide (NaOH) were prepared in distilled water, separately. Then, the beaker containing NaOH solution was heated at temperature of about 55°C and zinc nitrate solution was added drop wise to the heated sodium hydroxide solution under high speed

stirring. Then the beaker was sealed at this condition for 2 hrs. The precipitated ZnO NPs was cleaned with deionized water and ethanol respectively then dried in air at about 60°C. Finally, the product was calcination in muffle furnace at 300°C [1].

3.4: Characterization techniques for nanostructured ZnO

3.4.1: X-Ray Diffraction (XRD)

The X-Ray diffraction technique is a common technique for determining the crystallographic structure of a material. XRD study is the scattering of X-Rays from a sample after an incident X-Ray interacts with electrons in atoms. The incoming X-Ray collides with electron may produce elastic or inelastic scattering. No energy is lost in elastic collisions, therefore, the wavelength of the scattered X-Rays is the same as the incident wavelength and only momentum has been transferred. These scattered X-Rays transmit information about the electron distribution in the materials. The atomic planes of crystal cause an incident beam of X-Rays to interfere with one another as they leave the crystal and this phenomenon is called x-Ray diffraction [2].

Diffraction wave from different planes of atoms will interfere with each other creating a diffraction pattern. Atoms that are arranged in a periodic fashion will yield a diffraction pattern with sharp interference maxima. The peaks in an X-Ray diffraction pattern are related to the unit cell dimensions. The condition for a diffraction peak to occur can be found using Bragg's Law:

$$n\lambda = 2d \sin \theta$$

Where, d is the distance between lattice planes, θ is the scattering angle, n is an integer representing the order of the diffraction peak and λ is the wavelength of the X-Ray [3].

The lattice parameters of a crystal can be calculated by knowing the d-spacing value

which is determined from the peaks of the XRD image. For a hexagonal system, the d -spacing is related to the lattice parameters by:

$$\frac{l}{d^2} = \frac{4}{3} \left(\frac{h^2+hk+k^2}{a^2} \right) + \frac{l^2}{c^2} \quad (1)$$

Where, h , k and l are the Miller indices and a , b and c are the lattice parameters along the x , y and z directions.

The instrument used for the powdered sample is PANalytical Empyrean XRD [IISER Bhopal, MP].

X-Ray Diffractometer used is shown as Figure 1.3.



Fig. 3.1: XRD Instrument setup

The average crystallite size (D in nm) of the sample was calculated from the XRD pattern of the ZnO NPs according to the Scherrer equation.

$$D = k \left[\frac{\lambda}{\beta \cos \theta} \right] \quad (2)$$

Where, k is a shape factor, related to the crystallite shape, usually taken as 0.9, λ is the wavelength of X-Ray radiation, β is the full width at half maximum intensity of the peak and θ is the Bragg's angle of diffraction [4, 5].

3.4.2: High Resolution Field Emission Scanning Electron Microscope (HR FESEM):

The technique of High Resolution Field Emission Scanning Electron Microscope is used to capture very high resolution images of surface of nanoparticles. The benefits of SEM contain the capacity to image materials and the variety of analytical models available for determining the composition and nature of the sample. In present work, HR FESEM (Fig. 3.2) was used to characterize mean nanoparticle size and morphology of the sample [6].



Fig. 3.2: High Resolution Field Emission Scanning Electron Microscope

3.4.3: Fourier Transform Infrared Spectroscopy (FTIR):

The FT-IR is one of the powerful tools for identification of compounds by matching spectrum of unknown compounds with reference spectrum (finger printing) and identification of functional groups in unknown substances. The IR region of the electromagnetic spectrum is considered to cover the range from $50-12,500\text{cm}^{-1}$ approximately [7]. For the present study Bruker model ALPHA FTIR is used characterized ZnO NPs as shown in figure 3.3. [Department of Pharmaceutical Chemistry, Govt. Madhav Science P.G. College, Ujjain, MP]



Fig. 3.3: FT-IR Instrument

3.5: Photo-reactor Design and Experimental Conditions:

Photo-catalytic experimentations were carried out with 100ml of dye solution using ZnO NPs as photo-catalyst under exposure of visible light in a specially designed double-walled slurry type batch reactor vessel (height 7.5 cm x diameter 6 cm) made up of Pyrex glass surrounded by thermostatic water circulation arrangement to keep the temperature in the range of $30 \pm 0.5^{\circ}\text{C}$. Irradiation was carried out using 500W halogen lamp surrounded by aluminum reflector to avoid loss of irradiation.

During photo-catalytic experiment, after stirring for 10min. slurry composed of dye solution and catalyst was placed in dark for 30min. in order to establish equilibrium between adsorption and desorption phenomenon of dye molecule on photo-catalyst surface. Then slurry containing aqueous dye solution and ZnO NPs were stirred magnetically to ensure complete suspension of catalyst particle while exposing to visible light. At specific time intervals, aliquot (3mL) was withdrawn and centrifuged for 2 min at 3500 rpm to remove ZnO nanoparticles from aliquot to assess extent of decolourization photo-metrically. Changes in absorption spectra were recorded at 400-620nm λ_{max} on double-beam UV-Vis. Spectrophotometer (Systronic Model No.166). Intensity of visible

radiation was measured by a digital Lux-meter (Lutron LX - 101). A digital pH meter was used to measure the pH of the solution. The desired pH of the solution was adjusted by the addition of previously standardized 0.05M H₂SO₄ and 1.0M NaOH solutions. COD & CO₂ estimation were performed by using standard methods [8, 9]. Performance efficiency was calculated as

$$\% \text{ efficiency} = \frac{C_0 - C}{C_0} \times 100 \quad (3)$$

Where C₀ = initial COD/absorbance of dye solution before irradiation, C = final COD/absorbance of dye solution after irradiation time (t).

The schematic diagram of photo-reactor is shown in the Fig.3.4 and image of indigenous photo-reactor in Laboratory Fig. 3.5.

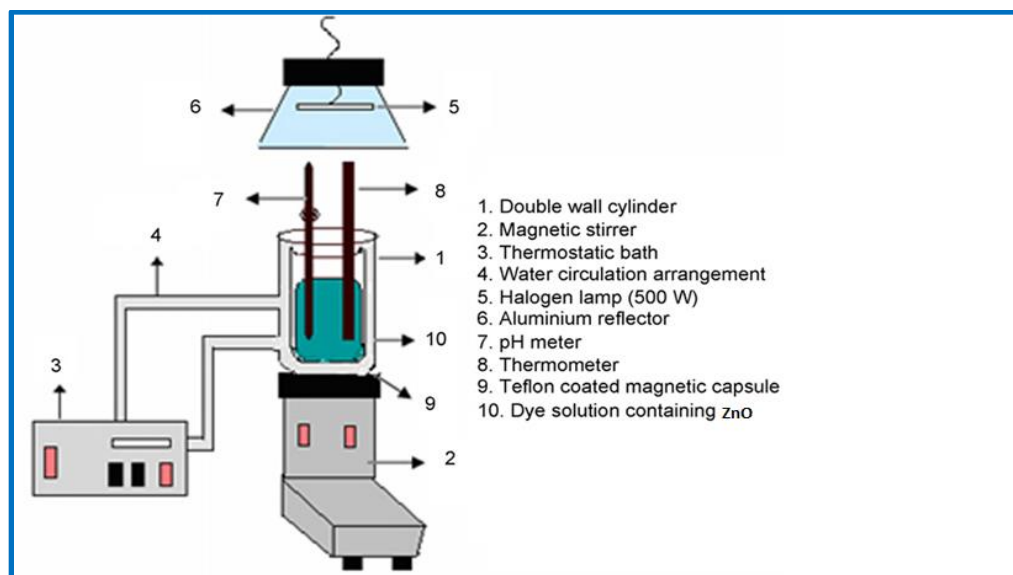


Fig. 3.4: Schematic diagram of photo-reactor

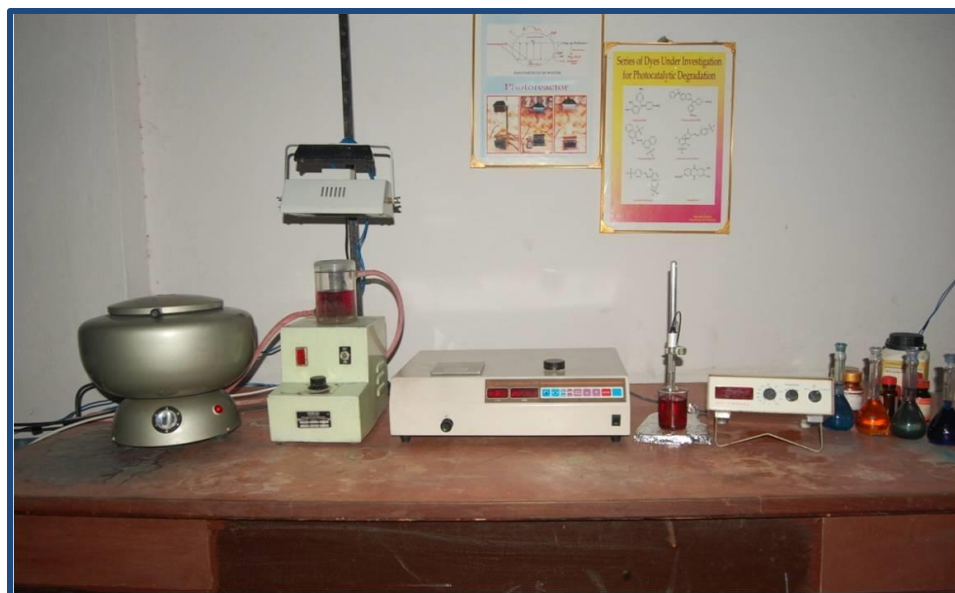


Fig. 3.5 Image of indigenous photo-reactor in Laboratory

3.6: Methods for identification of mineralized products:

Determination of Chemical Oxygen Demand (COD) [10, 11]:

Chemical oxygen demand (COD) is the measure of oxygen consumed during the oxidation of the oxidizable organic matter using a strong oxidizing agent. Potassium dichromate in presence of sulphuric acid is generally used as an oxidizing agent in determination of COD. The sample is refluxed with $K_2Cr_2O_7$ and H_2SO_4 in presence of mercuric sulphate to neutralize the effect of chlorides and silver sulphate. The excess of potassium dichromate is titrated against ferrous ammonium sulphate using ferroin indicator. The amount of $K_2Cr_2O_7$ used is proportional to the oxidizable organic matter present in the sample.

Reagents:

- a) Potassium dichromate solution, 0.25 M: Dissolve 12.259 g of dried A. R. grade $K_2Cr_2O_7$ in distilled water to make 1 litre of solution.
- b) Potassium dichromate solutions, 0.025 M: Dilute 0.25 M $K_2Cr_2O_7$ 10 times. (100 →1000 mL).

- c) Ferrous ammonium sulphate, 0.1 M: Dissolve 39.2 g of $\text{Fe}(\text{NH}_4)_2(\text{SO}_4)_2 \cdot 6\text{H}_2\text{O}$ in water adding 20 mL conc. H_2SO_4 to make 1 litre of solutions. Standardize this solution with $\text{K}_2\text{Cr}_2\text{O}_7$ for standardization, dilute 10.0 mL of $\text{K}_2\text{Cr}_2\text{O}_7$ to about 100 mL, add 30 mL of conc. H_2SO_4 and titrate with ferrous ammonium sulphate using ferroin as an indicator.
- d) Ferrous ammonium sulphate, 0.01 M: Dissolve 0.1 N ferrous ammonium sulphate to 10 times (100→1000 mL).
- e) Ferroin indicator: Dilute 1.485 g of 1, 10-phenanthroline and 0.695 g of ferrous sulphate (FeSO_4) (H_2O) in distilled water to make 100 mL of solution.
- f) Sulphuric acid: H_2SO_4 , conc. (Sp. gr. 1.84).
- g) Mercuric sulphate: HgSO_4 , solid.
- h) Silver sulphate: Ag_2SO_4 , solid.

Procedure:

1. Take 20mL of sample in a 500mL COD round bottom flask with a ground joint for Liebig reflux condenser.
2. If the sample is expected to have COD more than 50 mg/L, 10mL of 0.25M $\text{K}_2\text{Cr}_2\text{O}_7$ solutions is added and if COD is expected below 50mg/L then 10mL of 0.025M $\text{K}_2\text{Cr}_2\text{O}_7$ is added. Extreme care has been taken for low COD samples because a trace of organic matter in glassware may contribute a significant error.
3. A pinch of AgSO_4 and HgSO_4 is added to sample contains chloride in higher concentration; HgSO_4 is added in the ratio of 10:1, to the chlorides. COD cannot be determined accurately if the sample contains more than 2000 mg/L of chlorides.
4. Then 30mL of H_2SO_4 is added.
5. Add 25 mL of 0.02 M $\text{K}_2\text{Cr}_2\text{O}_7$ solution.

6. Reflux at least for 2hrs on water bath. Then cooled the flasks at RT and sufficient amount of distilled water is added to make the final volume 140mL.
7. Then 2-3 drops of ferroin indicator is added and mixed thoroughly and titrate with 0.1M ferrous ammonium sulphate.
8. Run blank distilled water using same quantity of the chemicals.

Calculations:

$$\text{COD mg/L} = \frac{(A-B) \times M \times 8000}{\text{Volume of the sample}}$$

Where, A = mL ferrous ammonium sulphate used for blank, B= mL ferrous ammonium sulphate used for sample and M = Molarity of FAS. The photo-degradation efficiency for each sample was calculated from the following expression:

$$\eta = \frac{\text{COD}_0 - \text{COD}_t}{\text{COD}_0} \times 100$$

Where, η = Photo-degradation efficiency

COD_0 = COD of dye solution before irradiation

COD_t = COD of dye solution after irradiation for time t.

Determination of CO₂ [12]:

Principle:

Free CO₂ can be determined by titrating the sample using a strong alkali (such as carbonate free NaOH) to pH 8.3. At this pH all the free CO₂ is converted into bicarbonates.

Reagents:

Sodium hydroxide, 0.05 M: Prepare 1.0 M NaOH in CO₂ free distilled water (boiled) to make 1 liter of solution. Dilute 50 mL of 1.0 M NaOH to 1 liter. Standardize with HCl.

Phenolphthalein indicator solution: Dissolve 0.5 g phenolphthalein in 50 mL, 95% ethyl alcohol and 50mL distilled water.

Procedure: Take 100mL of sample in a conical flask and add few drops of phenolphthalein indicator. If the color turns pink, free CO₂ is absent. If the sample remains colored then it is titrated against 5 x 10⁻² mol dm⁻³ NaOH solution. At the end point a pink color appears.

Calculation:

$$\text{CO}_2 \text{ mg/L} = \frac{(\text{A} \times \text{M}) \text{ of NaOH}}{\text{Volume of the sample}} \times 100$$

Where, A = mL titrant for sample, and

M = Molarity of NaOH

Determination of NO₃⁻

The NO₃⁻ determination was done using UV-Vis. Spectrophotometer (Lambda -20) at MP Pollution Control Board Laboratory, Ujjain, (M. P.).

References:

1. Moghaddam A. B., Nazari T., Badraghi J. and Kazemzad M., *Int. J. Electrochem. Sci.*, 4 (2009) 247.
2. Johnson R. L., *Master of Science Thesis, Iowa State University, Ames, Iowa (2005)*.
3. Philip D., William Lawrence Bragg., *Biographical Memories of Fellows of the Royal Society*, 25 (1975) 74.
4. <https://www.iiserb.ac.in/cif/xrd>
5. Cullity B. D. and Stocks S. R., *Elements of X- ray diffraction, prentice Hall, New Jersey, 3 edition, (2001)*.
6. <https://www.iiserb.ac.in/cif/sem>
7. Griffiths P. R. and de Haseth J. A., *Fourier Transform Infrared Spectrometry*, Wiley, New York, (1986).
8. More P., Swami D., Pandey H. and Pare B., *Int. J. Chem. Sci.*: 10 (2012) 1549.
9. Pare B., Singh P. and Jonnalagadda S. B., *Indian Journal of Chemistry* 17 (2010) 391.
10. APHA, *Standard methods for examination of water and wastewater*, 6th edition (1985) 535.
11. Pare B., Singh P. and Jannalgadda S. B., *J. Sci. Ind. Res.*, 68 (2009) 724.
12. Maiti S. K., *Handbook of methods in environmental studies: water and wastewater analysis* (ABD pub. Jaipur, India), Vol.1 (2001) 50.

CHAPTER-IV

Results and Discussion

4.1: Characterization techniques for ZnO NPs catalyst

4.1.1: X-Ray Diffraction (XRD) analysis:

X-Ray diffraction has been used to analyze the phase purity and crystal structure of the nano crystalline structures. All the samples were studied in the range $20-80^\circ$ (2θ) using PANalytical Empyrean XRD for XRD pattern. Scherrer formula was used to estimate the crystalline size using R-Silicon as a standard for broadening of instrumental line. Figure 4.1 shows the XRD pattern of prepared ZnO NPs for 2θ angle between 10° to 80° .

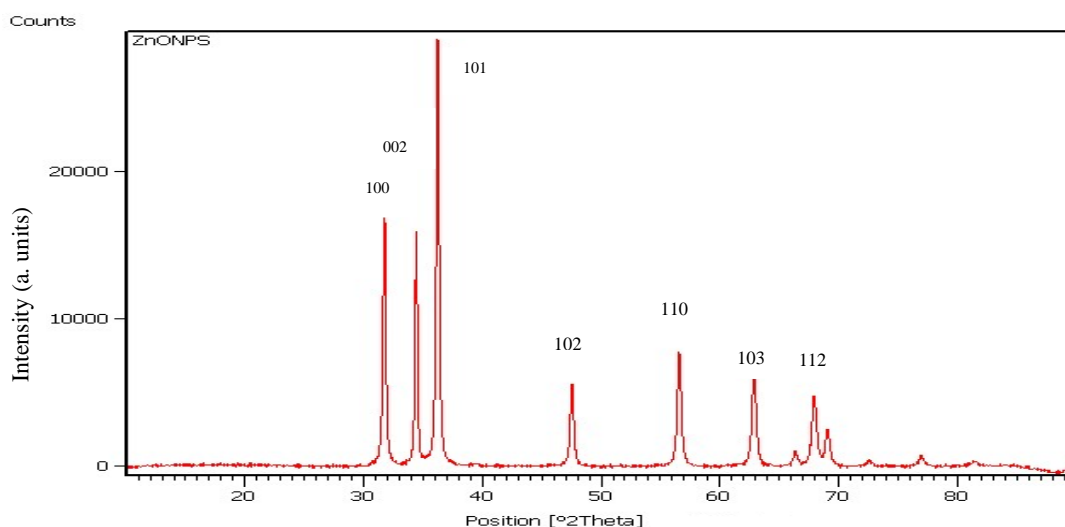


Fig. 4.1 ZnO nanoparticles: XRD pattern

As seen in the pattern of as-synthesized ZnO, the diffraction peaks are more intensive and narrower which suggested that product has a good crystalline structure. A series of characteristic peaks of ZnO NPs were detected like 31.46° (100), 34.41° (002), 36.57° (101), 47.66° (102), 56.72° (110), 62.70° (103) and 67.95° (112), which confirmed the synthesis of ZnO NPs. The diffraction peaks of sample could be readily index as wurtzite type (hexagonal structure) which matches well with the reported data (JCPDS card No. 36-1451) [1, 2]. Purity of the synthesized ZnO NPs was indicated by no extra peaks in XRD pattern. The peak (101) is dominant and higher intensity than other peaks signifying

the preferential growth of (101) orientation along c-axis for the sample. Table 4.1 shows that the calculated d-values and lattice parameters [$a=b=3.256\text{ \AA}$ and $c=5.220\text{ \AA}$ (calculated values) and $a=b=3.250\text{ \AA}$ and 5.207 \AA (JCPDS 36-1451)] which are also in good agreement with those taken from JCPDS card file data for ZnO powder. The calculated average crystallite size of ZnO NPs is 30nm by using Debye-Scherer formula [3, 4].

4.1.2: High Resolution Field Emission Scanning Electron Microscope (HR FESEM)

Analysis: The shape and size of the synthesized ZnO nanostructured were analyzed by SEM. As shown in Figure 4.2, which clearly indicated that the particles are cylindrical like shape and average nano particles size is the range 20-30nm diameter and about 150nm length. These size matches with that of XRD data obtained and calculated by Debye-Scherer formula. [5-7]

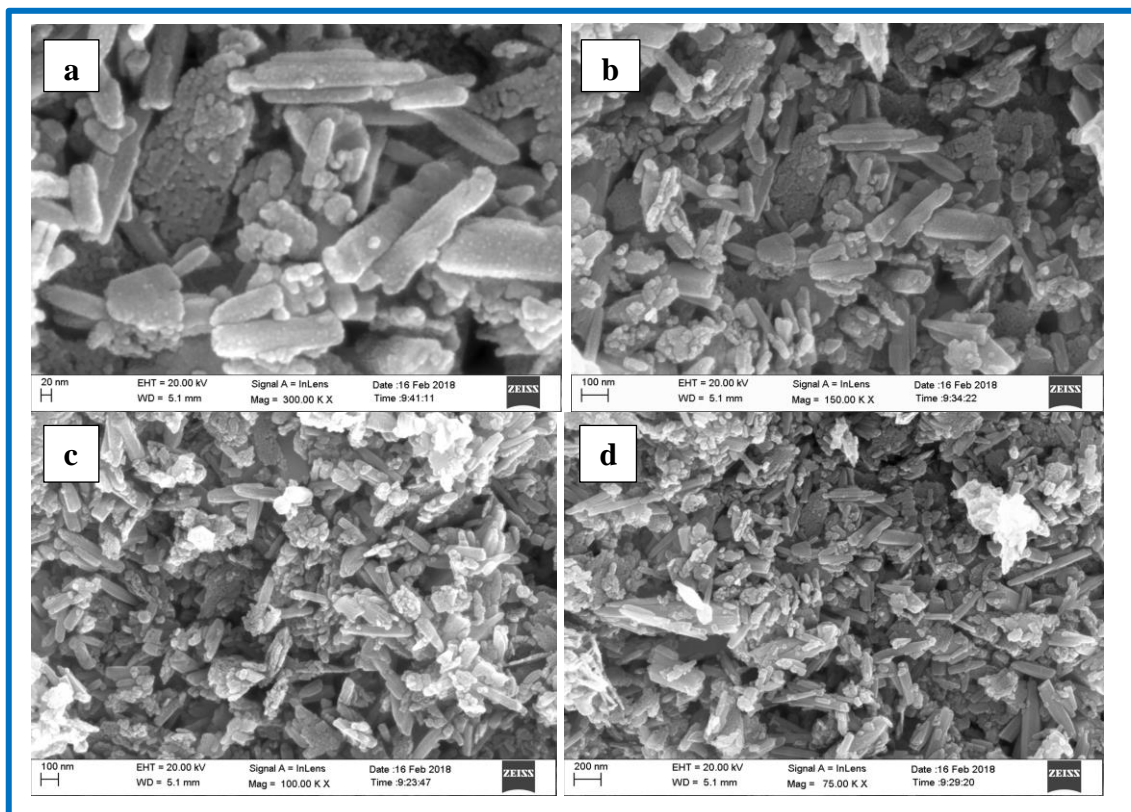


Fig. 4.2: HRFESEM image of ZnO NPs

4.1.3: Fourier Transform Infrared Spectroscopy (FT-IR):

The presence of functional groups of the compound was identified by FT-IR study [8]. The formation of ZnO wurtzite structures in the synthesis ZnO NPs samples was supported by FT-IR spectrum (Fig. 4.3) and absorption peak at 531.30 cm^{-1} could be attributed to the ZnO stretching modes and no other peaks observed indicated the absence of impurities [9,10].

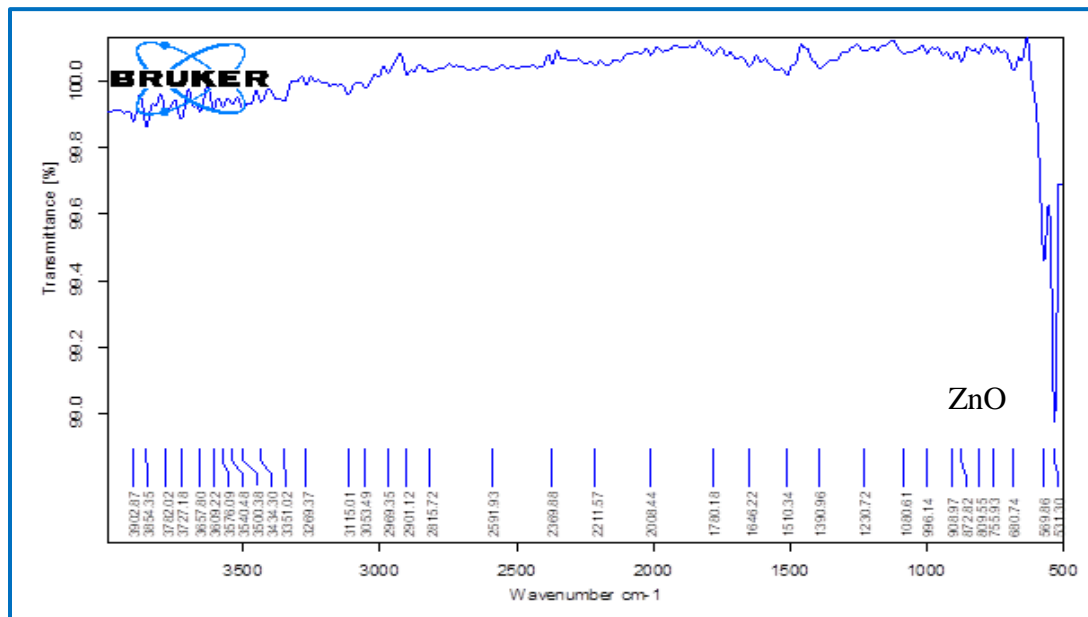
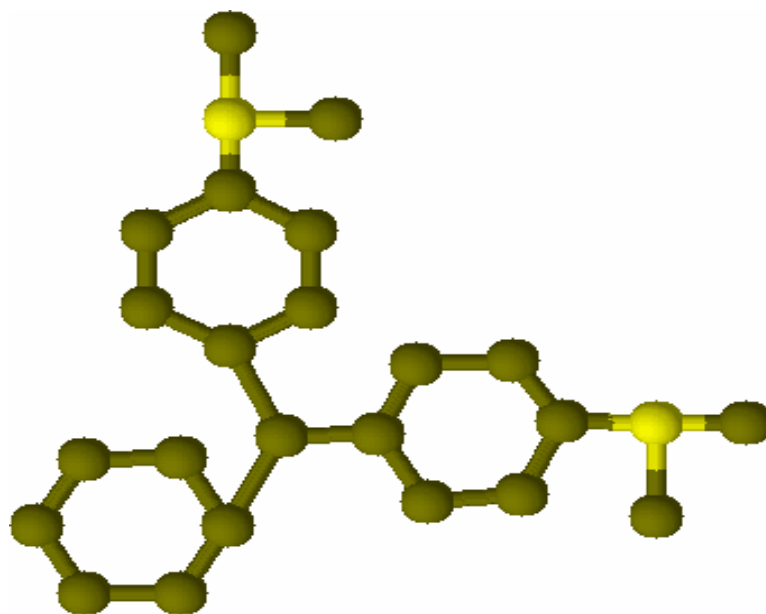


Fig. 4.3: FT-IR spectra of ZnO

Malachite Green



Malachite green is an organic compound that is used as a dyestuff. It is traditionally used as a dye for materials such as silk, leather, and paper. Malachite green also is used as a direct dye for silk, wool, jute, and leather and to dye cotton that has been mordant with tannin.

4.2: Effect of various experimental parameters on the degradation rate of Malachite Green (MG) dye

4.2.1: Photo-catalytic degradation of Malachite Green (MG):

On the surface of catalyst classical Langmuir–Hinshelwood expression was followed by the photo-catalytic degradation rate of Malachite Green dye and followed most often Langmuir sorption isotherm for the sorption of the dye to the catalyst surface. This theory is usually used kinetic model for unfolding photo-catalytic behavior. For treatment of heterogeneous surface reactions degradation rate is explained by pseudo first-order kinetics in Langmuir–Hinshelwood [11-14]. Such kinetics is streamlined in terms of modified model to accommodate reactions taking place at solid-liquid interface as

$$r = \frac{-dc}{dt} = \frac{k_r KC}{(1+KC)} \quad (1)$$

Where, r = rate of dye disappearance and C = variable dye concentration at time t . K = equilibrium constant for adsorption of MG dye on photo-catalyst and k_r = limiting reaction rate at maximum coverage in operational conditions. The integrated form can be written as

$$t = \ln\left(\frac{C_0}{C}\right) + \frac{1}{Kk_r} \frac{C_0 - C}{k_r} \quad (2)$$

Where t = time required for the initial concentration of dye C_0 to C . At low dye concentration in equation 2, value of C_0 is very less and hence can be neglected.

$$\ln\left(\frac{C_0}{C}\right) = k_r Kt = kt \quad (3)$$

Where k = apparent rate constant of degradation. The Half-life time ($t_{1/2}$) for the photo-catalytic degradation of Malachite Green dye on the ZnO NPs surface can be calculated by using following Eq. (4)

$$t_{1/2} = \frac{0.693}{k} \quad (4)$$

The Malachite Green dye degradation results are reported here for three conditions: (1) MG dye + ZnO NPs + visible light (2) MG dye + visible light only and (3) MG dye + ZnO nanoparticles only (dark) were shown in figure 4.4 (a). It was observed carefully that maximum degradation occurred in the first condition, while in dark and during photolysis, no significant changes in the absorbance values were observed. Therefore, in second and third condition, degradation process was not observed. Absorption spectrum Changes were recorded at 620nm wavelength.

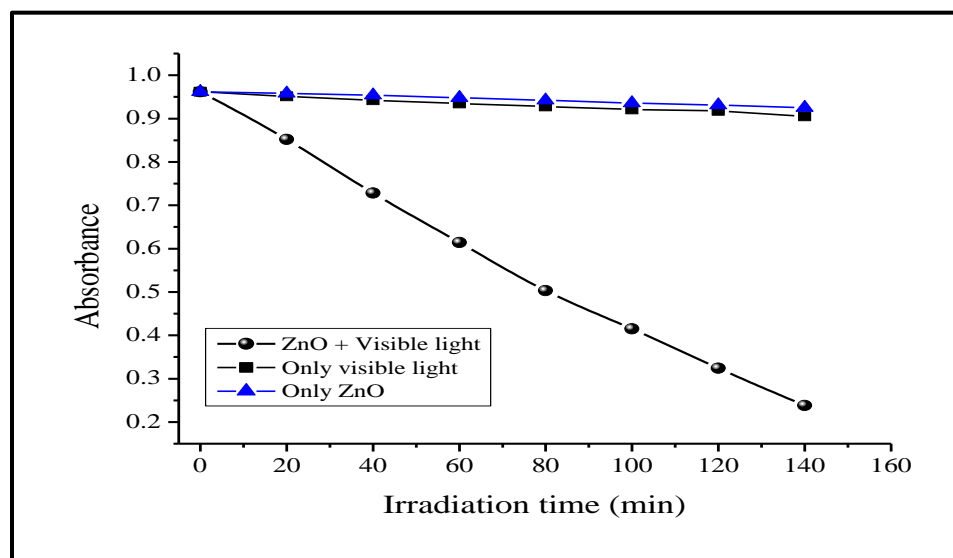


Fig. 4.4 (a) Degradation of Malachite Green: [MG] = $4.0 \times 10^{-5} \text{ mol dm}^{-3}$,

ZnO NPs = 60 mg/100mL, pH = 8.0, Light intensity = $30 \times 10^3 \text{ Lux}$.

Plotting the semi-logarithmic graph of concentration versus irradiation time (min) of MG dye in presence of ZnO NPs yielded a linear relationship as shown in Figure 4.4 (b). Therefore, reaction dye of degradation by ZnO nanoparticles is pseudo-1st order reaction kinetics and observes rate constant for MG dye is $4.05 \times 10^{-4} \text{ s}^{-1}$, with regression coefficient of 0.978. The rate constant is the slope of the straight line. In all cases

R^2 (correlation constant for the fitted line) values were close to 0.99 which confirmed pseudo 1st-order kinetics for the decolorization of MG dye in this method.

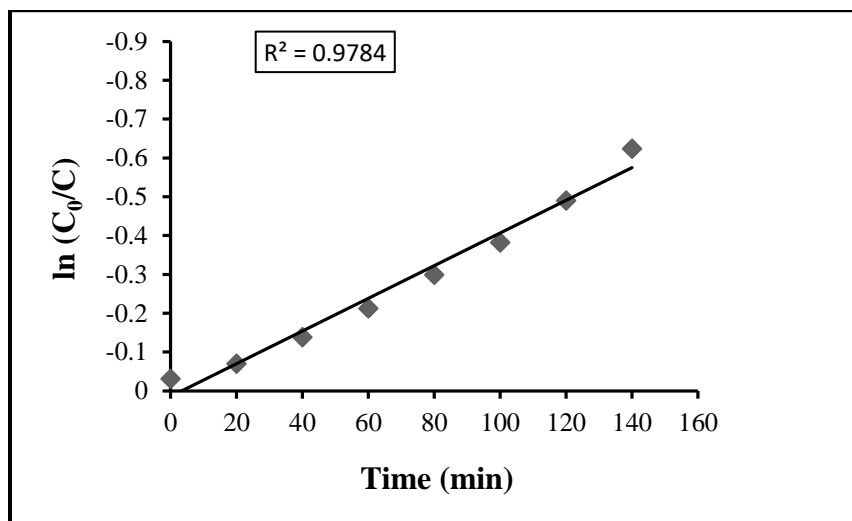


Fig. 4.4 (b): Pseudo first order kinetics: $[MG] = 4.0 \times 10^{-5} \text{ mol dm}^{-3}$,
ZnO NPs = 60 mg/100mL, pH = 8.0, Light intensity = $30 \times 10^3 \text{ Lux}$.

4.2.2: Effect of change in pH:

Solution pH played an important role in the photo-catalytic reactions and hence we studied the degradation of MG dye between pH 4 to 11. The degradation rate constant of MG dye and effect of pH variation are shown in Table 4.1 and figure 4.5. The rate of degradation of MG dye was found to be optimum at pH 8.0. But further increase in pH, decrease of photo-degradation rate was observed. We mentioned the reason for this optimum pH i.e. 8.0 because at high pH range 'OH radicals bound on the active site of the catalyst and at lower pH value i.e. pH~4, ZnO forms salts and formed zincates. If the pH value is too high, ZnO gets converted into zincates [15, 16].



Photo-catalytic activity of ZnO nanoparticles photo-catalyst was investigated by measuring the Malachite Green dye in aqueous medium under visible light. Since, on

surface of photo catalyst, photo-catalytic degradation of dye takes place hence as we decreases the particle size of ZnO increases and photo-catalytic degradation activity against dye increases [17-19].

Table 4.1: Effect of change in pH: [MG] = 4.0×10^{-5} mol dm⁻³, ZnO NPs = 60 mg/100mL, Light intensity = 30×10^3 Lux.

pH	$k \times 10^{-4} \text{ s}^{-1}$	$t_{1/2} \times 10^3 \text{ s}$
4	0.99	7.00
5	1.63	4.25
6	2.11	3.28
7	3.15	2.20
8	4.05	1.71
9	3.22	2.15
10	2.37	2.92
11	1.58	4.38

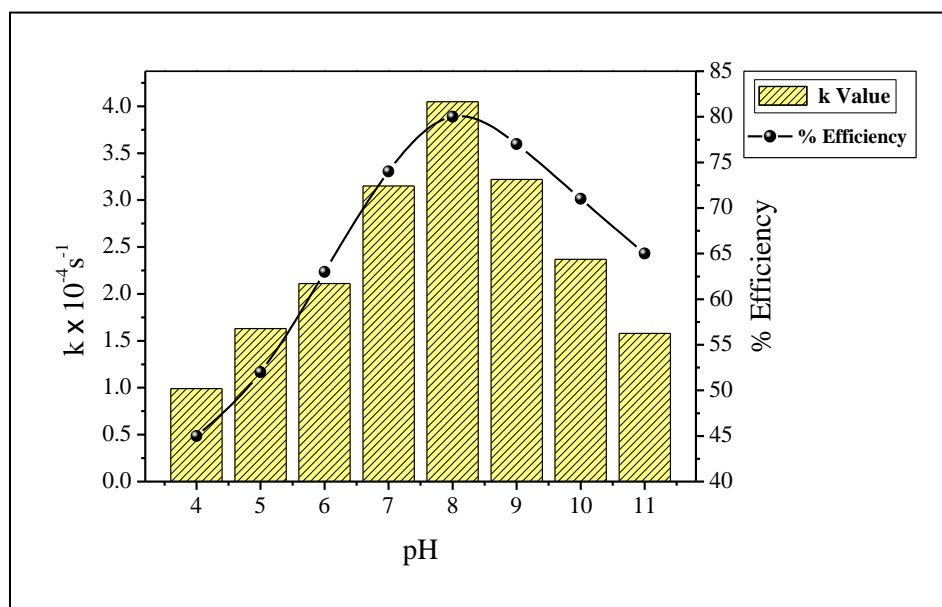


Fig. 4.5: Effect of change in pH on photo-catalytic degradation of MG

4.2.3: Effect of change in catalyst amount:

The effect of ZnO NPs catalyst concentration on the photo-catalytic degradation is one of the main aspects of the study. A significant increase in the photo-catalytic degradation rate was observed up to an optimal catalyst amount i.e. degradation rate constant increased from $0.94 \times 10^{-4} \text{s}^{-1}$ to $4.05 \times 10^{-4} \text{s}^{-1}$ with increase in catalyst amount from 20mg/100mL to 60mg/100mL because with the increased in catalyst amount, total active surface area increased. Therefore, the enhancement of the active sites of catalyst surface which also enhanced number of hydroxide and superoxide radicals on the surface. The degradation rate constant increased can be accredited to the high penetration of visible light into the suspension up to optimum catalyst amount. The optimal amount of catalyst was found to be 60mg/100mL to 100mg/100mL below the experimental conditions detailed in Table 4.2 and Figure 4.6 [20-22].

Hence, excess catalyst should be avoided to ensure total absorption of visible light photons for efficient photo-degradation of dye. This has been totally in agreement with investigated for heterogeneous system [23]. Since the most effective Mineralization of Malachite Green dye was experimental with 60mg/100mL of ZnO NPs, the other experiments were performed in this amount of ZnO NPs.

Table 4.2: Effect of change in catalyst amount: [MG] = 4.0×10^{-5} mol dm⁻³, pH = 8.0,
Light intensity = 30×10^3 Lux.

ZnO mg/100mL	$k \times 10^{-4} \text{ s}^{-1}$	$t_{1/2} \times 10^3 \text{ s}$
20	0.94	7.37
30	1.54	4.50
40	2.18	3.17
50	3.29	2.10
60	4.05	1.71
70	3.15	2.20
80	2.14	3.23
90	1.24	5.58
100	0.78	8.88

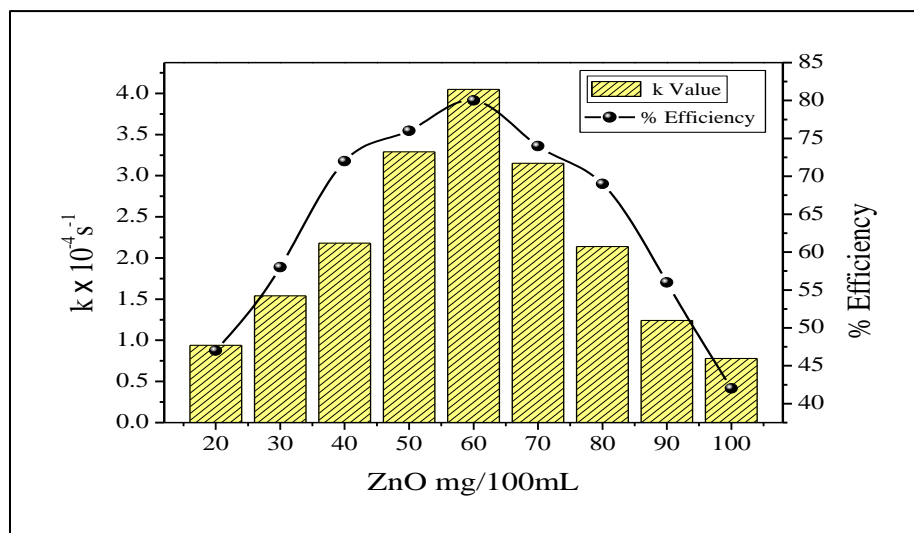


Fig. 4.6: Effect of change in catalyst amount on photo-catalytic degradation of MG

4.2.4: Effect of change in dye concentration:

We studied the dependence of the photo-catalytic rate of reaction on the dye concentration for systematic and application point of view. The possibility of $\cdot\text{OH}$

radical's formation on the semiconductor surface has been related to the degradation rate and to the probability of $\cdot\text{OH}$ radicals reacting with dye molecules [24, 25]. The initial Malachite Green dye concentration has been varied from $1.0 \times 10^{-5} \text{ mol dm}^{-3}$ to $7.0 \times 10^{-5} \text{ mol dm}^{-3}$. The results are shown in Table 4.3 and Figure 4.7. The rate constant of degradation increased $1.08 \times 10^{-4} \text{ s}^{-1}$ to $4.05 \times 10^{-4} \text{ s}^{-1}$ with increase in Malachite Green dye concentration from $1.0 \times 10^{-5} \text{ mol dm}^{-3}$ to $4.0 \times 10^{-5} \text{ mol dm}^{-3}$. Thereafter, rate constant of degradation decreased from $4.05 \times 10^{-4} \text{ s}^{-1}$ to $1.38 \times 10^{-4} \text{ s}^{-1}$ with increased dye solution concentration $4.0 \times 10^{-5} \text{ mol dm}^{-3}$ to $7.0 \times 10^{-5} \text{ mol dm}^{-3}$. The degradation rate constant is optimum at $4.0 \times 10^{-5} \text{ mol dm}^{-3}$ of Malachite Green dye concentration.

It is outstanding to detail that more dye molecules are presented in photoactive volume for the photo-degradation procedure. But, it has been noted that the degradation rate constant decreased with further increase in Malachite Green concentration above optimum value. This decrement is might be due to that the dye itself will start acting as filter for occurrence irradiation and reducing the photoactive volume [26]. At low concentration the reverse effect has been seeing whereas the irradiation time and catalyst amount has been taken as constant. Therefore on the surface of ZnO the relative numbers of $\text{O}_2\cdot$ and $\text{OH}\cdot$ radicals formed were also constant. Unnecessary adsorption of dye molecule on the catalyst surface mired the competitive adsorption of OH^- ions and depressed the rate of hydroxyl radical formation. Therefore, above optimal concentration with increment in dye concentration the rate of degradation decreased [27-29].

Table 4.3: Effect of change in dye concentration: ZnO NPs = 60 mg/100mL, pH = 8.0,
Light intensity = 30×10^3 Lux.

[MG] $\times 10^{-5}$ mol dm ⁻³	k $\times 10^{-4}$ s ⁻¹	t _{1/2} $\times 10^3$ s
1.0	1.08	6.41
2.0	2.04	3.39
3.0	3.13	2.21
4.0	4.05	1.71
5.0	3.24	2.13
6.0	2.21	3.13
7.0	1.38	5.02

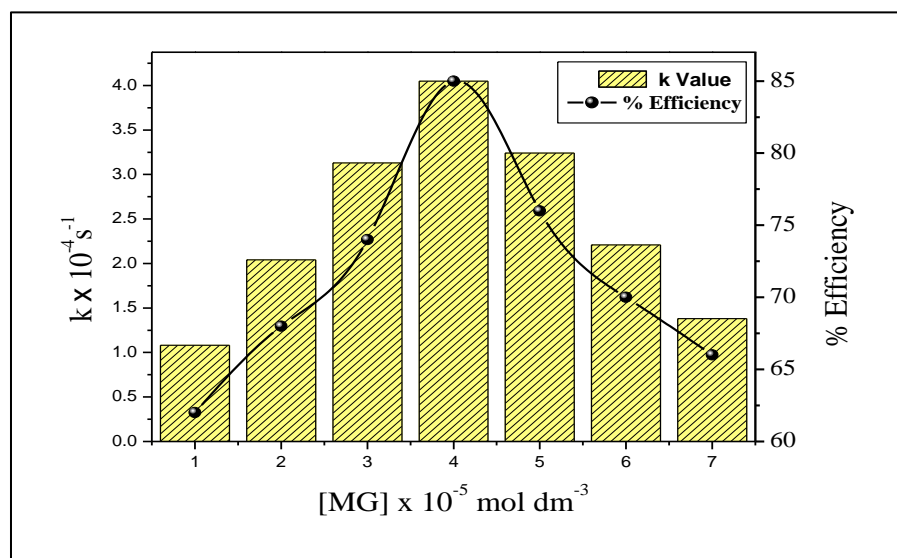
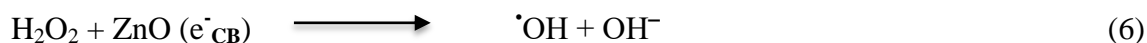


Fig. 4.7: Effect of change in dye concentration on photo-catalytic degradation of MG

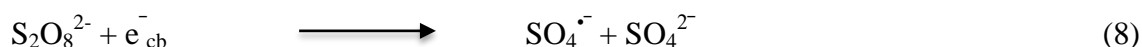
4.2.5: Effect of change in oxidant's concentration:

The degradation rate has been considered by the recombination of photo-generated electron-hole pairs. This can be overcome by the addition of the electron acceptor to the reaction. It is evident from relevant reports that oxidizing agents such as H₂O₂ and

$K_2S_2O_8$ as electron acceptors have a great deal of influence on the photo-catalytic degradation of dyes. The photo-catalytic degradation of MG dye has been examined by change in H_2O_2 and $K_2S_2O_8$ concentration. The rate constant of degradation of Malachite Green dye increased from $4.46 \times 10^{-4} s^{-1}$ to $6.42 \times 10^{-4} s^{-1}$ with increasing H_2O_2 concentrations from $2.0 \times 10^{-6} mol dm^{-3}$ to $8 \times 10^{-6} mol dm^{-3}$ and the rate constant of degradation of Malachite Green dye increased from $4.32 \times 10^{-4} s^{-1}$ to $6.03 \times 10^{-4} s^{-1}$ with increasing $K_2S_2O_8$ concentrations from $2.0 \times 10^{-6} mol dm^{-3}$ to $8 \times 10^{-6} mol dm^{-3}$ respectively and reached to an optimum but above this concentration range, the increased H_2O_2 and $K_2S_2O_8$ concentration retarded the rate of degradation as shown in Table 4.4 and Figure 4.8. At their respective low concentrations H_2O_2 and $K_2S_2O_8$ accelerate the reaction rate by producing an extremely strong and non-selective oxidant hydroxyl radical ($E^0 = +3.06V$). These hydroxyl radicals got generated by H_2O_2 and $K_2S_2O_8$ on account of scavenging the electrons from the conduction band of the photo-catalyst and this inhibited the process of electron-hole recombination [30-33]. H_2O_2 may also split photo-catalytically to produce hydroxyl radicals directly by the absorption of visible light by the following reactions:



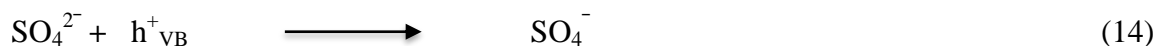
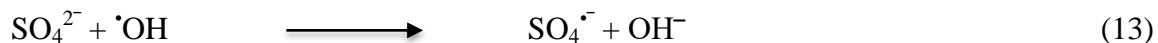
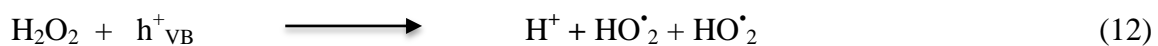
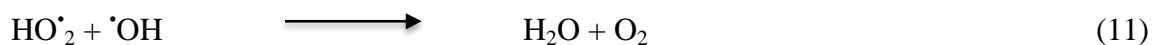
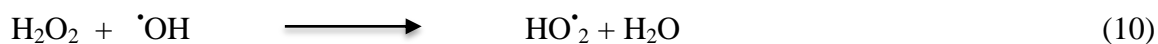
The $S_2O_8^{2-}$ anions generate strong oxidizing $SO_4^{\cdot-}$ radicals anion after trapping the photo-generated conduction band electrons of ZnO nanoparticles as shown in the following reaction:



The generated sulfate radical anions ($SO_4^{\cdot-}$) participate in reaction with the solvent, according to the following reaction:



Contrary to this behavior, H_2O_2 and $\text{K}_2\text{S}_2\text{O}_8$ start behaving as scavenger for $\cdot\text{OH}$ radical and hole at an excessive concentration. The photo-catalytic degradation of Malachite Green dye will be inhibited in the condition of excess of H_2O_2 and $\text{K}_2\text{S}_2\text{O}_8$ as these are strong oxidants for organic pollutants. Furthermore, H_2O_2 and SO_4^{2-} can be adsorbed onto ZnO NPs deactivating a section of photo-catalyst and consequently decrease its photo-catalytic activity [34, 35].



Subsequently, photo-degradation rate of Malachite Green dye can be accelerated by proper addition of H_2O_2 and $\text{K}_2\text{S}_2\text{O}_8$. However, in order to keep the efficiency of the added H_2O_2 and $\text{K}_2\text{S}_2\text{O}_8$, it was necessary to choose the proper dosage of H_2O_2 and $\text{K}_2\text{S}_2\text{O}_8$, according to the dyes concentration.

Table 4.4: Effect of change in H₂O₂ and K₂S₂O₈: [MG] = 4.0 × 10⁻⁵ mol dm⁻³, ZnO NPs = 60 mg/100mL, pH = 8.0, Light intensity = 30 × 10³ Lux.

[Oxidant] × 10 ⁻⁶ mol dm ⁻³	[H ₂ O ₂]		[K ₂ S ₂ O ₈]	
	k × 10 ⁻⁴ s ⁻¹	t _{1/2} × 10 ³ s	k × 10 ⁻⁴ s ⁻¹	t _{1/2} × 10 ³ s
0.0	4.05	1.71	4.05	1.71
2.0	4.46	1.55	4.32	1.60
4.0	4.76	1.45	4.55	1.52
6.0	5.52	1.25	5.11	1.35
8.0	6.42	1.07	6.03	1.14
10.0	5.64	1.22	5.57	1.24
12.0	5.06	1.36	5.02	1.38
14.0	4.37	1.58	4.39	1.57
16.0	3.43	2.02	4.09	1.69

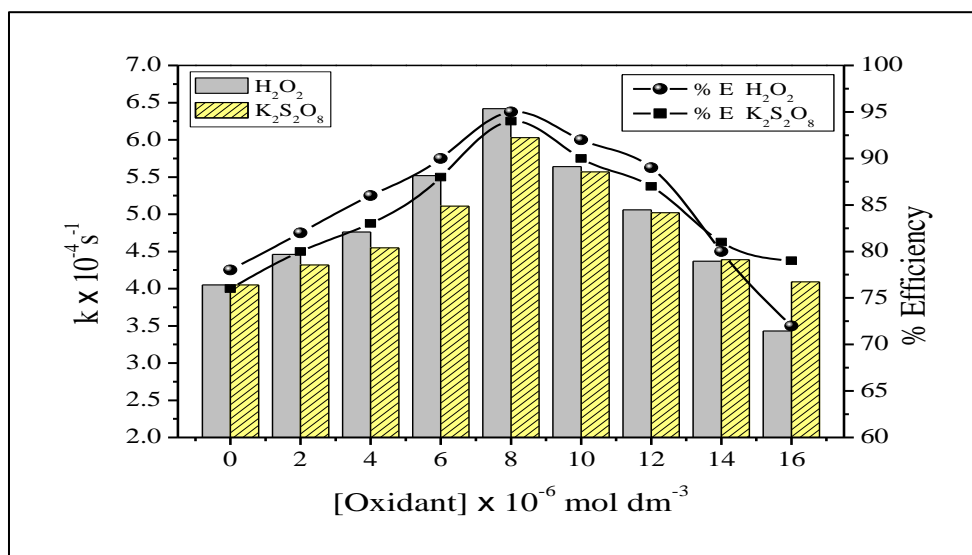
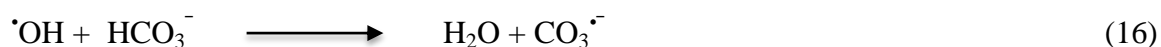
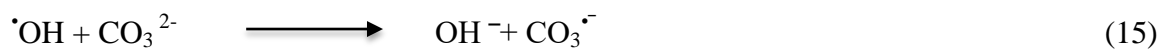


Fig. 4.8: Effect of change in oxidants on photo-catalytic degradation of MG

4.2.6: Effect of change in salts concentration:

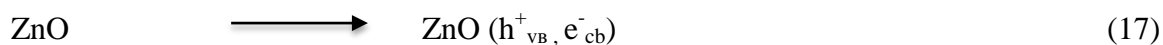
The Na₂CO₃ is mainly used in the dyeing bath in order to adjust the pH of the bath as it plays an important role in fixing of dye on the fabrics and in the fastness of color.

Therefore the wastewater from the dyeing process will contain considerable amount of carbonate ion [36]. With an increase in the amount of carbonate ion from $2.0 \times 10^{-5} \text{ mol dm}^{-3}$ to $12.0 \times 10^{-5} \text{ mol dm}^{-3}$ resulted into reduction of rate constant from $3.47 \times 10^{-4} \text{ s}^{-1}$ to $0.66 \times 10^{-4} \text{ s}^{-1}$. The degradation of dye inhibition might be due to the hydroxyl scavenging property of carbonate ions, which can be accounted from the following equation.



The $\cdot\text{OH}$ radical which is a primary oxidant for the photo-catalytic degradation of dye found to decrease slowly with an increase in carbonate ions and degradation of the dye significantly decreased [37].

NaCl generally comes out in the effluent along with wastewater and therefore we studied the photo-catalytic degradation rate in presence of Cl^- ions by varying Cl^- concentration from $2.0 \times 10^{-5} \text{ mol dm}^{-3}$ to $12 \times 10^{-5} \text{ mol dm}^{-3}$. It brings about the reduction of rate constant from $3.66 \times 10^{-4} \text{ s}^{-1}$ to $1.08 \times 10^{-4} \text{ s}^{-1}$. Hole scavenging properties of chloride ion is probably the reason behind the decrease in the degradation. [38]



The dependency of reaction rate constant on the concentration of Na_2CO_3 and NaCl is results are shown in Table 4.5 and Figure 4.9.

Table 4.5: Effect of change in Na₂CO₃ and NaCl: [MG] = 4.0 × 10⁻⁵ mol dm⁻³, ZnO NPs = 60 mg/100mL, pH = 8.0, Light intensity = 30 × 10³ Lux.

[Salt] × 10 ⁻⁵ mol dm ⁻³	[Na ₂ CO ₃]		[NaCl]	
	k × 10 ⁻⁴ s ⁻¹	t _{1/2} × 10 ³ s	k × 10 ⁻⁴ s ⁻¹	t _{1/2} × 10 ³ s
0.0	4.05	1.71	4.05	1.71
2.0	3.47	1.99	3.66	1.89
4.0	2.85	2.43	3.15	2.20
6.0	2.25	3.08	2.71	2.55
8.0	1.65	4.20	2.16	3.20
10.0	1.12	6.18	1.51	4.58
12.0	0.66	10.50	1.08	6.41

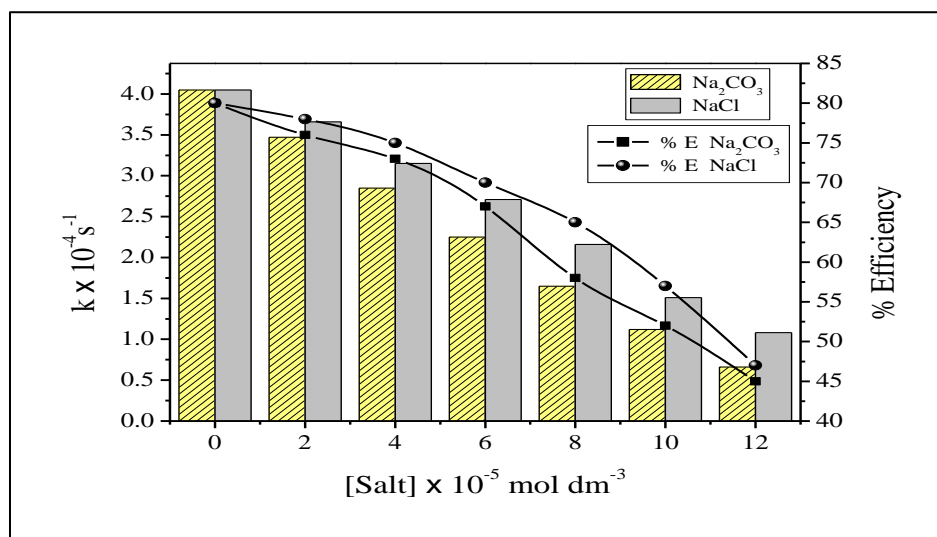
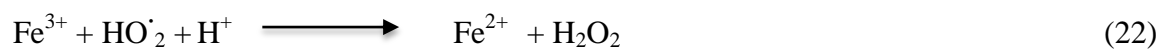


Fig. 4.9: Effect of change in salts on photo-catalytic degradation of MG

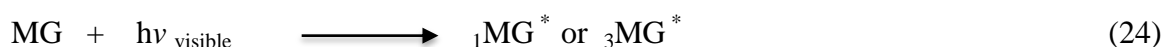
4.2.7: Effect of change in FeCl₃ concentration:

An ion Fe³⁺ could be used as sensitizers during photo-catalytic degradation of dye. In present study, effect of FeCl₃ on the photo-catalytic degradation of Malachite Green has been investigated by changing the concentration from 2.0 × 10⁻⁵ mol dm⁻³ to 14.0 × 10⁻⁵ mol dm⁻³. The decolorization rate constant values increased from 4.35 × 10⁻⁴ s⁻¹ to

$6.05 \times 10^{-4} \text{ s}^{-1}$ with the increase in amount of FeCl_3 from $2.0 \times 10^{-5} \text{ mol dm}^{-3}$ to $8.0 \times 10^{-5} \text{ mol dm}^{-3}$. Thereafter, decolorization rate constant decreased to $3.03 \times 10^{-4} \text{ s}^{-1}$ on further increase in amount of FeCl_3 up to $14.0 \times 10^{-5} \text{ mol dm}^{-3}$. The results are shown in Table 4.6 and Figure 4.10. In fact the increase in ferric ions concentration in the reaction mixture resulted into the increase of Fe^{2+} ions concentration, which is accompanied by enhanced production of $\cdot\text{OH}$ radicals, consequently growing the rate of degradation of FeCl_3 prevents the degradation rate by hostile $\cdot\text{OH}$ radical production. [39-41]



The photo-activation of surface adsorbed complex ion ($\text{Fe}^{3+}\text{OH}^-$) results in the formation of $\text{Fe}^{2+}\text{OH}\cdot$ specie which injects electrons to the conduction band of ZnO as shown in [Eq. 25-26]. When FeCl_3 is applied, rate of decolorization is reasonable due to rapid scavenging of conduction band electrons [42, 43] [Eq. (26)].



In the presence higher concentration of FeCl_3 , there is excessive surface adsorption of anionic dye on the surfaces of catalyst [44]. This reduced the total photoactive area of ZnO NPs catalyst and lowers the reaction rate [45].

Table 4.6: Effect of change in FeCl₃ concentration: [MG] = 4.0 × 10⁻⁵ mol dm⁻³, ZnO NPs = 60 mg/100mL, pH = 8.0, Light intensity = 30 × 10³ Lux.

FeCl ₃ × 10 ⁻⁵ mol dm ⁻³	k × 10 ⁻⁴ s ⁻¹	t _{1/2} × 10 ³ s
0.0	4.05	1.71
2.0	4.35	1.59
4.0	4.69	1.47
6.0	5.22	1.32
8.0	6.05	1.14
10.0	5.57	1.24
12.0	4.42	1.56
14.0	3.03	2.28

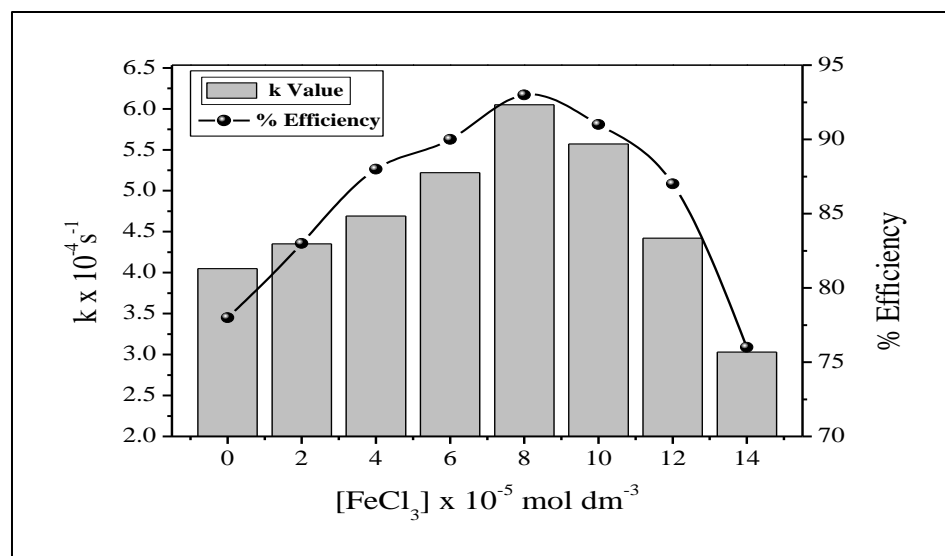


Fig. 4.10: Effect of change in FeCl₃ on photo-catalytic degradation of MG

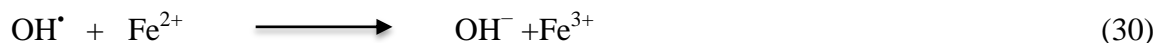
4.2.8: Effect of change in Fenton’s reagent concentration:

Fenton’s reagent, a mixture of ferrous iron and H₂O₂ (oxidizing agent), has been known as a powerful oxidant for organic pollutants [46]. Among advanced oxidation processes,

catalytic oxidation using Fenton and similar reagent is a striking procedure for the effective dye degradation due to low cost and lack of poisonousness [47-49].



OH^\bullet radicals may be scavenged by reaction with another Fe^{2+} :



Efficiency of $\text{Fe}^{3+}/\text{H}_2\text{O}_2$ method has been investigated for degradation of MG in presence of ZnO NPs and visible light. The degradation rate constant has a value of $4.51 \times 10^{-4} \text{ s}^{-1}$ on the addition of ($\text{Fe}^{3+}:\text{H}_2\text{O}_2$) in molar ratio (3:1). In the presence of ($\text{Fe}^{3+}:\text{H}_2\text{O}_2$) in molar ratio (1.4:1), rate constant has been found $5.38 \times 10^{-4} \text{ s}^{-1}$. The results are shown in Table 4.7 and Figure 4.11. Upon irradiation of $\text{Fe}^{3+}/\text{H}_2\text{O}_2/\text{ZnO}/\text{MG}$ method in the presence of visible light, formation of OH^\bullet radicals increases relating a very complex mechanism. Visible light radiations are absorbed by dye and excited to high-energy state. These excited dye molecules reduced the ferric to ferrous ion complex [50]. The reduced ferrous ions react with H_2O_2 to decompose and produce OH^\bullet [Eq. (34)]. OH^\bullet radicals also decompose H_2O_2 to HO_2^\bullet .

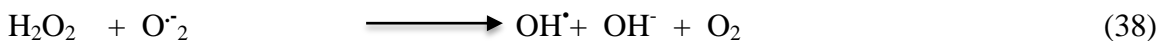
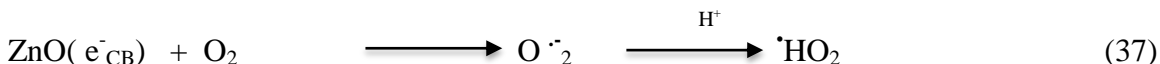
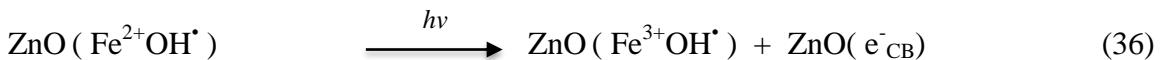
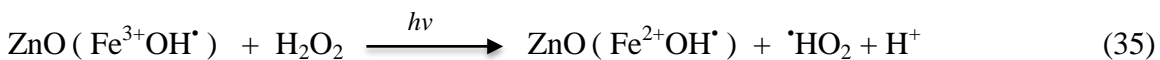
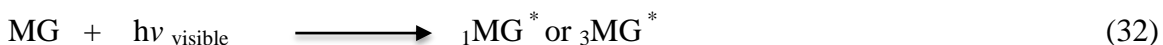




Table 4.7: Effect of change in $\text{Fe}^{3+}/\text{H}_2\text{O}_2$: [Malachite Green] = $4.0 \times 10^{-5} \text{ mol dm}^{-3}$, ZnO NPs = 60 mg/100mL, pH = 8.0, Light intensity = $30 \times 10^3 \text{ Lux}$. OH^\bullet

$\text{Fe}^{3+} : \text{H}_2\text{O}_2$	Without ZnO		With ZnO	
	$k \times 10^{-4} \text{ s}^{-1}$	$t_{1/2} \times 10^3 \text{ s}$	$k \times 10^{-4} \text{ s}^{-1}$	$t_{1/2} \times 10^3 \text{ s}$
3:1	0.93	7.45	4.51	1.53
1.4:1	1.28	5.41	6.93	1.00
1:1.4	1.68	4.12	5.38	1.28
1:3	2.04	3.39	4.16	1.66
11:1	2.32	2.98	3.01	2.30

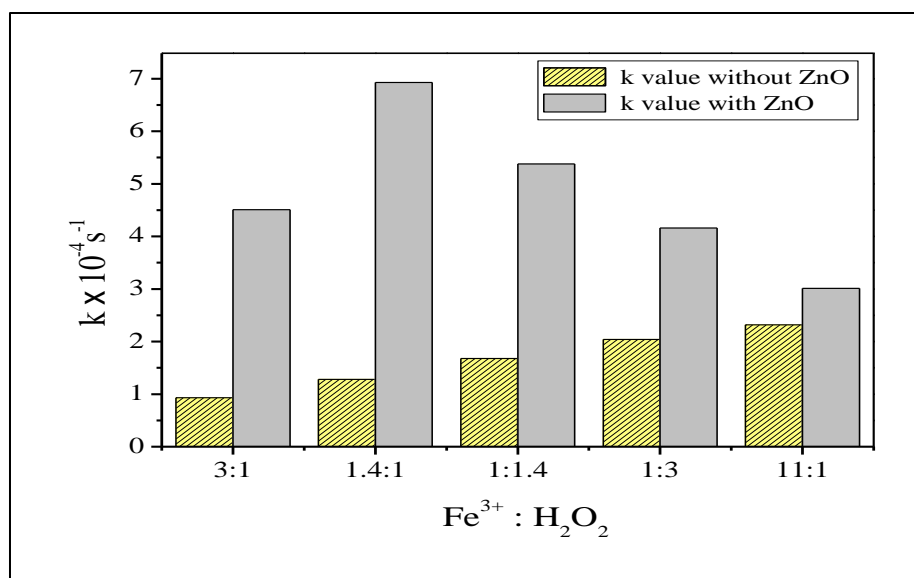


Fig. 4.11: Effect of change in Fenton's reagent on photo-catalytic degradation of MG

4.2.9: Effect of change in light intensity:

The effect of light intensity on the degradation rate has been studied at constant MG dye solution concentration $4.0 \times 10^{-5} \text{ mol dm}^{-3}$, ZnO NPs catalyst amount 60 mg/100mL and

pH 8.0. The degradation rate constant increases from $3.75 \times 10^{-4} \text{ s}^{-1}$ to $7.48 \times 10^{-4} \text{ s}^{-1}$ on increasing light intensity from $20 \times 10^3 \text{ Lux}$ to $60 \times 10^3 \text{ Lux}$, because at higher intensity competition might be in electron-hole separation with electron-hole recombination and resulted in high reaction rate [51, 52]. Results are shown in Table 4.8 and Figure 4.12.

Table 4.8: Effect of change in light intensity: $[\text{MG}] = 4.0 \times 10^{-5} \text{ mol dm}^{-3}$,
ZnO NPs = 60 mg/100mL, pH = 8.0.

Light intensity $\times 10^3 \text{ Lux}$	$k \times 10^{-4} \text{ s}^{-1}$	$t_{1/2} \times 10^3 \text{ s}$
20	3.75	1.84
30	4.05	1.71
40	5.36	1.29
50	6.88	1.00
60	7.48	0.92

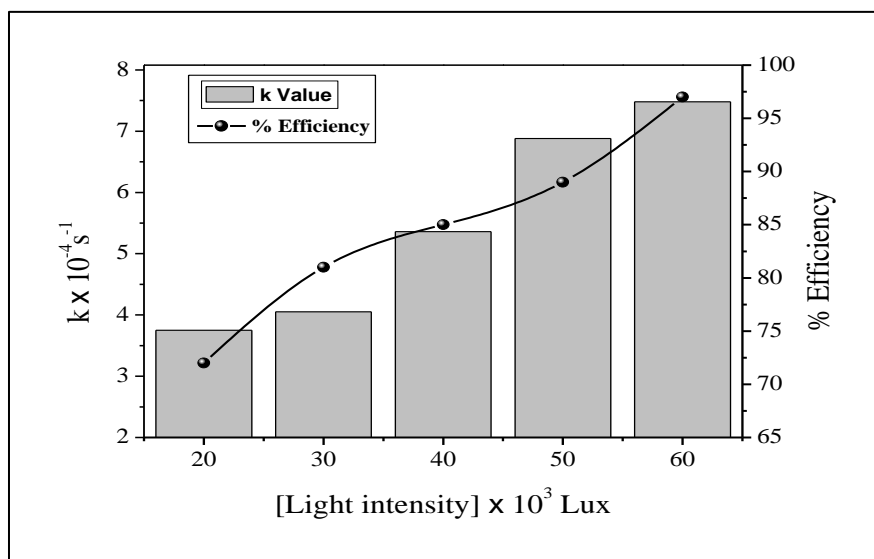
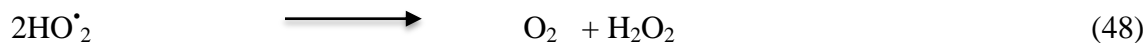
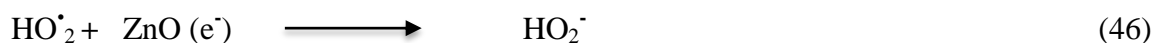
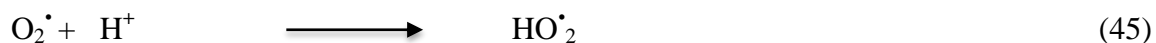
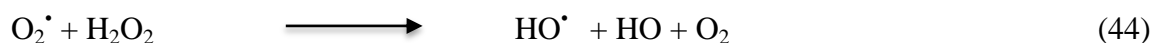
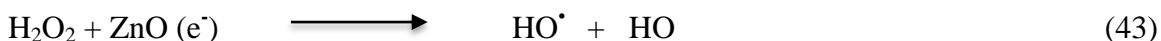


Fig. 4.12: Effect of change in light intensity on photo-catalytic degradation of MG

4.2.10: Effect of bubbling of N₂ and O₂ purging:

In the present study pure nitrogen and oxygen were purged into the photo-reactor in order to understand their effect on the photo-catalytic degradation of dye i.e. Malachite Green. The results are shown in Figure 4.13. These observations confirm the proposed assumption that dissolved oxygen as a precursor of main oxidant. The role of DO is to trap the photo-generated electrons to produce O₂^{•-} radicals, which particles in photo-catalytic process to accelerate the MG photo-degradation. The oxygen is adsorbed on the surface of the ZnO NPs and the surface redox reactions initiated by photo-generated electrons and generating superoxide anion radical. Dye degradation is started by superoxide anion radical photo-catalytically. Although, the conduction band (CB) electrons were blocked in nitrogen medium and the formation of superoxide anion radical is also prevented. Hence suppression in the rate of reaction is observed [53, 54].



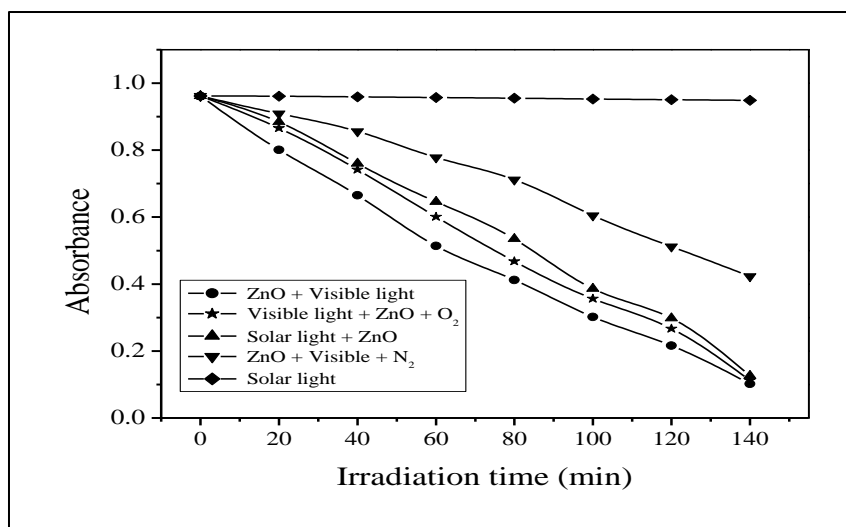


Fig. 4.13: Decolorization of MG under various photo-catalytic systems:
[MG] = 4.0×10^{-5} mol dm⁻³, ZnO NPs = 60 mg/100mL, pH = 8.0,
Light intensity = 30×10^3 Lux.

4.2.11: Comparison of solar and visible light:

The efficiency of solar and visible light on photo-catalytic degradation of dye was comparatively studied. The degradation efficiency of Malachite Green dye with visible light was found to be more efficient than that of solar light. Figure 4.13 shows the comparisons of color removal efficiency of Malachite Green with two light sources under different conditions. It was noticed that if same experiments were carried out in the absence of ZnO, then no absorbance loss of dye was found [55, 56].

4.2.12: Effect of other photo-catalysts:

The photo-catalyst on illuminating with light having energy equal to or more than band gap energy, a heterogeneous photo-catalyst reaction occurs on surface of semiconducting materials [57]. We have investigated the relative efficiencies of other photo-catalysts as well Table 4.9 and Figure 4.14. The order of photo-activity followed the order: ZnO NPs > ZnO > BiOCl > TiO₂ > BaCrO₄ on photo-catalytic degradation have been studied at

same condition. It has already been found that catalysts such as ZnO NPs, ZnO, BiOCl and TiO₂ have band gaps larger than 3 eV strong photo-catalytic activities. Redox potentials of H⁺/H₂ and H₂O/O₂ are greater than that of conduction and valence band potentials of both ZnO NPs and TiO₂. BaCrO₄ with smaller band gap shows less activity since its conduction band is much lower than that of ZnO NPs and TiO₂. The lesser band gap allows rapid recombination of electron-hole. So, electrons cannot move into the electron acceptors in the solution in such catalysts, rapidly. Hence low photo-catalytic activity was observed in these semiconductors [58]. It is for these reasons; the prepared ZnO nano photo-catalyst has more photo-catalytic efficiency than other photo-catalysts.

Table 4.9: Effect of other photo-catalysts: [Malachite Green] = 4.0 × 10⁻⁵ mol dm⁻³, pH = 8.0, Light intensity = 30 × 10³ Lux.

Catalysts (60mg/100mL)	k × 10 ⁻⁴ s ⁻¹	t _{1/2} × 10 ³ s
ZnO NPs	4.05	1.71
ZnO	3.20	2.16
BiOCl	2.76	2.51
TiO ₂	2.18	3.17
BaCrO ₄	1.62	4.27

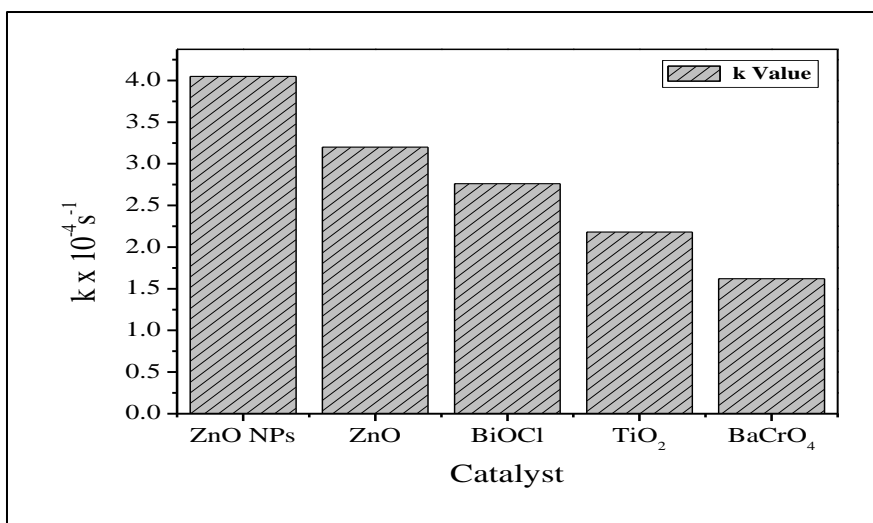


Fig. 4.14: Effect of other photo-catalysts on photo-catalytic degradation of MG

4.2.13: Test for reusability of ZnO NPs:

To determine the activity of ZnO NPs, this catalyst was further tested for two extra cycles and noted that no significant loss of photo-degradation activity against Malachite Green was detected. This indicates that ZnO is more stable and has better photo-catalytic performance on Malachite Green dye degradation. Fig. 4.15 shown as:

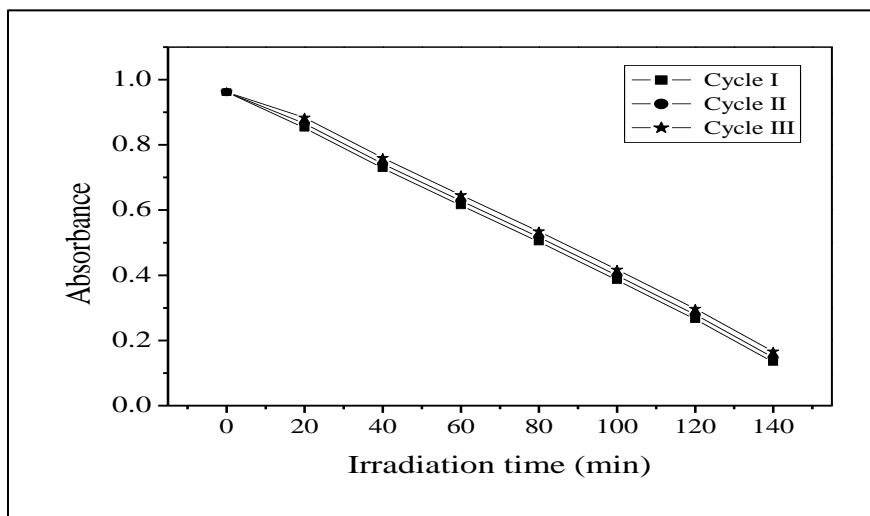


Fig. 4.15: Decolorization of Malachite Green by ZnO NPs: (I) Cycle; (II) Cycle; (III) Cycle; [MG] = 4.0×10^{-5} mol dm⁻³, ZnO NPs = 60 mg/100mL, pH = 8.0, Light intensity = 30×10^3 Lux.

4.2.14: COD and CO₂ measurements during degradation of Malachite Green:

The COD test commonly has been used as an effective method to measure the organic strength of wastewater. This test permits the measurement the total amount of oxygen mandatory for the oxidation of organic matter to CO₂ and H₂O [59]. Here, results of COD were occupied to note the possibility of the reduction process for the degradation of MG dye. The COD of the MG dye solution before and after the treatment was estimated. Mineralization of the dye molecule and decolorization as well are indicated by decrease in COD value of the treated dye solution. The decrease in the COD valued 265 mg/L to 0 mg/L and increase in CO₂ values from 41 mg/L to 236 mg/L in 115 min of presence of visible light the completed mineralization of treated dye solution [60]. The results were shown as Table 4.10 and Figure 4.16 (a) and (b).

Table 4.10: COD and CO₂ measurements during degradation of Malachite Green:

[MG] = 4.0×10^{-5} mol dm⁻³, ZnO NPs = 60 mg/100mL, pH = 8.0,
Light intensity = 30×10^3 Lux.

Time (min)	COD (mg/L)	CO ₂ (mg/L)	Efficiency (%)	NO ₃ ⁻ (mg/L)
0	265	41	0	0
15	232	87	12	7.5
30	148	118	44	13.2
45	76	147	71	18.3
60	34	175	87	22.5
75	18	195	93	27.2
90	8	225	96	29.1
115	0	236	100	33.4

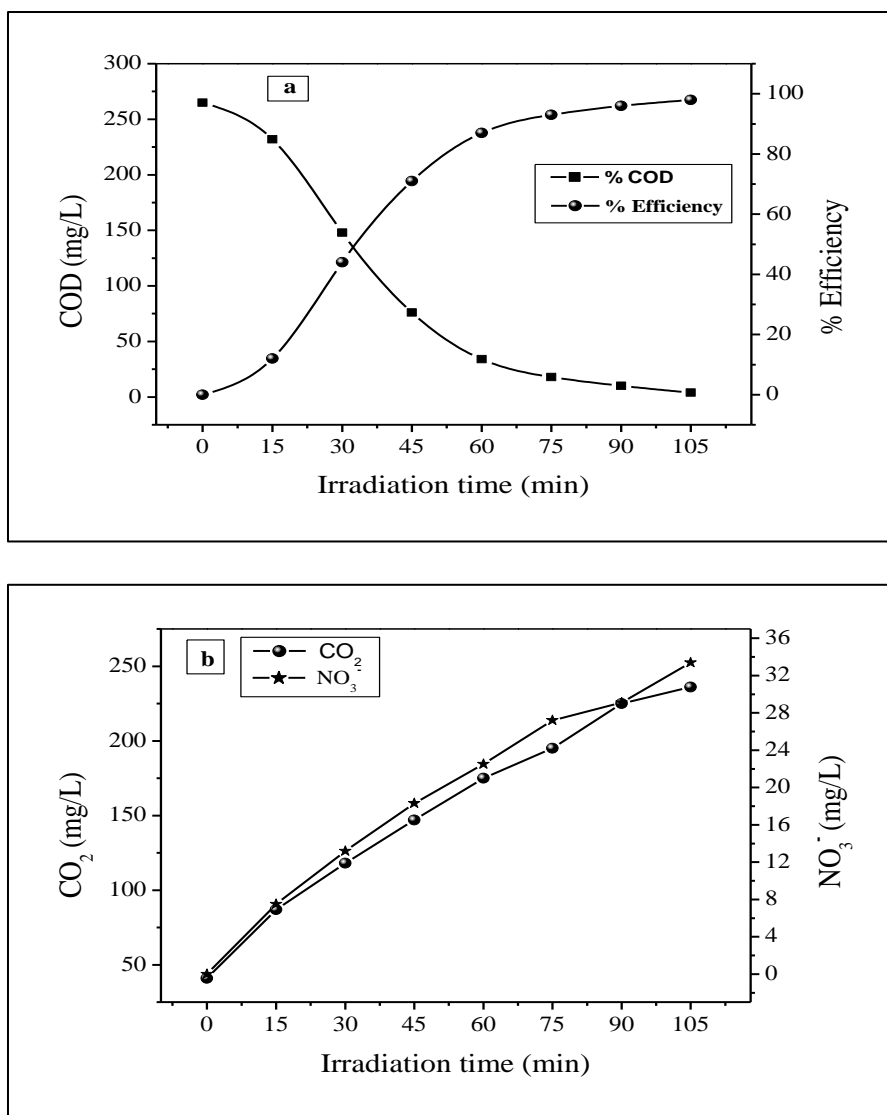
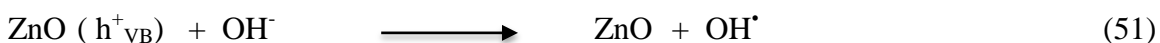
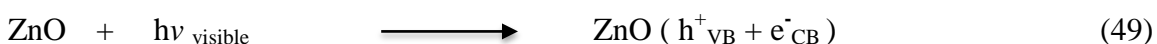


Fig. 4.16: (a) COD trend and % Efficiency (b) CO₂ trend and formation of NO₃⁻ during mineralization of Malachite Green: [MG] = 4.0 x 10⁻⁵ mol dm⁻³, ZnO NPs = 60 mg/100mL, pH = 8.0, Light intensity = 30 x 10³ Lux.

4.2.15: Mechanism of Malachite Green dye degradation:

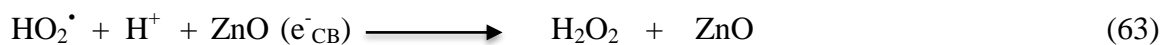
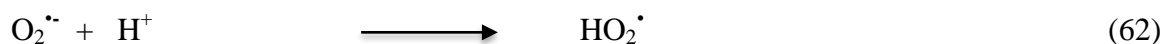
The photo-catalytic degradation of the Malachite Green dye was studied by the use of additives such as H₂O₂, K₂S₂O₈ etc. electron scavengers like H₂O₂ and K₂S₂O₈ accept a photo-generated electron from the conduction band (CB) and thus avoid electron-hole recombination producing OH[•] [61]. Valence band holes (h_{vb}⁺) and conduction band

electrons (e_{cb}^-) are generated when aqueous ZnO NPs suspension is irradiated with visible light energy when band gap energy is greater than ($E_g = 3.2$ eV) and these electron-hole pairs interact separately with another molecule. Conduction band electrons (e_{cb}^-) reduce molecular oxygen to generate superoxide radicals, as shown in Eq. (49) to Eq. (58) [62-64]. Such electron generated disrupted the conjugation system of dye and decomposition of dye and the hole so generated creates OH^\bullet from water which again leads to degradation of dye. The mechanism is as follows: [65, 66]

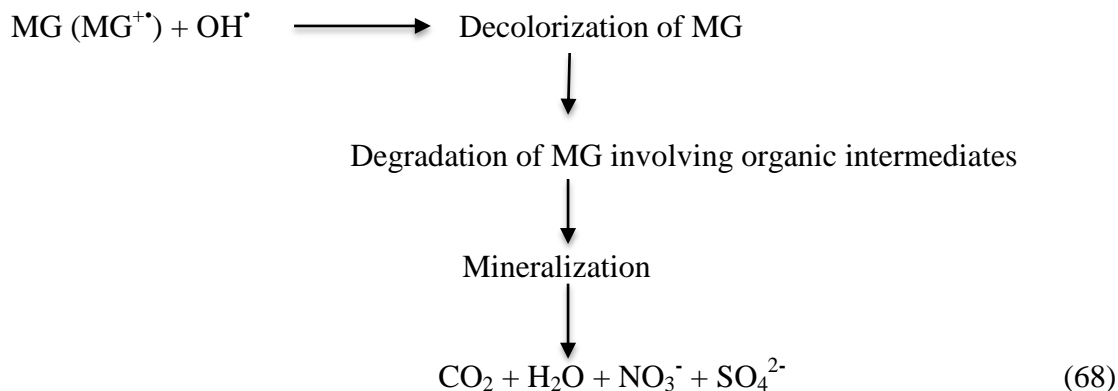


Secondly, sensitization of Dye molecule sensitization by visible light leads to excitation of dye molecule in singlet or triplet state, followed by electron injection from excited dye molecule onto conduction band of semiconductor particles. The mechanism of dye sensitization is summarized as in Eq. (59) to Eq. (68) [67-71].



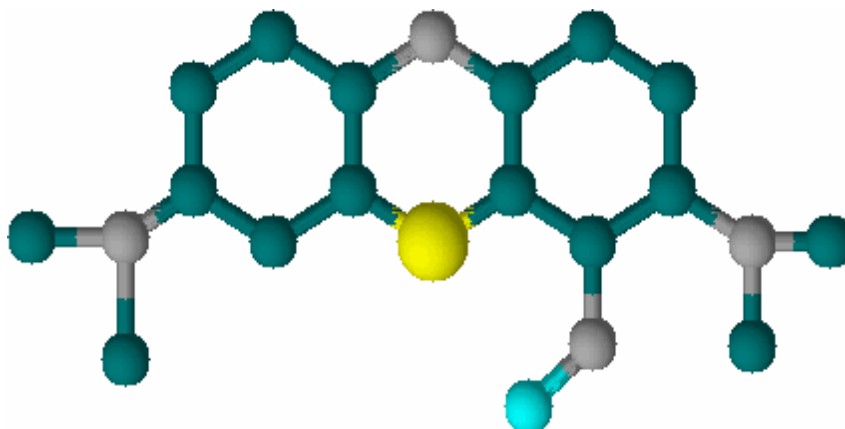


The mechanism of photo-catalysis is of very complex nature. Dye molecules interact with $\text{O}_2^{\bullet-}$, HO_2^{\bullet} , or OH^{\bullet} species to generate intermediates ultimately lead to degradation products. OH^{\bullet} radical are very strong oxidizing agent and mineralized dye into simple products [72, 73].



MG = Malachite Green

Methylene Green



Methylene green, a methylated homologue of basic dye, is a cationic thiazine dye showing deep greenish-blue color in the oxidized state. It is a highly hygroscopic, dark green crystalline powder having a bronze-like luster. It stains nuclei green and is sometimes used as counter stain to red purple primary stains. It is also used for coloring paper, tannin, mordant cotton and silk.

4.3: Effect of various experimental parameters on the degradation rate of Methylene Green (MG) dye

4.3.1: Photo-catalytic degradation of Methylene Green (MG):

On the surface of catalyst classical Langmuir–Hinshelwood expression was followed by the photo-catalytic degradation rate of Methylene Green dye and followed most often Langmuir sorption isotherm for the sorption of the dye to the catalyst surface. This theory is usually used kinetic model for unfolding photo-catalytic behavior. For treatment of heterogeneous surface reactions degradation rate is explained by pseudo first-order kinetics in Langmuir–Hinshelwood [11-14]. Such kinetics is streamlined in terms of modified model to accommodate reactions taking place at solid-liquid interface as

$$r = \frac{-dc}{dt} = \frac{k_r KC}{(1+KC)} \quad (1)$$

Where, r = rate of dye disappearance and C = variable dye concentration at time t . K = equilibrium constant for adsorption of MG dye on photo-catalyst and k_r = limiting reaction rate at maximum coverage in operational conditions. The integrated form can be written as

$$t = \ln\left(\frac{C_0}{C}\right) + \frac{1}{Kk_r} \frac{C_0 - C}{k_r} \quad (2)$$

Where t = time required for the initial concentration of dye C_0 to C . At low dye concentration in equation 2, value of C_0 is very less and hence can be neglected.

$$\ln\left(\frac{C_0}{C}\right) = k_r Kt = kt \quad (3)$$

Where k = apparent rate constant of degradation. The Half-life time ($t_{1/2}$) for the photo-catalytic degradation of Methylene Green dye on the ZnO NPs surface can be calculated by using following Eq. (4)

$$t_{1/2} = \frac{0.693}{k} \quad (4)$$

The Methylene Green dye degradation results are reported here for three conditions: (1) Methylene Green dye + ZnO NPs + visible light (2) Methylene Green dye + visible light only and (3) Methylene Green dye + ZnO nanoparticles only (dark) were shown in figure 4.17 (a). It was observed carefully that maximum degradation occurred in the first condition, while in dark and during photolysis, no significant changes in the absorbance values were observed. Therefore, in second and third condition, degradation process was not observed. Absorption spectrum changes were recorded at 620nm wavelength.

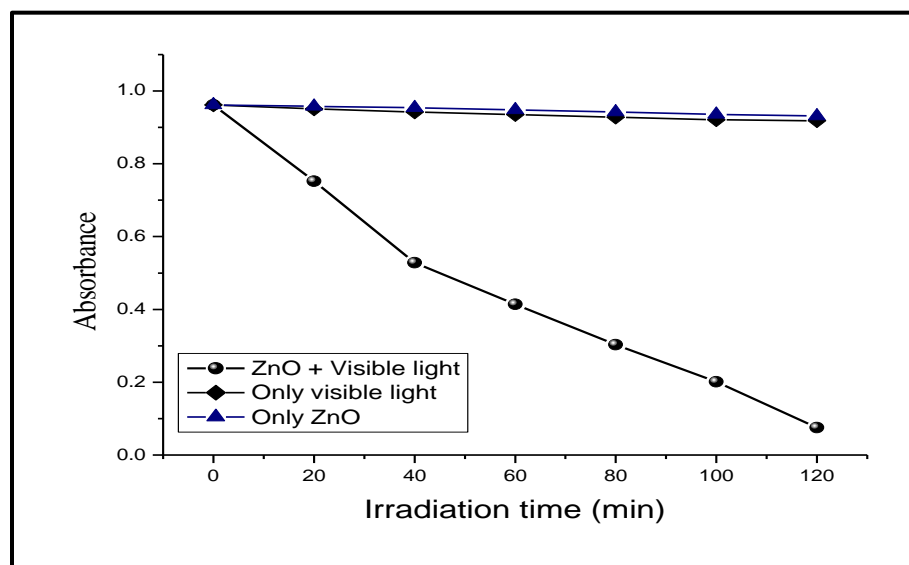


Fig. 4.17 (a) Degradation of Methylene Green: $[MG] = 4.5 \times 10^{-5} \text{ mol dm}^{-3}$,

ZnO NPs = 120 mg/100mL, pH = 8.5, Light intensity = $25 \times 10^3 \text{ Lux}$.

Plotting the semi-logarithmic graph of Methylene Green dye concentration versus irradiation time (min) the presence of ZnO NPs yielded a linear relationship as shown in figure 4.17 (b). Therefore, reaction dye of degradation by ZnO nanoparticles is pseudo-1st order reaction kinetics, with regression coefficient of 0.987, rate constant of $5.61 \times 10^{-4} \text{ s}^{-1}$. The rate constant is the slope of the straight line. In all cases

R^2 (correlation constant for the fitted line) values were close to 0.99 which confirmed pseudo 1st-order kinetics for degradation of MG dye mineralization in this method.

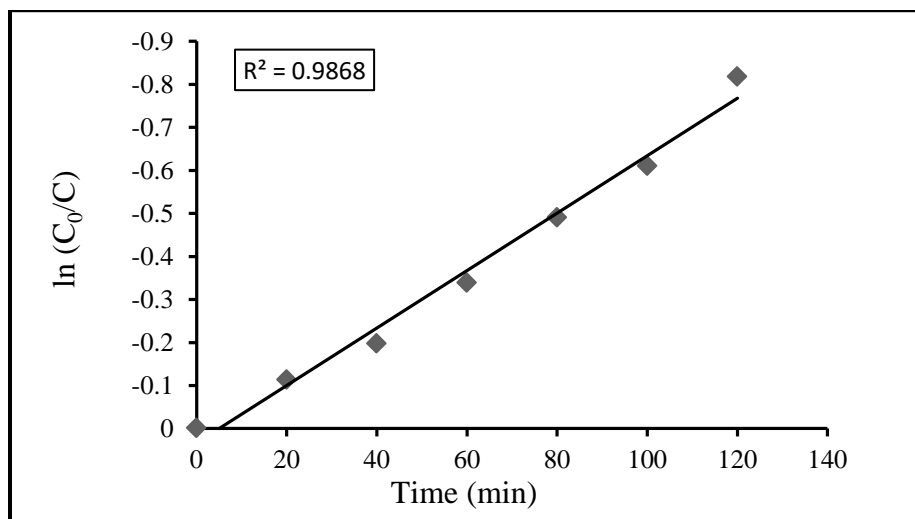
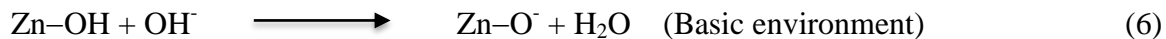
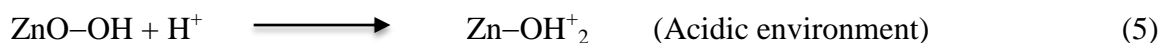


Fig. 4.17 (b): Pseudo first order kinetics: [Methylene Green] = 4.5×10^{-5} mol dm⁻³,
ZnO NPs = 120 mg/100mL, pH = 8.5, Light intensity = 25×10^3 Lux.

4.3.2: Effect of change in pH:

The pH of the aqueous solution also an important variable for the determination of photo-catalytic degradation process, because change in solution pH affected the adsorption of organic pollutants and process of adsorption on semiconductor surface. As the result, the photo-catalytic degradation efficiency got greatly affected by pH changes. The effect of pH on the photo-catalytic reaction could be mainly explained by the surface charge of ZnO NPs [74]. Hydroxide layers (Zn-OH) is formed in presence of water by hydroxylation on zinc oxide nanoparticles surface of zinc hydroxide is charged by amphoteric reaction with hydrogen ion or hydroxyl ion in acidic and alkaline environment respectively [75].



Experimentations were carried out at pH values, from 4 to 12 for constant dye concentration ($4.5 \times 10^{-5} \text{ mol dm}^{-3}$) and catalyst amount (120mg/100ml). The reaction rate increased with increase in pH exhibiting optimum determined rate of degradation at pH 8.5. The results were shown in Table 4.11 and Figure 4.18. Consequently, at higher pH value about 8.5, strong adsorption between negatively charged active sites on zinc oxide nanoparticles and electropositive nature of Methylene Green dye is observed because of electrostatic attraction among them, but if the pH value is too high, ZnO undergo dissolution and gets converted into zincates $[\text{Zn}(\text{OH})_4]^{2-}$.



Under acidic conditions, the MG dye was difficult to adsorb on the ZnO nanoparticles surface and hence the photo-catalytic degradation of Methylene Green dye was found to be very slow [76].

Table 4.11: Effect of change in pH: [Methylene Green] = $4.5 \times 10^{-5} \text{ mol dm}^{-3}$, ZnO NPs = 120 mg/100mL, Light intensity = $25 \times 10^3 \text{ Lux}$.

pH	$k \times 10^{-4} \text{ s}^{-1}$	$t_{1/2} \times 10^3 \text{ s}$
4	1.19	5.82
5	1.84	3.76
6	2.71	2.55
7.5	4.14	1.67
8.5	5.61	1.23
9	3.70	1.87
11	2.69	2.57
12	1.70	4.07

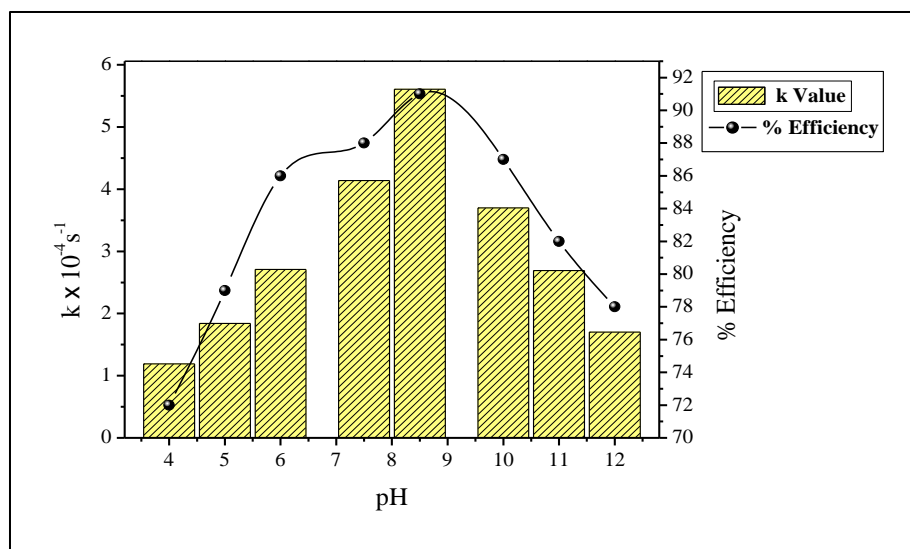


Fig. 4.18: Effect of change in pH on photo-catalytic degradation of MG

4.3.3: Effect of change in catalyst amount:

The photo-catalytic degradation rate constant of dye is generally related to the catalyst amount. The rate of reaction as a role of catalyst amount in photo-catalytic degradation process has been examined by numerous authors. A series of experiments have been carried out to assess the optimal catalyst amount by variable the amount of ZnO NPs catalyst from 60mg/100mL to 180mg/100mL at optimized $4.5 \times 10^{-5} \text{ mol dm}^{-3}$ dye concentration. The rate of degradation increased form $1.26 \times 10^{-4} \text{ s}^{-1}$ to $5.61 \times 10^{-4} \text{ s}^{-1}$ with increased in catalyst amount from 60mg/100mL to 120mg/100mL. Thereafter, rate constant decreases to $1.10 \times 10^{-4} \text{ s}^{-1}$ with increased catalyst amount 180mg/100mL. The rate of reaction is highest at 120mg/100mL of catalyst amount. The results are shown in Table 4.12 and Figure 4.19. Increase in amount of catalyst results in an increase of the available active sites in reaction condition. But higher concentration of catalyst also causes light scattering and decrease in infiltration of light in photo-active volume. Hence photo-active volume shrinks. This tendency can be rationalized in terms of accessibility of active sites on semiconductor surface and the light infiltration of visible light into the

suspension. At optimum ZnO nanoparticles amount of 120mg/100mL, both these conflicting aspects are evenly poised [77, 78]. All these aspects suggest that optimal loading of ZnO NPs catalyst has to be added in the order to avoid unnecessary excess of catalyst also to ensure total absorption of light photons for efficient photo-catalytic degradation of Methylene Green dye [79].

Table 4.12: Effect of change in catalyst amount: [Methylene Green] = 4.5×10^{-5} mol dm^{-3} , pH = 8.5, Light intensity = 25×10^3 Lux.

ZnO mg/100mL	$k \times 10^{-4} \text{ s}^{-1}$	$t_{1/2} \times 10^3 \text{ s}$
60	1.26	5.50
80	2.16	3.20
100	3.56	1.94
120	5.61	1.23
140	4.28	1.61
160	2.74	2.52
180	1.10	6.30

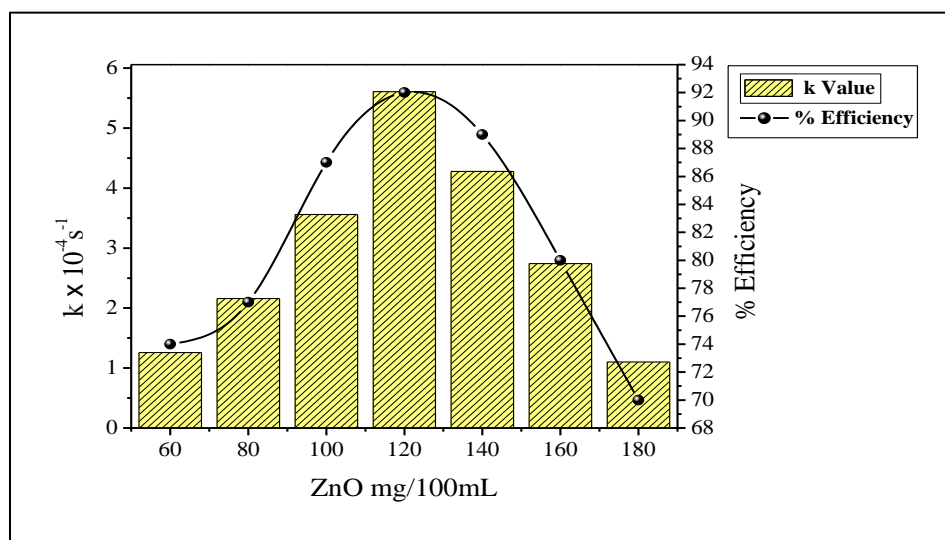


Fig. 4.19: Effect of change in catalyst amount on photo-catalytic degradation of MG

4.3.4: Effect of change in dye concentration:

It is observed that dye concentration is also a very important parameter in treatment of wastewater. The decolourization of Methylene Green dye at varying initial concentrations in the ranging from $1.0 \times 10^{-5} \text{ mol dm}^{-3}$ to $7.5 \times 10^{-5} \text{ mol dm}^{-3}$ was studied under the optimized reaction conditions (ZnO NPs amount=120mg/100mL, pH=8.5). The results are shown in Table 4.13 and Figure 4.20. It has been found that the rate of degradation increased from $1.05 \times 10^{-4} \text{ s}^{-1}$ to $5.61 \times 10^{-4} \text{ s}^{-1}$ with increase in Methylene Green dye concentration from $1.0 \times 10^{-5} \text{ mol dm}^{-3}$ to $4.5 \times 10^{-5} \text{ mol dm}^{-3}$. Thereafter, rate constant of degradation decreased from $5.61 \times 10^{-4} \text{ s}^{-1}$ to $2.07 \times 10^{-4} \text{ s}^{-1}$ with increased dye solution concentration $4.5 \times 10^{-5} \text{ mol dm}^{-3}$ to $7.5 \times 10^{-5} \text{ mol dm}^{-3}$. For Methylene Green dye the optimum degradation rate constant is found at $4.5 \times 10^{-5} \text{ mol dm}^{-3}$. At high concentration of dye, the absorbed reactant molecules might occupy all the active sites of ZnO nanoparticles surface and this led to decrease in rate of degradation [80]. From literature studies we came to know that as the target organic pollutant concentration increase adsorbed of these molecules on the catalyst surface also increases. Hence relative no. of O_2^\bullet and OH^\bullet radicals on the ZnO surface increased [81]. Consequently, excess dye molecule adsorption on catalyst surface hindered the OH^\bullet ions adsorption and finally rate of hydroxyl radical formation is lowered. It is concluded from above discussion that above optimum dye concentration rate of degradation decreased [27-29].

Table 4.13: Effect of change in dye concentration: ZnO NPs = 120 mg/100mL, pH = 8.5, Light intensity = 25×10^3 Lux.

$[MG] \times 10^{-5} \text{ mol dm}^{-3}$	$k \times 10^{-4} \text{ s}^{-1}$	$t_{1/2} \times 10^3 \text{ s}$
1.0	1.05	6.60
1.5	1.86	3.72
2.5	2.92	2.37
3.5	3.94	1.75
4.5	5.61	1.23
5.5	4.37	1.58
6.5	3.40	2.03
7.5	2.07	3.34

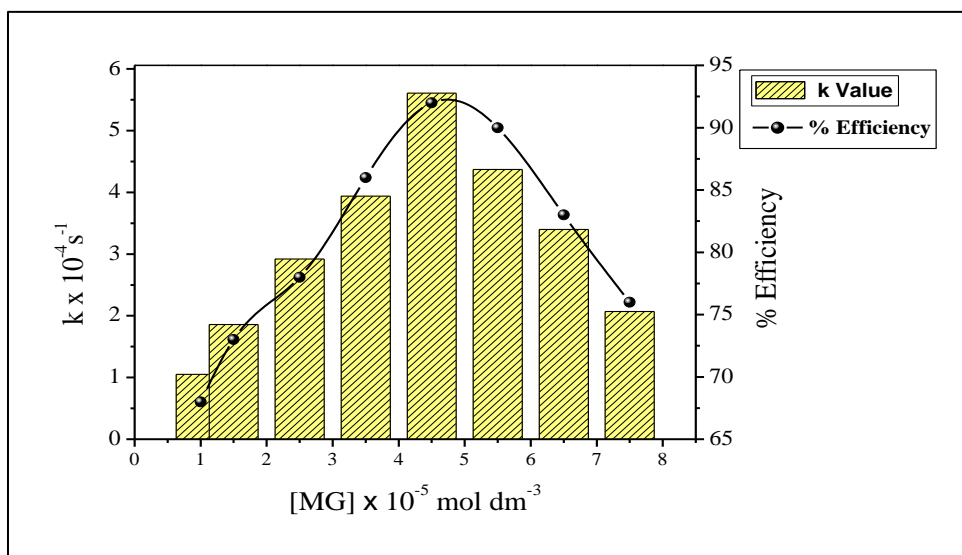
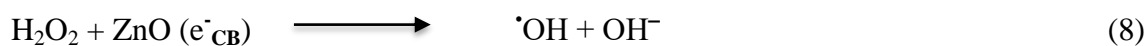


Fig. 4.20: Effect of change in dye concentration on photo-catalytic degradation of MG

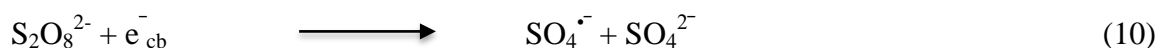
4.3.5: Effect of change in oxidant's concentration:

The addition of other power oxidizing agent like H_2O_2 and $\text{K}_2\text{S}_2\text{O}_8$ to ZnO nanoparticles suspension is a well-known method and lead to an increase in the rate of photo-oxidation.

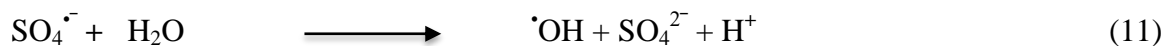
The rate of degradation has been attributed to the recombination of photo-generated electron-hole pairs. Addition of electron acceptors (scavengers) to the reaction is one of the best ways to inhibit electron-hole pair recombination. Relevant reports reveals that oxidizing agents such as H_2O_2 and $\text{K}_2\text{S}_2\text{O}_8$ as electron acceptors have a great deal of influence on the photo-catalytic degradation of dyes. Different concentration of H_2O_2 and $\text{K}_2\text{S}_2\text{O}_8$ has been studies for Methylene Green dye degradation. Rate constant of degradation of Methylene Green dye increased from $6.21 \times 10^{-4}\text{s}^{-1}$ to $8.24 \times 10^{-4}\text{s}^{-1}$ with increasing H_2O_2 concentrations from $2.0 \times 10^{-6} \text{ mol dm}^{-3}$ to $8 \times 10^{-6} \text{ mol dm}^{-3}$ and rate constant of degradation of Methylene Green dye increased from $5.89 \times 10^{-4}\text{s}^{-1}$ to $7.85 \times 10^{-4}\text{s}^{-1}$ with increasing $\text{K}_2\text{S}_2\text{O}_8$ concentrations from $2.0 \times 10^{-6} \text{ mol dm}^{-3}$ to $8 \times 10^{-6} \text{ mol dm}^{-3}$ respectively and reached to an optimum but above this concentration range, the increased H_2O_2 and $\text{K}_2\text{S}_2\text{O}_8$ concentration retarded the degradation rate as shown in Table 4.14 and Figure 4.21. At their respective low concentrations H_2O_2 and $\text{K}_2\text{S}_2\text{O}_8$ accelerate the reaction rate by producing an extremely strong and non-selective oxidant hydroxyl radical ($E^0 = +3.06\text{V}$). These hydroxyl radicals got generated by H_2O_2 and $\text{K}_2\text{S}_2\text{O}_8$ on account of scavenging the electrons from the conduction band of the photo-catalyst and this led to inhibit the electron-hole recombination process [30-33]. H_2O_2 may also split photo-catalytically to produce hydroxyl radicals directly by the absorption of visible light by the following reactions:



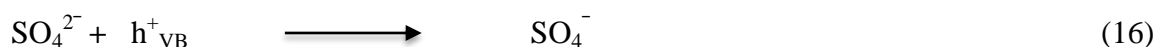
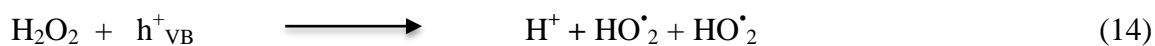
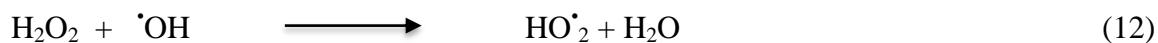
The $\text{S}_2\text{O}_8^{2-}$ anions generate strong oxidizing $\text{SO}_4^{\cdot-}$ radicals anion after trapping the photo-generated conduction band electrons of ZnO nanoparticles as shown in the following reaction:



The generated sulfate radical anions ($\text{SO}_4^{\cdot-}$) participate in reaction with the solvent, according to the following reaction:



Different to this behavior, H_2O_2 and $\text{K}_2\text{S}_2\text{O}_8$ start behaving as scavenger for $\cdot\text{OH}$ radicals and hole at an excessive concentration. The photo-catalytic degradation of Methylene Green dye is covered on excess addition of H_2O_2 and $\text{K}_2\text{S}_2\text{O}_8$ as both $\cdot\text{OH}$ radicals and h_{VB}^+ are strong oxidants for organic dyes. Furthermore, H_2O_2 and SO_4^{2-} can be adsorbed onto ZnO NPs deactivating a section of photo-catalyst and consequently decrease its photo-catalytic activity [34, 35].



Consequently, the proper addition of H_2O_2 and $\text{K}_2\text{S}_2\text{O}_8$ could accelerate the photo-degradation rate of Methylene Green dye. However, in order to keep the efficiency of the added H_2O_2 and $\text{K}_2\text{S}_2\text{O}_8$, it was necessary to choose the proper dosage of H_2O_2 and $\text{K}_2\text{S}_2\text{O}_8$, according to the dye concentration.

Table 4.14: Effect of change in H₂O₂ and K₂S₂O₈: [Methylene Green] = 4.5 × 10⁻⁵ mol dm⁻³, ZnO NPs = 120 mg/100mL, pH = 8.5, Light intensity = 25 × 10³ Lux.

[Oxidant] × 10 ⁻⁶ mol dm ⁻³	[H ₂ O ₂]		[K ₂ S ₂ O ₈]	
	k × 10 ⁻⁴ s ⁻¹	t _{1/2} × 10 ³ s	k × 10 ⁻⁴ s ⁻¹	t _{1/2} × 10 ³ s
0.0	5.61	1.23	5.61	1.23
2.0	6.21	1.11	5.89	1.17
4.0	6.74	1.02	6.37	1.08
6.0	7.20	0.96	6.83	1.01
8.0	8.24	0.84	7.85	0.88
10.0	7.55	0.91	6.93	1.00
12.0	6.17	1.12	6.31	1.09
14.0	5.73	1.20	5.13	1.35

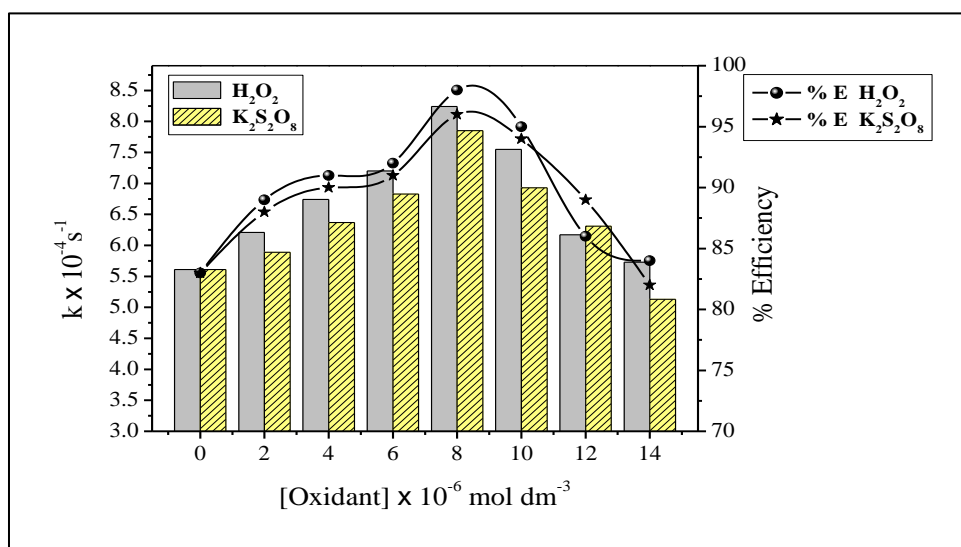
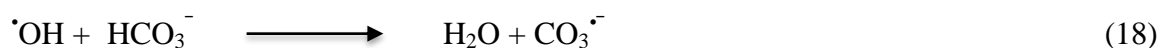
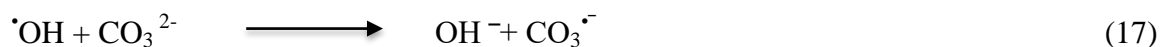


Fig. 4.21: Effect of change in oxidant's on photo-catalytic degradation of MG

4.3.6: Effect of change in salts concentration:

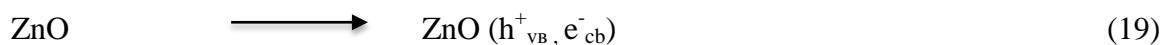
The different concentrations of industrial wastes contain different salts, apart from the pollutants. The inorganic anion may have an influence on the rate of photo-catalytic

degradation. The presence of several anions chloride, carbonate and bicarbonate is industrial wastes. Adsorption of degrading species are affected by these ions and acting as OH⁻ ion scavengers as well as adsorbs light radiation, which also an important factor in mainly photo-catalytic degradation of dye. Here mainly sodium carbonate is used dyeing bath which adjusted bath pH and as it effected fixing of dye on fabrics and color fastness [82]. Therefore the wastewater from the dyeing process will contain considerable amount of carbonate ion [36]. With an increase in the amount of carbonate ion from 2.0 x 10⁻⁵ mol dm⁻³ to 12.0 x 10⁻⁵ mol dm⁻³ resulted into reduction of rate constant from 5.15 x 10⁻⁴ s⁻¹ to 2.87 x 10⁻⁴ s⁻¹. Carbonate ions have hydroxyl ion scavenging property which inhibited the dye degradation and it degradation is calculated by following equation:



The $\cdot\text{OH}$ radical which is a primary oxidant for the photo-catalytic degradation of dye found to decrease slowly with an increase in carbonate ions and degradation of the dye significantly decreased [37].

Similarly, sodium chloride generally comes out in the effluent along with wastewater. Therefore photo-catalytic degradation rate in presence of Cl⁻ ions has been studied by increase in concentration of Cl⁻ ions from 2.0 x 10⁻⁵ mol dm⁻³ to 12 x 10⁻⁵ mol dm⁻³ that conclude into decrease of rate constant from 4.85 x 10⁻⁴ s⁻¹ to 1.95 x 10⁻⁴ s⁻¹. Chloride ions might have hole scavenging property and hence in presence of Cl⁻ ions dye degradation decreases [38].





The dependency of reaction rate constant on the concentration of Na_2CO_3 and NaCl is results are shown in Table 4.15 and Figure 4.22.

Table 4.15: Effect of change in Na_2CO_3 and NaCl : [Methylene Green] = 4.5×10^{-5} mol dm^{-3} , ZnO NPs = 120 mg/100mL, pH = 8.5, Light intensity = 25×10^3 Lux.

[Salt] x 10^{-5} mol dm^{-3}	[Na_2CO_3]		[NaCl]	
	k x 10^{-4} s $^{-1}$	$t_{1/2}$ x 10^3 s	k x 10^{-4} s $^{-1}$	$t_{1/2}$ x 10^3 s
0.0	5.61	1.23	5.61	1.23
2.0	5.15	1.34	4.85	1.42
4.0	4.74	1.46	4.32	1.60
6.0	4.19	1.65	3.73	1.85
8.0	3.86	1.79	3.27	2.11
10.0	3.17	2.18	2.69	2.57
12.0	2.87	2.41	1.95	3.55

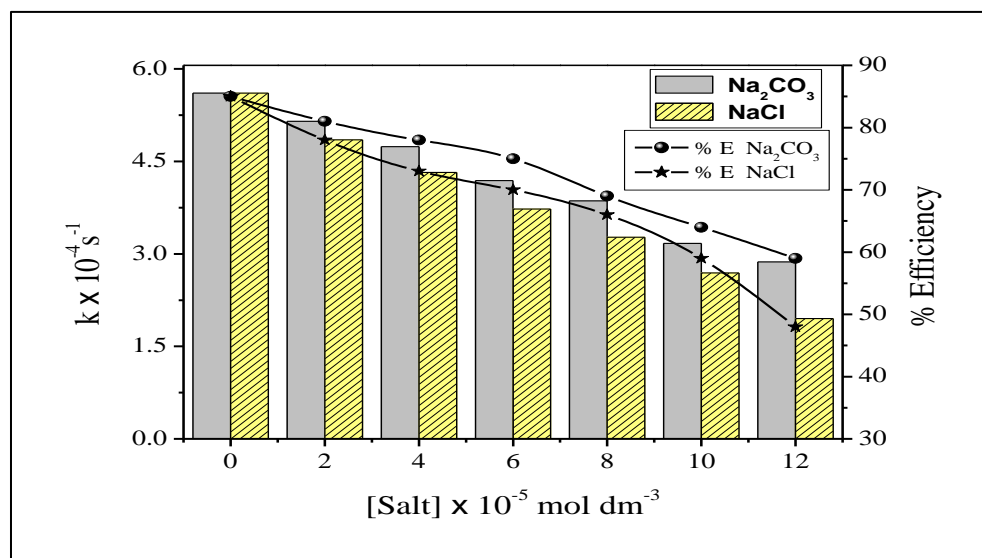


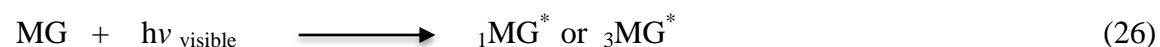
Fig. 4.22: Effect of change in salts on photo-catalytic degradation of MG

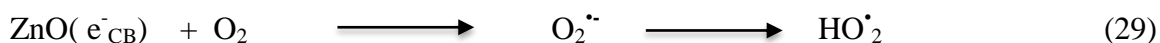
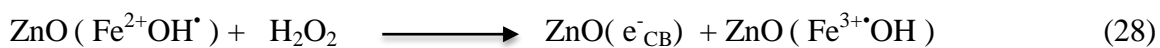
4.3.7: Effect of change in FeCl₃ concentration:

The photo-catalytic degradation process was evaluated observed effect of FeCl₃ on Methylene Green dye oxidation with Zinc oxide nanoparticles using visible light. It was observed that when FeCl₃ was varied concentration from 2.0 x 10⁻⁵ mol dm⁻³ to 14.0 x 10⁻⁵ mol dm⁻³. It is observed from experimental data that on increase concentration of FeCl₃ from 2.0 x 10⁻⁵ mol dm⁻³ to 8.0 x 10⁻⁵ mol dm⁻³ with the degradation rate constant value increased from 5.94 x 10⁻⁴ s⁻¹ to 7.02 x 10⁻⁴ s⁻¹ respectively. Thereafter, rate constant of photo-catalytic degradation decreased to 5.02 x 10⁻⁴ s⁻¹ on further increase in amount of FeCl₃ up to 14.0 x 10⁻⁵ mol dm⁻³. The results are tabulated in Table 4.16 and Figure 4.23. It can be conclude that Fe³⁺ metal ion can be used as photosensitizer for photo-catalytic degradation of dye. In fact the increase in ferric ions concentration in the reaction mixture resulted into the increase of Fe²⁺ ions concentration, which is accompanied by improved generation of [•]OH radicals, therefore increasing rate of degradation of FeCl₃ inhibits the reaction rate of degradation by competing with formation of [•]OH radicals [39-41].



The photo-activation of surface adsorbed complex ion (Fe³⁺OH⁻) results in the formation of Fe²⁺OH[•] specie which injects electrons to the conduction band of ZnO as shown in [Eq. 27-28]. The rate of photo-catalytic degradation in case of FeCl₃ is explicable due to rapid scavenging of conduction band (CB) electrons by molecular oxygen leading to formation of superoxide and hydroperoxide radicals [42, 43] [Eq. (28)].





In the presence of higher concentration of FeCl_3 , there is excessive surface adsorption of dye on the surfaces of catalyst [44]. This reduced the total photoactive area of ZnO NPs catalyst and lowered rate of reaction [45].

Table 4.16: Effect of change in FeCl_3 concentration: $[\text{MG}] = 4.5 \times 10^{-5} \text{ mol dm}^{-3}$,
ZnO NPs = 120 mg/100mL, pH = 8.5, Light intensity = $25 \times 10^3 \text{ Lux}$.

$\text{FeCl}_3 \times 10^{-5} \text{ mol dm}^{-3}$	$k \times 10^{-4} \text{ s}^{-1}$	$t_{1/2} \times 10^3 \text{ s}$
0.0	5.61	1.23
2.0	5.94	1.16
4.0	6.24	1.11
6.0	6.67	1.03
8.0	7.02	0.98
10.0	6.60	1.05
12.0	5.87	1.18
14.0	5.02	1.38

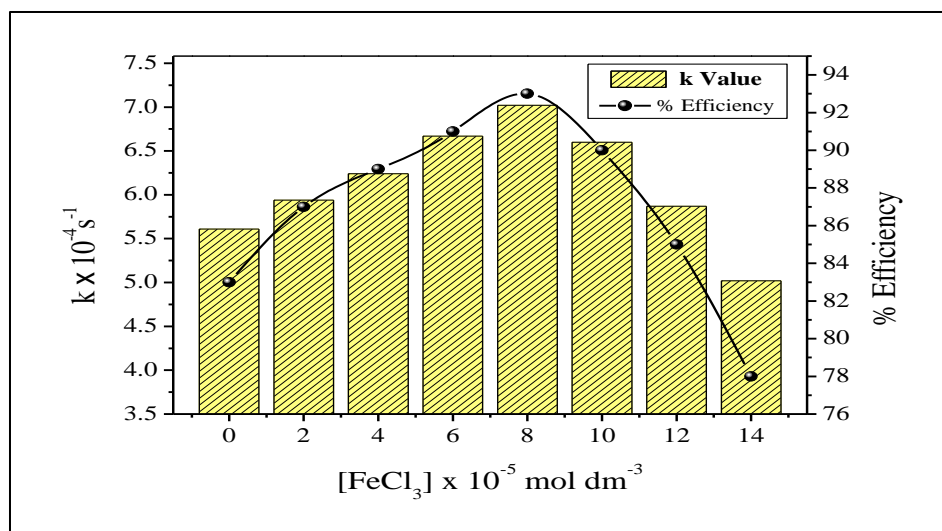


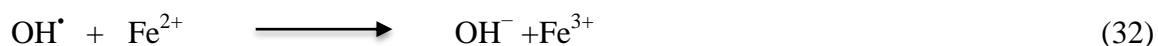
Fig. 4.23: Effect of change in FeCl₃ on photo-catalytic degradation of MG

4.3.8: Effect of change in Fenton's reagent concentration:

Fenton reagent makes attractive AOPs for the wastewater treatment and usage for the effective degradation of dyes due to low cost and less toxicity [83]. It is very well known that for textile dye Fenton's reagent is powerful oxidant. Many researcher studied degradation of dyes using Fenton's and visible light system past few years. Photo-Fenton's process is one of the most common AOPs which is based on the formation of very reactive species such as $\cdot\text{OH}$ radicals, which have a ver strong oxidative potential after fluorine [48, 49].



$\text{OH}\cdot$ radicals may be scavenged by reaction with another Fe^{2+} :



In present study Fenton's reagent for degradation of Methylene Green dye in presence of ZnO nanoparticles in visible light has been studied. The degradation rate constant has a value of $5.96 \times 10^{-4} \text{ s}^{-1}$ on the addition of $\text{Fe}^{3+}:\text{H}_2\text{O}_2$ in molar ratio 1:2. In the presence of

$\text{Fe}^{3+}:\text{H}_2\text{O}_2$ in molar ratio 1:4, rate constant has been found $7.57 \times 10^{-4} \text{ s}^{-1}$. The results are shown in Table 4.17 and Figure 4.24. Upon irradiation of $\text{Fe}^{3+}/\text{H}_2\text{O}_2/\text{ZnO}/\text{MG}$ technique in the presence of visible light, formation of OH^\bullet radicals increases relating a complex mechanism. Visible radiation is absorbed by dye and excited in to high energy state from ground state and this excited dye molecules reduce ferric ion complex into ferrous ion complex followed by the transfer to ferric ion [50]. This ferrous ion complex produced hydroxyl radical on the reaction with hydrogen peroxide [Eq. (36)]. OH^\bullet radicals also decompose H_2O_2 to $^\bullet\text{HO}_2$.

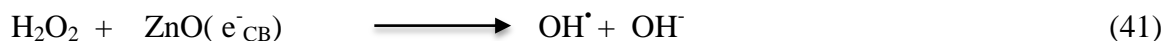
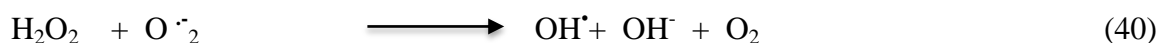
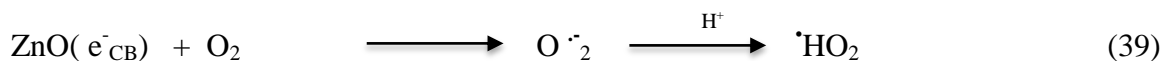
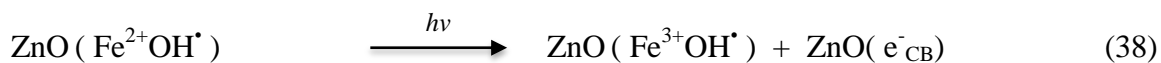
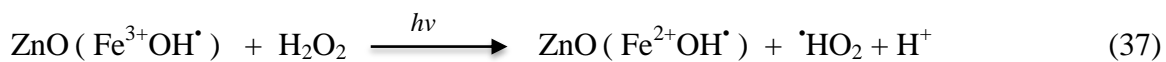


Table 4.17: Effect of change in $\text{Fe}^{3+}/\text{H}_2\text{O}_2$: [Methylene Green] = $4.5 \times 10^{-5} \text{ mol dm}^{-3}$,
ZnO NPs = 120 mg/100mL, pH = 8.5, Light intensity = $25 \times 10^3 \text{ Lux}$.

$\text{Fe}^{3+} : \text{H}_2\text{O}_2$	Without ZnO		With ZnO	
	$k \times 10^{-4} \text{ s}^{-1}$	$t_{1/2} \times 10^3 \text{ s}$	$k \times 10^{-4} \text{ s}^{-1}$	$t_{1/2} \times 10^3 \text{ s}$
1:2	0.85	8.15	5.96	1.16
1:1.3	1.63	4.25	6.49	1.06
1:4	2.02	2.79	7.57	0.91
1.3:3	2.32	2.98	6.81	1.01
3:4	2.48	3.43	6.12	1.13

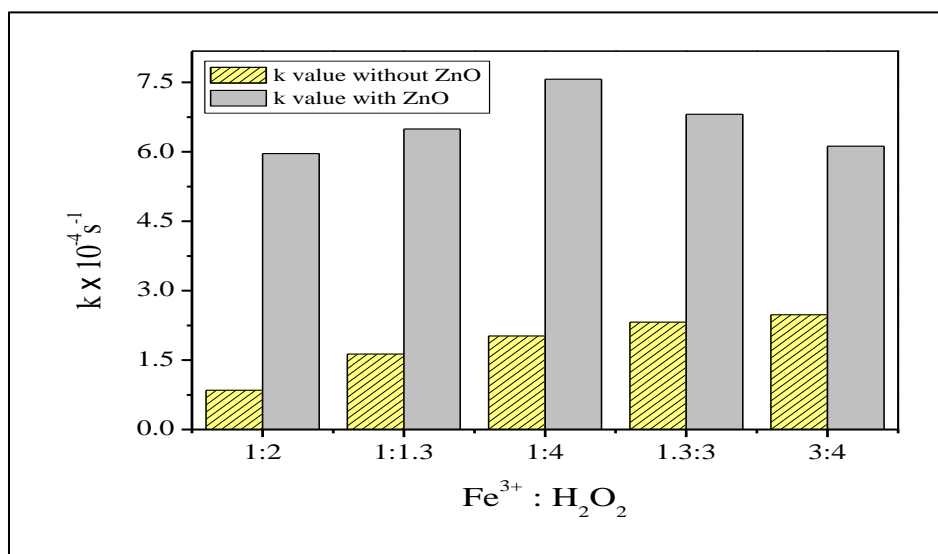


Fig. 4.24: Effect of change in Fenton's reagent on photo-catalytic degradation of MG

4.3.9: Effect of change in light intensity:

The effect of the variation of the intensity of light on the rate of degradation has been investigated by varying the light intensity increasing from $15 \times 10^3 \text{ Lux}$ to $35 \times 10^3 \text{ Lux}$. Methylene Green dye solution concentration $4.5 \times 10^{-5} \text{ mol dm}^{-3}$, ZnO NPs catalyst

amount 120 mg/100mL and pH 8.5. To examine the effect of light intensity on photocatalytic degradation of Methylene Green dye, the distance between the light source and the exposed surface area was varied. The degradation rate constant increased from $3.96 \times 10^{-4} \text{ s}^{-1}$ to $6.54 \times 10^{-4} \text{ s}^{-1}$ with increase in light intensity on semiconductor surface as shown in Table 4.18 and Figure 4.25. The data show that the rate of degradation was accelerated as the light intensity was increased because any increase in the intensity of light increased the photons striking per unit time per unit area of the ZnO NPs catalyst powder resulted in more OH^\bullet radicals. A linear behavior between intensity of light and rate of degradation was observed [84].

Table 4.18: Effect of change in light intensity: $[\text{MG}] = 4.5 \times 10^{-5} \text{ mol dm}^{-3}$, ZnO NPs = 120 mg/100mL, pH = 8.5.

Light intensity $\times 10^3 \text{ lux}$	$k \times 10^{-4} \text{ s}^{-1}$	$t_{1/2} \times 10^3 \text{ s}$
15	3.96	1.75
20	4.26	1.62
25	5.61	1.23
30	5.84	1.18
35	6.54	1.05

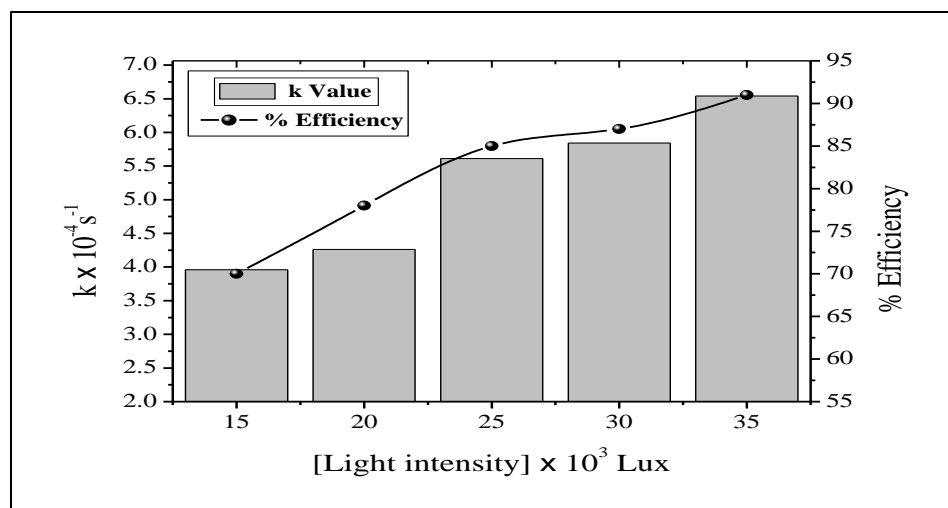


Fig. 4.25: Effect of change in light intensity on photo-catalytic degradation of MG

4.3.10: Effect of bubbling of N₂ and O₂:

The reactions of photo-catalytic degradation were carried out in presence of ZnO NPs catalyst by bubbling oxygen and nitrogen in a closed reactor. The degradation percentage of Methylene Green dye after a given irradiation time with ZnO nanoparticles in the presence and absence of oxygen was found. It is confirmed from the observation that proposed assumption oxygen dissolve in water is main oxidant, that is, the role of DO is to trap the photo-generated electrons to produce O₂^{•-} radicals, which particles in photo-catalytic process to accelerate the photo-degradation of Methylene Green dye. The Oxygen got adsorbed on the surface of the ZnO NPs and the surface redox reactions initiated by photo-generated electrons and generating superoxide anion radical and this superoxide anion radical started the photo-catalytic degradation of organic pollutant. However in the presence of nitrogen the conduction band electrons were blocked and the formation of superoxide anion radical is prevented. Hence the reaction rate is suppressed. The results are shown in Figure 4.26 [53, 54].



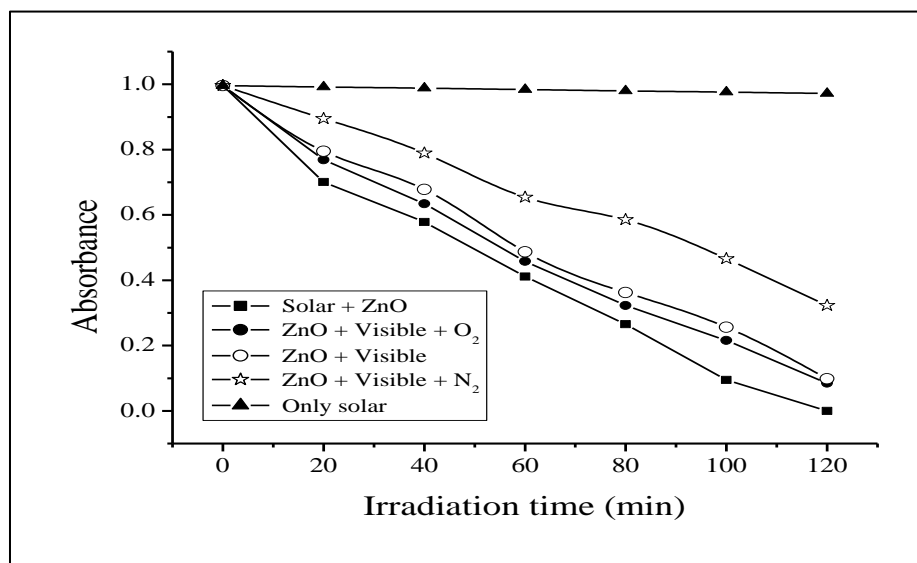
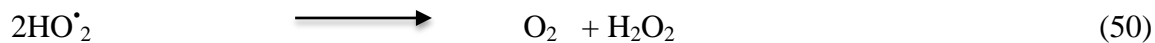
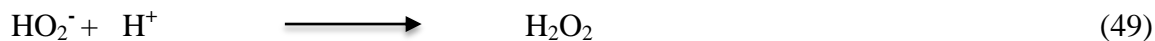
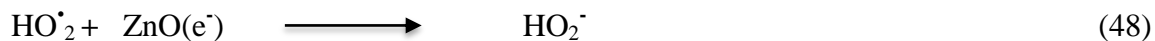
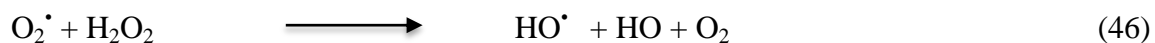
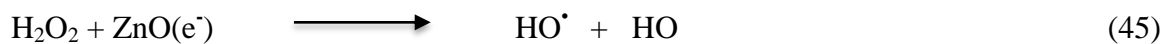


Fig. 4.26: Decolorization of MG under various photo-catalytic systems: [MG] = 4.5×10^{-5} mol dm⁻³, ZnO NPs = 120 mg/100mL, pH = 8.5, Light intensity = 25×10^3 Lux.

4.3.11: Comparison of solar and visible light:

The efficiency of solar and visible light on photo-catalytic degradation of dye was comparatively studied. The degradation efficiency of Methylene Green dye with visible light was found to be more efficient than that of solar light. Figure 4.26 shows the comparisons of color removal efficiency of Methylene Green with two light sources under different conditions. It was noticed that if same experiments were carried out in the absence of ZnO, then no absorbance loss of dye was found [55, 56].

4.3.12: Effect of other photo-catalysts:

The order of photo-activity followed the order: ZnO NPs > ZnO > BiOCl > TiO₂ > BaCrO₄ on photo-catalytic degradation have been studied at same condition. It has already been found that catalysts such as ZnO NPs, ZnO, BiOCl and TiO₂ have band gaps larger than 3 eV strong photo-catalytic activities. The heterogeneous photo-catalyst i. e. ZnO nanoparticles reaction occurred on surface when illumination with light of energy equal or more than band gap of photo-catalyst [57]. We have investigated the relative efficiencies of other photo-catalysts. The conduction band (CB) and valence band (VB) potentials of both ZnO NPs and TiO₂ are larger than the corresponding redox potentials of H⁺/H₂ and H₂O/O₂ and the photo-generated electron and hole can be separated efficiently. BaCrO₄ with smaller band gap shows less activity since its conduction band is much lower than that of ZnO nanoparticles and TiO₂. Rapid recombination of electron-hole and so electron is permitted by smaller band gap in such catalyst and these cannot move towards electron scavengers rapidly. Hence low photo-catalytic activity was observed in these semiconductors [58]. It is for these reasons; the prepared ZnO nanoparticles photo-catalyst has more photo-catalytic efficiency than other photo-catalysts. The results are shown in Table 4.19 and 4.27.

Table 4.19: Effect of other photo-catalysts: [Methylene Green] = $4.5 \times 10^{-5} \text{ mol dm}^{-3}$, pH = 8.5, Light intensity = $25 \times 10^3 \text{ Lux}$.

Catalysts (120mg/100mL)	$k \times 10^{-4} \text{ s}^{-1}$	$t_{1/2} \times 10^3 \text{ s}$
ZnO NPs	5.61	1.23
ZnO	3.93	1.76
BiOCl	2.85	2.43
TiO ₂	2.23	3.10
BaCrO ₄	1.57	4.41

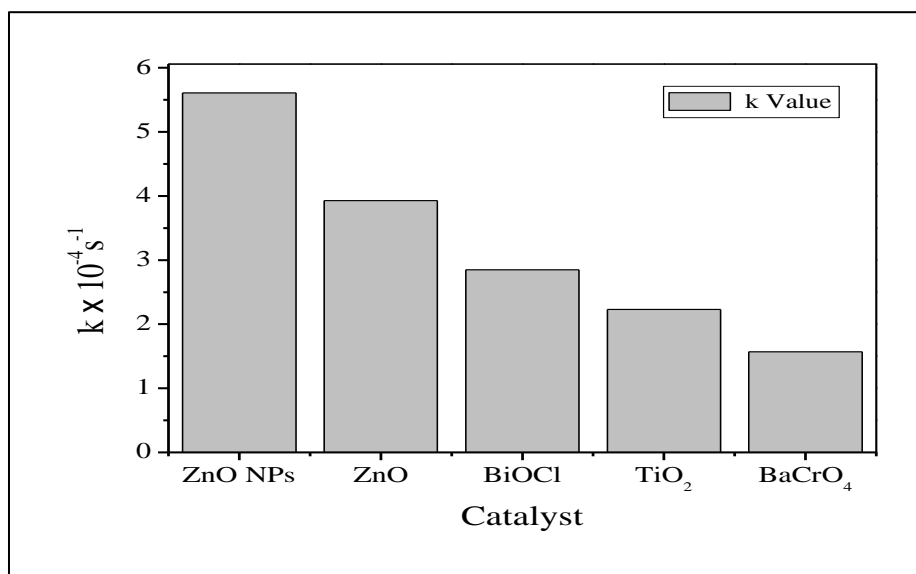


Fig. 4.27: Effect of other photo-catalysts on photo-catalytic degradation of MG

4.3.13: Test for reusability of ZnO NPs:

The reusability of ZnO nanoparticles photo-catalyst was tested for dye degradation. The ZnO nanoparticles catalyst used for degradation of dye was filtered, washed and dried in air and then in oven for 30 minutes. This dried ZnO photo-catalyst was used for the

degradation of dyes under similar reaction conditions. It was observed that the ZnO photo-catalyst can be used repeatedly even up to three batches of reaction without any treatment and reused catalyst showed almost similar catalyst activity with fresh (original) catalyst. The initial rate of photo-degradation of the dye has found very low decrement even after the third second cycle of reuse. ZnO nanoparticles reusability is shown in figure 4.28. The less of activity was observed and losses of Zn^{++} ions were more pounced only after third cycle of its reuse.

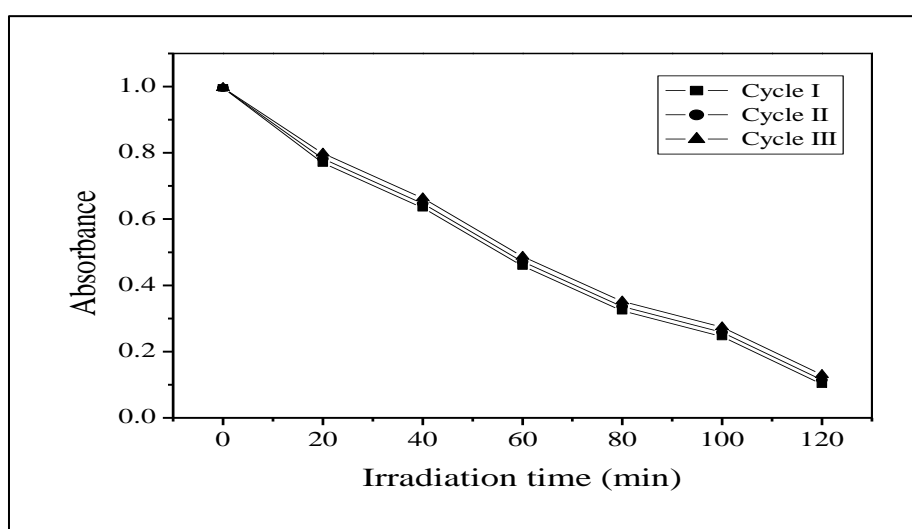


Fig. 4.28: Decolorization of Methylene Green by ZnO NPs: (I) Cycle; (II) Cycle; (III) Cycle; [MG] = 4.5×10^{-5} mol dm⁻³, ZnO = 120 mg/100mL, pH = 8.5, Light intensity = 25×10^3 Lux.

4.3.14: COD and CO₂ measurements during degradation of Methylene Green:

The efficiency of photo-catalytic treatment to mineralize the dyes was studied. Chemical oxygen demand resulted were taken as one of the parameter to determine the feasibility of the reduction process for Methylene Green dye degradation. COD and free CO₂ measurement were carried out to record the quantity of mineralization of the organic compounds under consideration over ZnO suspension, COD test allowed the

measurements of waste in terms of the total quantity of oxygen required for the degradation of organic matter to CO₂ and inorganic ions [59]. The decrease in COD values of the treated dye solution indicated the mineralization of dye molecules along with the color removal. The reduction in the estimated COD from 196 mg/L to 5 mg/L and increase in CO₂ values from 24mg/L to 158mg/L of illumination indicated the complete mineralization of treated dye solution. From estimated value of COD and CO₂, it is evident that 97 % of COD removal has been completed in 150 min of irradiation under optimum reaction condition. A decrease in COD and increase in CO₂ confirm the degradation of dye. Significant amount of NO₃⁻ were released into reaction during the mineralization of dye. A decrease in pH has also been observed with increase in the quantity of mineralization [85]. The results were shown as Table 4.20 and Fig. 4.29 (a, b).

Table 4.20: COD and CO₂ measurements during degradation of Methylene Green:

[Methylene Green] = 4.5×10^{-5} mol dm⁻³, ZnO NPs = 120 mg/100mL, pH = 8.5, Light intensity = 25×10^3 Lux.

Time (min)	COD (mg/L)	CO ₂ (mg/L)	Efficiency (%)	NO ₃ ⁻ (mg/L)
0	196	24	0	0
30	152	68	22	6.1
60	120	90	38	7.5
90	65	108	66	9.2
120	18	142	90	12.5
150	5	158	97	15.2

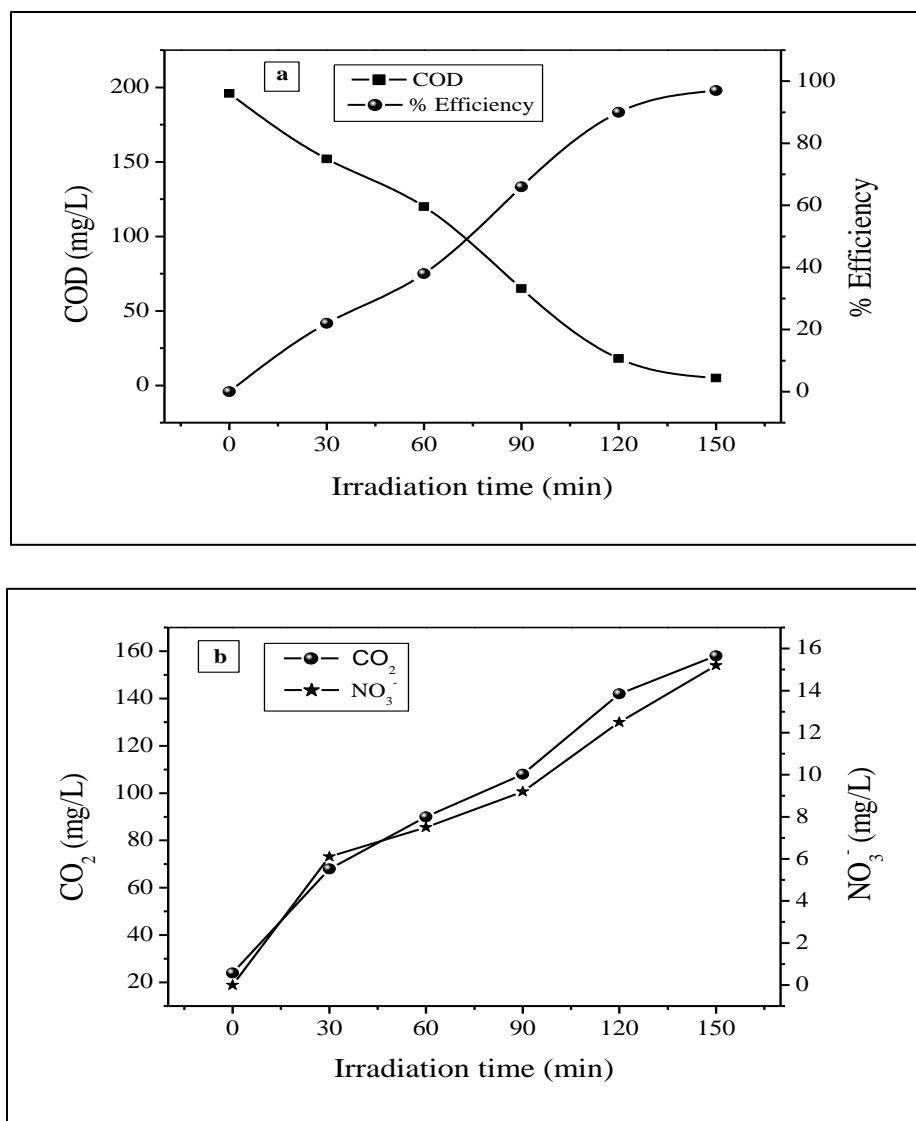
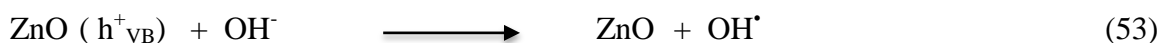
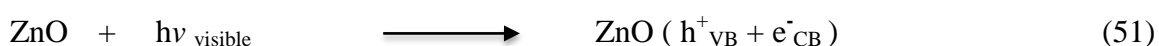


Fig. 4.29: (a) COD trend and % Efficiency (b) CO₂ trend and formation of NO₃⁻ during mineralization of Methylene Green: [MG] = 4.5×10^{-5} mol dm⁻³, ZnO NPs = 120 mg/100mL, pH = 8.5, Light intensity = 25×10^3 Lux.

4.3.15: Mechanism of Methylene Green dye degradation:

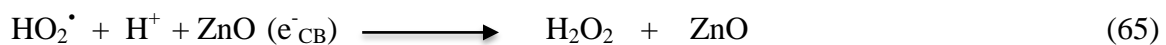
The photo-catalytic degradation of the Methylene Green dye was studied by the use of additives such as H₂O₂, K₂S₂O₈ etc. electron scavengers like H₂O₂ and K₂S₂O₈ accept a photo-generated electron from the conduction band (CB) and thus avoid electron-hole recombination producing OH[•] [61]. Valence band holes (h_{vb}⁺) and conduction band

electrons(e_{cb}^-) are generated when aqueous ZnO NPs suspension is irradiated with visible light energy when band gap energy is greater than ($E_g = 3.2$ eV) and these electron-hole pairs interact separately with another molecule. Conduction band electrons (e_{cb}^-) reduce molecular oxygen to generate superoxide radicals, as shown in Eq. (51) to Eq. (60) [62-64]. Such electron generated disrupted the conjugation system of dye and decomposition of dye and the hole so generated creates OH^\bullet from water which again leads to degradation of dye. The mechanism is as follows: [65, 66]

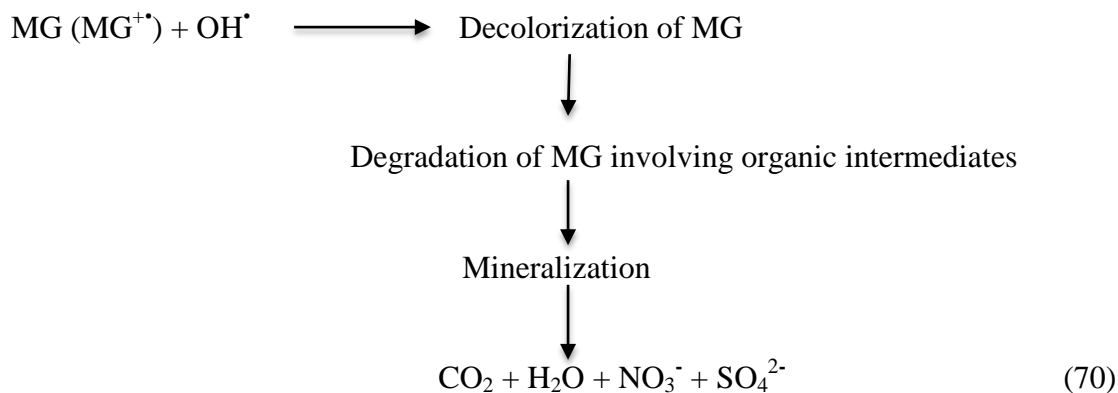


Secondly, sensitization of dye molecule by visible light leads to excitation of dye molecule in singlet or triplet state, subsequently followed by electron injection from excited dye molecule onto conduction band of semiconductor particles. The mechanism of dye sensitization is summarized in Eq. (61) to Eq. (70) [67-71].



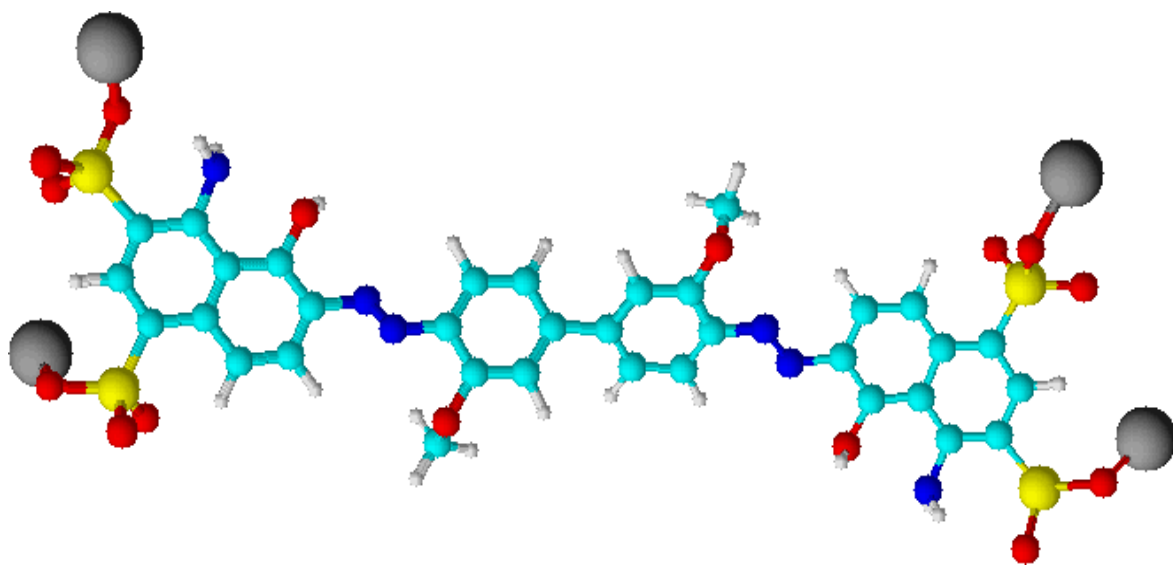


The mechanism of semiconductor photo-catalysis is of very complex nature. Dye molecules interact with $\text{O}_2^{\bullet-}$, HO_2^{\bullet} , or OH^{\bullet} species to generate intermediates ultimately lead to degradation products. OH^{\bullet} radical being very strong oxidizing agent (oxidation potential 3.2 eV) mineralizes dye to various end products. The role of reductive pathways in heterogeneous photo-catalysis has been found to be in minor extent as compared to oxidation [72, 73].



MG = Methylene Green

Direct Blue-1



Direct blue-1 is an anionic azo group dye and soluble in water. It is the compound able to dye cellulose fibers without the aid of mordent's. It is widely used in the textile, cosmetic, paper, drug and food processing industries large quantities.

4.4: Effect of various experimental parameters for the degradation rate of Direct Blue-1 (DB-1) dye

4.4.1: Photo-catalytic degradation of Direct Blue-1 (DB-1):

On the surface of catalyst classical Langmuir–Hinshelwood expression was followed by the photo-catalytic degradation rate of Direct Blue-1 dye and followed most often Langmuir sorption isotherm for the sorption of the dye to the catalyst surface. This theory is usually used kinetic model for unfolding photo-catalytic behavior. For treatment of heterogeneous surface reactions degradation rate is explained by pseudo first order kinetics in Langmuir–Hinshelwood [11-14]. Such kinetics is streamlined in terms of modified model to accommodate reactions taking place at solid-liquid interface as

$$r = \frac{-dc}{dt} = \frac{k_r KC}{(1+KC)} \quad (1)$$

Where, r = rate of dye disappearance and C = variable dye concentration at time t . K = equilibrium constant for adsorption of DB-1 dye on photo-catalyst and k_r = limiting reaction rate at maximum coverage in operational conditions. The integrated form can be written as

$$t = \ln\left(\frac{C_0}{C}\right) + \frac{1}{Kk_r} \frac{C_0 - C}{k_r} \quad (2)$$

Where t = time required for the initial concentration of dye C_0 to C . At low dye concentration in equation 2, value of C_0 is very less and hence can be neglected.

$$\ln\left(\frac{C_0}{C}\right) = k_r Kt = kt \quad (3)$$

Where k = apparent rate constant of degradation. The Half-life time ($t_{1/2}$) for the photo-catalytic degradation of DB-1 dye on the ZnO NPs surface can be calculated by using following Eq. (4)

$$t_{1/2} = \frac{0.693}{k} \quad (4)$$

The Direct Blue-1 dye degradation results are reported here for three conditions: (1) Direct Blue-1+ ZnO NPs + visible light (2) Direct Blue-1 dye + visible light only and (3) Direct Blue-1 dye + ZnO nanoparticles only (dark) were show in figure 4.30 (a). It was observed carefully that maximum degradation occurred in the first condition, while in dark and during photolysis, no significant changes in the absorbance values were observed. Therefore, in second and third condition, degradation process was not observed. Absorption spectrum Changes were recorded at 610nm wavelength.

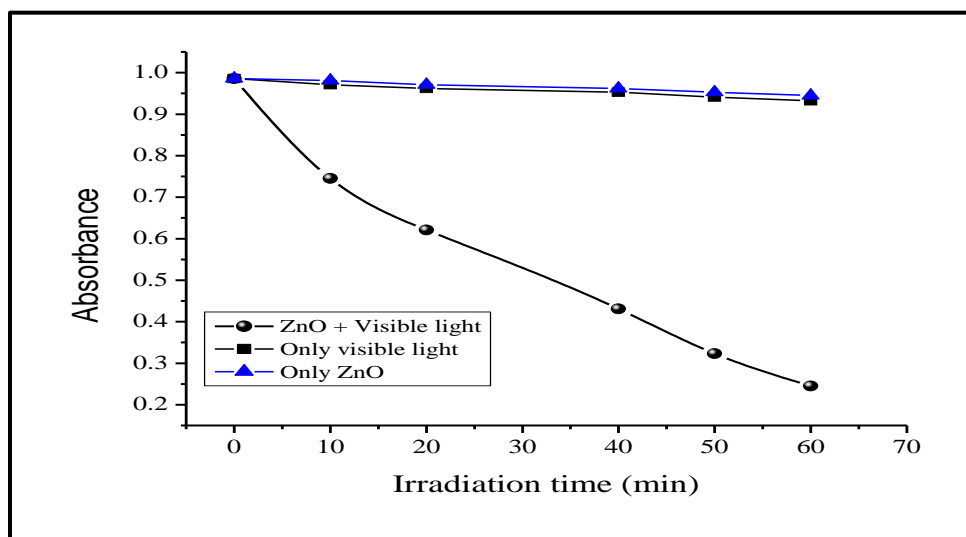


Fig. 4.30 (a) Degradation of Direct Blue-1: [DB-1] = 2.0×10^{-5} mol dm⁻³, ZnO NPs = 160 mg/100mL, pH = 6.5, Light intensity = 40×10^3 Lux.

Plotting the semi-logarithmic graph of Direct Blue-1 dye concentration versus irradiation time (min) in presence of ZnO NPs yielded a linear relationship as shown in Figure 4.30 (b). Therefore, reaction dye of degradation by ZnO nanoparticles is pseudo- 1st order reaction kinetics, with regression coefficient of 0.993, DB-1 dye degradation rate constant of 7.62×10^{-4} s⁻¹. The rate constant is the slope of the straight line. In all cases

R^2 (correlation constant for the fitted line) values were close to 0.99 which confirmed pseudo 1st-order kinetics for Direct Blue-1 dye mineralization in this method.

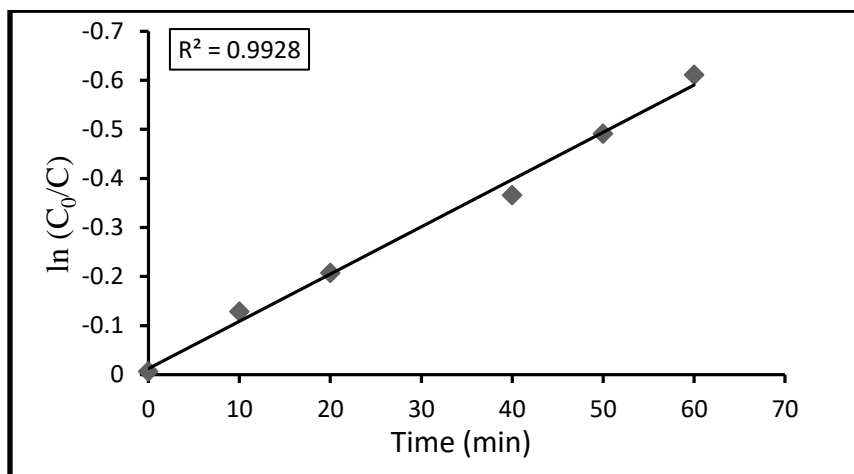


Fig. 4.30 (b): Pseudo first order kinetics: [DB-1] = 2.0×10^{-5} mol dm⁻³, ZnO NPs = 160 mg/100mL, pH = 6.5, Light intensity = 40×10^3 Lux.

4.4.2: Effect of change in pH:

The role of pH is very important in textile waste and hydroxyl radical generation as well. Hence several researchers studied the pH effect on dye degradation in presence of visible light. Photo-catalytic degradation process has been studied at pH values from 3.5 to 9.5. The effect of pH on the rate of degradation is shown in Table 4.21 and Figure 4.31. With increase in pH from 3.5 to 6.5, degradation rate constant increases from 3.15×10^{-4} s⁻¹ to 7.62×10^{-4} s⁻¹. Further increase in pH results in reduction in degradation rate constant. At higher pH value about 7.5, negatively charged active sites on the surface of ZnO NPs catalyst result in high concentration of positively charged dye molecules on the surface of ZnO NPs. In highly acidic medium, adsorption of lesser dye molecules inhibits the reaction rate. But ZnO has amphoteric nature and dissolving at low pH and salt formation takes place. At higher pH, it forms zincates such as $[\text{Zn}(\text{OH})_4]^{2-}$ [86]. All these factors were responsible for optimal value of photo-degradation of Direct Blue-1 dye at pH 6.5.

Table 4.21: Effect of change in pH: [DB-1] = 2.0×10^{-5} mol dm⁻³, ZnO NPs = 160mg/100mL, Light intensity = 40×10^3 Lux.

pH	$k \times 10^{-4} \text{ s}^{-1}$	$t_{1/2} \times 10^3 \text{ s}$
3.5	3.15	2.20
4.5	4.39	1.57
5.4	5.94	1.16
6.5	7.62	0.90
7.5	6.14	1.12
8.6	4.65	1.49
9.5	3.24	2.13

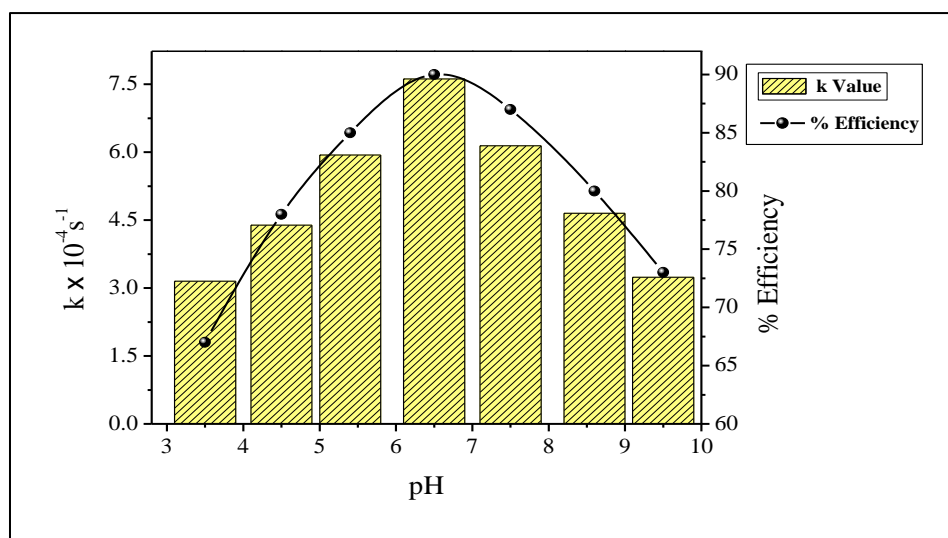


Fig. 4.31: Effect of change in pH on photo-catalytic degradation of DB-1

4.4.3: Effect of change in catalyst amount:

The effect of ZnO nanoparticles catalyst loading is basic parameter to assess the decolorization of DB-1 dye. Use of excess catalyst is a wastewater and it also hindered the rate of degradation of dye. A series of experiments have been carried out to assess the optimal catalyst amount by different amount of ZnO NPs catalyst from 80mg/100mL to 220mg/100mL at 2.0×10^{-5} mol dm⁻³ dye concentration in reaction solution. The rate of

degradation increased from $4.12 \times 10^{-4} \text{ s}^{-1}$ to $7.62 \times 10^{-4} \text{ s}^{-1}$ with increased in catalyst amount from 80mg/100mL to 160mg/100mL. Thereafter, rate constant decreases to $5.13 \times 10^{-4} \text{ s}^{-1}$ with increased catalyst amount 220mg/100mL. The rate of degradation is highest at 160mg/100mL of catalyst amount. This parameter analysis indicated that beyond optimum catalyst concentration, other factor applied also affected the dye degradation. Increase in amount of catalyst results in an increase of the available active sites in reaction condition. But higher concentration of catalyst also causes light scattering and decrease in infiltration of light in photo-active volume. Hence photo-active volume shrinks. At optimum ZnO nanoparticles amount of 160mg/100mL, both these conflicting aspects are evenly poised [77, 78]. All these factors suggest that optimal amount of ZnO NPs catalyst has to be added in the order to avoid unnecessary excess of catalyst also to ensure total absorption of light photons for efficient photo-catalytic degradation of DB-1 dye [87]. The results were shown in Table 4.22 and Figure 4.32.

Table 4.22: Effect of change in catalyst amount: [DB-1] = $2.0 \times 10^{-5} \text{ mol dm}^{-3}$, pH = 6.5, Light intensity = $40 \times 10^3 \text{ Lux}$.

ZnO mg/100mL	$k \times 10^{-4} \text{ s}^{-1}$	$t_{1/2} \times 10^3 \text{ s}$
80	4.12	1.68
100	5.04	1.37
120	5.82	1.19
140	6.34	1.09
160	7.62	0.90
180	6.72	1.03
200	6.01	1.15
220	5.13	1.35

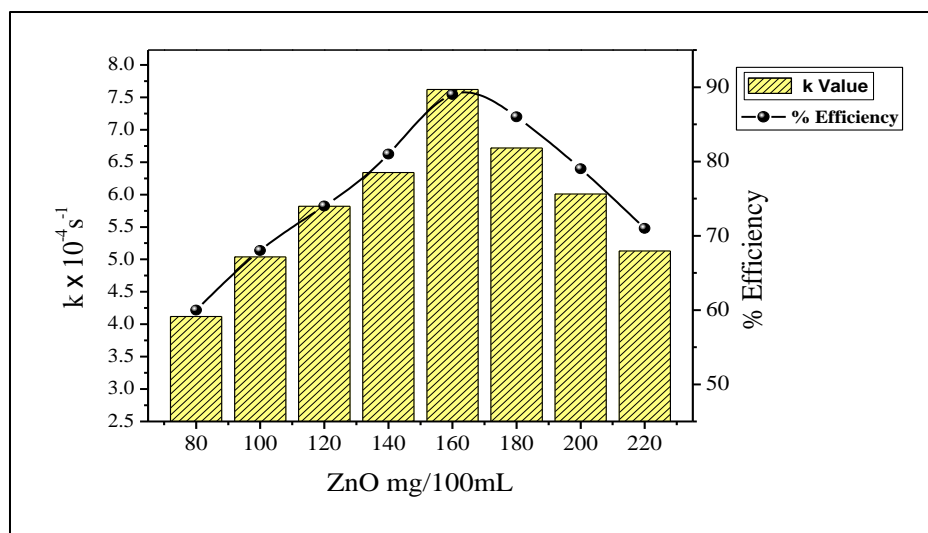


Fig. 4.32: Effect of change in catalyst amount on photo-catalytic degradation of DB-1

4.4.4: Effect of change in dye concentration:

The amount of industrial textile dye concentration is very important parameter in degradation of textile dye [80]. The decolorization of Direct Blue-1 dye at different initial concentrations from $1.0 \times 10^{-5} \text{ mol dm}^{-3}$ to $3.5 \times 10^{-5} \text{ mol dm}^{-3}$ was investigated under the optimized reaction conditions. It has been found that the rate of degradation increased from $3.08 \times 10^{-4} \text{ s}^{-1}$ to $7.62 \times 10^{-4} \text{ s}^{-1}$ with increase in Direct Blue-1 dye concentration from $1.0 \times 10^{-5} \text{ mol dm}^{-3}$ to $2.0 \times 10^{-5} \text{ mol dm}^{-3}$. Thereafter, rate constant of dye degradation decreased from $7.62 \times 10^{-4} \text{ s}^{-1}$ to $3.18 \times 10^{-4} \text{ s}^{-1}$ with increased dye solution concentration $2.0 \times 10^{-5} \text{ mol dm}^{-5}$ to $3.5 \times 10^{-5} \text{ mol dm}^{-3}$. The rate constant of degradation is optimum at $2.0 \times 10^{-5} \text{ mol dm}^{-3}$ of Direct Blue-1 dye concentration. Therefore, above optimal concentration with increase in dye concentration the rate of degradation decreases [81]. The results are shown in Table 4.23 and Figure 4.33. Several reports it is discussed that as the concentration of target textile dye increases more number of molecules get adsorbed on the catalyst surface. As the concentration of dye molecules increase may be occupied all the active sites of ZnO nanoparticle surface and

consequently, decrement of rate of degradation occurred. Hence the relative numbers of O_2^{\bullet} and hydroxyl radicals formed on the surface of semiconductors were also constant. Excessive adsorption of dye molecule on the catalyst surface hindered the viable adsorption of OH^- ions and lowers the formation rate of OH^{\bullet} radicals [27-29].

Table 4.23: Effect of change in dye concentration: ZnO NPs = 160 mg/100mL, pH = 6.5, Light intensity = 40×10^3 Lux.

[DB-1] $\times 10^{-5} \text{ mol dm}^{-3}$	k $\times 10^{-4} \text{ s}^{-1}$	$t_{1/2} \times 10^3 \text{ s}$
1.0	3.08	2.25
1.5	5.20	1.33
2.0	7.62	0.90
2.5	6.47	1.07
3.0	4.42	1.56
3.5	3.18	2.17

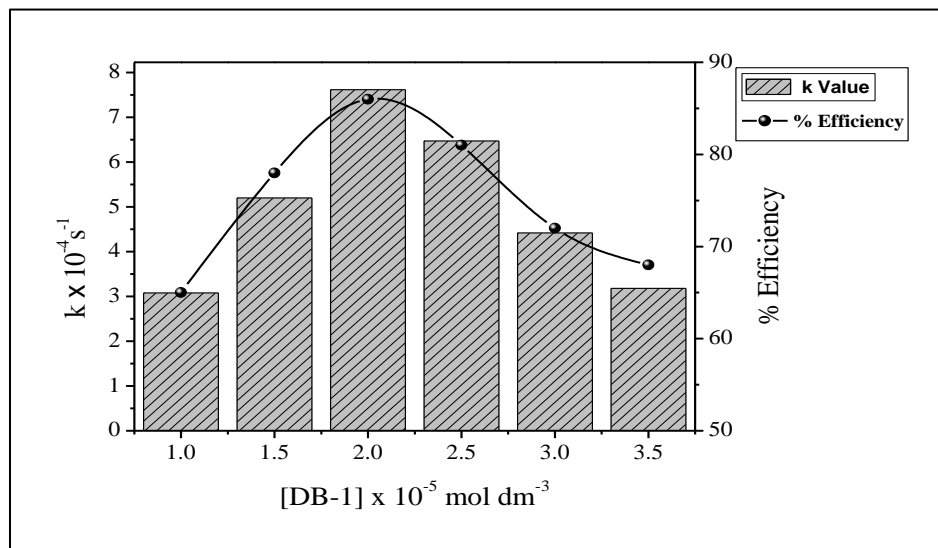
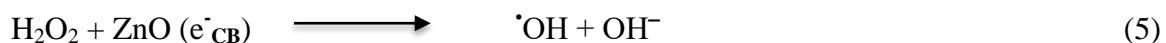


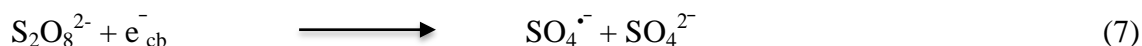
Fig. 4.33: Effect of change in dye concentration on photo-catalytic degradation of DB-1

4.4.5: Effect of change in oxidant's concentration:

The photo-catalytic degradation of Direct Blue-1 dye has been investigated at varied concentration of H_2O_2 and $\text{K}_2\text{S}_2\text{O}_8$. Rate constant of degradation of DB-1 dye increased from $8.03 \times 10^{-4} \text{s}^{-1}$ to $11.23 \times 10^{-4} \text{s}^{-1}$ with increasing H_2O_2 concentrations from $2.0 \times 10^{-6} \text{mol dm}^{-3}$ to $8 \times 10^{-6} \text{mol dm}^{-3}$ and rate constant of degradation of DB-1 dye increased from $8.12 \times 10^{-4} \text{s}^{-1}$ to $10.93 \times 10^{-4} \text{s}^{-1}$ with increasing $\text{K}_2\text{S}_2\text{O}_8$ concentrations from $2.0 \times 10^{-6} \text{mol dm}^{-3}$ to $8 \times 10^{-6} \text{mol dm}^{-3}$ respectively and reached to an optimum but above this concentration range, the increased H_2O_2 and $\text{K}_2\text{S}_2\text{O}_8$ concentration retarded the rate of degradation. The results are shown in Table 4.24 and Figure 4.34. At their respective low concentrations H_2O_2 and $\text{K}_2\text{S}_2\text{O}_8$ accelerate the reaction rate by producing an extremely strong and non-selective oxidant hydroxyl radical [88]. These hydroxyl radicals got generated by H_2O_2 and $\text{K}_2\text{S}_2\text{O}_8$ on account of scavenging the electrons from the conduction band of the photo-catalyst and this led to inhibit the electron-hole recombination process [30-33]. H_2O_2 may also split photo-catalytically to produce hydroxyl radicals directly by the absorption of visible light by the following reactions:



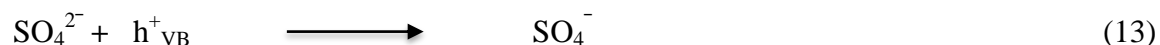
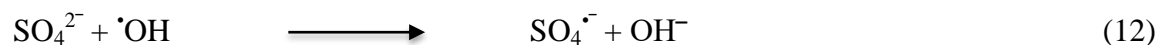
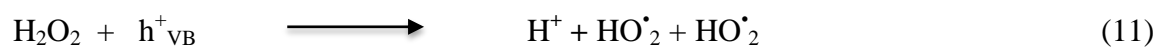
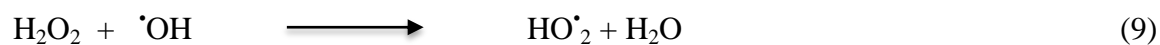
The $\text{S}_2\text{O}_8^{2-}$ anions generate strong oxidizing $\text{SO}_4^{\cdot-}$ radicals anion after trapping the photo-generated conduction band electrons of ZnO NPs as shown in the following reaction:



The generated sulfate radical anions ($\text{SO}_4^{\cdot-}$) participate in reaction with the solvent, according to the following reaction:



Different to this behavior, H_2O_2 and $\text{K}_2\text{S}_2\text{O}_8$ start behaving as scavenger for $\cdot\text{OH}$ radicals and hole at an excessive concentration. The photo-catalytic degradation of Direct Blue-1 dye will be inhibited in the condition of excess of H_2O_2 and $\text{K}_2\text{S}_2\text{O}_8$ as these are strong oxidants for organic pollutants. Furthermore, H_2O_2 and SO_4^{2-} can be adsorbed onto ZnO NPs deactivating a section of photo-catalyst and consequently decrease its photo-catalytic activity [34, 35].



Consequently, the proper addition of H_2O_2 and $\text{K}_2\text{S}_2\text{O}_8$ could accelerate the photo-degradation rate of DB-1 dye. However, in order to keep the efficiency of the added H_2O_2 and $\text{K}_2\text{S}_2\text{O}_8$, it was necessary to choose the proper concentration of H_2O_2 and $\text{K}_2\text{S}_2\text{O}_8$, according to the dye concentration.

Table 4.24: Effect of change in H_2O_2 and $\text{K}_2\text{S}_2\text{O}_8$: $[\text{DB-1}] = 2.0 \times 10^{-5} \text{ mol dm}^{-3}$,
 $\text{ZnO NPs} = 160 \text{ mg}/100\text{mL}$, $\text{pH} = 6.5$, Light intensity = $40 \times 10^3 \text{ Lux}$.

[Oxidant] x $10^{-6} \text{ mol dm}^{-3}$	[H_2O_2]		[$\text{K}_2\text{S}_2\text{O}_8$]	
	$k \times 10^{-4} \text{ s}^{-1}$	$t_{1/2} \times 10^3 \text{ s}$	$k \times 10^{-4} \text{ s}^{-1}$	$t_{1/2} \times 10^3 \text{ s}$
0.0	7.62	0.90	7.62	0.90
2.0	8.03	0.86	8.12	0.85
4.0	9.94	0.69	9.74	0.71
6.0	10.38	0.66	10.15	0.68
8.0	11.23	0.61	10.93	0.63
10.0	10.29	0.67	9.09	0.76
12.0	9.76	0.71	8.77	0.79
14.0	9.11	0.76	8.15	0.85

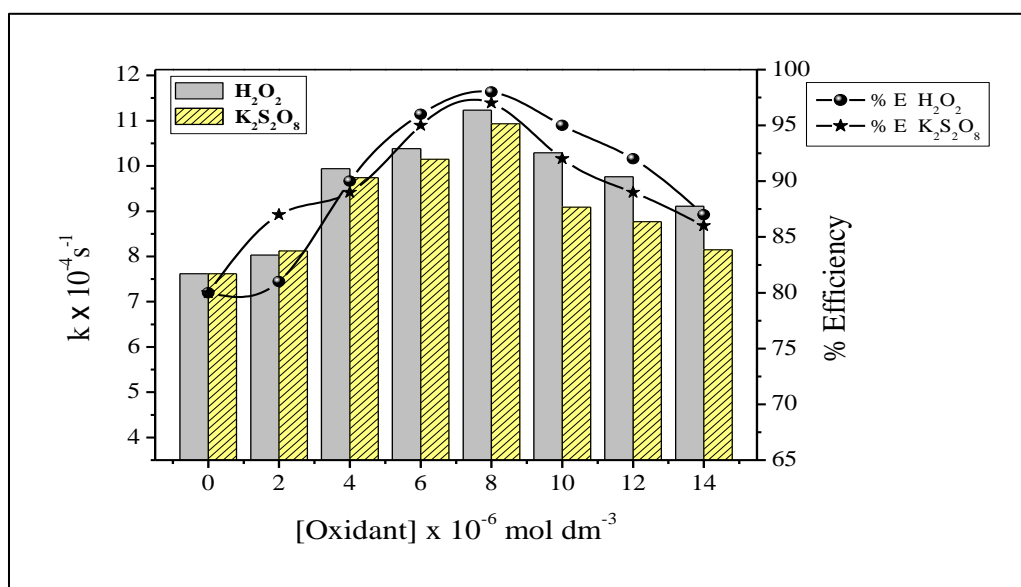
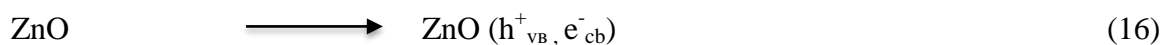
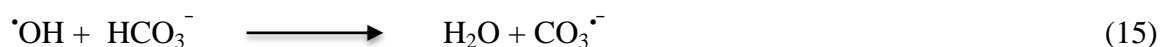
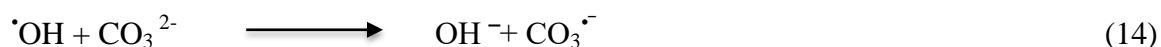


Fig. 4.34: Effect of change in oxidants on photo-catalytic degradation of DB-1

4.4.6: Effect of change in salts concentration:

The industrial textile wastewater from dyeing process usually contain considerable amount of CO_3^{2-} and Chloride ions. The chemicals are often used in textile processing for

adjust pH of the dye bath. The presence of several anions chloride, carbonate and bicarbonate is industrial wastes. Adsorption of degrading species are affected by these ions and acting as OH⁻ ion scavengers as well as adsorbs light radiation, which also an important factor in mainly photo-catalytic degradation of dye [89]. With an increase in the amount of carbonate ion from 2.0 x 10⁻⁵ mol dm⁻³ to 12.0 x 10⁻⁵ mol dm⁻³ resulted into decrease of rate constant from 6.95 x 10⁻⁴ s⁻¹ to 4.65 x 10⁻⁴ s⁻¹. The inhibition in the degradation of dye is due to the hydroxyl scavenging property of carbonate ions, which can be accounted from the following equation. Similarly, NaCl commonly comes out in the effluent along with wastewater. Therefore photo-catalytic degradation rate in presence of Cl⁻ ions has been studied by increase in concentration of Cl⁻ ions from 2.0 x 10⁻⁵ mol dm⁻³ to 12 x 10⁻⁵ mol dm⁻³ that resulted into reduction of rate constant from 6.86 x 10⁻⁴ s⁻¹ to 4.92 x 10⁻⁴ s⁻¹. The decrease in the degradation of dye in the presence of Cl⁻ ion might be due to the hole scavenging properties of chloride ion [38].



The $\cdot\text{OH}$ radical which is a primary oxidant for the photo-catalytic degradation of dye reported to decrease slowly with an increase in carbonate ions and degradation of the dye significantly decreased [37]. The results are shown in Table 4.25 and Figure 4.35 is the dependency of reaction rate constant on the concentration of Na₂CO₃ and NaCl.

Table 4.25: Effect of change in Na₂CO₃ and NaCl: [DB-1] = 2.0 × 10⁻⁵ mol dm⁻³, ZnO NPs = 160 mg/100mL, pH = 6.5, Light intensity = 40 × 10³ Lux.

[Salt] × 10 ⁻⁵ mol dm ⁻³	[Na ₂ CO ₃]		[NaCl]	
	K × 10 ⁻⁴ s ⁻¹	t _{1/2} × 10 ³ s	k × 10 ⁻⁴ s ⁻¹	t _{1/2} × 10 ³ s
0.0	7.62	0.90	7.62	0.90
2.0	6.95	0.99	6.86	1.01
4.0	6.54	1.05	6.68	1.03
6.0	6.07	1.14	6.26	1.10
8.0	5.66	1.22	5.87	1.18
10.0	5.18	1.33	5.36	1.29
12.0	4.65	1.49	4.92	1.40

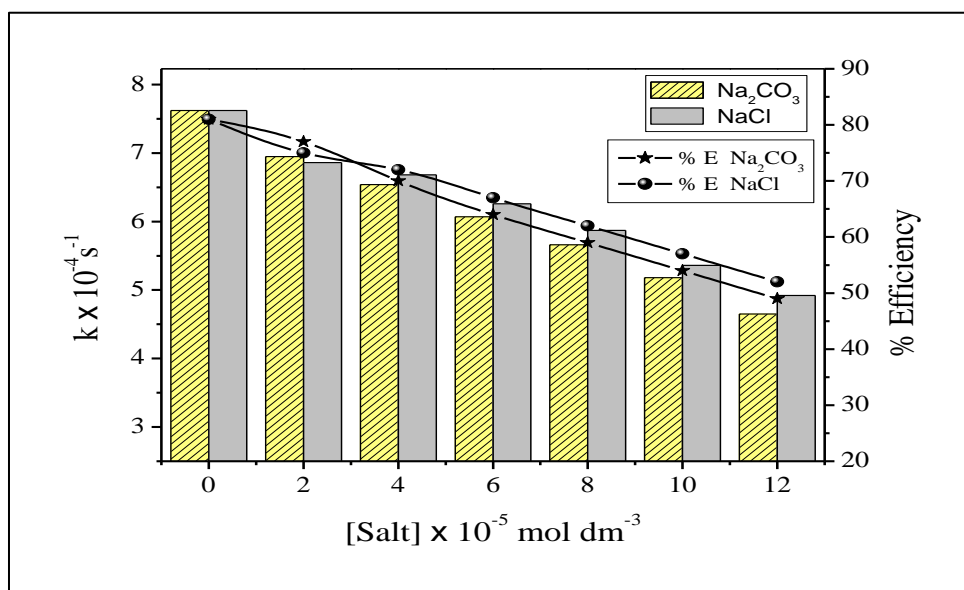
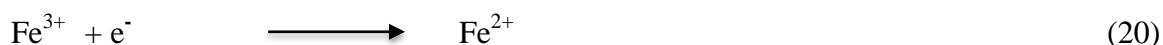


Fig. 4.35: Effect of change in salts on photo-catalytic degradation of DB-1

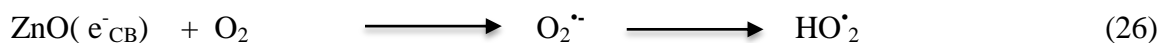
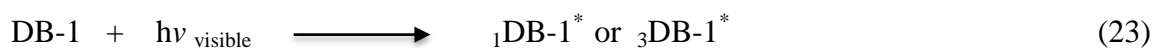
4.4.7: Effect of FeCl₃ change in concentration:

The effect of FeCl₃ on the photo-catalytic mineralization of Direct Blue-1 dye has been studied. The metal ions such as Fe³⁺ could be used as sensitizers during photo-catalytic degradation of dye. The photo-catalytic degradation process was evaluated observed

effect of FeCl₃ on Direct Blue-1 dye oxidation with Zinc oxide nanoparticles using visible light. It was observed that when FeCl₃ was varied concentration from 2.0 x 10⁻⁵ mol dm⁻³ to 12.0 x 10⁻⁵ mol dm⁻³. The degradation rate constant increased from 8.19 x 10⁻⁴ s⁻¹ to 10.06 x 10⁻⁴ s⁻¹ with the increase in concentration of FeCl₃ from 2.0 x 10⁻⁵ mol dm⁻³ to 8.0 x 10⁻⁵ mol dm⁻³. Thereafter, degradation rate constant decreased to 8.12 x 10⁻⁴ s⁻¹ on further increase in amount of FeCl₃ up to 12.0 x 10⁻⁵ mol dm⁻³. The results are shown in Table 4.26 and Fig. 4.36. In fact the increase in ferric ions concentration in the reaction mixture resulted into the increase of Fe²⁺ ions concentration, which is accompanied by improved formation of [•]OH radicals, consequently increasing rate of degradation of FeCl₃ inhibits the reaction rate of degradation by competing with formation of [•]OH radicals [90, 91].



The photo-activation of surface adsorbed complex ion (Fe³⁺OH⁻) results in the formation of Fe²⁺OH[•] specie which injects electrons to the conduction band of ZnO as shown in [Eq. 24-25]. The rate of decolorization in case of FeCl₃ is explicable due to rapid scavenging of conduction band electrons by molecular oxygen leading to formation of superoxide and hydroperoxide radicals [42, 43] [Eq. (25)].



In the presence of higher concentration of FeCl_3 , there is excessive surface adsorption of dye on the surfaces of catalyst [44]. This reduced the total photoactive area of ZnO NPs catalyst and lowered the rate of reaction [45].

Table 4.26: Effect of change in FeCl_3 concentration: $[\text{DB-1}] = 2.0 \times 10^{-5} \text{ mol dm}^{-3}$,
ZnO NPs = 160 mg/100mL, pH = 6.5, Light intensity = $40 \times 10^3 \text{ Lux}$.

$\text{FeCl}_3 \times 10^{-5} \text{ mol dm}^{-3}$	$k \times 10^{-4} \text{ s}^{-1}$	$t_{1/2} \times 10^3 \text{ s}$
0.0	7.62	0.90
2.0	8.19	0.84
4.0	8.63	0.80
6.0	9.58	0.72
8.0	10.06	0.68
10.0	9.16	0.75
12.0	8.42	0.82

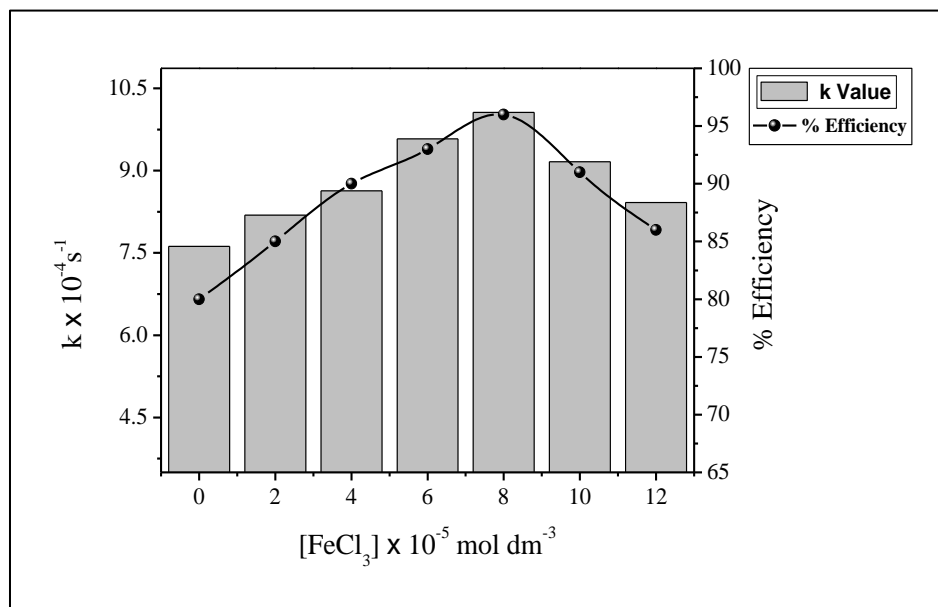


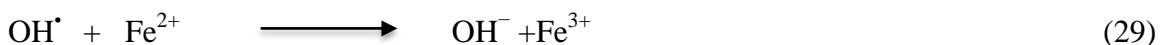
Fig. 4.36: Effect of change in FeCl_3 on photo-catalytic degradation of DB-1

4.4.8: Effect of change in Fenton's reagent concentration:

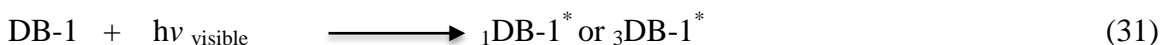
Photo-Fenton's process is one of the most common AOPs which is based on the formation of very reactive species such as $\cdot\text{OH}$ radicals, which have a very strong oxidative potential second only to fluorine. $\cdot\text{OH}$ radicals rapidly and non selectively oxidize a broad range of dyes pollutants. Fenton like reagent is an attractive usage for the effective degradation of dyes because of its low cost and lack of toxicity of the reagents like H_2O_2 and Fe^{2+} or Fe^{3+} [92]. Fenton's reagent, a mixture of Fe^{3+} and H_2O_2 has been known as a powerful oxidant for textile dyes [48, 49].



$\text{OH}\cdot$ radicals may be scavenged by reaction with another Fe^{2+} :



In present study Fenton's reagent for degradation of Direct Blue-1 dye in presence of ZnO nanoparticles in visible light has been studied. The degradation rate constant has a value of $8.06 \times 10^{-4} \text{ s}^{-1}$ on the addition of $\text{Fe}^{3+}:\text{H}_2\text{O}_2$ in molar ratio 1:2. In the presence of $\text{Fe}^{3+}:\text{H}_2\text{O}_2$ in molar ratio 3:4, rate constant has been found $10.13 \times 10^{-4} \text{ s}^{-1}$. The results are shown in Table 4.27 and Figure 4.37. Upon irradiation of $\text{Fe}^{3+}/\text{H}_2\text{O}_2/\text{ZnO}/\text{DB-1}$ system in the presence of visible light, formation of $\text{OH}\cdot$ radicals increased relating a complex mechanism. Visible radiation is absorbed by dye and excited to high energy state from ground state and this excited dye molecules reduce ferric ion complex into ferrous ion complex followed by the transfer to ferric ion [93]. The reduced ferrous ions react with hydrogen peroxide to decompose and produce hydroxyl radical [Eq. (33)]. $\text{OH}\cdot$ radicals also decompose H_2O_2 to $\cdot\text{HO}_2$.



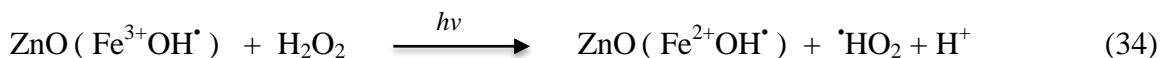


Table 4.27: Effect of change in $\text{Fe}^{3+}/\text{H}_2\text{O}_2$: $[\text{DB-1}] = 2.0 \times 10^{-5} \text{ mol dm}^{-3}$,

ZnO NPs = 160 mg/100mL, pH = 6.5, Light intensity = $40 \times 10^3 \text{ Lux}$.

$\text{Fe}^{3+}:\text{H}_2\text{O}_2$	Without ZnO		With ZnO	
	$k \times 10^{-4} \text{ s}^{-1}$	$t_{1/2} \times 10^3 \text{ s}$	$k \times 10^{-4} \text{ s}^{-1}$	$t_{1/2} \times 10^3 \text{ s}$
1:2	0.87	7.96	8.06	0.85
1.5:2	1.24	5.58	8.75	0.79
2.5:4	1.91	3.62	9.35	0.74
3:4	2.32	2.98	10.13	0.68
4:5	2.67	2.59	9.69	0.71
5:6	2.94	2.35	8.26	0.83

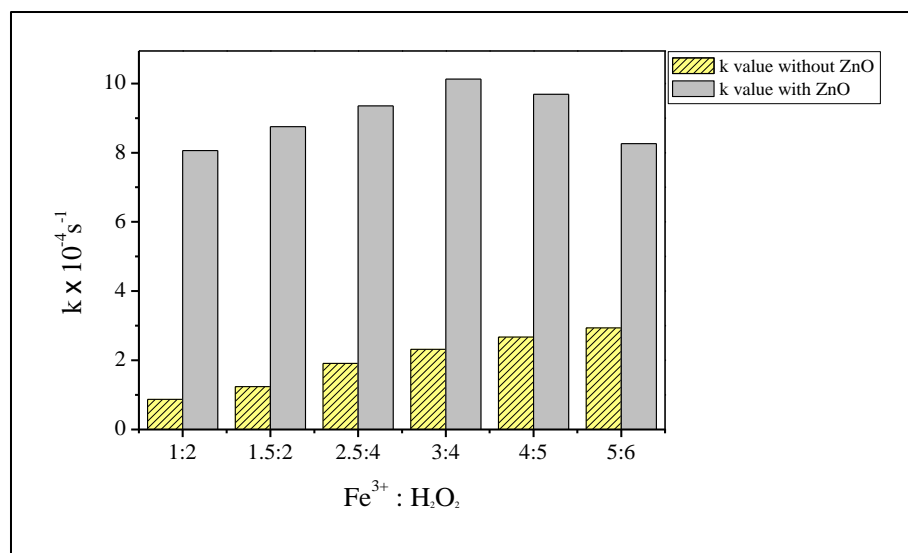


Fig. 4.37: Effect of change in Fenton's reagent on photo-catalytic degradation of DB-1

4.4.9: Effect of change in light intensity:

The effect of light intensity on photo-catalytic degradation rate was investigated and the results are given in Table 4.28 and Figure 4.38. By varying the intensity of light increasing from 20×10^3 Lux to 60×10^3 Lux for DB-1 dye solution concentration 2.0×10^{-5} mol dm⁻³, ZnO NPs catalyst amount 160 mg/100mL and pH 6.5. The rate of degradation constant increased from 5.27×10^{-4} s⁻¹ to 8.95×10^{-4} s⁻¹ as shown in the figure. It may be explained on the basis of number of excited molecules. As more light intensity falls on ZnO molecules, more number of molecules get excited which in turn may degrade more dye molecules and thus the rate of photo-catalytic degradation was found to increase with increase in light intensity [94].

Table 4.28: Effect of change in light intensity: [DB-1] = 2.0×10^{-5} mol dm⁻³, ZnO NPs = 160 mg/100mL, pH = 6.5.

Light intensity $\times 10^3$ lux	$k \times 10^{-4} \text{ s}^{-1}$	$t_{1/2} \times 10^3 \text{ s}$
20	5.27	1.31
30	6.74	1.02
40	7.62	0.90
50	8.29	0.83
60	8.95	0.77

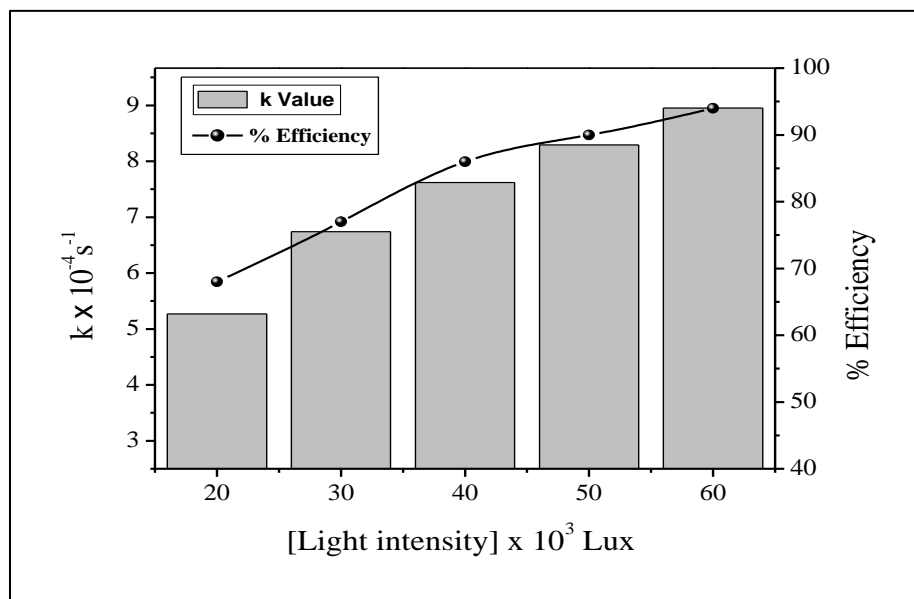


Fig. 4.38: Effect of change in light intensity on photo-catalytic degradation of DB-1

4.4.10: Effect of bubbling of N₂ and O₂:

The photo-catalytic degradation reactions were carried out in presence of catalyst by bubbling O₂ or N₂ in a closed reactor. The degradation of DB-1 dye has been severely retarded by bubbling of pure N₂ decrease in rate constant but increases rapidly on bubbling oxygen through the dye solution. These observations confirm the proposed

assumption that dissolved oxygen is a precursor of main oxidant, that is, the role of DO is to trap the photo-generated electrons to produce $O_2^{\cdot-}$ radicals, which particles in photo-catalytic process to accelerate the DB-1 dye photo-degradation. In the oxygenated solution oxygen get adsorb on the surface of the photo-catalyst, preventing electron-hole recombination by trapping electron and producing superoxide anion radicals. With the improved charge separation more numbers of photo-generated holes becomes available to take part in photo oxidation reactions. The results are shown in Fig. 4.39 [53, 54].

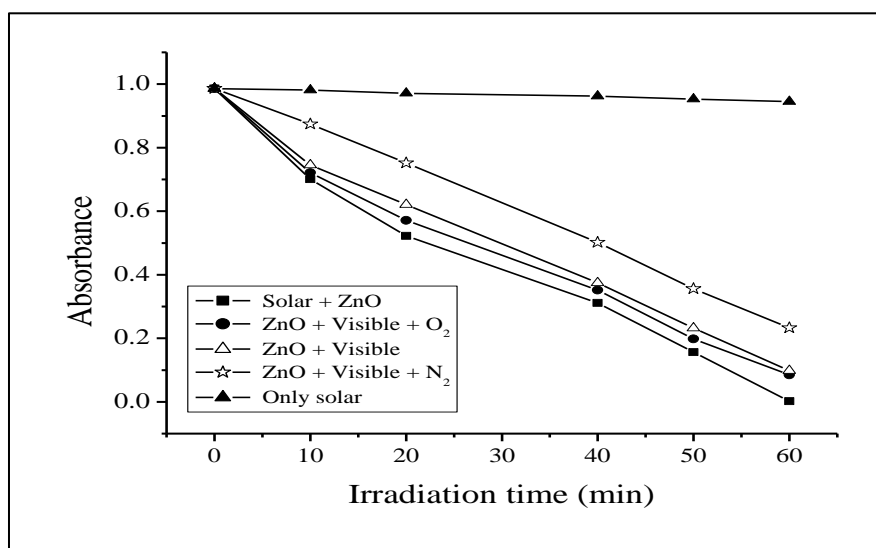
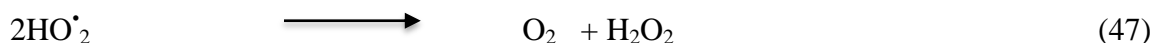
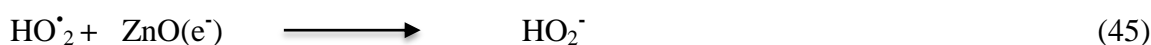
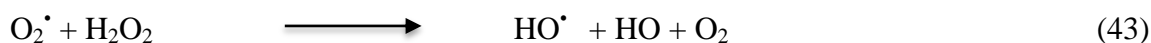
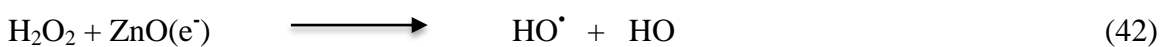


Fig. 4.39: Decolorization of DB-1 under various photo-catalytic systems: [DB-1] = $2.0 \times 10^{-5} \text{ mol dm}^{-3}$, ZnO NPs = 160 mg/100mL, pH = 6.5, Light intensity = $40 \times 10^3 \text{ Lux}$.

4.4.11: Comparison of solar and visible light:

The efficiency of solar and visible light on photo-catalytic degradation of dye was comparatively studied. The degradation efficiency of Direct Blue-1 dye with visible light was found to be more efficient than that of solar light. Figure 4.39 shows the comparisons of color removal efficiency of Direct Blue-1 dye with two light sources under different conditions. It was noticed that if same experiments were carried out in the absence of ZnO, then no absorbance loss of dye was found [55, 56].

4.4.12: Effect of other photo-catalysts:

In order to understand the more photo-catalytic efficiency of ZnO NPs towards photo-catalytic degradation of DB-1 dye, identical experiments were carried out with commercial ZnO, BiOCl, TiO₂ and BaCrO₄ using visible light irradiated. The results are shown in Table 4.29 and Figure 4.40. The heterogeneous photo-catalyst i. e. ZnO nanoparticles reaction occurred on surface when illumination with light of energy equal or more than band gap of photo-catalyst [57]. We have investigated the relative efficiencies of other photo-catalysts. BaCrO₄ with smaller band gap shows less activity since its conduction band is much lower than that of ZnO NPs and TiO₂. The smaller band gap permits rapid recombination of electron-hole and so electron in these catalysts cannot move into the electron acceptors in the solution rapidly. Hence low photo-catalytic activity was observed in these semiconductors [58]. It is for these reasons; the prepared ZnO nano photo-catalyst has more photo-catalytic efficiency than other photo-catalysts.

Table 4.29: Effect of other photo-catalysts: [DB-1] = 2.0×10^{-5} mol dm⁻³, pH = 6.5,
Light intensity = 40×10^3 Lux.

Catalysts (160mg/100mL)	$k \times 10^{-4} \text{ s}^{-1}$	$t_{1/2} \times 10^3 \text{ s}$
ZnO NPs	7.62	0.90
ZnO	5.36	1.29
BiOCl	4.58	1.51
TiO ₂	3.61	1.91
BaCrO ₄	2.34	2.96

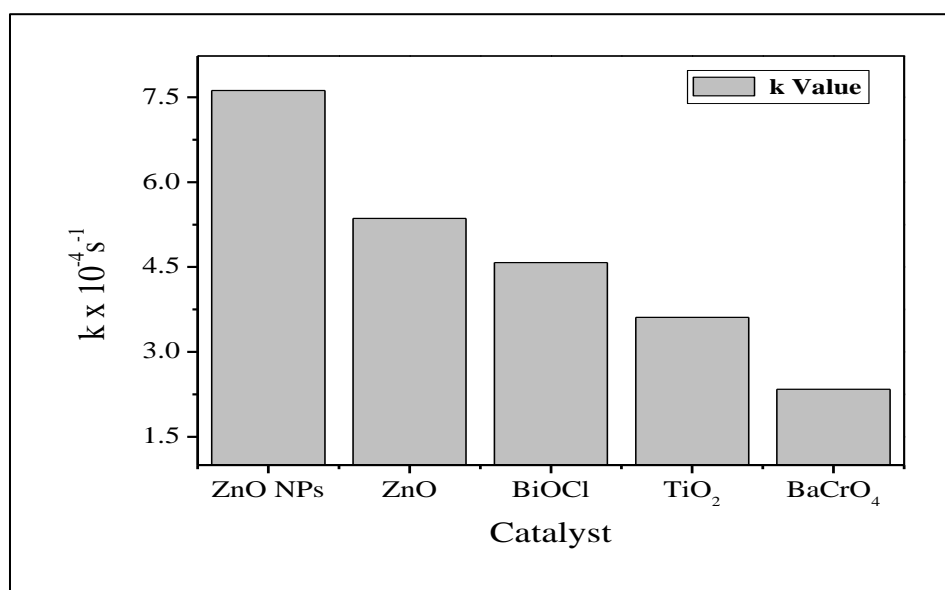


Fig. 4.40: Effect of other photo-catalysts on photo-catalytic degradation of DB-1

4.4.13: Test for reusability of ZnO NPs:

To determine the activity of ZnO NPs, this catalyst was further tested for two extra cycles and noted that catalyst did not show any significant loss of photo-degradation activity

against Direct Blue-1 dye. This indicates that ZnO is more stable and has better photo-catalytic performance on Direct Blue-1 dye degradation. Fig.4.41 shown as:

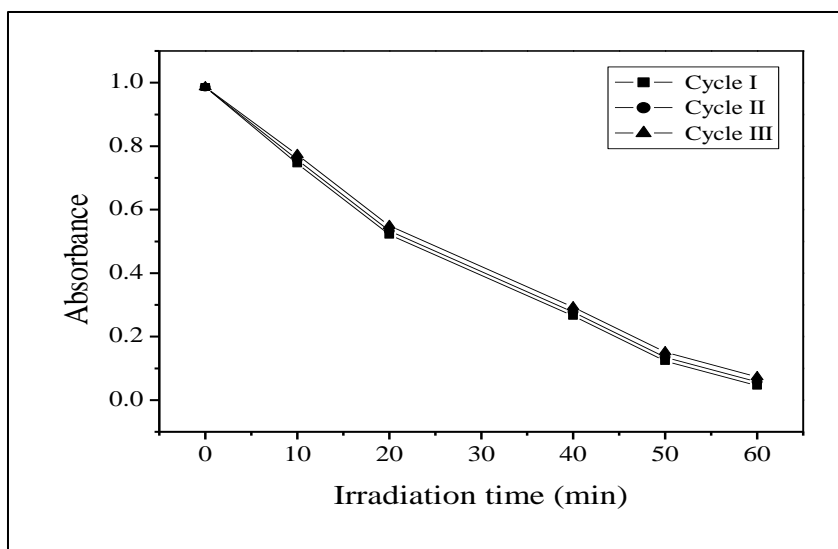


Fig. 4.41: Decolorization of DB-1 by ZnO NPs: (I) Cycle; (II) Cycle; (III) Cycle:
[DB-1] = 2.0×10^{-5} mol dm⁻³, ZnO NPs = 160 mg/100mL, pH = 6.5,
Light intensity = 40×10^3 Lux.

4.4.14: COD and CO₂ measurements during degradation of DB-1:

Chemical oxygen demand resulted were taken as one of the parameter to determine the feasibility of the reduction process for Direct Blue-1 dye degradation. The COD of the DB-1 dye solution before and after the treatment was valued. The efficiency of photo-catalytic treatment to mineralize the dyes was studied. COD test is one of the best and effective processor which is also largely used as most an effective and efficient procedure to determine the strength of wastewater. It measured the waste in terms of total oxygen required for the degradation of dye and other waste substance present in water [95]. Increases in COD of treated water in comparison with untreated solution showed that mineralization along with decoloration of dye molecules are taking place. The reduction

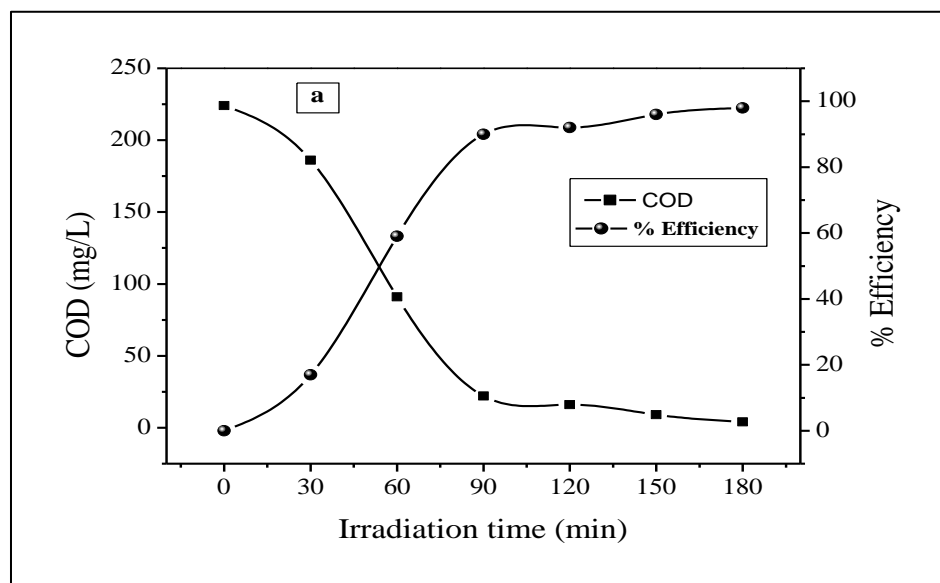
in the estimated COD from 224 mg/L to 4 mg/L and increase in CO₂ values from 24mg/L to 175 mg/L in 180 min of illumination indicated the complete mineralization of treated dye solution. A decrease in pH has also been observed with increase in the quantity of mineralization. The results were shown as Table 4.30 and Figure 4.42 (a) and (b).

Table 4.30: COD and CO₂ measurements during degradation of DB-1:

[DB-1] = 2.0×10^{-5} mol dm⁻³, ZnO NPs = 160 mg/100mL, pH = 6.5,

Light intensity = 40×10^3 Lux.

Time (min)	COD (mg/L)	CO ₂ (mg/L)	Efficiency (%)	NO ₃ ⁻ (mg/L)
0	224	24	0	0
30	186	36	17	8
60	91	54	59	14.5
90	22	96	90	17.2
120	16	136	92	21.4
150	9	154	96	29
180	4	175	98	31



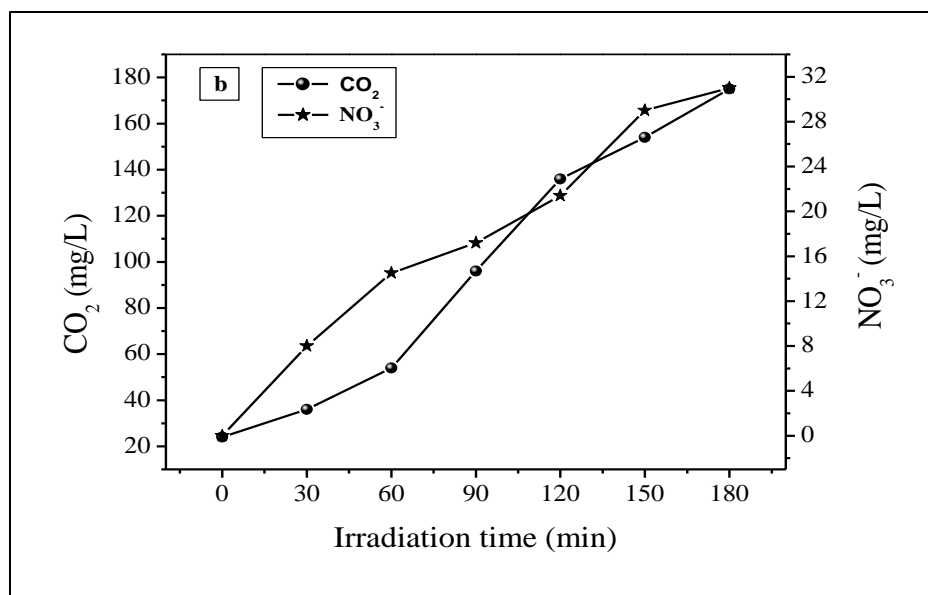
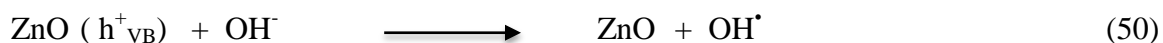


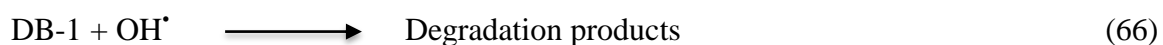
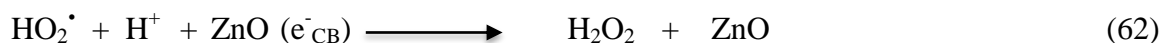
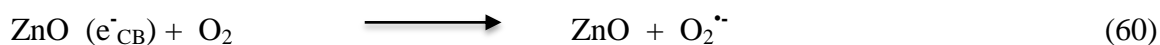
Fig. 4.42: (a) COD trend and % Efficiency (b) CO₂ trend and formation of NO₃⁻ during mineralization of Direct Blue-1: [DB-1] = 2.0 × 10⁻⁵ mol dm⁻³, ZnO NPs = 160 mg/100mL, pH = 6.5, Light intensity = 40 × 10³ Lux.

4.4.15: Mechanism of Direct Blue-1 dye degradation:

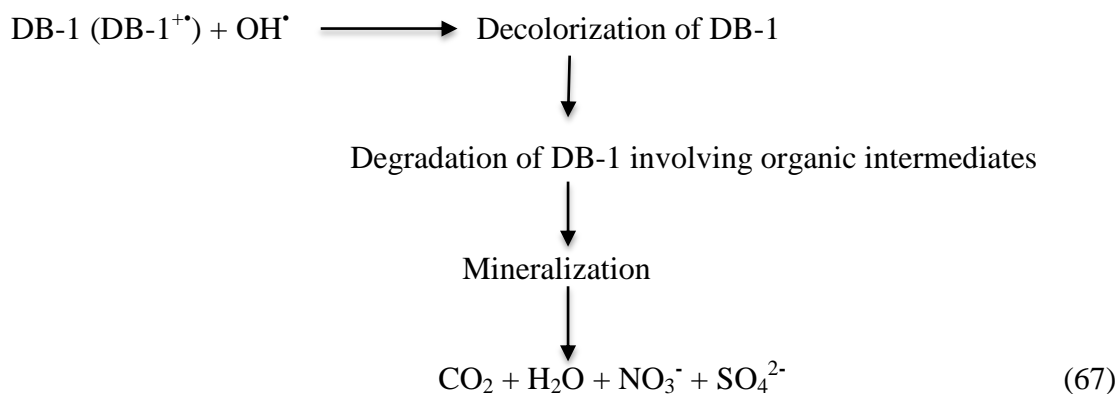
The photo-catalytic degradation of the Direct Blue-1 dye was studied by the use of additives such as H₂O₂, K₂S₂O₈ etc. electron scavengers like H₂O₂ and K₂S₂O₈ accept a photo-generated electron from the conduction band (CB) and thus avoid electron-hole recombination producing OH[•] [61]. Valence band holes (h_{vb}⁺) and conduction band electrons (e_{cb}⁻) are generated when aqueous ZnO NPs suspension is irradiated with visible light energy when band gap energy is greater than (E_g = 3.2 eV) and these electron-hole pairs interact separately with another molecule. Conduction band electrons (e_{CB}⁻) reduce molecular oxygen to generate superoxide radicals, as shown in Eq. (48) to Eq. (57) [62-64]. Such electron generated disrupted the conjugation system of dye and decomposition of dye and the hole so generated creates OH[•] from water which again leads to degradation of dye. The mechanism is as follows: [65, 66]



Secondly, sensitization of dye molecule by visible light leads to excitation of dye molecule in singlet or triplet state, subsequently followed by electron injection from excited dye molecule onto conduction band of semiconductor particles. The mechanism of dye sensitization is summarized in Eq. (58) to Eq. (67) [67-71].

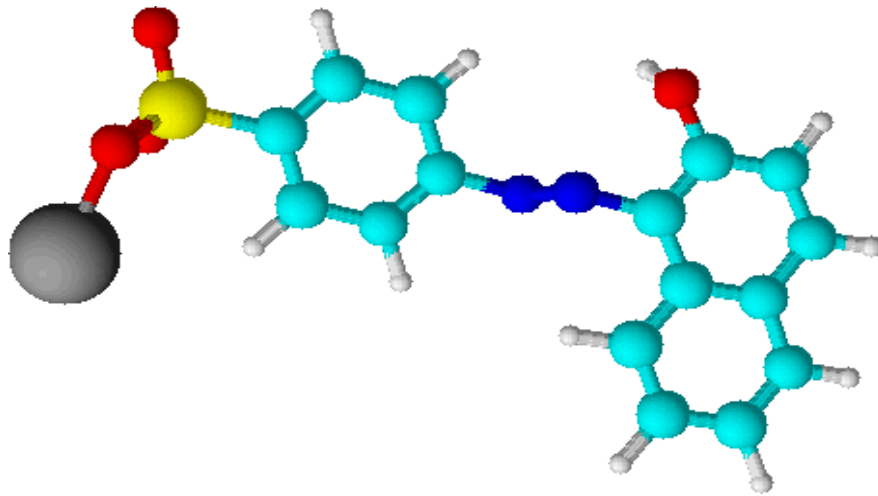


The mechanism of semiconductor photo-catalysis is of very complex nature. Dye molecules interact with $O_2^{\cdot-}$, $\cdot OH_2$, or OH^{\cdot} species to generate intermediates ultimately lead to degradation products. OH^{\cdot} radical being very strong oxidizing agent (oxidation potential 3.2 eV) mineralizes dye to various end products. The role of reductive pathways in heterogeneous photo-catalysis has been found to be in minor extent as compared to oxidation [72, 73].



DB-1 = Direct Blue-1

Orange II



Orange II has a chromophoric system containing azo group-N=N- in association with two aromatic system. It is anionic in nature attach strongly to cationic groups in the fiber directly. They can be applicable to use for natural fibers like wool, cotton and silk as well as to synthetics like polyesters, acrylic and rayon, paints, inks, plastics and leather.

4.5: Effect of various experimental parameters on the degradation rate of Orange-II (OII) dye

4.5.1: Photo-catalytic degradation of Orange-II (OII):

On the surface of catalyst classical Langmuir–Hinshelwood expression was followed by the photo-catalytic degradation rate of Orange II dye and followed most often Langmuir sorption isotherm for the sorption of the dye to the catalyst surface. This theory is usually used kinetic model for unfolding photo-catalytic behavior. For treatment of heterogeneous surface reactions degradation rate is explained by pseudo first order kinetics in Langmuir–Hinshelwood [11-14]. Such kinetics is streamlined in terms of modified model to accommodate reactions taking place at solid-liquid interface as

$$r = \frac{-dc}{dt} = \frac{k_r KC}{(1+KC)} \quad (1)$$

Where, r = rate of dye disappearance and C = variable dye concentration at time t . K = equilibrium constant for adsorption of Orange II dye on photo-catalyst and k_r = limiting reaction rate at maximum coverage in operational conditions. The integrated form can be written as

$$t = \ln\left(\frac{C_0}{C}\right) + \frac{1}{Kk_r} \frac{C_0 - C}{k_r} \quad (2)$$

Where t = time required for the initial concentration of dye C_0 to C . At low dye concentration in equation 2, value of C_0 is very less and hence can be neglected.

$$\ln\left(\frac{C_0}{C}\right) = k_r Kt = kt \quad (3)$$

Where k = apparent rate constant of degradation. The Half-life time ($t_{1/2}$) for the photo-catalytic degradation of Orange II dye on the ZnO NPs surface can be calculated by using following Eq. (4)

$$t_{1/2} = \frac{0.693}{k} \quad (4)$$

The Orange II dye degradation results are reported here for three conditions: (1) Orange II dye + ZnO NPs + visible light (2) Orange II dye + visible light only and (3) Orange II dye + ZnO nanoparticles only (dark) were shown in figure 4.43 (a). It was observed carefully that maximum degradation occurred in the first condition, while in dark and during photolysis, no significant changes in the absorbance values were observed. Therefore, in second and third condition, degradation process was not observed. Absorption spectrum changes were recorded at 480nm wavelength.

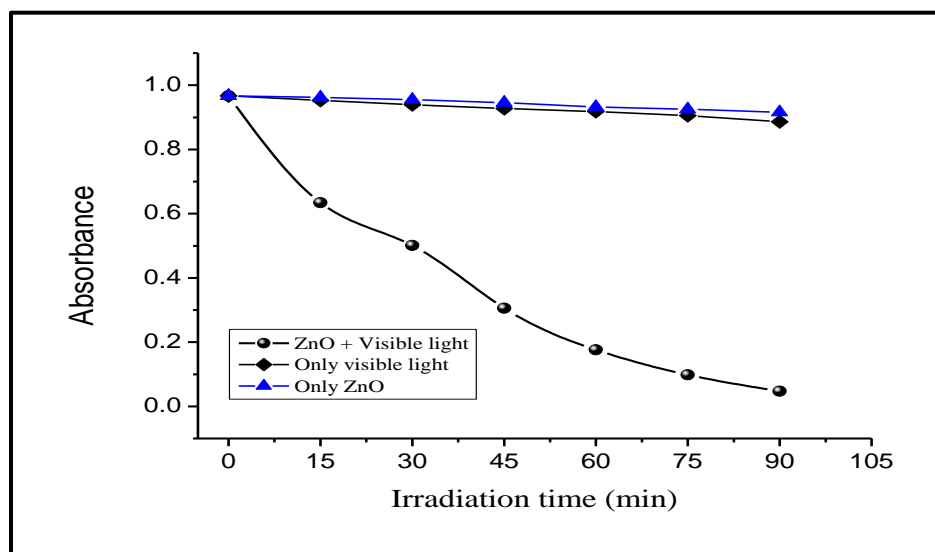


Fig. 4.43 (a) Degradation of Orange-II: $[OII] = 5.2 \times 10^{-5} \text{ mol dm}^{-3}$, ZnO NPs = 90 mg/100mL, pH = 7.5, Light intensity = $35 \times 10^3 \text{ Lux}$.

Plotting the semi-logarithmic graph of concentration versus irradiation time (min) of Orange-II dye in the presence of ZnO NPs yielded a linear relationship as shown in figure 4.43 (b). Therefore, reaction dye of degradation by ZnO nanoparticles is pseudo-first order reaction kinetics, with regression coefficient of 0.978, Orange II dye degradation rate constant of $4.95 \times 10^{-4} \text{ s}^{-1}$. The rate constant is the slope of the straight line. In all

cases R^2 (correlation constant for the fitted line) values were close to 0.99 which confirmed pseudo 1st-order kinetics for Orange-II dye mineralization in this process.

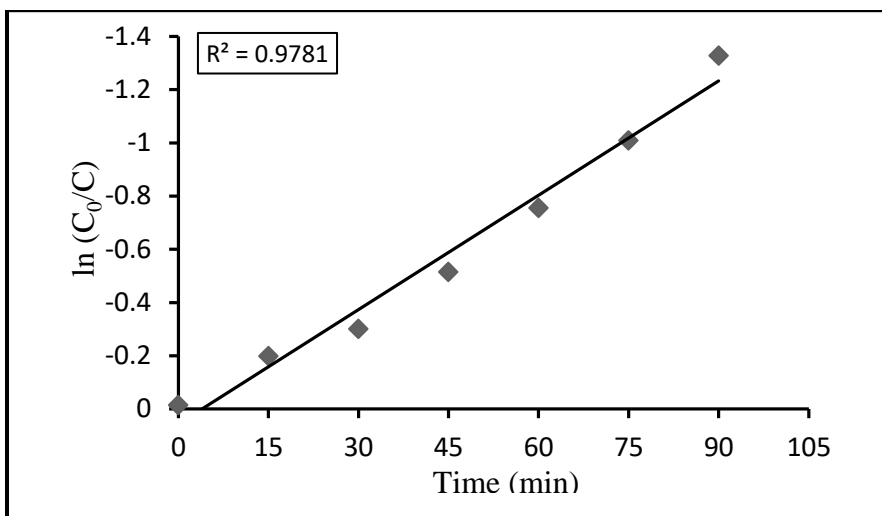


Fig. 4.43 (b): Pseudo first order kinetics: $[OII] = 5.2 \times 10^{-5} \text{ mol dm}^{-3}$, ZnO NPs = 90 mg/100mL, pH = 7.5, Light intensity = $35 \times 10^3 \text{ Lux}$.

4.5.2: Effect of change in pH:

The pH is very important parameter in the photo-catalytic degradation reaction. Wastewater containing dyes is discharged at different pH; consequently it is important to study the role of pH on the decolorization of dye. In order to investigate the influence of pH on the degradation efficiency, experiments were carried out at various pH values, ranging from 4.5 to 10.5. The effect of pH on the rate of degradation results is shown in Table 4.31 and Figure 4.44. With increase in pH from 4.5 to 7.5, degradation rate constant increases from $3.13 \times 10^{-4} \text{ s}^{-1}$ to $4.95 \times 10^{-4} \text{ s}^{-1}$. Further increase in pH results in reduction in degradation rate constant. The pH of zero point charge for ZnO is about 9.3 [96, 97]. At higher value of pH about 7.5, negatively charged active sites on the surface of ZnO NPs catalyst result in high concentration of positively charged dye molecules on the surface of ZnO NPs. It gets dissolved at lower pH, forming salts. At higher pH, it

forms zincates [98]. All these factors are responsible for optimal value of photo-degradation of Orange II dye at pH 7.5.

Table 4.31: Effect of change in pH: [Orange-II] = 5.2×10^{-5} mol dm⁻³, ZnO NPs = 90 mg/100mL, Light intensity = 35×10^3 Lux.

pH	$k \times 10^{-4} \text{ s}^{-1}$	$t_{1/2} \times 10^3 \text{ s}$
4.5	3.13	2.21
5.5	3.84	1.80
6.5	4.35	1.59
7.5	4.95	1.40
8.5	4.44	1.56
9.5	3.75	1.84
10.5	3.06	2.26

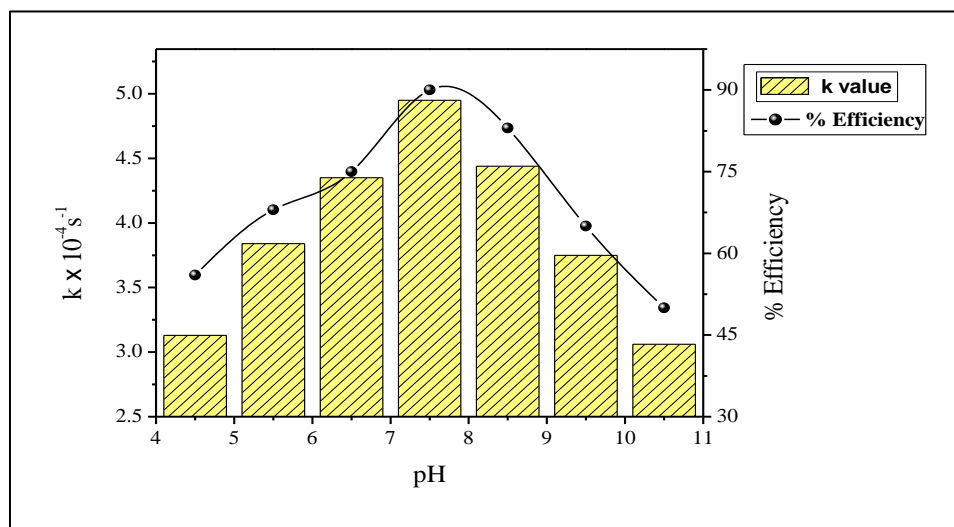


Fig. 4.44: Effect of change in pH on photo-catalytic degradation of O-II

4.5.3: Effect of change in catalyst amount:

The effect of catalyst amount is an important parameter affecting the efficiency of photo-catalytic degradation. The initial rate of reaction has been observed to be directly

proportional to ZnO NPs catalyst amount indicating the heterogeneous system. In order to investigate the optimum amount of ZnO NPs catalyst, a series of experiments has been carried out using by different amount of ZnO NPs catalyst from 60mg/100mL to 120mg/100mL at optimized pH 7.5. The rate of degradation increased form $1.03 \times 10^{-4} \text{ s}^{-1}$ to $4.95 \times 10^{-4} \text{ s}^{-1}$ with increased in catalyst amount from 60mg/100mL to 90mg/100mL. Thereafter, rate constant decreases to $2.67 \times 10^{-4} \text{ s}^{-1}$ with increased catalyst amount 120mg/100mL. The results are shown in Table 4.32 and Figure 4.45. The rate of degradation is optimum at 90mg/100mL of catalyst amount. This observation indicated that beyond the optimum catalyst concentration, other factors affected the degradation of dyes. Increase in amount of catalyst resulted in an increase of the available active sites in reaction condition. Completely all these aspects suggest that optimal amount of ZnO NPs catalyst has to be added in the order to aviod unnecessary excess of catalyst also to essure total absorption of light photons for efficient photo-catalytic degradation of Orange II dye [99, 100].

Table 4.32: Effect of change in catalyst amount: [Orange-II] = $5.2 \times 10^{-5} \text{ mol dm}^{-3}$, pH = 7.5, Light intensity = $35 \times 10^3 \text{ Lux}$.

ZnO NPs mg/100mL	$k \times 10^{-4} \text{ s}^{-1}$	$t_{1/2} \times 10^3 \text{ s}$
60	1.03	6.72
70	2.25	3.08
80	3.43	2.02
90	4.95	1.40
100	4.23	1.63
110	3.77	1.83
120	2.67	2.59

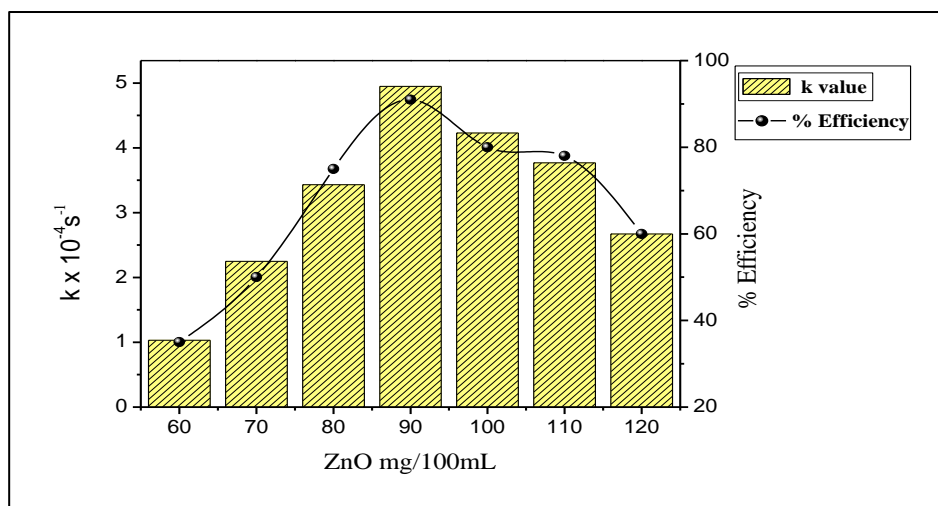


Fig. 4.45: Effect of change in catalyst amount on photo-catalytic degradation of O-II

4.5.4: Effect of change in dye concentration:

The effect of different initial dye concentration on the photo-catalytic degradation of Orange II dye has been studied from $2.2.0 \times 10^{-5} \text{ mol dm}^{-3}$ to $8.2 \times 10^{-5} \text{ mol dm}^{-3}$ was investigated under the optimized experimental reaction conditions. It has been observed that the rate of degradation increased from $2.51 \times 10^{-4} \text{ s}^{-1}$ to $4.95 \times 10^{-4} \text{ s}^{-1}$ with increase in Orange II dye concentration from $2.2 \times 10^{-5} \text{ mol dm}^{-3}$ to $5.2 \times 10^{-5} \text{ mol dm}^{-3}$. Thereafter, rate constant of dye degradation decreased from $4.95 \times 10^{-4} \text{ s}^{-1}$ to $3.06 \times 10^{-4} \text{ s}^{-1}$ with increased dye solution concentration $5.2 \times 10^{-5} \text{ mol dm}^{-5}$ to $8.2 \times 10^{-5} \text{ mol dm}^{-3}$. The rate constant of degradation is optimum at $5.2 \times 10^{-5} \text{ mol dm}^{-3}$ of Orange II dye concentration. From literature studies we came to know that as the target textile dye concentration increase adsorbed of these molecules on the catalyst surface also increases [80]. Hence relative no. of O_2^{\bullet} and OH^{\bullet} radicals on the catalyst surface increased. Therefore, excess dye molecule adsorption on catalyst surface hindered the OH^- ions adsorption and finally rate of OH^{\bullet} formation is lowered. It is concluded from above discussion that above

optimum dye concentration rate of degradation decreased [101, 102]. The data are given in Table 4.33 and Figure 4.46.

Table 4.33: Effect of change in dye concentration: ZnO NPs = 90 mg/100mL, pH = 7.5, Light intensity = 35×10^3 Lux.

[OII] x 10^{-5} mol dm $^{-3}$	k x 10^{-4} s $^{-1}$	t $_{1/2}$ x 10^3 s
2.2	2.51	2.76
3.2	3.64	1.90
4.2	4.17	1.66
5.2	4.95	1.40
6.2	4.30	1.61
7.2	3.79	1.82
8.2	3.06	2.26

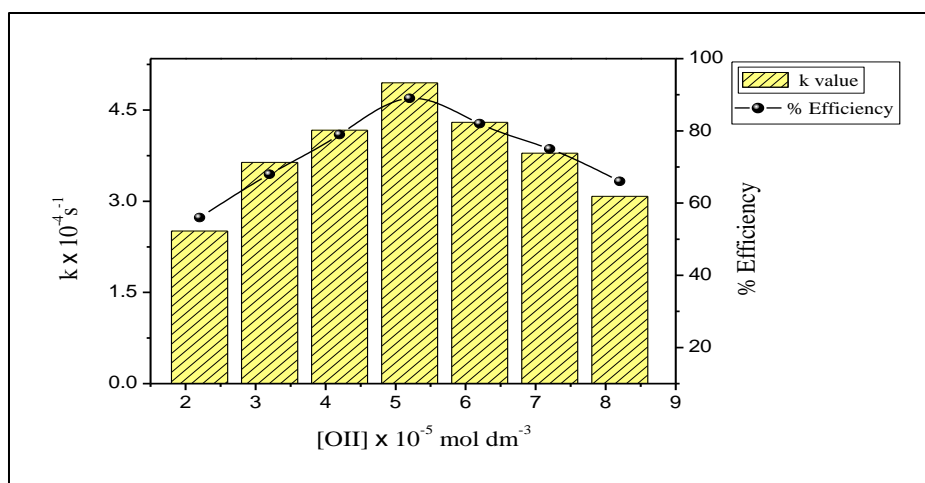
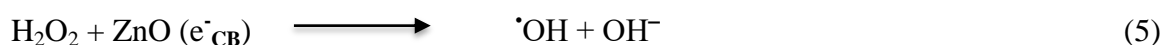


Fig. 4.46: Effect of change in dye concentration on photo-catalytic degradation of O-II

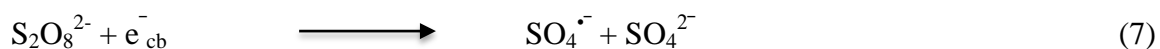
4.5.5: Effect of change in oxidant's concentration:

The rate of photo-catalytic degradation of organic compound is significantly improved either in the presence of oxygen or by addition of H₂O₂ and K₂S₂O₈. The photo-catalytic degradation of Orange II dye has been investigated at varied concentration 2.0×10^{-6} mol

dm⁻³ to 14 x 10⁻⁶ mol dm⁻³ of H₂O₂ and K₂S₂O₈. The rate constant of photo-catalytic degradation of Orange II dye increased from 5.25 x 10⁻⁴s⁻¹ to 6.77 x 10⁻⁴s⁻¹ with increasing H₂O₂ concentrations from 2.0 x 10⁻⁶ mol dm⁻³ to 8 x 10⁻⁶ mol dm⁻³ and rate constant of photo-catalytic degradation of Orange II dye increased from 5.32 x 10⁻⁴s⁻¹ to 6.93 x 10⁻⁴s⁻¹ with increasing K₂S₂O₈ concentrations from 2.0 x 10⁻⁶ mol dm⁻³ to 8 x 10⁻⁶ mol dm⁻³ respectively and reached to an optimum but above this concentration range, the increased H₂O₂ and K₂S₂O₈ concentration retarded the rate of degradation. The results are shown in Table 4.34 and Figure 4.47. At their respective low concentrations H₂O₂ and K₂S₂O₈ accelerate the reaction rate by producing an extremely strong and non-selective oxidant [•]OH radical. These [•]OH radicals got generated by H₂O₂ and K₂S₂O₈ on account of scavenging the electrons from the conduction band of the photo-catalyst and this led to inhibit the electron-hole recombination process [30-33]. H₂O₂ may also split photo-catalytically to produce [•]OH radicals directly by the absorption of visible light by the following reactions:



The S₂O₈²⁻ anions generate strong oxidizing SO₄^{•-} radicals anion after trapping the photo-generated conduction band electrons of ZnO NPs as shown in the following reaction:

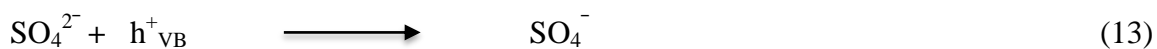
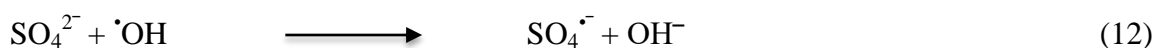
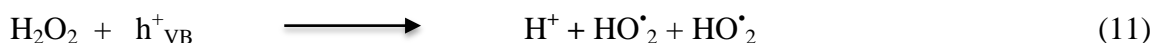
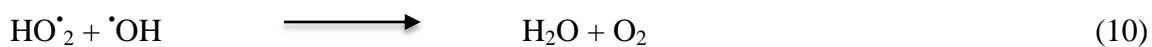
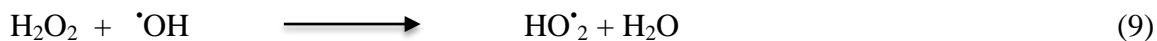


The generated sulfate radical anions (SO₄^{•-}) participate in reaction with the solvent, according to the following reaction:



Different to this behavior, H₂O₂ and K₂S₂O₈ start behaving as scavenger for [•]OH radicals and hole at an excessive concentration. As both [•]OH radical and h_{VB}⁺ are strong oxidants

for organic dye pollutants, the photo-catalytic degradation of Orange II dye will be inhibited in the condition of additional of H₂O₂ and K₂S₂O₈. Furthermore, H₂O₂ and SO₄²⁻ can be adsorbed onto ZnO NPs deactivating a section of photo-catalyst and consequently decrease its photo-catalytic activity [103, 104].



Consequently, higher concentration of H₂O₂ and K₂S₂O₈ inhibited the reaction rate of dye degradation by competing with Orange II dye for available $\cdot\text{OH}$ radicals [105].

Table 4.34: Effect of change in H₂O₂ and K₂S₂O₈: [Orange-II] = 5.2 x 10⁻⁵ mol dm⁻³, ZnO NPs = 90 mg/100mL, pH = 7.5, Light intensity = 35 x 10³ Lux.

[Oxidant] x 10 ⁻⁶ mol dm ⁻³	[H ₂ O ₂]		[K ₂ S ₂ O ₈]	
	k x 10 ⁻⁴ s ⁻¹	t _{1/2} x 10 ³ s	k x 10 ⁻⁴ s ⁻¹	t _{1/2} x 10 ³ s
0.0	4.95	1.40	4.95	1.40
2.0	5.25	1.32	5.32	1.30
4.0	5.64	1.22	5.71	1.21
6.0	6.17	1.12	6.22	1.11
8.0	6.77	1.02	6.93	1.00
10.0	6.28	1.10	6.37	1.08
12.0	5.71	1.21	5.82	1.19
14.0	5.34	1.29	5.43	1.27

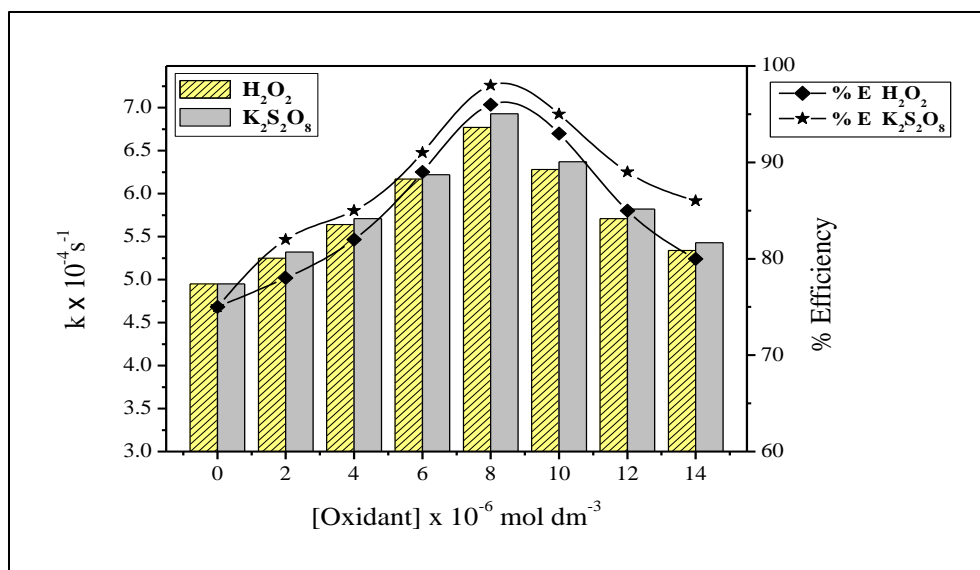
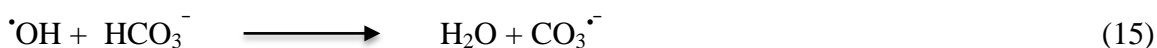
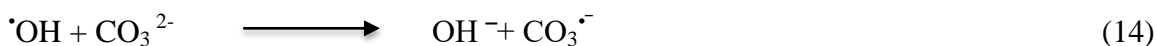


Fig. 4.47: Effect of change in oxidants on photo-catalytic degradation of O-II

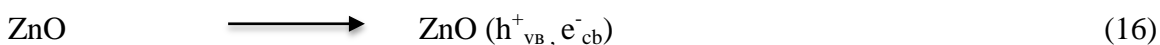
4.5.6: Effect of change in salts concentration:

The textile wastewater from dyeing process usually contains considerable amount of carbonate and Chloride ions. The substances are often used in textile processing for adjust pH of the dye bath. The presence of several anions chloride, carbonate and bicarbonate is industrial wastes. These ions affects the adsorption of the degrading species, acts as hydroxyl ion scavengers and may absorb light as well [89]. With an increase in the amount of carbonate ion from $2.0 \times 10^{-5} \text{ mol dm}^{-3}$ to $12.0 \times 10^{-5} \text{ mol dm}^{-3}$ resulted into reduction of rate constant from $4.42 \times 10^{-4} \text{ s}^{-1}$ to $2.07 \times 10^{-4} \text{ s}^{-1}$. The inhibition in the degradation of dye is due to the hydroxyl scavenging property of carbonate ions, which can be accounted from the following equation.



The $\cdot\text{OH}$ radical which is a primary oxidant for the photo-catalytic degradation of dye reported to decrease slowly with an increase in carbonate ions and degradation of the dye significantly decreased [37].

Similarly, NaCl generally comes out in the effluent along with wastewater. Therefore photo-catalytic degradation rate in presence of Cl⁻ ions has been studied by increase in concentration of Cl⁻ ions from 2.0 x 10⁻⁵ mol dm⁻³ to 12 x 10⁻⁵ mol dm⁻³ that resulted into reduction of rate constant from 4.03 x 10⁻⁴ s⁻¹ to 1.61 x 10⁻⁴ s⁻¹. The decrease in the degradation of dye in the presence of chloride ion might be due to the hole scavenging properties of chloride ion [38]



The results are shown in Table 4.35 and Figure 4.48 is the dependency of reaction rate constant on the concentration of Na₂CO₃ and NaCl.

Table 4.35: Effect of change in Na₂CO₃ and NaCl: [Orange-II] = 5.2 x 10⁻⁵ mol dm⁻³, ZnO NPs = 90 mg/100mL, pH = 7.5, Light intensity = 35 x 10³ Lux.

[Salt] x 10 ⁻⁵ mol dm ⁻³	[Na ₂ CO ₃]		[NaCl]	
	k x 10 ⁻⁴ s ⁻¹	t _{1/2} x 10 ³ s	k x 10 ⁻⁴ s ⁻¹	t _{1/2} x 10 ³ s
0.0	4.95	1.40	4.95	1.40
2.0	4.42	1.56	4.03	1.71
4.0	3.89	1.78	3.66	1.89
6.0	3.24	2.13	3.15	2.20
8.0	2.78	2.49	2.60	2.66
10.0	2.44	2.84	2.02	3.43
12.0	2.07	3.34	1.61	4.30

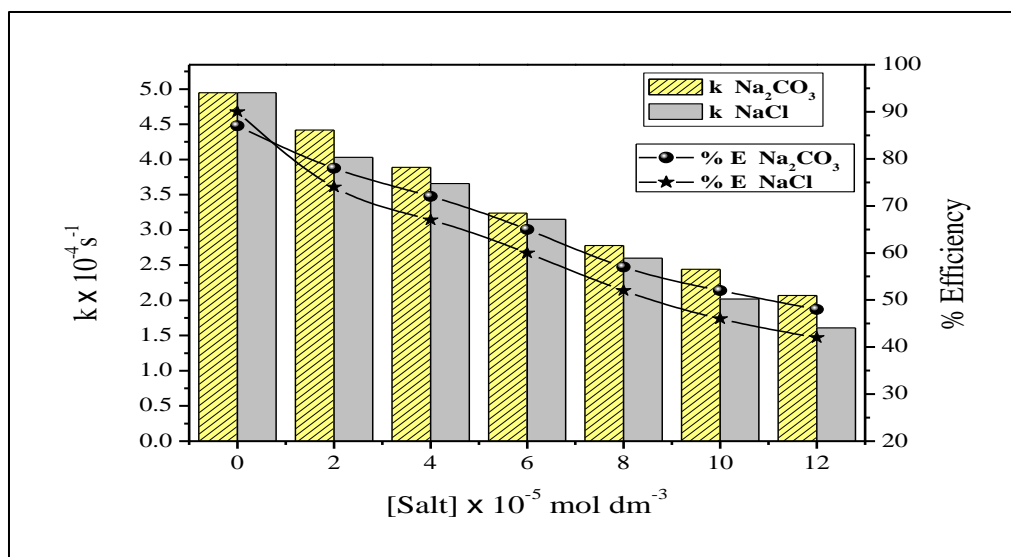


Fig. 4.48: Effect of change in salts on photo-catalytic degradation of O-II

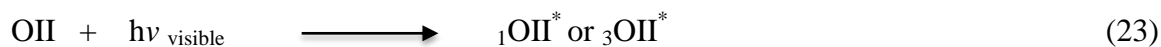
4.5.7: Effect of change in FeCl₃ concentration:

The metal ions such as Fe³⁺ could be used as sensitizers during photo-catalytic degradation of dye. In present study, effect of FeCl₃ on the photo-catalytic degradation of Orange II has been investigated by changing the concentration from 2.0 × 10⁻⁵ mol dm⁻³ to 12.0 × 10⁻⁵ mol dm⁻³. The degradation rate constant values increased from 5.38 × 10⁻⁴ s⁻¹ to 7.11 × 10⁻⁴ s⁻¹ with the increase in amount of FeCl₃ from 2.0 × 10⁻⁵ mol dm⁻³ to 8.0 × 10⁻⁵ mol dm⁻³. Thereafter, degradation rate constant values decreased to 6.01 × 10⁻⁴ s⁻¹ on further increase in amount of FeCl₃ up to 12.0 × 10⁻⁵ mol dm⁻³. The results are shown in Table 4.36 and Fig. 4.49. In fact the increase in ferric ions concentration in the reaction mixture resulted into the increase of Fe²⁺ ions concentration, which is accompanied by improved generation of [•]OH radicals, therefore increasing the rate of degradation of FeCl₃ inhibits the reaction rate of decolorization by competing with formation of [•]OH radicals [90, 91].





The photo-activation of surface adsorbed complex ion ($\text{Fe}^{3+}\text{OH}^-$) results in the formation of $\text{Fe}^{2+}\text{OH}^\cdot$ species which injects electrons to the conduction band of ZnO as shown in [Eq. 22-25]. When FeCl_3 is applied, rate of decolorization is reasonable due to rapid scavenging of conduction band electrons [42, 43] [Eq. (25)].



In the presence higher concentration of FeCl_3 , there is excessive surface adsorption of anionic dye on the surfaces of catalyst. This reduced the total photoactive area of ZnO NPs catalyst and lowered the reaction rate [45].

Table 4.36: Effect of change in FeCl_3 : [Orange-II] = 5.2×10^{-5} mol dm^{-3} ,

ZnO NPs = 90 mg/100mL, pH = 7.5, Light intensity = 35×10^3 Lux.

$\text{FeCl}_3 \times 10^{-5} \text{ mol dm}^{-3}$	$k \times 10^{-4} \text{ s}^{-1}$	$t_{1/2} \times 10^3 \text{ s}$
0.0	4.95	1.40
2.0	5.38	1.28
4.0	6.05	1.14
6.0	6.90	1.00
8.0	7.11	0.97
10.0	6.56	1.05
12.0	6.01	1.15

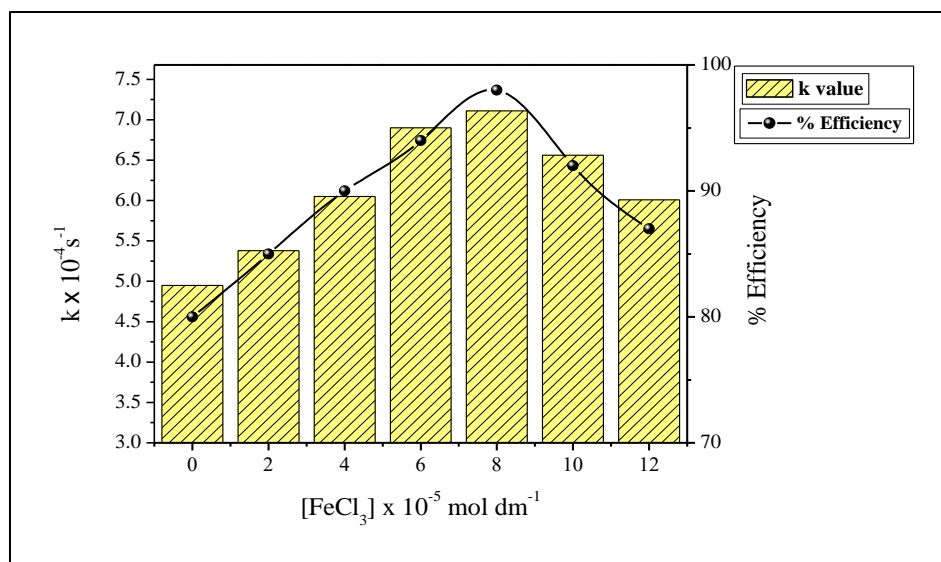


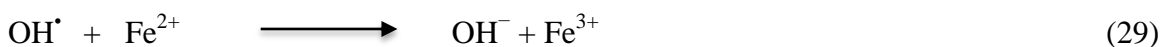
Fig. 4.49: Effect of change in FeCl₃ on photo-catalytic degradation of O-II

4.5.8: Effect of change in Fenton's reagent concentration:

Fenton's reagent system has been investigated for degradation of Orange II dye in presence of visible light and ZnO nanoparticles. In recent years, many research workers have studied the degradation of dyes using Fenton and visible/solar light system. Fenton reagent makes an attractive AOPs for the wastewater treatment and usage for the effective degradation of dyes because of its low cost and lack of toxicity of the reagents like H₂O₂ and Fe²⁺ or Fe³⁺ [106]. Photo-Fenton's process is one of the most common AOPs which is based on the formation of very reactive species such as [•]OH radicals, which have a very strong oxidative potential second only to fluorine. [•]OH radicals rapidly and non selectively oxidize a broad range of organic pollutants [48, 49].



OH[•] radicals may be scavenged by reaction with another Fe²⁺:



The rate constant of degradation has a value of $5.31 \times 10^{-4} \text{ s}^{-1}$ on the addition of Fe^{3+} : H_2O_2 in molar ratio 3:1. In the presence of Fe^{3+} : H_2O_2 in molar ratio 1:1.4, rate constant has been found $7.04 \times 10^{-4} \text{ s}^{-1}$. The results are shown in Table 4.37 and Figure 4.50. Fenton's reagent system, a mixture of Fe^{3+} and H_2O_2 has been known as a powerful oxidant for textile dyes. Upon irradiation of $\text{Fe}^{3+}/\text{H}_2\text{O}_2/\text{ZnO}/\text{Orange II}$ dye system in the presence of visible light, formation of OH^\bullet radicals increased relating a complex mechanism. Dye absorbs visible irradiation and is excited into high-energy state. This excited dye molecules reduction the ferric ion complex to ferrous ion complex followed by the transfer to ferric ion [50]. The reduced ferrous ions react with H_2O_2 to decompose and produce hydroxyl radical [Eq. (33)]. OH^\bullet radicals also decompose H_2O_2 to $^\bullet\text{HO}_2$.

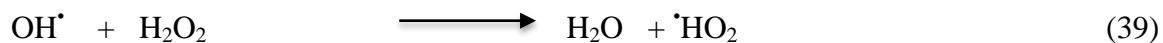
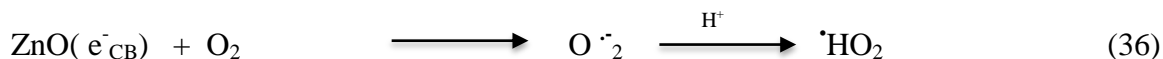
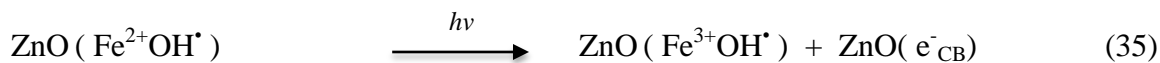
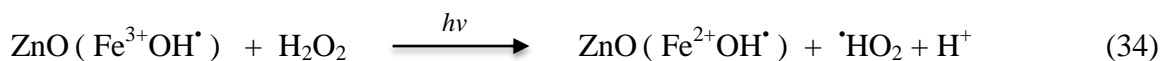
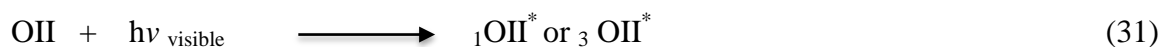


Table 4.37: Effect of change in $\text{Fe}^{3+}/\text{H}_2\text{O}_2$: [Orange-II] = 5.2×10^{-5} mol dm⁻³, ZnO NPs = 90 mg/100mL, pH = 7.5, Light intensity = 35×10^3 Lux.

$\text{Fe}^{3+} : \text{H}_2\text{O}_2$	Without ZnO		With ZnO	
	$k \times 10^{-4} \text{ s}^{-1}$	$t_{1/2} \times 10^3 \text{ s}$	$k \times 10^{-4} \text{ s}^{-1}$	$t_{1/2} \times 10^3 \text{ s}$
3:1	0.89	7.78	5.31	1.30
1.4:1	1.58	4.38	6.44	1.07
1:1.4	2.30	3.01	7.04	0.98
1:3	2.57	2.69	6.72	1.03
11:1	2.97	2.33	6.26	1.10

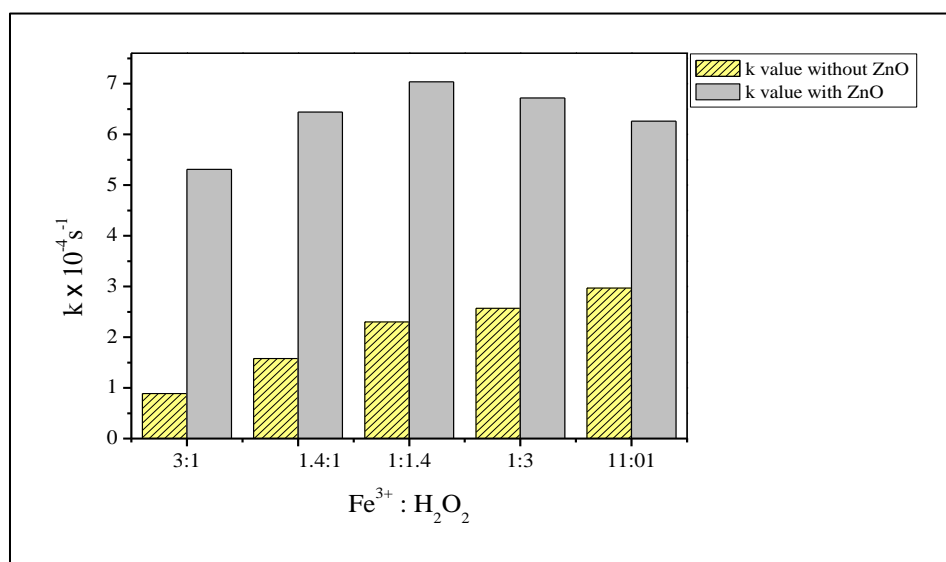


Fig. 4.50: Effect of change in Fenton's reagent on photo-catalytic degradation of O-II

4.5.9: Effect of change in light intensity:

The effect of light intensity on photo-catalytic degradation rate was investigated and the resulted are given in Table 4.38 and Figure 4.51. By varying the intensity of light increasing from 25×10^3 Lux to 45×10^3 Lux for Orange II dye solution concentration

$5.0 \times 10^{-5} \text{ mol dm}^{-3}$, ZnO NPs catalyst amount 90 mg/100mL and pH 7.5. The rate of degradation constant increased from $2.34 \times 10^{-4} \text{ s}^{-1}$ to $6.67 \times 10^{-4} \text{ s}^{-1}$ as shown in the figure. It may be explained on the basis of number of excited molecules. As more light intensity falls on ZnO molecules, more number of molecules get excited which in turn may degrade more dye molecules and thus the rate of photo-catalytic degradation was found to increase with increase in light intensity [94]. The data show that the rate of degradation was accelerated as the light intensity was increased because any increase in the intensity of light increased the photons striking per unit time per unit area of the ZnO NPs catalyst powder resulted in more OH^\bullet radicals. A linear behavior between intensity of light and rate of degradation was observed [84].

Table 4.38: Effect of change in light intensity: [Orange-II] = $5.2 \times 10^{-5} \text{ mol dm}^{-3}$, ZnO NPs = 90 mg/100mL, pH = 7.5.

Light intensity $\times 10^3 \text{ Lux}$	$k \times 10^{-4} \text{ s}^{-1}$	$t_{1/2} \times 10^3 \text{ s}$
25	2.34	2.96
30	3.45	2.00
35	4.95	1.40
40	5.66	1.22
45	6.67	1.03

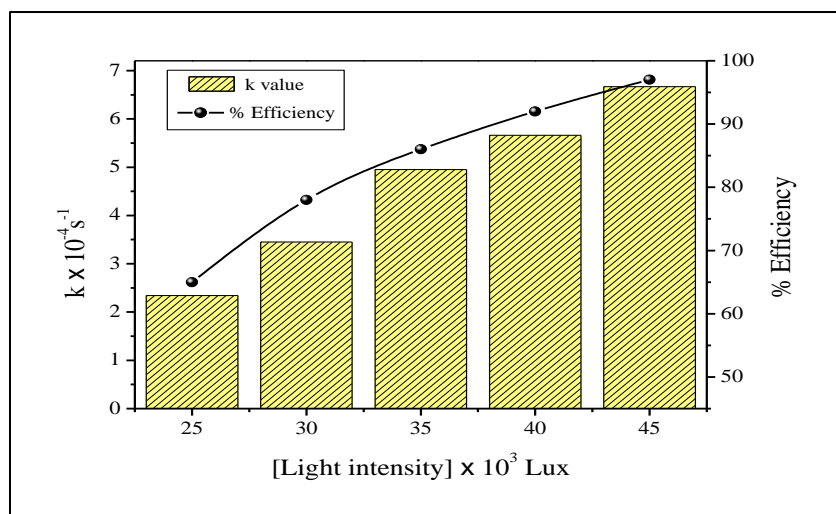
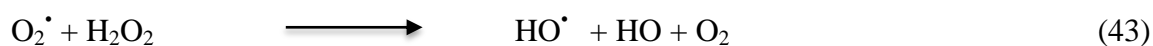
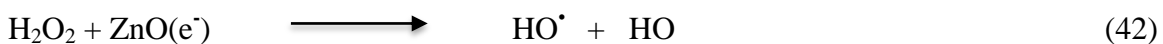


Fig. 4.51: Effect of change in light intensity on photo-catalytic degradation of O-II

4.5.10: Effect of bubbling of N₂ and O₂:

An important role of dissolved gases in a real aqueous sample play in the degradation of dissolved organic pollutants. The degradation of Orange II has been severely retarded by bubbling of pure N₂ decrease in rate constant but increases rapidly on bubbling oxygen through the dye solution. These observations confirm the proposed assumption that dissolved oxygen is a precursor of main oxidant, that is, the role of DO is to trap the photo-generated electrons to produce O₂^{•-} radicals, which particles in photo-catalytic process to accelerate the Orange II dye photo-degradation. In the oxygenated solution oxygen get adsorb on the surface of the photo-catalyst, preventing electron-hole recombination by trapping electron and producing superoxide anion radicals. With the improved charge separation more numbers of photo-generated holes becomes available to take part in photo oxidation reactions. The results are shown in Fig. 4.52 [53, 54].



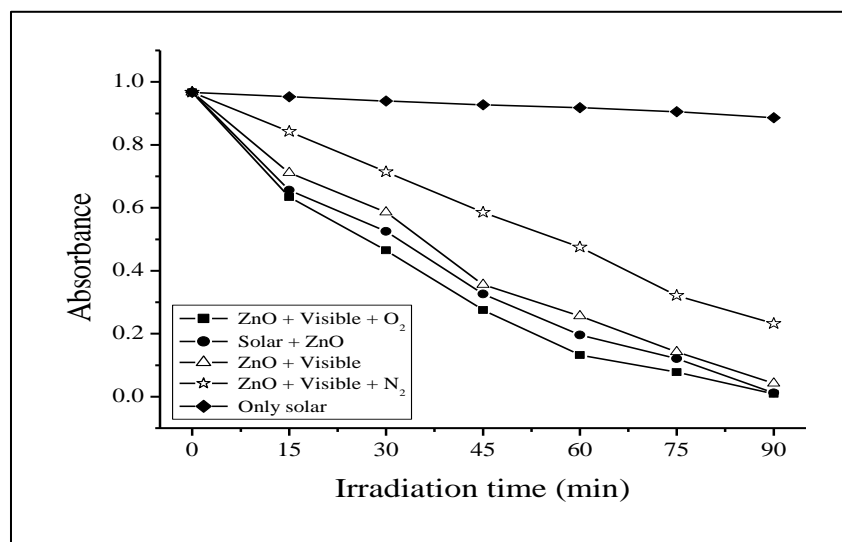
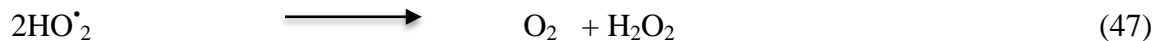
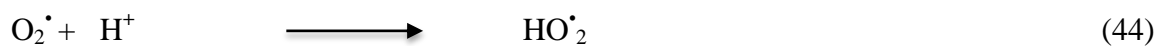


Fig. 4.52: Decolorization of Orange II under various photo-catalytic systems:

[Orange II] = 5.2×10^{-5} mol dm⁻³, ZnO NPs = 90 mg/100mL, pH = 7.5, Light intensity = 35×10^3 Lux.

4.5.11: Comparison of solar and visible light:

The efficiency of solar and visible light on photo-catalytic degradation of dye was comparatively studied. The degradation efficiency of Orange II dye with visible light was found to be more efficient than that of solar light. Figure 4.52 shows the comparisons of color removal efficiency of Orange II with two light sources under different conditions. It was noticed that if same experiments were carried out in the absence of ZnO, then no absorbance loss of dye was found [55, 56].

4.5.12: Effect of other photo-catalysts:

The results shown in Table 4.39 and Figure 4.53, the photo-catalytic degradation of Orange II dye with prepared ZnO NPs and varied catalyst such as ZnO, BiOCl, TiO₂ and BaCrO₄ using visible light. The photo-catalyst on illuminating with light having energy equal to or more than band gap energy, a heterogeneous photo-catalyst reaction occurs on surface of semiconducting materials [57]. The order of photo-activity followed the order: ZnO NPs > ZnO > BiOCl > TiO₂ > BaCrO₄ on photo-catalytic degradation have been studied at same condition. It has already been found that catalysts such as ZnO NPs, ZnO, BiOCl and TiO₂ have band gaps larger than 3 eV strong photo-catalytic activities. The conduction and valence band potentials of both ZnO NPs and TiO₂ are larger than the corresponding redox potentials of H⁺/H₂ and H₂O/O₂ and the photo-generated electron and hole can be separated efficiently. BaCrO₄ with smaller band gap shows less activity since its conduction band is much lower than that of ZnO NPs and TiO₂. The smaller band gap permits rapid recombination of electron-hole and so electron in these catalysts cannot move into the electron acceptors in the solution rapidly. Hence low photo-catalytic activity was observed in these semiconductors [58]. It is for these reasons; the prepared ZnO nano photo-catalyst has more photo-catalytic efficiency than other photo-catalysts.

Table 4.39: Effect of other photo-catalysts: [Orange-II] = 5.2×10^{-5} mol dm⁻³, pH = 7.5, Light intensity = 35×10^3 Lux.

Catalysts (90mg/100mL)	$k \times 10^{-4} \text{ s}^{-1}$	$t_{1/2} \times 10^3 \text{ s}$
ZnO NPs	4.95	1.40
ZnO	2.64	2.62
BiOCl	2.35	2.94
TiO ₂	1.29	5.37
BaCrO ₄	1.08	6.41

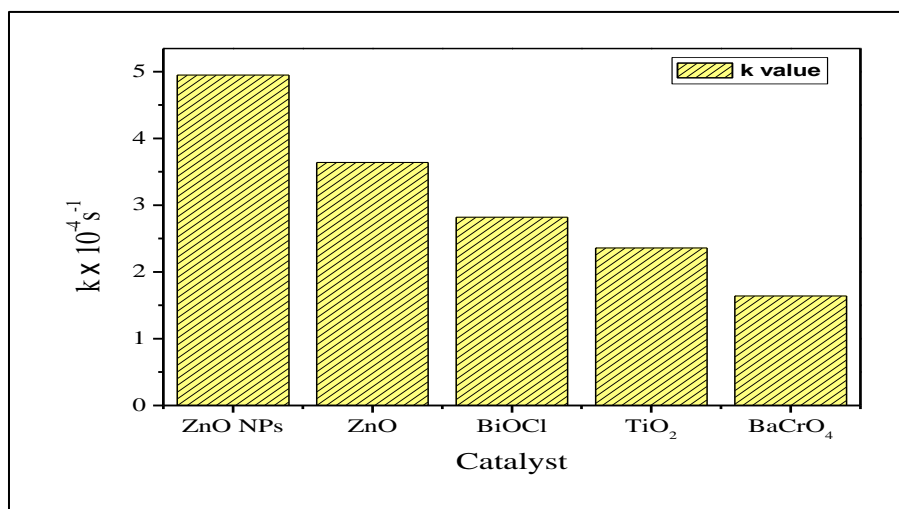


Fig. 4.53: Effect of other photo-catalysts on photo-catalytic degradation of Orange-II

4.5.13: Test for reusability of ZnO NPs:

The reusability of ZnO nanoparticles photo-catalyst was tested for dye degradation. The ZnO nanoparticles catalyst used for degradation of dye was filtered, washed and dried in air and then in oven for 30 minutes. This dried ZnO photo-catalyst was used for the degradation of dyes under similar reaction conditions. It was observed that the ZnO

photo-catalyst can be used repeatedly even up to three batches of reaction without any treatment and reused catalyst showed almost similar catalyst activity with fresh (original) catalyst. The initial rate of photo-degradation of the dye has found very low decrement even after the third second cycle of reuse. The results were shown in figure 4.54. The less of activity was observed and losses of Zn^{++} ions were more pounced only after third cycle of its reuse.

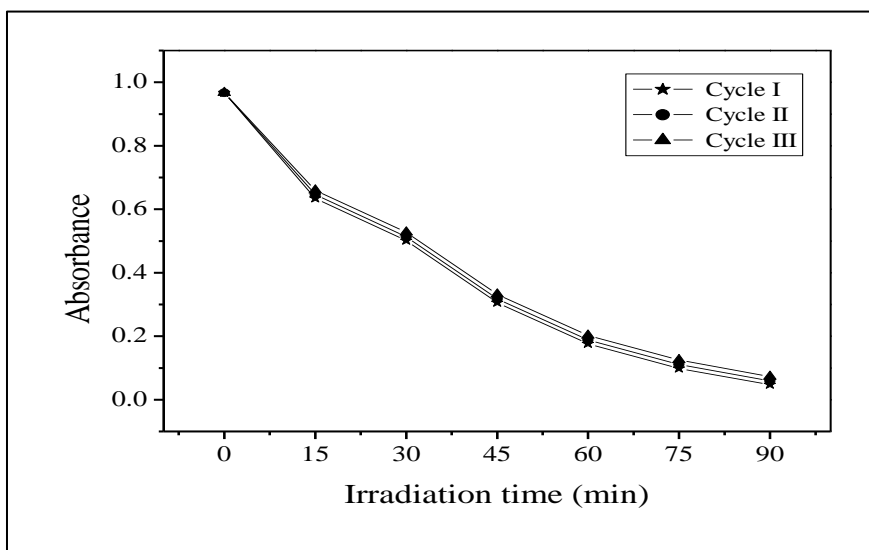


Fig. 4.54: Decolorization of Orange-II by ZnO NPs: (I) Cycle; (II) Cycle; (III) Cycle; [Orange-II] = 5.2×10^{-5} mol dm^{-3} , ZnO NPs = 90 mg/100mL, pH = 7.5, Light intensity = 35×10^3 Lux.

4.5.14: COD and CO₂ measurements during degradation of Orange-II:

The COD test has widely been used as an effective method to measure the organic strength of wastewater. The test allows the measurement of waste in terms of the total amount of oxygen required for the oxidation of organic matter to CO₂ and H₂O. Here, results of COD were occupied to note the possibility of the reduction process for the degradation of Orange II dye. Increases in COD of treated water in comparison with untreated solution showed that mineralization along with decoloration of dye molecules

are taking place. The decrease in the COD valued 216 mg/L to 0 mg/L and increase in CO₂ values from 32 mg/L to 232 mg/L in 4 h of presence of visible light the completed mineralization of treated dye solution. A decrease in COD and increase in CO₂ confirm the degradation of Orange II dye. Significant amount of NO₃⁻ were released into reaction during the mineralization of dye. A decrease in pH has also been observed with increase in the quantity of mineralization. The results were shown as Table 4.40 and Figure 4.55 (a) and (b) [107].

Table 4.40: COD and CO₂ measurements during degradation of Orange-II:

[Orange-II] = 5.2×10^{-5} mol dm⁻³, ZnO NPs = 90 mg/100mL, pH = 7.5, Light intensity = 35×10^3 Lux.

Time (h)	COD (mg/L)	CO ₂ (mg/L)	Efficiency (%)	NO ₃ ⁻ (mg/L)
0	216	32	0	0
1	142	74	34	6.5
2	86	124	60	9.2
3	36	168	83	16.3
4	0	232	100	28.5

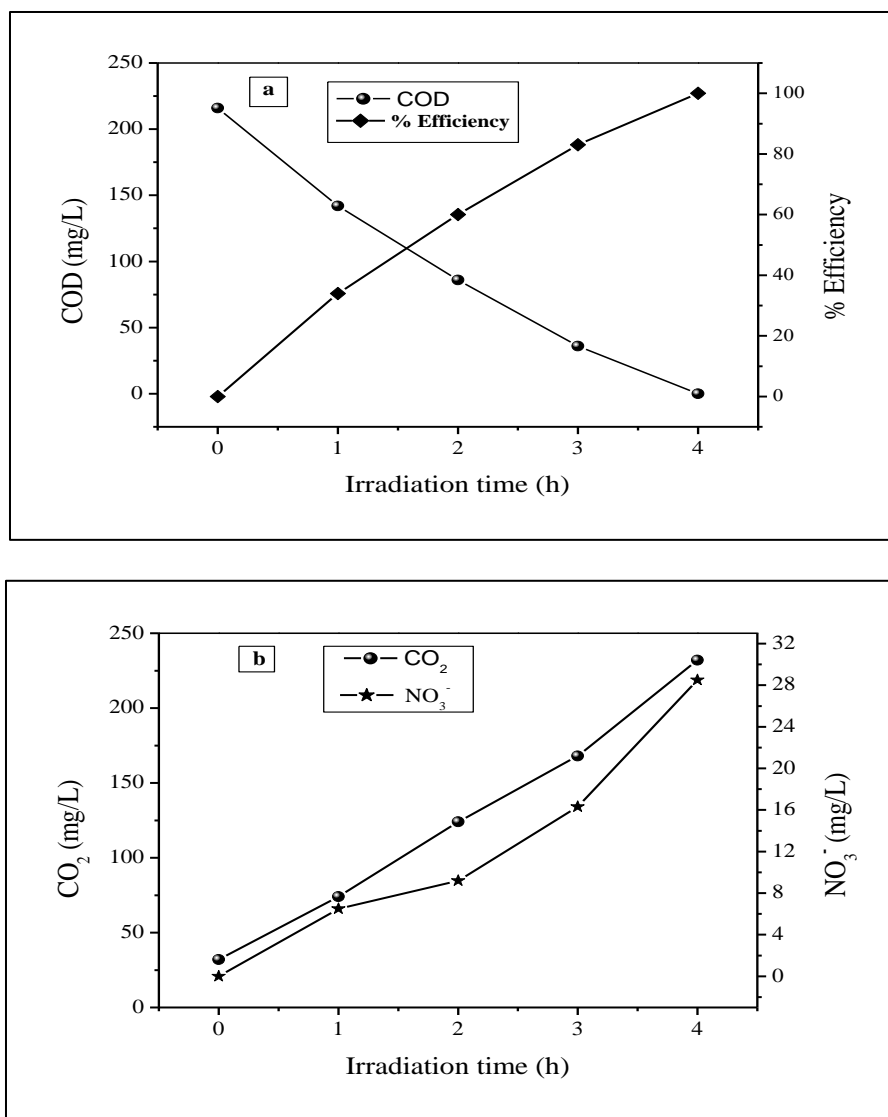


Fig. 4.55: (a) COD trend and % Efficiency (b) CO₂ trend and formation of NO₃⁻ during mineralization of Orange-II: [OII] = 5.2×10^{-5} mol dm⁻³, ZnO NPs = 90 mg/100mL, pH = 7.5, Light intensity = 35×10^3 Lux.

4.5.15: Mechanism of Orange II dye degradation:

The photo-catalytic degradation of the Orange II dye was studied by the use of additives such as H₂O₂, K₂S₂O₈ etc. electron scavengers like H₂O₂ and K₂S₂O₈ accept a photo-generated electron from the conduction band (CB) and thus avoid electron-hole recombination producing OH[•] [61]. Valence band holes (h_{vb}^+) and conduction band

electrons (e_{cb}^-) are generated when aqueous ZnO NPs suspension is irradiated with visible light having more energy than (3.2 eV) band gap energy. These electron and hole pairs interacts with another molecules separately. Now valance band holes (h_{VB}^+) reacted with H_2O or OH^- radical's bonded on surface to procedure hydroxyl radical (OH^\bullet). And molecule oxygen generated superoxide radicals, as shown in Eq. (48) to Eq. (57) [62-64]. Such electron generated disrupted the conjugation system of dye and decomposition of dye and the hole so generated creates OH^\bullet from water which again leads to degradation of dye. The mechanism is as follows: [65, 66]

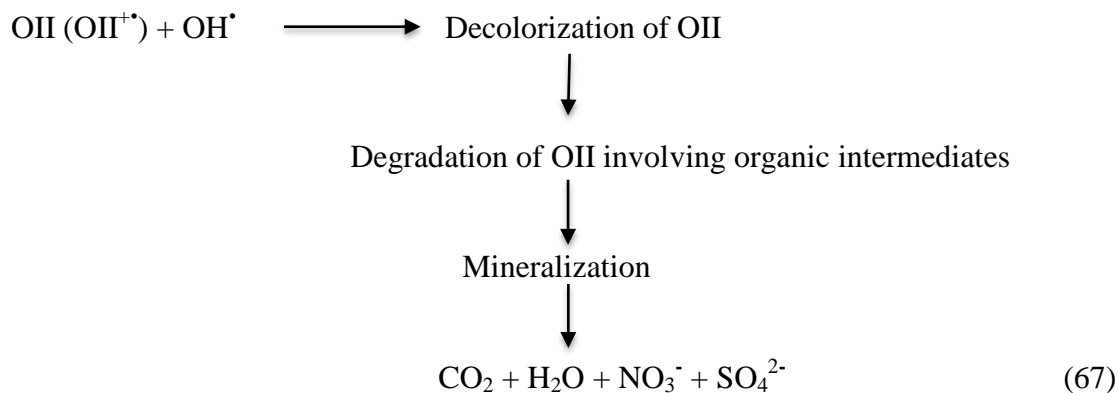


Secondly, sensitization of dye molecule by visible light leads to excitation of dye molecule in singlet or triplet state, subsequently followed by electron injection from excited dye molecule onto conduction band of semiconductor particles. The mechanism of dye sensitization is summarized in Eq. (58) to Eq. (67) [67-71].



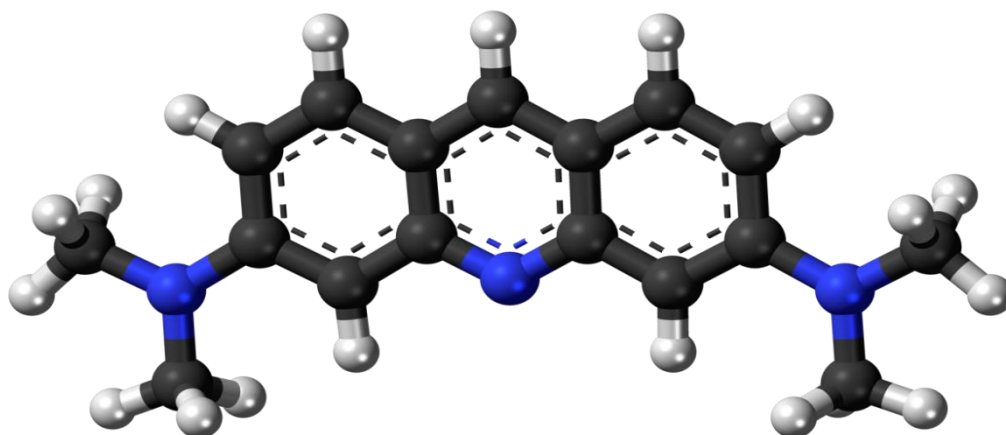


The mechanism of semiconductor photo-catalysis is of very complex nature. Dye molecules interact with $\text{O}_2^{\bullet -}$, HO_2^{\bullet} , or OH^{\bullet} species to generate intermediates ultimately lead to degradation products. OH^{\bullet} radical being very strong oxidizing agent (oxidation potential 3.2 eV) mineralizes dye to various end products. The role of reductive pathways in heterogeneous photo-catalysis has been found to be in minor extent as compared to oxidation [72, 73].



OII = Orange II

Acridine Orange



Acridine Orange belongs to the oldest group of synthetic dyes. Acridine Orange is a fluorescent pH indicator, orange colored at pH 8.4 and exhibiting a green fluorescence at pH 10.4. It may be used to differentially stain DNA and RNA within Individual unfixed cells of as a viability stain. It also stains tumor cells selectively and retards tumor growth. Among the non-textile uses are coloration of leather, paper, lacquer and spirit inks.

4.6: Effect of various experimental parameters on the degradation rate of Acridine Orange (AO) dye

4.6.1: Photo-catalytic degradation of Acridine Orange (AO):

On the surface of catalyst classical Langmuir–Hinshelwood expression was followed by the photo-catalytic degradation rate of AO dye and followed most often Langmuir sorption isotherm for the sorption of the dye to the catalyst surface. This theory is usually used kinetic model for unfolding photo-catalytic behavior. For treatment of heterogeneous surface reactions degradation rate is explained by pseudo first-order kinetics in Langmuir–Hinshelwood [11-14]. Such kinetics is streamlined in terms of modified model to accommodate reactions taking place at solid-liquid interface as

$$r = \frac{-dc}{dt} = \frac{k_r KC}{(1+KC)} \quad (1)$$

Where, r = rate of dye disappearance and C = variable dye concentration at time t . K = equilibrium constant for adsorption of AO dye on photo-catalyst and k_r = limiting reaction rate at maximum coverage in operational conditions. The integrated form can be written as

$$t = \ln\left(\frac{C_0}{C}\right) + \frac{1}{Kk_r} \frac{C_0 - C}{k_r} \quad (2)$$

Where t = time required for the initial concentration of dye C_0 to C . At low dye concentration in equation 2, value of C_0 is very less and hence can be neglected.

$$\ln\left(\frac{C_0}{C}\right) = k_r Kt = kt \quad (3)$$

Where k = apparent rate constant of degradation. The Half-life time ($t_{1/2}$) for the photo-catalytic degradation of AO dye on the ZnO NPs surface can be calculated by using following Eq. (4)

$$t_{1/2} = \frac{0.693}{k} \quad (4)$$

The Acridine Orange dye degradation results are reported here for three conditions: (1) Acridine Orange dye + ZnO NPs + visible light (2) Acridine Orange dye + visible light only and (3) Acridine Orange dye + ZnO NPs only (dark) were shown in figure 4.56 (a). It was observed carefully that maximum degradation occurred in the first condition, while in dark and during photolysis, no significant changes in the absorbance values were observed. Therefore, in second and third condition, degradation process was not observed. Absorption spectrum Changes were recorded at 450nm wavelength.

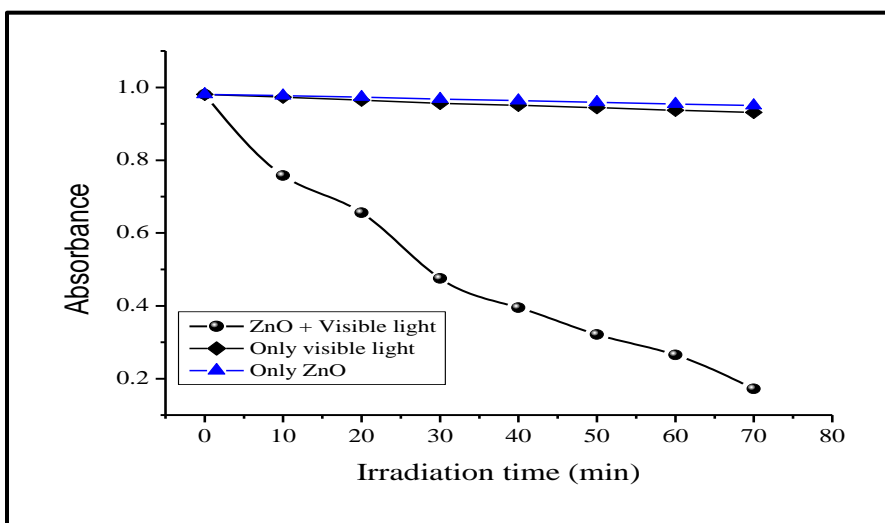


Fig. 4.56 (a) Degradation of Acridine Orange: [AO] = 2.5×10^{-5} mol dm⁻³, ZnO = 80 mg/100mL, pH = 8.4, Light intensity = 25×10^3 Lux.

Plotting the semi-logarithmic graph of concentration versus irradiation time (min) of AO dye in presence of ZnO NPs yielded a linear relationship as shown in Figure 4.56 (b). Therefore, reaction dye of degradation by ZnO nanoparticles is pseudo-first order reaction kinetics, AO dye rate constant of 3.86×10^{-4} s⁻¹, with regression coefficient of 0.988. The rate constant is the slope of the straight line. In all cases R² (correlation

constant for the fitted line) values were close to 0.99 which confirmed pseudo 1st-order kinetics for the degradation of AO dye in this method.

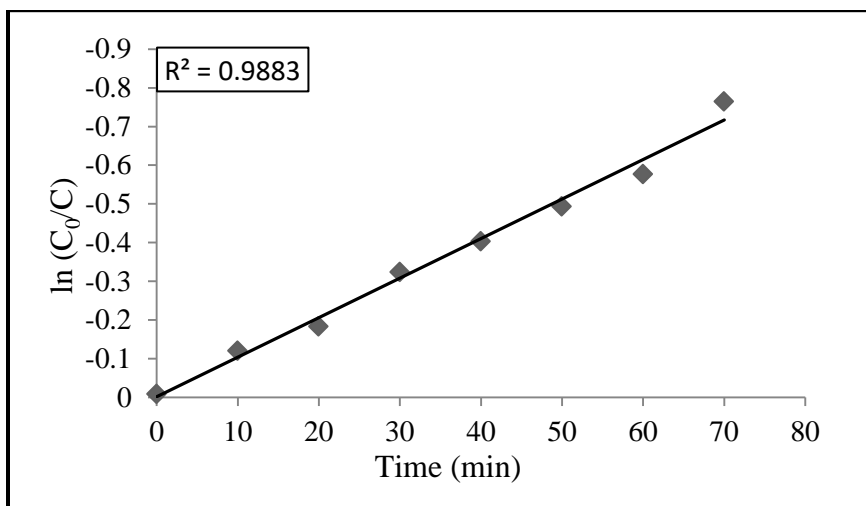
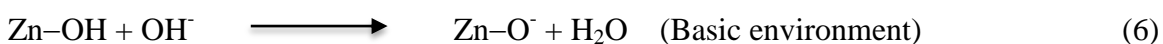
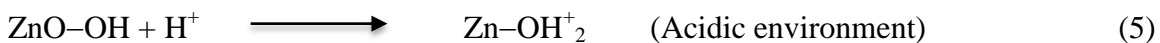


Fig. 4.56 (b): Pseudo first order kinetics: [AO] = 2.5×10^{-5} mol dm⁻³, ZnO = 80mg/100mL, pH = 8.4, Light intensity = 25×10^3 Lux.

4.6.2: Effect of change in pH:

The effect of pH on the photo-catalytic reaction could be mainly explained by the surface charge of ZnO NPs. The pH of the aqueous solution also an important variable for the determination of degradation process, because change in solution pH affected the adsorption of organic pollutants and process of adsorption on catalyst surface. As the resulted, the photo-catalytic degradation efficiency got greatly affected by pH changed. Hydroxide layers (Zn-OH) is formed in presence of water by hydroxylation on zinc oxide nanoparticles surface of zinc hydroxide is charged by amphoteric reaction with hydrogen ion or hydroxyl ion in acidic and alkaline environment respectively [75].



Experimentations were carried out at pH values, from 5.5 to 11.5 for constant dye concentration ($2.5 \times 10^{-5} \text{ mol dm}^{-3}$) and catalyst amount (80mg/100ml). The reaction rate increased with increase in pH exhibiting optimum determined rate of degradation at pH 8.4. The results were shown in Table 4.41 and Figure 4.57. Consequently, at higher pH value about 8.4, the electrostatic attraction between the negatively charged active sites on the surface of ZnO NPs and positive AO dye molecule causes strong adsorption, but if the pH value is too high, ZnO undergo dissolution and gets converted into zincates $[\text{Zn}(\text{OH})_4]^{2-}$.



Under acidic conditions, the Acridine Orange dye was difficult to adsorb on the ZnO nanoparticles surface and hence the photo-catalytic degradation of Acridine Orange dye was very slow [76].

Table 4.41: Effect of change in pH: $[\text{AO}] = 2.5 \times 10^{-5} \text{ mol dm}^{-3}$, $\text{ZnO} = 80 \text{ mg}/100\text{mL}$,
Light intensity = $25 \times 10^3 \text{ Lux}$.

pH	$k \times 10^{-4} \text{ s}^{-1}$	$t_{1/2} \times 10^3 \text{ s}$
5.5	0.97	7.14
6.5	1.36	5.09
7.5	2.53	2.73
8.4	3.86	1.79
9.5	3.04	2.27
10.5	2.62	2.64
11.5	1.06	6.53

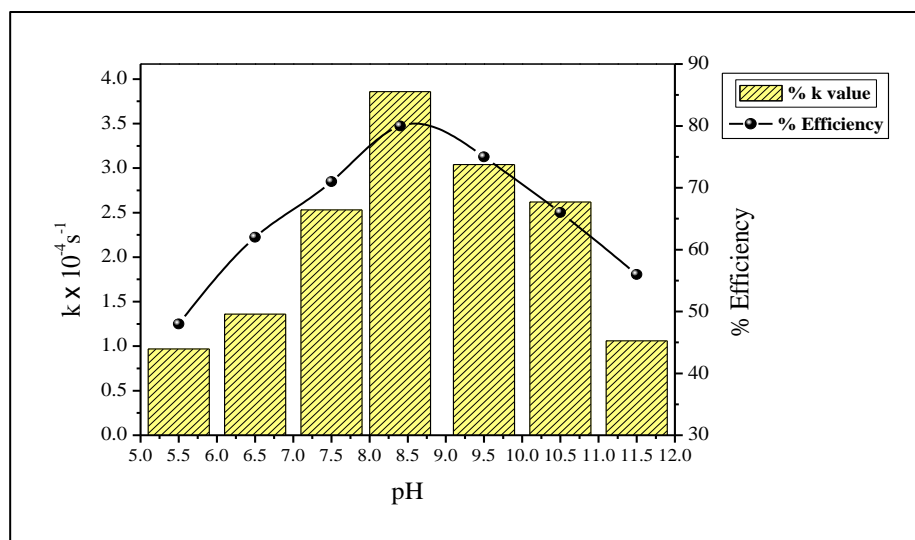


Fig. 4.57: Effect of change in pH on photo-catalytic degradation of AO

4.6.3: Effect of change in catalyst amount:

The ZnO nanoparticles catalyst amount added to the reaction vessel is an important parameter affecting the efficiency of photo-catalytic degradation. The initial rate of reaction has been observed to be directly proportional to ZnO NPs catalyst amount indicating the heterogeneous system. When excess catalyst is used for treatment of wastewater it showed adverse effect on rate of dye degradation. A series of experiments have been carried out to assess the optimal catalyst amount by various amount of ZnO NPs catalyst from 50mg/100mL to 110mg/100mL at $2.5 \times 10^{-5} \text{ mol dm}^{-3}$ dye concentration in reaction solution. The rate of degradation increased from $1.03 \times 10^{-4} \text{ s}^{-1}$ to $3.86 \times 10^{-4} \text{ s}^{-1}$ with increased in catalyst amount from 50mg/100mL to 80mg/100mL. Thereafter, rate constant decreases to $1.22 \times 10^{-4} \text{ s}^{-1}$ with increased catalyst amount 110mg/100mL. The results are shown in Table 4.42 and Figure 4.58. The rate of degradation is optimum at 80mg/100mL of catalyst amount. This observation indicated that beyond the optimum catalyst concentration, other factors affect the degradation of dyes. Increase in amount of catalyst results in an increase of the available active sites in

reaction condition. All these factors suggest that optimal amount of ZnO NPs catalyst has to be added in the order to avoid unnecessary excess of catalyst also to ensure total absorption of light photons for efficient photo-catalytic degradation of Acridine Orange dye [79].

Table 4.42: Effect of change in catalyst amount: [AO] = 2.5×10^{-5} mol dm⁻³, pH = 8.4, Light intensity = 25×10^3 Lux.

ZnO mg/100mL	k x 10 ⁻⁴ s ⁻¹	t _{1/2} x 10 ³ s
50	1.03	6.72
60	1.91	3.62
70	2.74	2.52
80	3.86	1.79
90	3.24	2.13
100	2.53	2.73
110	1.22	5.68

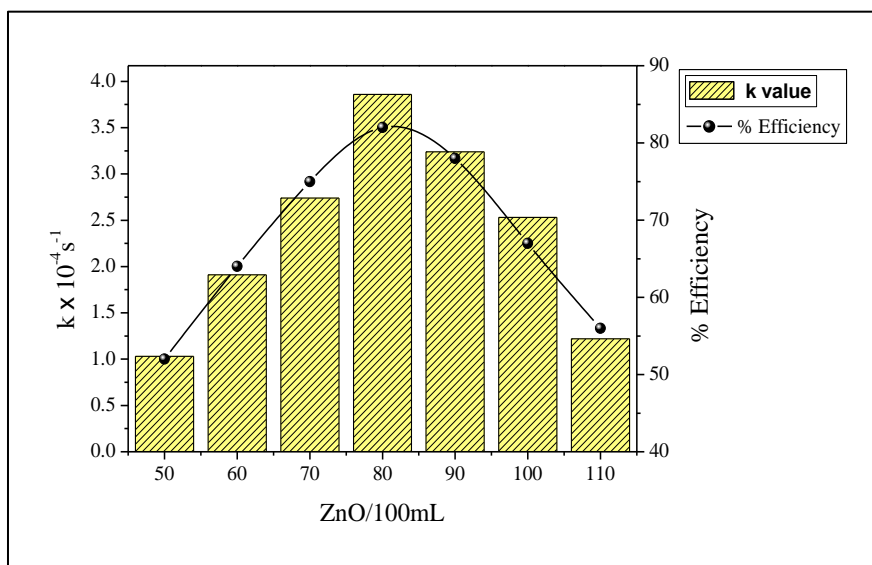


Fig. 4.58: Effect of catalyst change in amount on photo-catalytic degradation of AO

4.6.4: Effect of change in dye concentration:

Another crucial parameter for the treatment of wastewater is substrate concentration effectively. The decolorization of AO dye at varied initial concentrations in the ranging from $1.0 \times 10^{-5} \text{ mol dm}^{-3}$ to $4.5 \times 10^{-5} \text{ mol dm}^{-3}$ was studied under the optimized reaction conditions (ZnO NPs amount=80mg/100mL, pH=8.4). The results are shown in Table 4.43 and Figure 4.59. It has been found that the rate of degradation increased from $1.17 \times 10^{-4} \text{ s}^{-1}$ to $3.86 \times 10^{-4} \text{ s}^{-1}$ with increase in AO dye concentration from $1.0 \times 10^{-5} \text{ mol dm}^{-3}$ to $2.5 \times 10^{-5} \text{ mol dm}^{-3}$. Thereafter, rate constant of dye degradation decreased from $3.86 \times 10^{-4} \text{ s}^{-1}$ to $1.31 \times 10^{-4} \text{ s}^{-1}$ with increased dye concentration $2.5 \times 10^{-5} \text{ mol dm}^{-3}$ to $4.5 \times 10^{-5} \text{ mol dm}^{-3}$. The rate constant of degradation is optimum at $2.5 \times 10^{-5} \text{ mol dm}^{-3}$ of AO dye concentration. All the active sites of catalyst surface may be occupied as the concentration become higher than optimum condition which led to slow the rate of degradation. From literature studies we came to know that as the target organic pollutant concentration increase adsorbed of these molecules on the Zinc oxide photo-catalyst surface also increases. Hence relative number of O_2^{\bullet} and hydroxyl radicals on the ZnO surface increased. Therefore, excess dye molecule adsorption on catalyst surface hindered the OH^{\bullet} ions adsorption and finally rate of hydroxyl radical formation is lowered. Hence, more dye concentration than optimum value it decreased the rate of dye degradation [108, 109].

Table 4.43: Effect of change in dye concentration: ZnO = 80 mg/100mL, pH = 8.4, Light intensity = 25×10^3 Lux.

[AO] $\times 10^{-5}$ mol dm ⁻³	k $\times 10^{-4}$ s ⁻¹	t _{1/2} $\times 10^3$ s
1.0	1.17	5.92
1.5	2.09	3.31
2.0	3.25	2.13
2.5	3.86	1.79
3.0	3.13	2.21
3.5	2.69	2.57
4.0	2.18	3.17
4.5	1.31	5.29

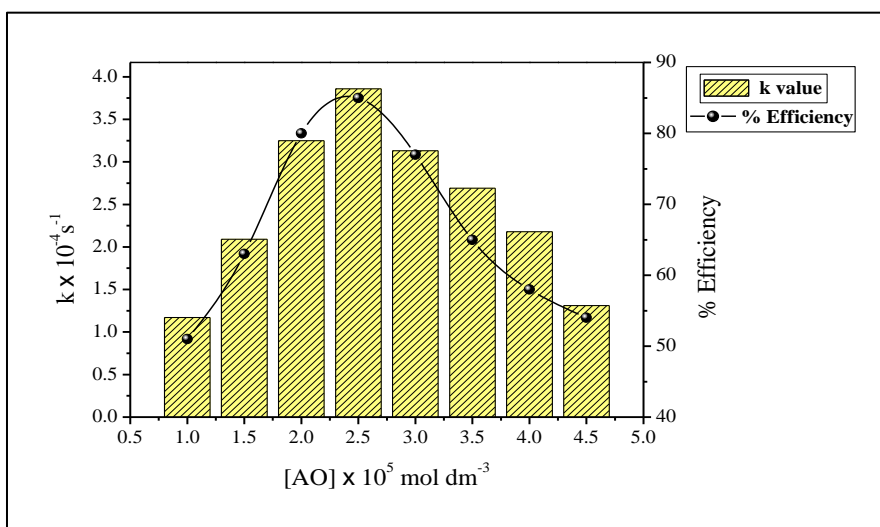
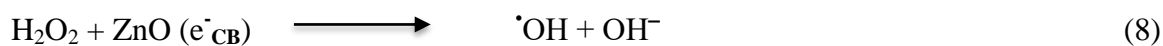


Fig. 4.59: Effect of change in dye concentration on photo-catalytic degradation of AO

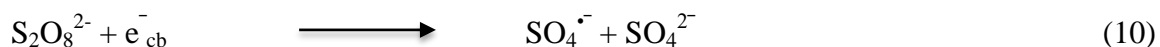
4.6.5: Effect of change in oxidant's concentration:

It was found that addition of oxidants such as H₂O₂ and K₂S₂O₈ was useful for the photo-catalytic oxidation of the dyes. The reactive intermediates are such as [•]OH and SO₄^{-•} radicals are generated. The photo-catalytic degradation of AO dye has been investigated

at varied concentration $2.0 \times 10^{-6} \text{ mol dm}^{-3}$ to $16 \times 10^{-6} \text{ mol dm}^{-3}$ of H_2O_2 and $\text{K}_2\text{S}_2\text{O}_8$. Rate constant of degradation of AO dye increased from $4.35 \times 10^{-4} \text{ s}^{-1}$ to $7.23 \times 10^{-4} \text{ s}^{-1}$ with increasing H_2O_2 concentrations from $2.0 \times 10^{-6} \text{ mol dm}^{-3}$ to $10 \times 10^{-6} \text{ mol dm}^{-3}$ and rate constant of degradation of AO dye increased from $4.53 \times 10^{-4} \text{ s}^{-1}$ to $7.87 \times 10^{-4} \text{ s}^{-1}$ with increasing $\text{K}_2\text{S}_2\text{O}_8$ concentrations from $2.0 \times 10^{-6} \text{ mol dm}^{-3}$ to $8 \times 10^{-6} \text{ mol dm}^{-3}$ respectively and reached to an optimum but above this concentration range, the increased H_2O_2 and $\text{K}_2\text{S}_2\text{O}_8$ concentration retarded the rate of degradation. The results were shown in Table 4.44 and Figure 4.60. These hydroxyl radicals got generated by H_2O_2 and $\text{K}_2\text{S}_2\text{O}_8$ on account of scavenging the electrons from the conduction band of the photo-catalyst and this led to inhibit the electron-hole recombination process [110]. H_2O_2 may also split photo-catalytically to produce $\cdot\text{OH}$ radicals directly by the absorption of visible light by the following reactions:



The $\text{S}_2\text{O}_8^{2-}$ anions generate strong oxidizing $\text{SO}_4^{\cdot-}$ radicals anion after trapping the photo-generated conduction band electrons of ZnO NPs as shown in the following reaction:

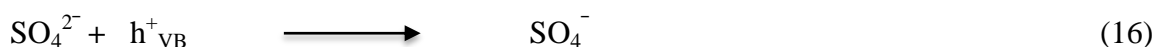
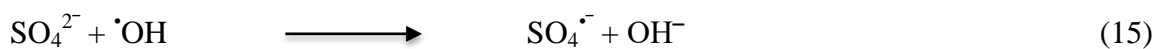
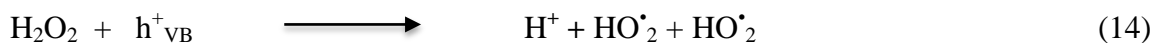
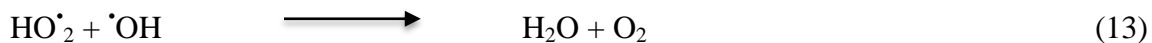
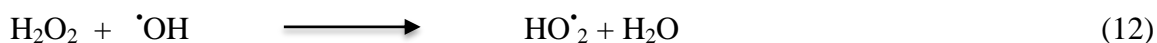


The generated sulfate radical anions ($\text{SO}_4^{\cdot-}$) participate in reaction with the solvent, according to the following reaction:



Different to this behavior, H_2O_2 and $\text{K}_2\text{S}_2\text{O}_8$ start behaving as scavenger for $\cdot\text{OH}$ radicals and hole at an excessive concentration. As both $\cdot\text{OH}$ radical and $h\nu_{\text{B}}^+$ are strong oxidants for organic dye pollutants, the photo-catalytic degradation of AO dye will be inhibited in the condition of additional of H_2O_2 and $\text{K}_2\text{S}_2\text{O}_8$. Furthermore, H_2O_2 and SO_4^{2-} can be

adsorbed onto ZnO NPs deactivating a section of photo-catalyst and consequently decrease its photo-catalytic activity [34, 35].



Consequently, the proper addition of H₂O₂ and K₂S₂O₈ could accelerate the photo-degradation rate of AO dye. However, in order to keep the efficiency of the added H₂O₂ and K₂S₂O₈, it was necessary to choose the proper concentration of H₂O₂ and K₂S₂O₈, according to the dyes concentration.

Table 4.44: Effect of change in H₂O₂ and K₂S₂O₈: [AO] = 2.5 × 10⁻⁵ mol dm⁻³, ZnO = 80 mg/100mL, pH = 8.4, Light intensity = 25 × 10³ Lux.

[Oxidant] × 10 ⁻⁶ mol dm ⁻³	[H ₂ O ₂]		[K ₂ S ₂ O ₈]	
	k × 10 ⁻⁴ s ⁻¹	t _{1/2} × 10 ³ s	k × 10 ⁻⁴ s ⁻¹	t _{1/2} × 10 ³ s
0.0	3.86	1.79	3.86	1.79
2.0	4.35	1.59	4.53	1.52
4.0	4.79	1.44	5.34	1.29
6.0	5.22	1.32	6.65	1.04
8.0	6.17	1.12	7.87	0.88
10.0	7.23	0.95	6.42	1.07
12.0	6.33	1.09	5.29	1.31
14.0	5.57	1.24	4.46	1.55
16.0	4.16	1.66	3.93	1.76

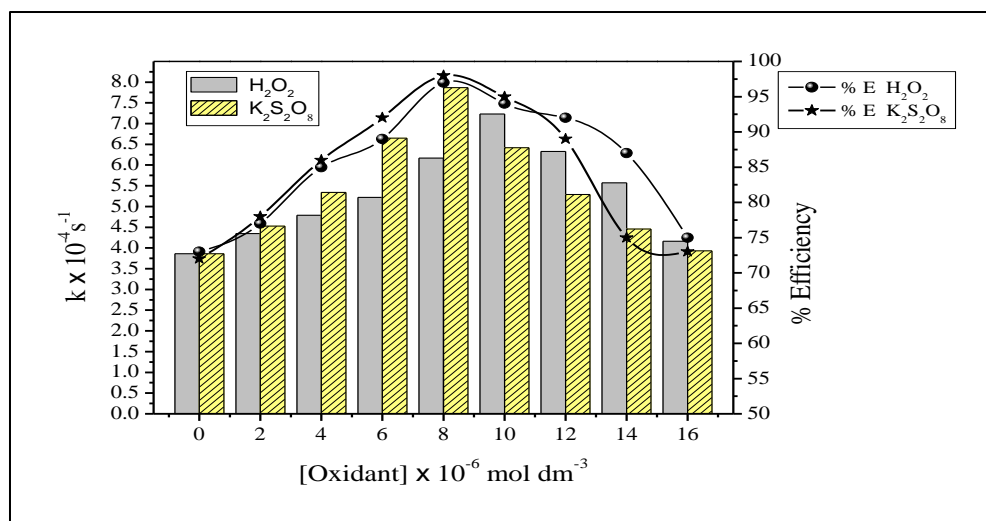
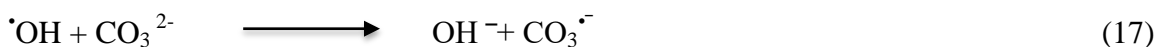
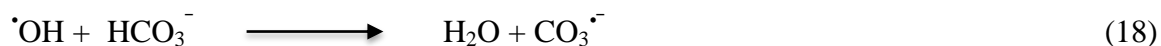


Fig. 4.60: Effect of change in oxidants on photo-catalytic degradation of AO

4.6.6: Effect of change in salts concentration:

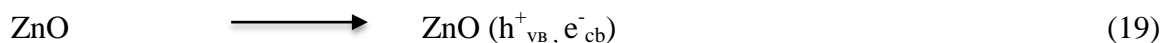
The inorganic anion may have an influence on the rate of photo-catalytic degradation. The different concentrations of industrial wastes contain, apart from the pollutants and different salts. The presence of several anions chloride, carbonate and bicarbonate is industrial wastes. The presence of several anions chloride, carbonate and bicarbonate is industrial wastes. Adsorption of degrading species are affected by these ions and acting as OH⁻ ion scavengers as well as adsorbs light radiation, which also an important factor in mainly degradation of dye. Here mainly sodium carbonate is used dyeing bath which adjusted bath pH and as it effected fixing of dye on fabrics and color fastness. Therefore the wastewater from the dyeing process will contain considerable amount of carbonate ion [82]. With an increase in the amount of carbonate ion from $2.0 \times 10^{-5} \text{ mol dm}^{-3}$ to $12.0 \times 10^{-5} \text{ mol dm}^{-3}$ resulted into reduction of rate constant from $3.59 \times 10^{-4} \text{ s}^{-1}$ to $1.45 \times 10^{-4} \text{ s}^{-1}$. The inhibition in the degradation of dye is due to the hydroxyl scavenging property of carbonate ions, which can be accounted from the following equation.





The $\cdot\text{OH}$ radical which is a primary oxidant for the photo-catalytic degradation of dye reported to decrease slowly with an increase in carbonate ions and degradation of the dye significantly decreased [37].

Similarly, NaCl commonly comes out in the effluent along with wastewater. Therefore photo-catalytic degradation rate in presence of Cl^- ions has been studied by increase in concentration of Cl^- ions from $2.0 \times 10^{-5} \text{ mol dm}^{-3}$ to $12 \times 10^{-5} \text{ mol dm}^{-3}$ that resulted into reduction of rate constant from $3.68 \times 10^{-4} \text{ s}^{-1}$ to $1.54 \times 10^{-4} \text{ s}^{-1}$. The decrease in the degradation of dye in the presence of chloride ion might be due to the hole scavenging properties of chloride ion [38].



The results are shown in Table 4.45 and Figure 4.61 is the dependency of reaction rate constant on the concentration of Na_2CO_3 and NaCl.

Table 4.45: Effect of change in Na₂CO₃ and NaCl: [AO] = 2.5 × 10⁻⁵ mol dm⁻³, ZnO = 80 mg/100mL, pH = 8.4, Light intensity = 25 × 10³ Lux.

[Salt] × 10 ⁻⁵ mol dm ⁻³	[Na ₂ CO ₃]		[NaCl]	
	k × 10 ⁻⁴ s ⁻¹	t _{1/2} × 10 ³ s	k × 10 ⁻⁴ s ⁻¹	t _{1/2} × 10 ³ s
0.0	3.86	1.79	3.86	1.79
2.0	3.59	1.93	3.68	1.88
4.0	3.27	2.11	3.38	2.05
6.0	2.83	2.44	2.94	2.35
8.0	2.41	2.87	2.53	2.73
10.0	1.81	3.82	1.95	3.55
12.0	1.45	4.77	1.54	4.50

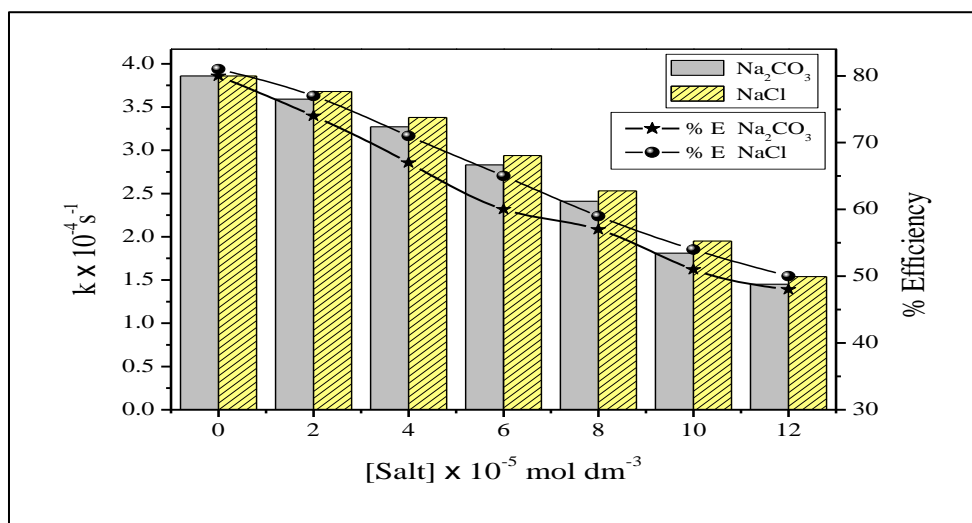
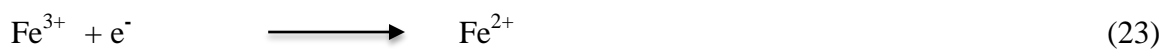


Fig. 4.61: Effect of change in salts on photo-catalytic degradation of AO

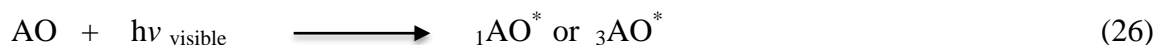
4.6.7: Effect of change in FeCl₃ concentration:

Keeping all the other parameters constant, the effect of FeCl₃ concentration on degradation of AO dye was investigated by varied FeCl₃ concentration from 2.0 × 10⁻⁵ mol dm⁻³ to 12.0 × 10⁻⁵ mol dm⁻³. The degradation rate constant values increased from 4.28 × 10⁻⁴ s⁻¹ to 6.12 × 10⁻⁴ s⁻¹ with the increase in concentration of FeCl₃ from 2.0 × 10⁻⁵

mol dm⁻³ to 8.0 x 10⁻⁵ mol dm⁻³. Thereafter, rate constant of photo-catalytic degradation decreased to 4.21 x 10⁻⁴ s⁻¹ on further increase in amount of FeCl₃ up to 12.0 x 10⁻⁵ mol dm⁻³. The results are shown in Table 4.46 and Figure 4.62. The metal ions such as Fe³⁺ could be used as sensitizers during photo-catalytic degradation of dye. In fact the increase in ferric ions concentration in the reaction mixture resulted into the increase of Fe²⁺ ions concentration, which is accompanied by improved generation of [•]OH radicals, consequently increasing rate of degradation of FeCl₃ inhibits the reaction rate of degradation by competing with formation of [•]OH radicals [39-41].



The photo-activation of surface adsorbed complex ion (Fe³⁺OH⁻) results in the formation of Fe²⁺OH[•] specie which injects electrons to the conduction band of ZnO as shown in [Eq. 27-28]. When FeCl₃ is applied, rate of decolorization is reasonable due to rapid scavenging of conduction band electrons [42, 43] [Eq. (28)].



In the presence of higher concentration of FeCl₃, there is excessive surface adsorption of dye on the surfaces of ZnO NPs catalyst. This reduced the total photoactive area of ZnO NPs catalyst and lowered rate of reaction [45].

Table 4.46: Effect of change in FeCl₃ concentration: [AO] = 2.5 × 10⁻⁵ mol dm⁻³, ZnO = 80 mg/100mL, pH = 8.4, Light intensity = 25 × 10³ Lux.

FeCl ₃ × 10 ⁻⁵ mol dm ⁻³	k × 10 ⁻⁴ s ⁻¹	t _{1/2} × 10 ³ s
0.0	3.86	1.79
2.0	4.28	1.61
4.0	4.74	1.46
6.0	5.38	1.28
8.0	6.12	1.13
10.0	5.53	1.25
12.0	4.21	1.64

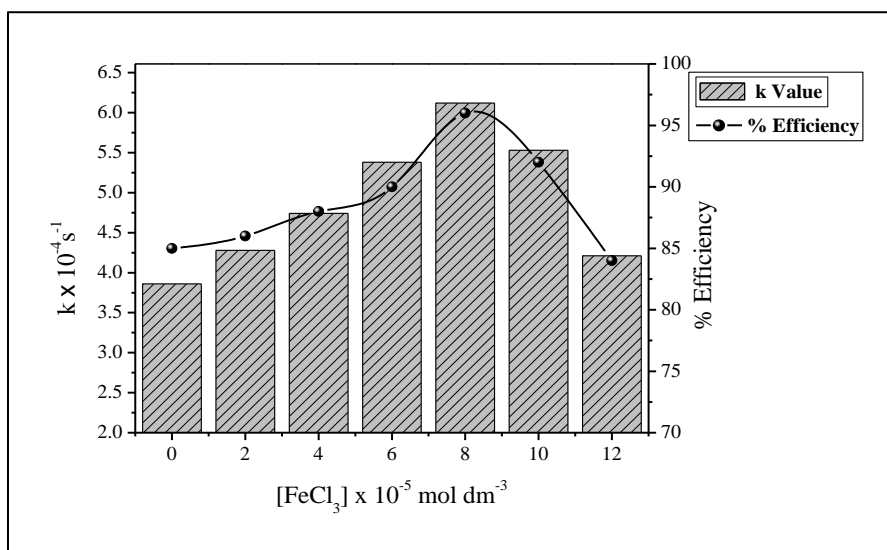


Fig. 4.62: Effect of change in FeCl₃ on photo-catalytic degradation of AO

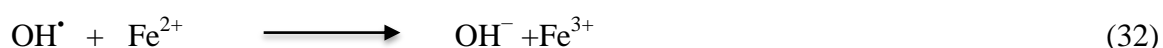
4.6.8: Effect of change in Fenton’s reagent concentration:

Fenton’s reagent system, a mixture of Fe³⁺ and H₂O₂ has been known as a powerful oxidant for textile dyes. Many researcher studied degradation of dyes using Fenton’s and visible light system past few years. Fenton reagent makes an attractive AOPs for the wastewater treatment and usage for the effective degradation of dyes because of its low

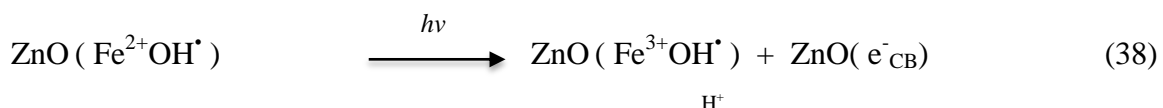
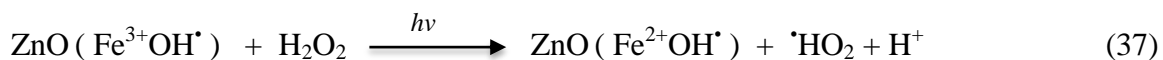
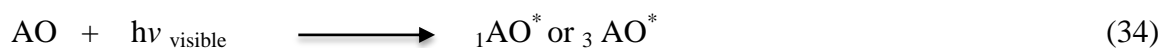
cost and lack of toxicity of the reagents like H_2O_2 and Fe^{2+} or Fe^{3+} [106]. Photo-Fenton's process is one of the most common AOPs which is based on the formation of very reactive species such as $\cdot\text{OH}$ radicals, which have a very strong oxidative potential second only to fluorine. $\cdot\text{OH}$ radicals rapidly and non selectively oxidize a broad range of dyes pollutants [48, 49].



$\text{OH}\cdot$ radicals may be scavenged by reaction with another Fe^{2+} :



The degradation rate constant has a value of $4.19 \times 10^{-4} \text{ s}^{-1}$ on the addition of Fe^{3+} : H_2O_2 in molar ratio 3:1. In the presence of Fe^{3+} : H_2O_2 in molar ratio 1:1.4, rate constant has been found $7.09 \times 10^{-4} \text{ s}^{-1}$. The results are shown in Table 4.47 and Figure 4.63. Fenton's system has been investigated for degradation of Acridine Orange dye in presence of visible light and ZnO nanoparticles. Upon irradiation of $\text{Fe}^{3+}/\text{H}_2\text{O}_2/\text{ZnO}/\text{AO}$ system in the presence of visible light, formation of $\text{OH}\cdot$ radicals increased relating a complex mechanism. Dye absorbs visible irradiation and is excited into high-energy state. This excited dye molecules reduction the ferric ion complex to ferrous ion complex followed by the transfer to ferric ion [50]. The reduced ferrous ions react with H_2O_2 to decompose and produce hydroxyl radical [Eq. (36)]. $\text{OH}\cdot$ radicals also decompose H_2O_2 to $\cdot\text{HO}_2$.



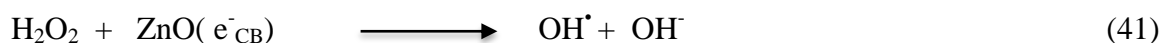
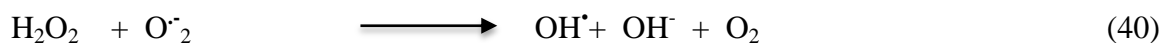
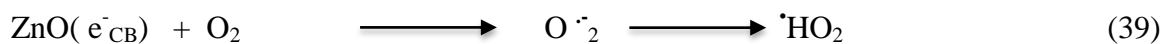


Table 4.47: Effect of change in $\text{Fe}^{3+}/\text{H}_2\text{O}_2$: $[\text{AO}] = 2.5 \times 10^{-5} \text{ mol dm}^{-3}$,
 $\text{ZnO} = 80 \text{ mg}/100\text{mL}$, $\text{pH} = 8.4$, Light intensity = $25 \times 10^3 \text{ Lux}$.

$\text{Fe}^{3+}:\text{H}_2\text{O}_2$	Without ZnO		With ZnO	
	$k \times 10^{-4} \text{ s}^{-1}$	$t_{1/2} \times 10^3 \text{ s}$	$k \times 10^{-4} \text{ s}^{-1}$	$t_{1/2} \times 10^3 \text{ s}$
3:1	1.35	5.13	4.19	1.65
1.4:1	1.54	4.50	5.78	1.19
1:1.4	1.82	3.80	7.09	0.97
1:3	2.12	3.26	6.26	1.10
11:1	2.34	2.96	5.15	1.34

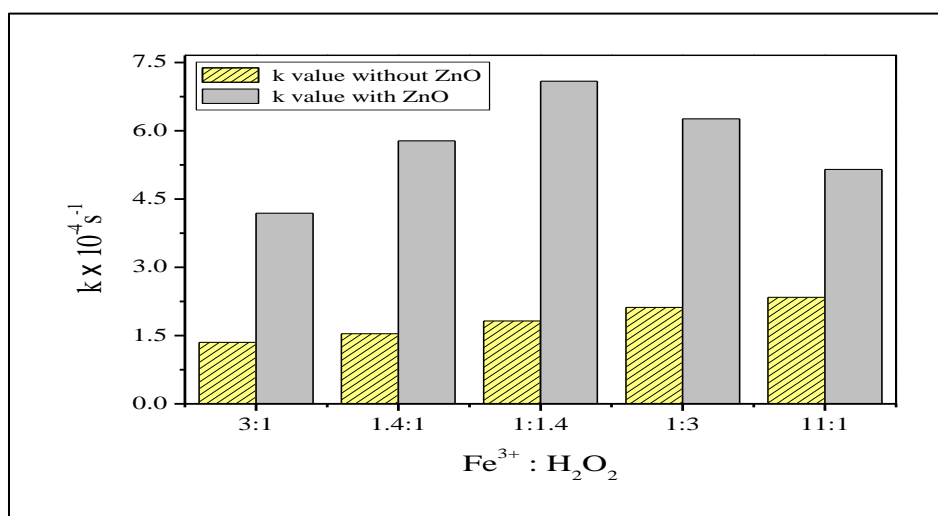


Fig. 4.63: Effect of change in Fenton's reagent on photo-catalytic degradation of AO

4.6.9: Effect of change in light intensity:

The influence of intensity of light on the degradation rate has been investigated at constant Acridine Orange dye solution concentration $2.5 \times 10^{-5} \text{ mol dm}^{-3}$, ZnO NPs catalyst amount 80 mg/100mL and pH 8.4. The degradation rate constant increases from $1.79 \times 10^{-4} \text{ s}^{-1}$ to $5.66 \times 10^{-4} \text{ s}^{-1}$ on increasing light intensity from $15 \times 10^3 \text{ Lux}$ to $35 \times 10^3 \text{ Lux}$. This is because at higher intensity electron-hole separation competes with the electron-hole recombination and results in high reaction rate. The data show that the rate of degradation was accelerated as the light intensity was increased because any increase in the intensity of light increased the photons striking per unit time per unit area of the ZnO NPs catalyst powder resulted in more OH^\bullet radicals. A linear behavior between intensity of light and rate of degradation was observed [51, 52]. The results were shown as Table 4.48 and Figure 4.64.

Table 4.48: Effect of change in light intensity: $[\text{AO}] = 2.5 \times 10^{-5} \text{ mol dm}^{-3}$, ZnO = 80 mg/100mL, pH = 8.4.

Light intensity $\times 10^3 \text{ Lux}$	$k \times 10^{-4} \text{ s}^{-1}$	$t_{1/2} \times 10^3 \text{ s}$
15	1.79	3.87
20	2.64	2.62
25	3.86	1.79
30	4.92	1.40
35	5.66	1.22

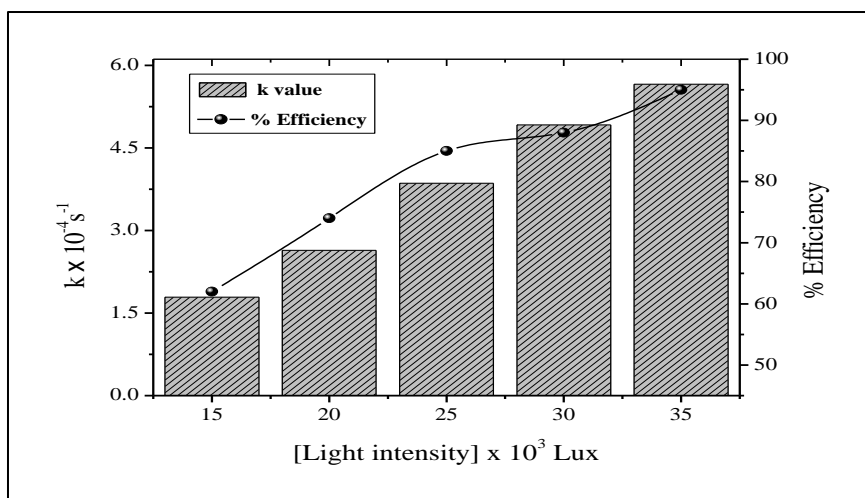
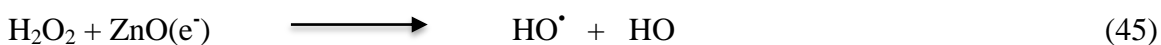


Fig. 4.65: Effect of change in light intensity on photo-catalytic degradation of AO

4.6.10: Effect of bubbling of N₂ and O₂:

The reactions of photo-catalytic degradation were carried out in presence of catalyst by bubbling oxygen or nitrogen in a closed reactor. The degradation of Acridine Orange dye has been severely retarded by bubbling of pure N₂ decrease in rate constant but increases rapidly on bubbling oxygen through the dye solution. These observations confirm the proposed assumption that dissolved oxygen is a precursor of main oxidant, that is, the role of DO is to trap the photo-generated electrons to produce O₂^{•-} radicals, which particles in photo-catalytic process to accelerate the Acridine Orange dye photo-degradation. In the oxygenated solution oxygen get adsorb on the surface of the photo-catalyst, preventing electron-hole recombination by trapping electron and producing superoxide anion radicals. With the improved charge separation more numbers of photo-generated holes becomes available to take part in photo oxidation reactions. The results are shown in Figure 4.65 [53, 54].



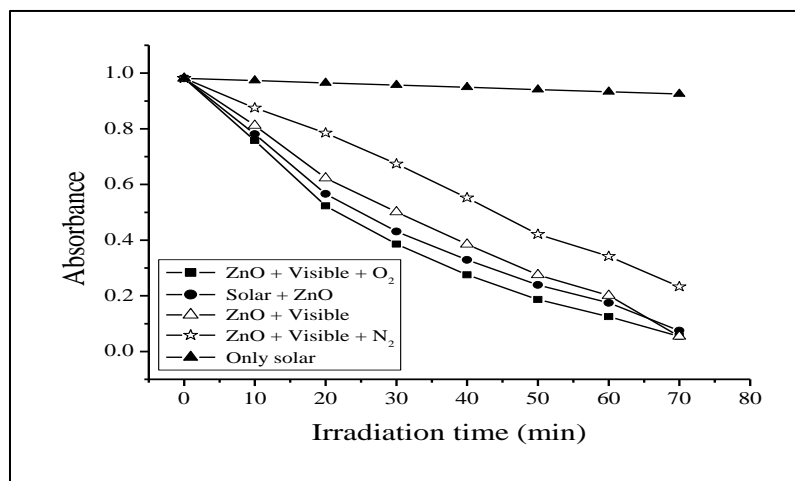
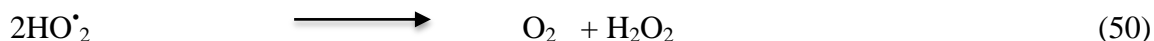
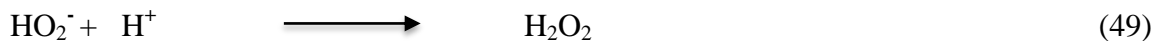
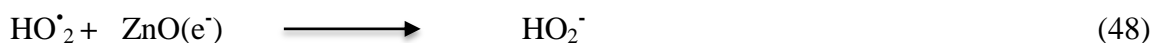


Fig. 4.65: Decolorization of AO under various photo-catalytic systems: [AO] = 2.5×10^{-5} mol dm⁻³, ZnO = 80 mg/100mL, pH = 8.4, Light intensity = 25×10^3 Lux.

4.6.11: Comparison of solar and visible light:

The efficiency of solar and visible light on photo-catalytic degradation of dye was comparatively studied. The degradation efficiency of Acridine Orange dye with visible light was found to be more efficient than that of solar light. Figure 4.65 shows the comparisons of color removal efficiency of Acridine Orange with two light sources under different conditions. It was noticed that if same experiments were carried out in the absence of ZnO, then no absorbance loss of dye was found [55, 56].

4.6.12: Effect of other photo-catalysts:

To observe the efficiency of nano-catalyst and commercial photo-catalysts towards photo-degradation of Acridine Orange dye, identical experiments were carried out with

ZnO NPs, ZnO, BiOCl, TiO₂ and BaCrO₄. The order of photo-activity followed the order: ZnO NPs > ZnO > BiOCl > TiO₂ > BaCrO₄ on photo-catalytic degradation have been studied at same condition. The photo-catalyst on illuminating with light having energy equal to or more than band gap energy, a heterogeneous photo-catalyst reaction occurs on surface of semiconducting materials [57]. We have investigated the relative efficiencies of other photo-catalysts. The conduction and valence band potentials of both ZnO NPs and TiO₂ are larger than the corresponding redox potentials of H⁺/H₂ and H₂O/O₂ and the photo-generated electron and hole can be separated efficiently. BaCrO₄ with smaller band gap shows less activity since its conduction band is much lower than that of ZnO NPs and TiO₂. The smaller band gap permits rapid recombination of electron-hole and so electron in these catalysts cannot move into the electron acceptors in the solution rapidly. Hence low photo-catalytic activity was observed in these semiconductors [58]. It is for these reasons; the prepared ZnO nano photo-catalyst has more photo-catalytic efficiency than other photo-catalysts. The results were shown in Table 4.49 and Figure 4.66.

Table 4.49: Effect of other photo-catalysts: [AO] = 2.5 × 10⁻⁵ mol dm⁻³, pH = 8.4, Light intensity = 25 × 10³ Lux.

Catalysts (80mg/100mL)	k × 10 ⁻⁴ s ⁻¹	t _{1/2} × 10 ³ s
ZnO NPs	3.86	1.79
ZnO	2.53	2.73
BiOCl	2.28	3.03
TiO ₂	1.93	3.59
BaCrO ₄	1.45	4.77

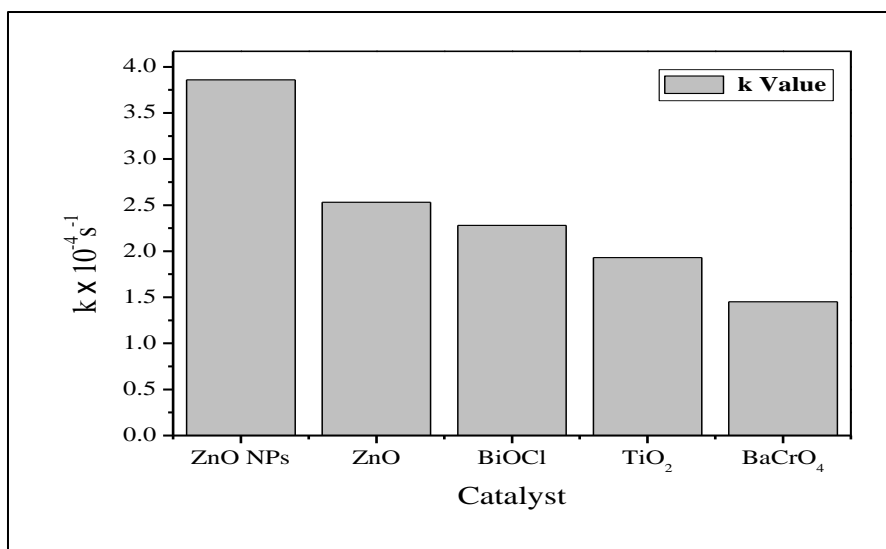


Fig. 4.66: Effect of other photo-catalysts on photo-catalytic degradation of AO

4.6.13: Test for reusability of ZnO NPs:

The reusability of ZnO nanoparticles photo-catalyst was tested for dye degradation. The ZnO nanoparticles catalyst used for degradation of dye was filtered, washed and dried in air and then in oven for 30 minutes. This dried ZnO photo-catalyst was used for the degradation of dyes under similar reaction conditions. It was observed that the ZnO photo-catalyst can be used repeatedly even up to three batches of reaction without any treatment and reused catalyst showed almost similar catalyst activity with fresh (original) catalyst. The initial rate of photo-degradation of the dye has found very low decrement even after the third second cycle of reuse. The results were shown in figure 4.67. The less of activity was observed and losses of Zn^{++} ions were more pounced only after third cycle of its reuse.

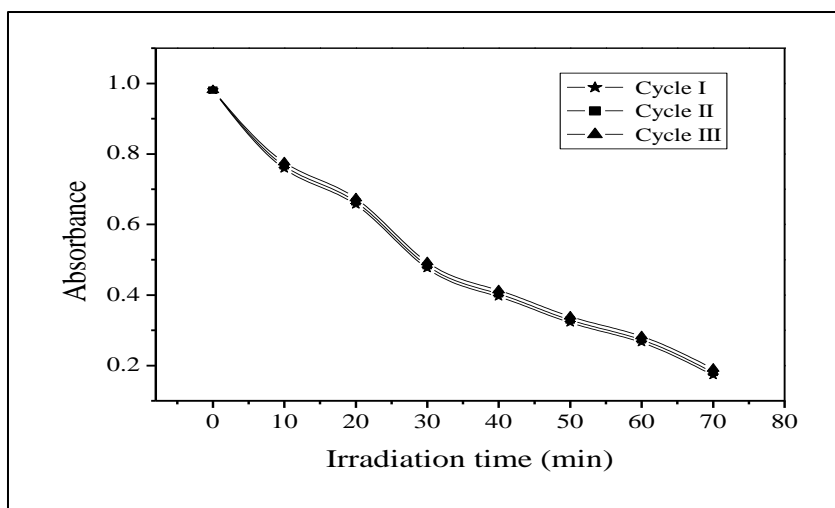


Fig. 4.67: Decolorization of AO by ZnO NPs: (I) Cycle; (II) Cycle; (III) Cycle;
[AO] = 2.5×10^{-5} mol dm⁻³, ZnO = 80 mg/100mL, pH = 8.4,
Light intensity = 25×10^3 Lux.

4.6.14: COD and CO₂ measurements during degradation of AO:

In the present work results of COD were taken as one of the parameter to judge the feasibility of the reduction procedure for the degradation of AO dye. The COD of the AO dye solution before and after the treatment was valued. The COD test widely has been used as an effective technique to measure the organic strength of wastewater. The test allows the measurement of waste in terms of the total amount of oxygen required for the oxidation of organic matter to CO₂ and H₂O [59]. The decrease in COD values of the treated dye solution indicated the mineralization of dye molecules along with the colour removal. The reduction in the estimated COD from 218 mg/L to 9 mg/L and increase in CO₂ values from 21 mg/L to 192 mg/L in 60 min of presence of visible light the complete mineralization of treated AO dye solution. The results were shown as Table 4.50 and Figure 4.68 (a) and (b).

Table 4.50: COD and CO₂ measurements during degradation of AO: [AO] = 2.5 × 10⁻⁵ mol dm⁻³, ZnO = 80 mg/100mL, pH = 8.4, Light intensity = 25 × 10³ Lux.

Time (min)	COD (mg/L)	CO ₂ (mg/L)	Efficiency (%)	NO ₃ ⁻ (mg/L)
0	218	21	0	0
15	161	35	26	9.2
30	89	112	59	13.5
45	28	171	87	19.4
60	9	192	95	24.5

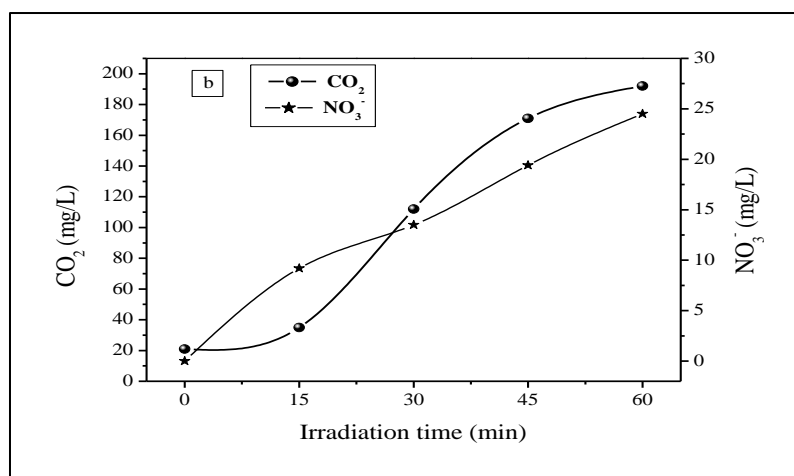
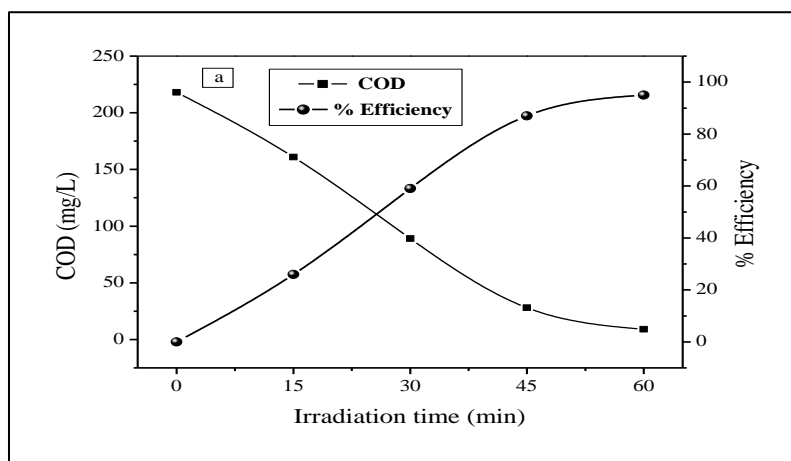
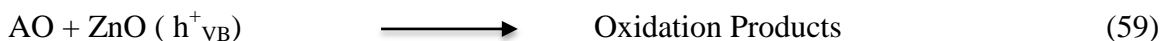
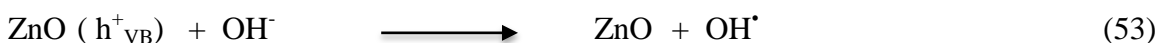


Fig. 4.68: (a) COD trend and % Efficiency (b) CO₂ trend and formation of NO₃⁻ during mineralization of AO: [AO] = 2.5 × 10⁻⁵ mol dm⁻³, ZnO = 80 mg/100mL, pH = 8.4, Light intensity = 25 × 10³ Lux.

4.6.15: Mechanism of Acridine Orange dye degradation:

The photo-catalytic degradation of the AO dye was studied by the use of additives such as H_2O_2 , $K_2S_2O_8$ etc. electron scavengers like H_2O_2 and $K_2S_2O_8$ accept a photo-generated electron from the conduction band (CB) and thus avoid electron-hole recombination producing OH^\bullet [61]. Valence band holes (h_{vb}^+) and conduction band electrons (e_{cb}^-) are generated when aqueous ZnO NPs suspension is irradiated with visible light energy when band gap energy is greater than ($E_g = 3.2$ eV) and these electron-hole pairs interact separately with another molecule. Conduction band electrons (e_{CB}^-) reduce molecular oxygen to generate superoxide radicals, as shown in Eq. (51) to Eq. (60) [62-64]. Such electron generated disrupted the conjugation system of dye and decomposition of dye and the hole so generated creates OH^\bullet from water which again leads to degradation of dye.

The mechanism is as follows: [65, 66]

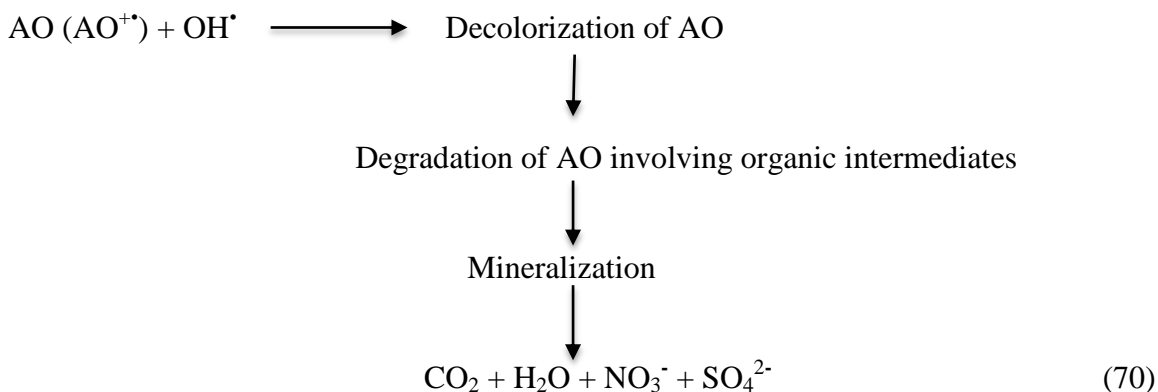


Secondly, sensitization of dye molecule by visible light leads to excitation of dye molecule in singlet or triplet state, subsequently followed by electron injection from

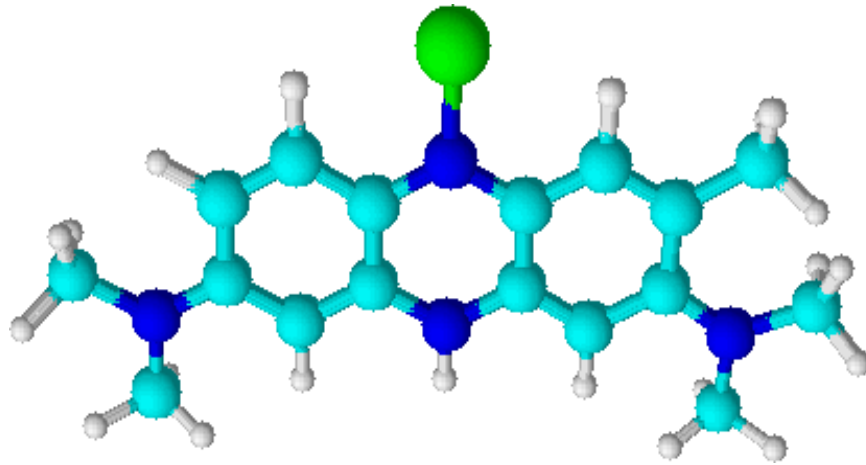
excited dye molecule onto conduction band of semiconductor particles. The mechanism of dye sensitization is summarized in Eq. (61) to Eq. (70) [67-71].



The mechanism of semiconductor photo-catalysis is of very complex nature. Dye molecules interact with $\text{O}_2^{\bullet-}$, HO_2^{\bullet} , or OH^{\bullet} species to generate intermediates ultimately lead to degradation products. OH^{\bullet} radical being very strong oxidizing agent mineralizes dye to various end products. The role of reductive pathways in heterogeneous photo-catalysis has been found to be in minor extent as compared to oxidation [72, 73].



Neutral Red



Neutral Red (or toluylene red, Basic Red 5, or C.I. 50040) is a eurythodan dye used for staining in histology. It is used as a general stain in histology, as a counterstain in combination with other dyes, and for many staining methods. Neutral Red is added to some growth media for bacteria and cell cultures. It usually comes as a chloride salt. Neutral Red acts as a pH indicator, changing from red to yellow between the pH 6.8-8.0.

4.7: Effect of various experimental parameters on the degradation rate of Neutral Red (NR) dye

4.7.1: Photo-catalytic degradation of Neutral Red (NR):

On the surface of catalyst classical Langmuir–Hinshelwood expression was followed by the photo-catalytic degradation rate of NR dye and followed most often Langmuir sorption isotherm for the sorption of the dye to the catalyst surface. This theory is usually used kinetic model for unfolding photo-catalytic behavior. For treatment of heterogeneous surface reactions degradation rate is explained by pseudo first order kinetics in Langmuir–Hinshelwood [11-14]. Such kinetics is streamlined in terms of modified model to accommodate reactions taking place at solid-liquid interface as

$$r = \frac{-dc}{dt} = \frac{k_r KC}{(1+KC)} \quad (1)$$

Where, r = rate of dye disappearance and C = variable dye concentration at time t . K = equilibrium constant for adsorption of NR dye on photo-catalyst and k_r = limiting reaction rate at maximum coverage in operational conditions. The integrated form can be written as

$$t = \ln\left(\frac{C_0}{C}\right) + \frac{1}{Kk_r} \frac{C_0 - C}{k_r} \quad (2)$$

Where t = time required for the initial concentration of dye C_0 to C . At low dye concentration in equation 2, value of C_0 is very less and hence can be neglected.

$$\ln\left(\frac{C_0}{C}\right) = k_r Kt = kt \quad (3)$$

Where k = apparent rate constant of degradation. The Half-life time ($t_{1/2}$) for the photo-catalytic degradation of NR dye on the ZnO NPs surface can be calculated by using following Eq. (4)

$$t_{1/2} = \frac{0.693}{k} \quad (4)$$

The Neutral Red dye degradation results are reported here for three conditions: (1) Neutral Red dye + ZnO NPs + visible light (2) Neutral Red dye + visible light only and (3) Neutral Red dye + ZnO nanoparticles only (dark) were shown in figure 4.69 (a). It was observed carefully that maximum degradation occurred in the first condition, while in dark and during photolysis, no significant changes in the absorbance values were observed. Therefore, in second and third condition, degradation process was not observed. Absorption spectrum changes were recorded at 520nm wavelength.

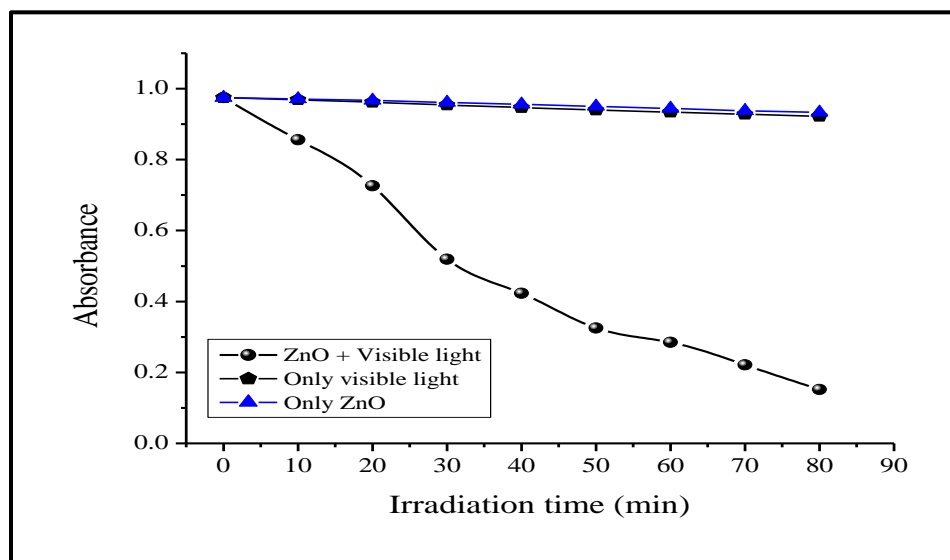


Fig. 4.69 (a) Degradation of Neutral Red: $[NR] = 5.5 \times 10^{-5} \text{ mol dm}^{-3}$,

ZnO NPs = 70 mg/100mL, pH = 9.2, Light intensity = $20 \times 10^3 \text{ Lux}$.

Plotting the semi-logarithmic graph of concentration versus irradiation time (min) of NR dye in presence of ZnO NPs yielded a linear relationship as shown in Figure 4.69 (b). Therefore, reaction dye of degradation by ZnO nanoparticles is pseudo-first order reaction kinetics, with regression coefficient of 0.990, the NR dye degradation rate

constant of $3.52 \times 10^{-4} \text{ s}^{-1}$. The rate constant is the slope of the straight line. In all cases R^2 (correlation constant for the fitted line) values were close to 0.99 which complete pseudo first-order kinetics for NR dye mineralization in this process.

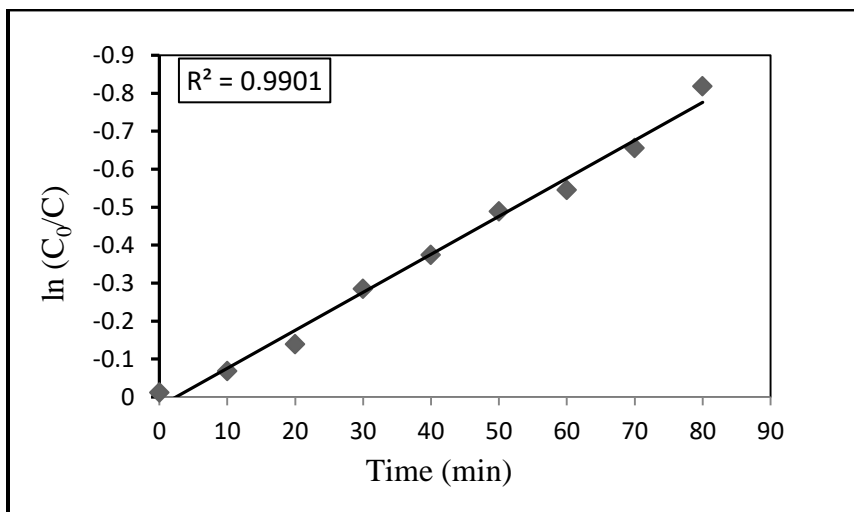


Fig.4.69 (b): Pseudo first order kinetics: $[\text{NR}] = 5.5 \times 10^{-5} \text{ mol dm}^{-3}$,
 $\text{ZnO NPs} = 70 \text{ mg}/100\text{mL}$, $\text{pH} = 9.2$, $\text{Light intensity} = 20 \times 10^3 \text{ Lux}$.

4.7.2: Effect of change in pH:

The pH plays an important role both in the characteristics of textile wastes and generation of OH^\bullet radicals. Hence, attempts have been made to investigate the effect of pH in the degradation of dyes in the presence of visible light. Photo-catalytic degradation process has been studied at pH values from 3.7 to 12.5. The effect of pH on the rate of degradation is shown in Table 4.51 and Figure 4.70. With the increase in pH from 3.7 to 9.2, degradation rate constant increased from $1.17 \times 10^{-4} \text{ s}^{-1}$ to $3.52 \times 10^{-4} \text{ s}^{-1}$. Further increase in pH resulted in reduction in degradation rate constant. At higher value of pH about 7.5, negatively charged active sites on the surface of ZnO NPs catalyst result in high concentration of positively charged of dye molecules on the surface of ZnO NPs. In highly acidic medium, adsorption of lesser dye molecules inhibited the reaction rate.

With increasing pH, surface concentration of dye molecules decreased and OH[•] radicals increased. But ZnO has amphoteric nature and dissolving at low pH and salt formation takes place. At higher pH, it forms zincates such as [Zn(OH)₄]²⁻ [96, 97]. All these factors are responsible for optimal value of photo-degradation of Neutral Red dye at pH 9.2.

Table 4.51: Effect of change in pH: [NR] = 5.5 x 10⁻⁵ mol dm⁻³, ZnO NPs = 70 mg/100mL, Light intensity = 20 x 10³ Lux.

pH	k x 10 ⁻⁴ s ⁻¹	t _{1/2} x 10 ³ s
3.7	1.17	5.93
5.4	2.27	3.05
7.5	2.78	2.49
9.2	3.52	1.96
11.0	2.57	2.69
12.5	1.63	4.25

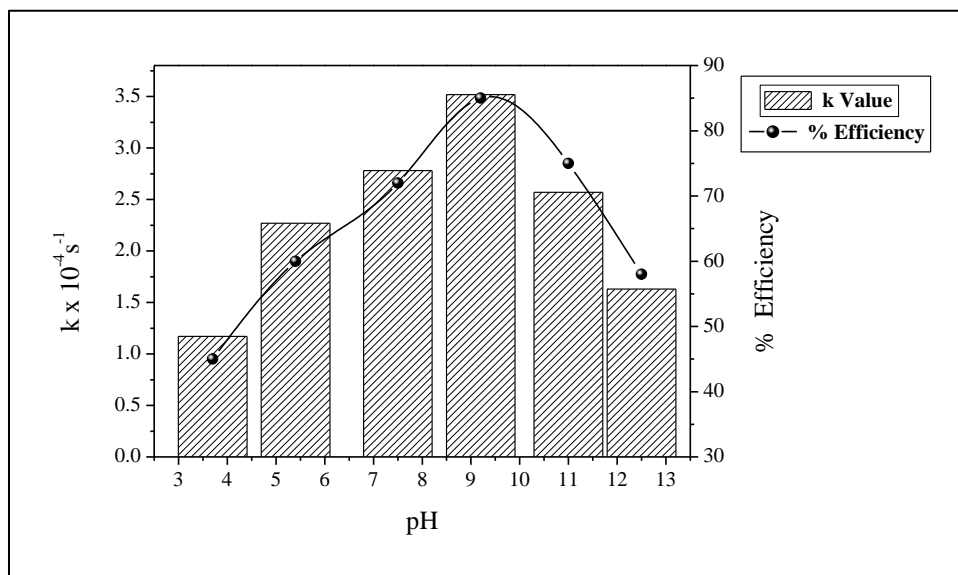


Fig. 4.70: Effect of change in pH on photo-catalytic degradation of NR

4.7.3: Effect of change in catalyst amount:

The influence of catalyst amount on the rate of degradation has been studied by varying its amount from 40mg/100mL to 100mg/100mL. The degradation rate constant values increased from $1.42 \times 10^{-4} \text{ s}^{-1}$ to $3.52 \times 10^{-4} \text{ s}^{-1}$ with the increase in catalyst amount from 40mg/100mL to 70mg/100mL. Further, degradation rate constant values decreased from $3.52 \times 10^{-4} \text{ s}^{-1}$ to $1.15 \times 10^{-4} \text{ s}^{-1}$ with the increased catalyst amount 70mg/100mL to 100mg/100mL. The degradation rate constant value has been reported to be maximal at 70mg/100mL of catalyst amount. The results are shown in Table 4.52 and Figure 4.71. The photo-catalytic degradation efficiency increased with an increase in catalysts mass. This behavior might be due to an increased in the amount of active site on surface of ZnO NPs. Thereafter the optimal amount of ZnO NPs, the activity of photo-catalytic degradation decreased with increased of ZnO NPs catalyst concentration. Because highest loading of ZnO NPs catalyst also causes increase in turbidity of the solution which reduced the light penetration in photoactive volume shrinks [79].

Table 4.52: Effect of change in catalyst amount: [NR] = $5.5 \times 10^{-5} \text{ mol dm}^{-3}$, pH = 9.2, Light intensity = $20 \times 10^3 \text{ Lux}$.

ZnO mg/100mL	$k \times 10^{-4} \text{ s}^{-1}$	$t_{1/2} \times 10^3 \text{ s}$
40	1.42	4.88
50	2.07	3.34
60	2.69	2.57
70	3.52	1.96
80	2.21	3.13
90	1.72	4.02
100	1.15	6.02

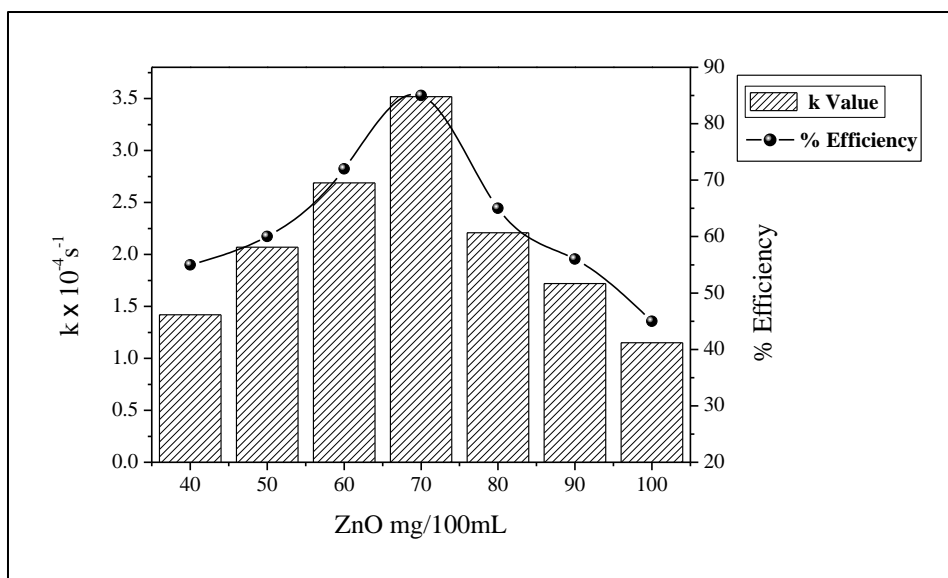


Fig. 4.71: Effect of catalyst amount on photo-catalytic degradation of NR

4.7.4: Effect of change in dye concentration:

The effect of Neutral Red dye concentration on degradation is an important aspect of the study. The possibility of $\cdot\text{OH}$ radical's formation on the semiconductor surface has been related to the degradation rate and to the probability of $\cdot\text{OH}$ radicals reacting with dye molecules [111]. The initial concentration of NR dye has been varied from $2.5 \times 10^{-5} \text{ mol dm}^{-3}$ to $8.5 \times 10^{-5} \text{ mol dm}^{-3}$. The results were shown in Table 4.53 and Figure 4.72. The degradation rate constant increased from $1.22 \times 10^{-4} \text{ s}^{-1}$ to $3.52 \times 10^{-4} \text{ s}^{-1}$ with increased in dye concentration from $2.5 \times 10^{-5} \text{ mol dm}^{-3}$ to $5.5 \times 10^{-5} \text{ mol dm}^{-3}$. Thereafter, degradation rate constant decreased to $1.08 \times 10^{-4} \text{ s}^{-1}$ with dye concentration increased $8.5 \times 10^{-5} \text{ mol dm}^{-3}$. The degradation rate constant is highest at $5.5 \times 10^{-5} \text{ mol dm}^{-3}$ of dye concentration. From literature studies we came to know that as the target organic pollutant concentration increase adsorbed of these molecules on the catalyst surface also increases. Hence relative no. of $\text{O}_2\cdot$ and $\text{OH}\cdot$ radicals on the ZnO surface increased. Consequently, excess dye molecule adsorption on catalyst surface hindered the $\text{OH}\cdot$ ions adsorption and finally

rate of hydroxyl radical formation is lowered. It is concluded from above discussion that above optimum dye concentration rate of degradation decreased [27-29].

Table 4.53: Effect of change in dye concentration: ZnO NPs = 70 mg/100mL, pH = 9.2, Light intensity = 20×10^3 Lux.

[NR] x 10^{-5} mol dm ⁻³	k x 10^{-4} s ⁻¹	t _{1/2} x 10^3 s
2.5	1.22	5.68
3.5	2.11	3.28
4.5	2.87	2.41
5.5	3.52	1.96
6.5	2.53	2.73
7.5	1.65	4.20
8.5	1.08	6.41

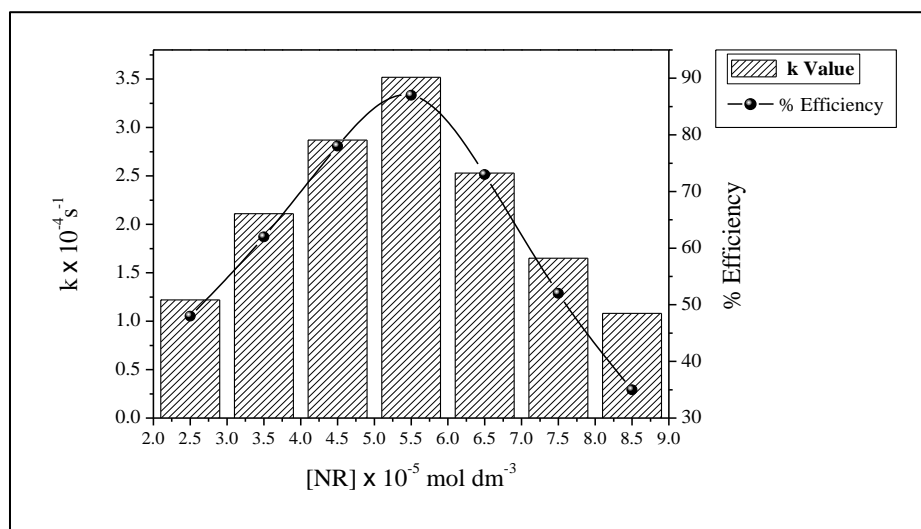


Fig. 4.72: Effect of change in dye concentration on photo-catalytic degradation of NR

4.7.5: Effect of change in oxidant's concentration:

The effect of oxidants concentration such as H₂O₂ and K₂S₂O₈ has been carried out. H₂O₂ and K₂S₂O₈ can play an important role in photo-catalytic degradation of dyes if organic

pollutants contain these oxidants along with dyes [112-114]. The effect of these two oxidants H_2O_2 and $\text{K}_2\text{S}_2\text{O}_8$ on photo-catalytic degradation of NR dye is showed in Table 4.54 and Figure 4.73. The degradation rate constant increased from $4.23 \times 10^{-4} \text{ s}^{-1}$ to $7.58 \times 10^{-4} \text{ s}^{-1}$ with increased in H_2O_2 from $2.0 \times 10^{-6} \text{ mol dm}^{-3}$ to $6.0 \times 10^{-6} \text{ mol dm}^{-3}$. This is because H_2O_2 inhibits the electron-hole recombination by accepting photo-generated electron from the conduction band of ZnO NPs and promotes separation charge and also it forms $\cdot\text{OH}$ radicals according to Eq. (5) to (6).



Further increase in concentration of H_2O_2 beyond optimum concentration, results in decreased in rate constant. When H_2O_2 is in excess, it may act as a hole or $\cdot\text{OH}$ scavenger having injurious effect on photo-catalytic degradation. This explains the need for an optimum concentration H_2O_2 for the highest effect [115, 116].



At optimum concentration of $\text{K}_2\text{S}_2\text{O}_8$, rate constant of degradation has been reported to be $6.98 \times 10^{-4} \text{ s}^{-1}$. $\text{K}_2\text{S}_2\text{O}_8$ can also trap the photo-generated conduction band results in the generation of $\text{SO}_4^{\cdot-}$, a strong oxidizing agent. In addition it can trap the photo-generated electrons and /or generated $\cdot\text{OH}$ radicals.



The results are shown in Table 4.54 and Figure 4.73, the decreased in rate constant optimum concentration $8.0 \times 10^{-6} \text{ mol dm}^{-3}$ is due to the adsorption of $\text{SO}_4^{\cdot-}$ formed during the reaction on surface of ZnO NPs deactivating a section of photo-catalyst [105].

Table 4.54: Effect of change in H₂O₂ and K₂S₂O₈: [NR] = 5.5 × 10⁻⁵ mol dm⁻³, ZnO NPs = 70 mg/100mL, pH = 9.2, Light intensity = 20 × 10³ Lux.

[Oxidant] × 10 ⁻⁶ mol dm ⁻³	[H ₂ O ₂]		[K ₂ S ₂ O ₈]	
	k × 10 ⁻⁴ s ⁻¹	t _{1/2} × 10 ³ s	k × 10 ⁻⁴ s ⁻¹	t _{1/2} × 10 ³ s
0.0	3.52	1.96	3.52	1.96
2.0	4.23	1.63	4.39	1.57
4.0	5.32	1.30	5.57	1.24
6.0	7.58	0.91	6.98	0.99
8.0	6.42	1.07	5.48	1.26
10.0	5.87	1.18	4.74	1.46
12.0	4.28	1.61	4.12	1.68

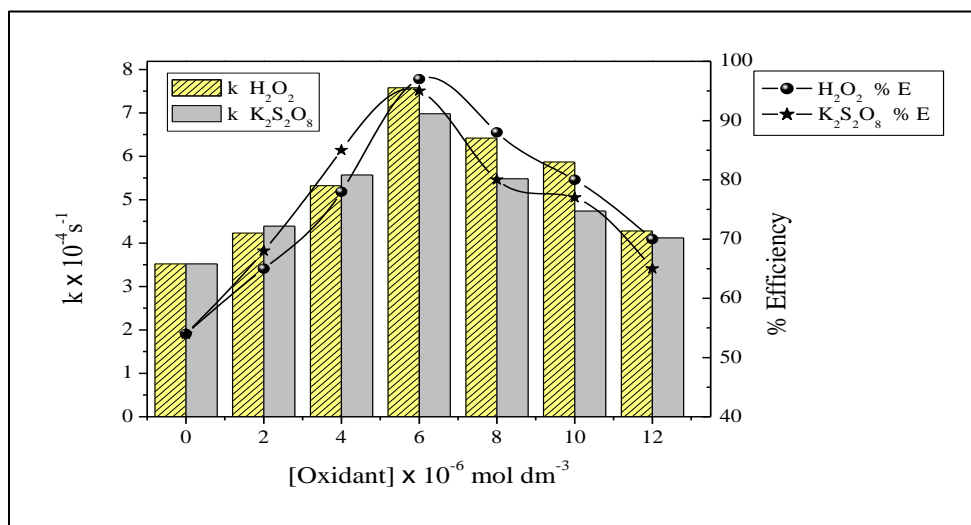
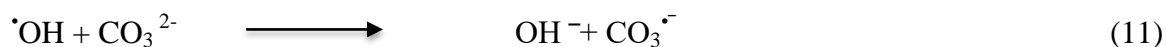


Fig. 4.73: Effect of change in oxidants on photo-catalytic degradation of NR

4.7.6: Effect of change in salts concentration:

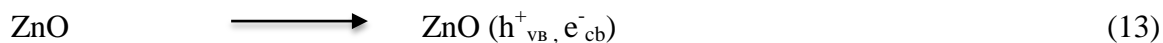
The Na₂CO₃ is mainly used in the dyeing bath in order to adjust the pH of the bath as it plays an important role in fixing of dye on the fabrics and in the fastness of color. Therefore, the wastewater from the dyeing operation will contain considerable amount of

carbonate ion [82]. With an increase in the amount of carbonate ion from 2.0×10^{-5} mol dm^{-3} to 12.0×10^{-5} mol dm^{-3} resulted into reduction of rate constant from $3.18 \times 10^{-4} \text{ s}^{-1}$ to $1.52 \times 10^{-4} \text{ s}^{-1}$. The inhibition in the degradation of dye is due to the hydroxyl scavenging property of carbonate ions, which can be accounted from the following equation.



The hydroxyl radical which is a primary oxidant for the photo-catalytic degradation found to decrease slowly with an increase in carbonate ions and degradation of the dye significantly decreased [37].

Similarly, NaCl commonly comes out in the effluent along with wastewater. Therefore photo-catalytic degradation rate in presence of Cl^- ions has been studied by increase in concentration of Cl^- ions from 2.0×10^{-5} mol dm^{-3} to 12×10^{-5} mol dm^{-3} that resulted into reduction of rate constant from $3.22 \times 10^{-4} \text{ s}^{-1}$ to $1.38 \times 10^{-4} \text{ s}^{-1}$. The decrease in the degradation of dye in the presence of chloride ion might be due to the hole scavenging properties of chloride ion [38]



The dependency of reaction rate constant on the concentration of Na_2CO_3 and NaCl is shown in Table 4.55 and Figure 4.74.

Table 4.55: Effect of change in Na_2CO_3 and NaCl : $[\text{NR}] = 5.5 \times 10^{-5} \text{ mol dm}^{-3}$,
 $\text{ZnO NPs} = 70 \text{ mg}/100\text{mL}$, $\text{pH} = 9.2$, Light intensity = $20 \times 10^3 \text{ Lux}$.

[Salt] x $10^{-5} \text{ mol dm}^{-3}$	[Na_2CO_3]		[NaCl]	
	$k \times 10^{-4} \text{ s}^{-1}$	$t_{1/2} \times 10^3 \text{ s}$	$k \times 10^{-4} \text{ s}^{-1}$	$t_{1/2} \times 10^3 \text{ s}$
0.0	3.52	1.96	3.52	1.96
2.0	3.18	2.17	3.22	2.15
4.0	2.83	2.44	2.92	2.37
6.0	2.42	2.86	2.62	2.64
8.0	2.09	3.31	2.25	3.08
10.0	1.82	3.80	1.61	4.30
12.0	1.52	4.55	1.38	5.02

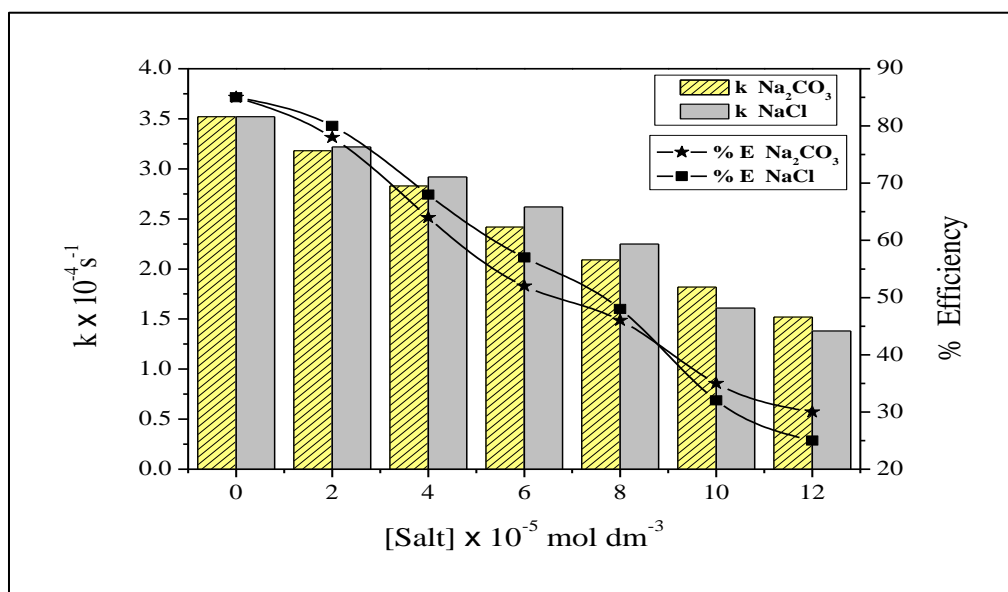
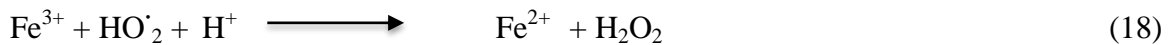


Fig. 4.74: Effect of change in salts on photo-catalytic degradation of NR

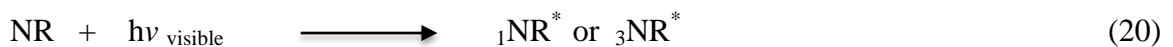
4.7.7: Effect of change in FeCl_3 concentration:

In present study, effect of FeCl_3 on the photo-catalytic degradation of NR dye has been investigated by varied the concentration from $2.0 \times 10^{-5} \text{ mol dm}^{-3}$ to $12.0 \times 10^{-5} \text{ mol dm}^{-3}$.

The degradation rate constant values increased from $4.32 \times 10^{-4} \text{ s}^{-1}$ to $5.62 \times 10^{-4} \text{ s}^{-1}$ with the increase in concentration of FeCl_3 from $2.0 \times 10^{-5} \text{ mol dm}^{-3}$ to $6.0 \times 10^{-5} \text{ mol dm}^{-3}$. Thereafter, degradation rate constant values decreased to $3.37 \times 10^{-4} \text{ s}^{-1}$ on further increase in amount of FeCl_3 up to $12.0 \times 10^{-5} \text{ mol dm}^{-3}$. The results are shown in Table 4.56 and Fig. 4.75. The metal ions such as Fe^{3+} could be used as sensitizers during photocatalytic degradation of dye. In fact the increase in ferric ions concentration in the reaction mixture resulted into the increase of Fe^{2+} ions concentration, which is accompanied by improved generation of $\cdot\text{OH}$ radicals, consequently increasing the rate of degradation of FeCl_3 inhibits the reaction rate of degradation by competing with formation of $\cdot\text{OH}$ radicals [90, 91].



The photo-activation of surface adsorbed complex ion ($\text{Fe}^{3+}\text{OH}^-$) results in the formation of $\text{Fe}^{2+}\text{OH}\cdot$ specie which injects electrons to the conduction band of ZnO as shown in [Eq. 21-22]. The rate of decolorization in case of FeCl_3 is explicable due to rapid scavenging of conduction band electrons by molecular oxygen leading to formation of superoxide and hydroperoxide radicals [42, 43] [Eq. (22)].



In the presence of higher concentration of FeCl_3 , there is excessive surface adsorption of anionic dye on the surfaces of catalyst. This reduced the total photoactive area of ZnO NPs catalyst and lowered the rate of reaction [45].

Table 4.56: Effect of change in FeCl_3 concentration: $[\text{NR}] = 5.5 \times 10^{-5} \text{ mol dm}^{-3}$, ZnO NPs = 70 mg/100mL, pH = 9.2, Light intensity = $20 \times 10^3 \text{ Lux}$.

$\text{FeCl}_3 \times 10^{-5} \text{ mol dm}^{-3}$	$k \times 10^{-4} \text{ s}^{-1}$	$t_{1/2} \times 10^3 \text{ s}$
0.0	3.52	1.96
2.0	4.32	1.60
4.0	4.56	1.51
6.0	5.62	1.23
8.0	4.83	1.43
10.0	4.26	1.62
12.0	3.73	1.85

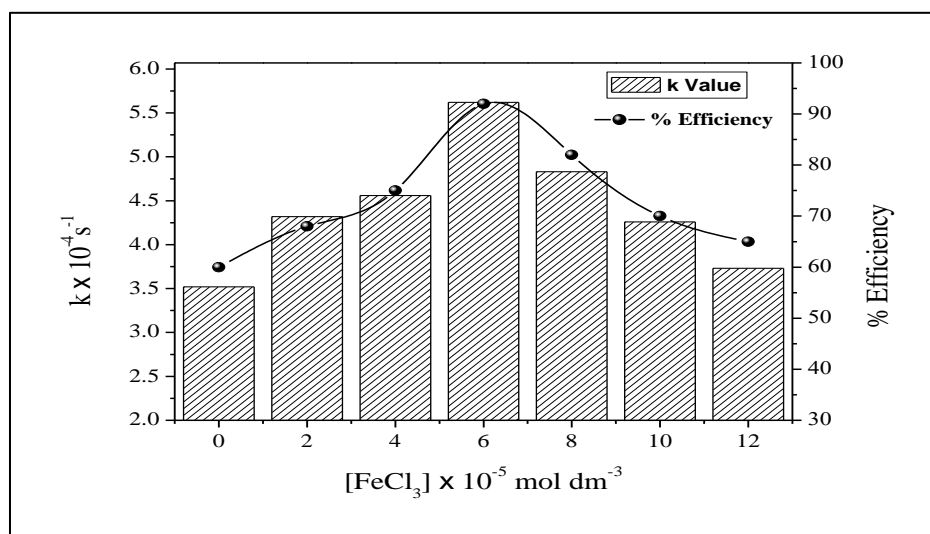


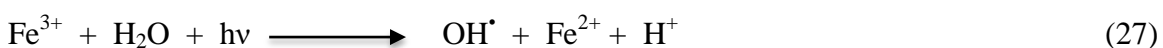
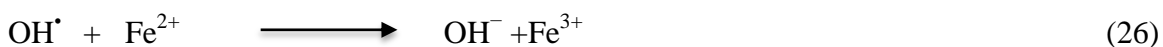
Fig. 4.75: Effect of change in FeCl_3 on photo-catalytic degradation of NR

4.7.8: Effect of change in Fenton's reagent concentration:

Among advanced oxidation processes, semiconductor oxidation using Fenton and Fenton like reagent is an attractive usage for the effective degradation of dyes because of its low cost and lack of toxicity of the reagents like H_2O_2 and Fe^{2+} or Fe^{3+} [106]. Fenton's reagent, a mixture of Fe^{3+} and H_2O_2 has been known as a powerful oxidant for textile dyes. In recent years, many research workers have studied the degradation of dyes using Fenton and visible/solar light system [48, 49].



OH^{\bullet} radicals may be scavenged by reaction with another Fe^{2+} :



Efficiency of $\text{Fe}^{3+}/\text{H}_2\text{O}_2$ method has been studied for degradation of Neutral Red dye in presence of visible light and ZnO nanoparticles. The degradation rate constant has a value of $4.24 \times 10^{-4} \text{ s}^{-1}$ on the addition of $\text{Fe}^{3+}:\text{H}_2\text{O}_2$ in molar ratio 3:1. In the presence of $\text{Fe}^{3+}:\text{H}_2\text{O}_2$ in molar ratio 1.4:1, rate constant has been found $8.19 \times 10^{-4} \text{ s}^{-1}$. The results are shown in Table 4.57 and Figure 4.76. Upon irradiation of $\text{Fe}^{3+}/\text{H}_2\text{O}_2/\text{ZnO}/\text{NR}$ method in the presence of visible light, formation of OH^{\bullet} radicals increases relating a complex mechanism. Dye absorbs visible irradiation and is excited into high-energy state. These excited dye molecules reduce the ferric ion complex to ferrous ion complex followed by the transfer to ferric ion [50]. The reduced ferrous ions react with hydrogen peroxide to decompose and produce hydroxyl radical [Eq. (30)]. OH^{\bullet} radicals also decompose H_2O_2 to HO_2^{\bullet} .



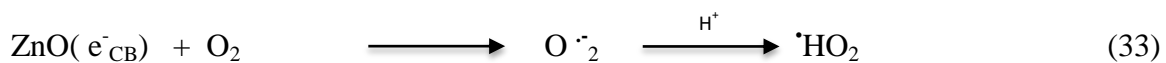


Table 4.57: Effect of change in Fe³⁺/H₂O₂: [NR] = 5.5 × 10⁻⁵ mol dm⁻³, ZnO NPs = 70 mg/100mL, pH = 9.2, Light intensity = 20 × 10³ Lux.

Fe ³⁺ : H ₂ O ₂	Without ZnO		With ZnO	
	k × 10 ⁻⁴ s ⁻¹	t _{1/2} × 10 ³ s	k × 10 ⁻⁴ s ⁻¹	t _{1/2} × 10 ³ s
3:1	1.20	5.77	4.24	1.63
1.4:1	1.57	4.41	6.47	1.07
1:1.4	1.93	3.59	8.19	0.84
1:3	2.18	3.17	7.46	0.92
1:11	2.55	2.71	6.77	1.02
11:1	2.67	2.59	6.14	1.12

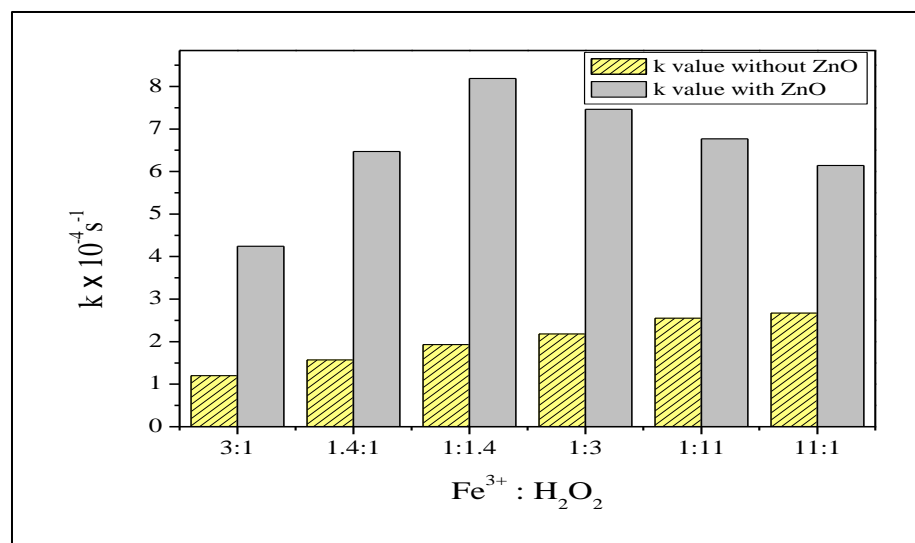


Fig. 4.76: Effect of change in Fenton's reagent on photo-catalytic degradation of NR

4.7.9: Effect of change in light intensity:

The effect of the variation of the light intensity on the degradation rate has been studied by varying the light intensity increasing from 10×10^3 Lux to 30×10^3 Lux. Neutral Red dye solution concentration 5.5×10^{-5} mol dm⁻³, ZnO NPs catalyst amount 70 mg/100mL and pH 9.2. To examine the effect of light intensity on photo-catalytic degradation of Neutral Red dye, the distance between the light source and the exposed surface area was varied. The degradation rate constant increased from 2.04×10^{-4} s⁻¹ to 5.08×10^{-4} s⁻¹ with increase in light intensity on semiconductor surface as shown in Table 4.58 and Figure 4.77. The data show that the rate of degradation was accelerated as the light intensity was increased because any increase in the intensity of light increased the photons striking per unit time per unit area of the ZnO NPs catalyst powder resulted in more OH[•] radicals. A linear behavior between intensity of light and rate of degradation was observed [84].

Table 4.58: Effect of change in light intensity: $[NR] = 5.5 \times 10^{-5} \text{ mol dm}^{-3}$,
ZnO NPs = 70 mg/100mL, pH = 9.2.

Light intensity $\times 10^3$ Lux	$k \times 10^{-4} \text{ s}^{-1}$	$t_{1/2} \times 10^3 \text{ s}$
10	2.04	3.39
15	2.74	2.52
20	3.52	1.96
25	4.46	1.55
30	5.08	1.36

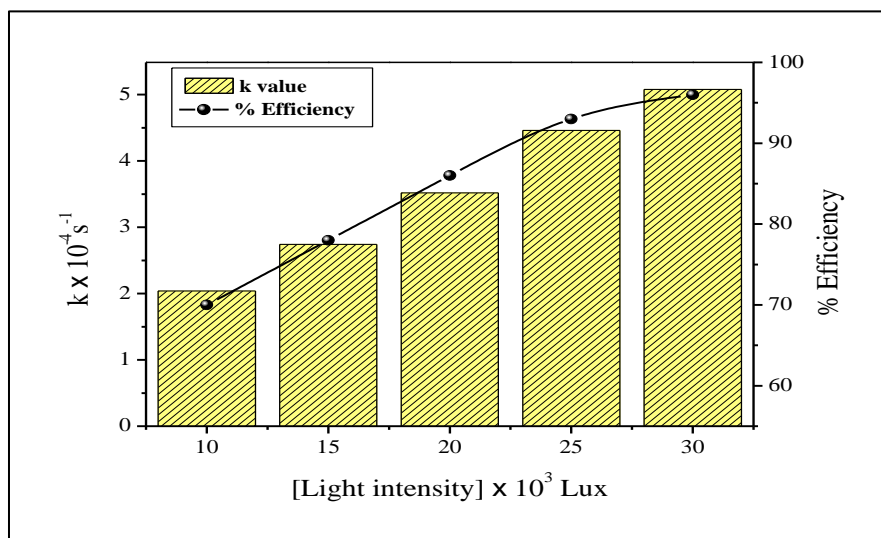


Fig. 4.77: Effect of change in light intensity on photo-catalytic degradation of NR

4.7.10: Effect of bubbling of N_2 and O_2 :

In the present study pure nitrogen and oxygen were purged into the photo-reactor in order to understand their effect on the photo-catalytic degradation of NR, respectively, the results are shown in Figure 4.78. These observations confirm the proposed assumption that dissolved oxygen is a precursor of main oxidant, that is, the role of DO is to trap the photo-generated electrons to produce $O_2^{\cdot-}$ radicals, which particles in photo-catalytic

process to accelerate the NR photo-degradation. The Oxygen got adsorbed on the surface of the ZnO NPs and the surface redox reactions initiated by photo-generated electrons and generating superoxide anion radical and this superoxide anion radical started the photo-catalytic degradation of dye pollutant. However in the presence of nitrogen the conduction band (CB) electrons were blocked and the formation of superoxide anion radical is prevented. Hence the reaction rate is suppressed [53, 54].

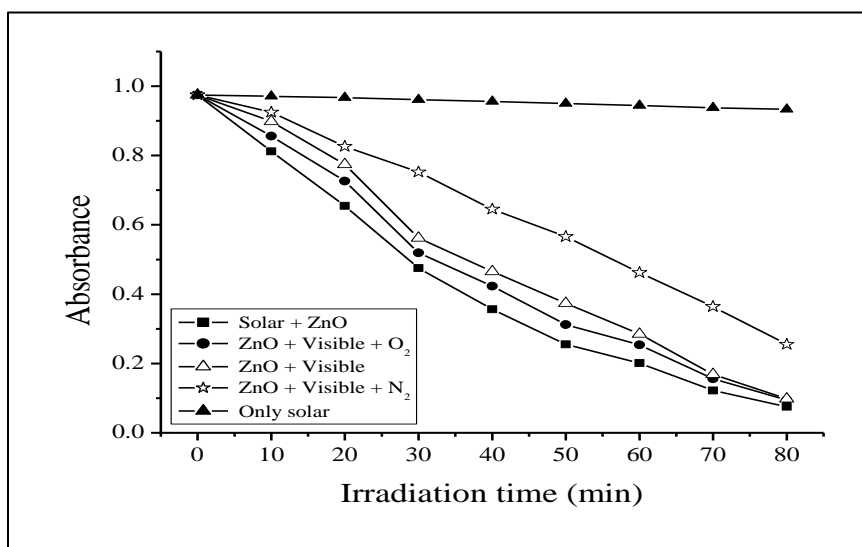
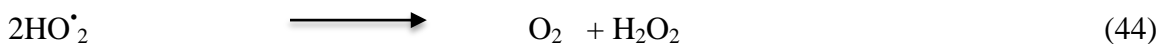
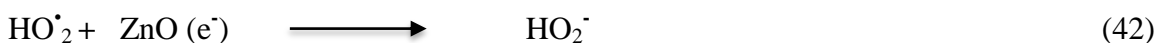
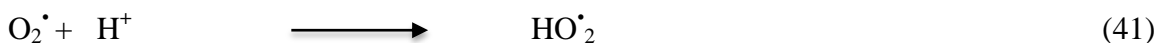
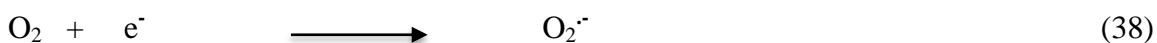


Fig. 4.78: Decolorization of NR under various photo-catalytic systems:

[NR] = 5.5×10^{-5} mol dm⁻³, ZnO NPs = 70 mg/100mL, pH = 9.2,
Light intensity = 20×10^3 Lux.

4.7.11: Comparison of solar and visible light:

The efficiency of solar and visible light on photo-catalytic degradation of dye was comparatively studied. The degradation efficiency of Neutral Red dye with visible light was found to be more efficient than that of solar light. Figure 4.78 shows the comparisons of color removal efficiency of Neutral Red with two light sources under different conditions. It was noticed that if same experiments were carried out in the absence of ZnO, then no absorbance loss of dye was found [55, 56].

4.7.12: Effect of other photo-catalysts:

We have investigated the relative efficiencies of other photo-catalysts as well Table 4.59 and Figure 4.79. The order of photo-activity followed the order: ZnO NPs > ZnO > BiOCl > TiO₂ > BaCrO₄ on photo-catalytic degradation have been studied at same condition. The photo-catalyst on illuminating with light having energy equal to or more than band gap energy, a heterogeneous photo-catalyst reaction occurs on surface of semiconducting materials. It has already been found that catalysts such as ZnO NPs, ZnO, BiOCl and TiO₂ have band gaps larger than 3 eV strong photocatalytic activities. The conduction and valence band potentials of both ZnO NPs and TiO₂ are larger than the corresponding redox potentials of H⁺/H₂ and H₂O/O₂ and the photo-generated electron and hole can be separated efficiently. BaCrO₄ with smaller band gap shows less activity since its conduction band is much lower than that of ZnO NPs and TiO₂. The smaller band gap permits rapid recombination of electron-hole and so electron in these catalysts cannot move into the electron acceptors in the solution rapidly. Hence low photo-catalytic activity was observed in these semiconductors. It is for these reasons; the prepared ZnO nano photo-catalyst has more photo-catalytic efficiency than other photo-catalysts [57, 58].

Table 4.59: Effect of other photo-catalysts: [NR] = $5.5 \times 10^{-5} \text{ mol dm}^{-3}$, pH = 9.2,
Light intensity = $20 \times 10^3 \text{ Lux}$.

Catalysts (70mg/100mL)	$k \times 10^{-4} \text{ s}^{-1}$	$t_{1/2} \times 10^3 \text{ s}$
ZnO NPs	3.52	1.96
ZnO	2.62	2.64
BiOCl	2.18	3.17
TiO ₂	1.56	4.44
BaCrO ₄	1.15	6.02

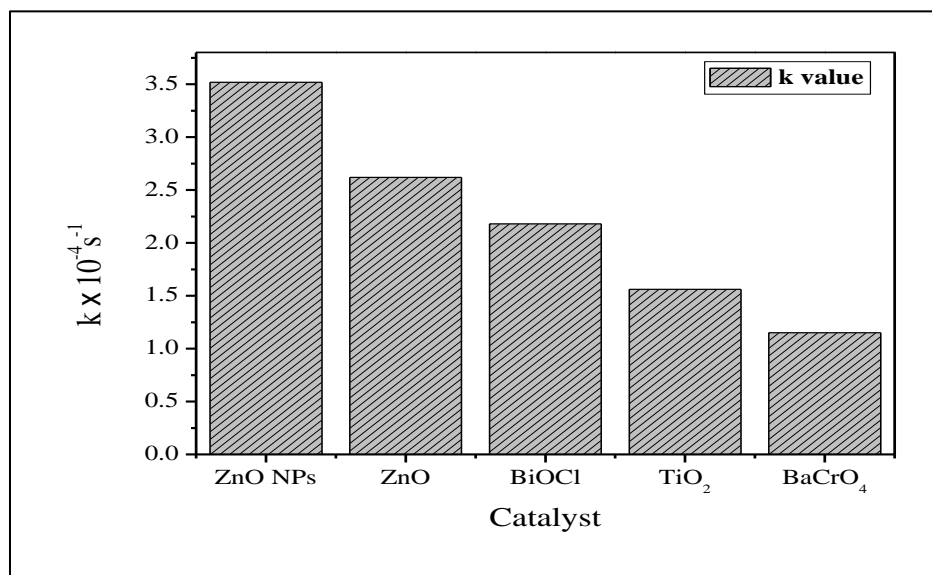


Fig. 4.79: Effect of other photo-catalysts on photo-catalytic degradation of NR

4.7.13: Test for reusability of ZnO NPs:

The reusability of ZnO nanoparticles photo-catalyst was tested for dye degradation. The ZnO nanoparticles catalyst used for degradation of dye was filtered, washed and dried in air and then in oven for 30 minutes. This dried ZnO photo-catalyst was used for the

degradation of dyes under similar reaction conditions. It was observed that the ZnO photo-catalyst can be used repeatedly even up to three batches of reaction without any treatment and reused catalyst showed almost similar catalyst activity with fresh (original) catalyst. The initial rate of photo-degradation of the dye has found very low decrement even after the third second cycle of reuse. The results were shown in figure 4.80. The less of activity was observed and losses of Zn^{++} ions were more pounced only after third cycle of its reuse.

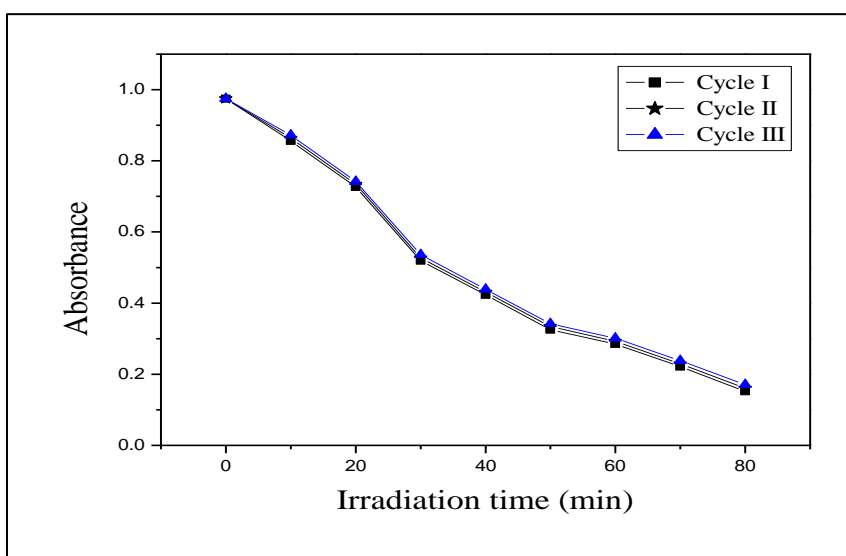


Fig. 4.80: Decolorization of NR by ZnO NPs: (I) Cycle; (II) Cycle; (III) Cycle:
[NR] = 5.5×10^{-5} mol dm^{-3} , ZnO NPs = 70 mg/100mL, pH = 9.2,
Light intensity = 20×10^3 Lux.

4.7.14: COD and CO₂ measurements during degradation of Neutral Red:

The efficiency of photo-catalytic treatment to mineralize the dyes was studied. Chemical oxygen demand resulted were taken as one of the parameter to determine the feasibility of the reduction process for Neutral Red dye degradation. COD and free CO₂ measurement were carried out to record the quantity of mineralization of the organic molecule under consideration over ZnO suspension, COD test allowed the measurements

of waste in terms of the total quantity of oxygen required for the degradation of organic matter to CO₂ and inorganic ions [59]. The decrease in COD values of the treated dye solution indicated the mineralization of dye molecules along with the colour removal. The reduction in the estimated COD from 208 mg/L to 1mg/L and increase in CO₂ values from 13 mg/L to 152 mg/L of illumination indicated the complete mineralization of treated dye solution. From estimated value of COD and CO₂, it is evident that 99 % of COD removal has been completed in 120 min of irradiation under optimum reaction condition. A decrease in COD and increase in CO₂ confirm the degradation of dye. Significant amount of NO₃⁻ were released into reaction during the mineralization of dye. A decrease in pH has also been observed with increase in the quantity of mineralization. The results were shown as Table 4.60 and Figure 4.81 (a) and (b) [60].

Table 4.60: COD and CO₂ measurements during degradation of Neutral Red:

[NR] = 5.5×10^{-5} mol dm⁻³, ZnO NPs = 70 mg/100mL, pH = 9.2,
Light intensity = 20×10^3 Lux.

Time (min)	COD (mg/L)	CO ₂ (mg/L)	Efficiency (%)	NO ₃ & (mg/L)
0	208	13	0	0
30	142	36	31	8.7
60	72	92	65	14.8
90	20	141	90	23.2
120	1	152	99	30.3

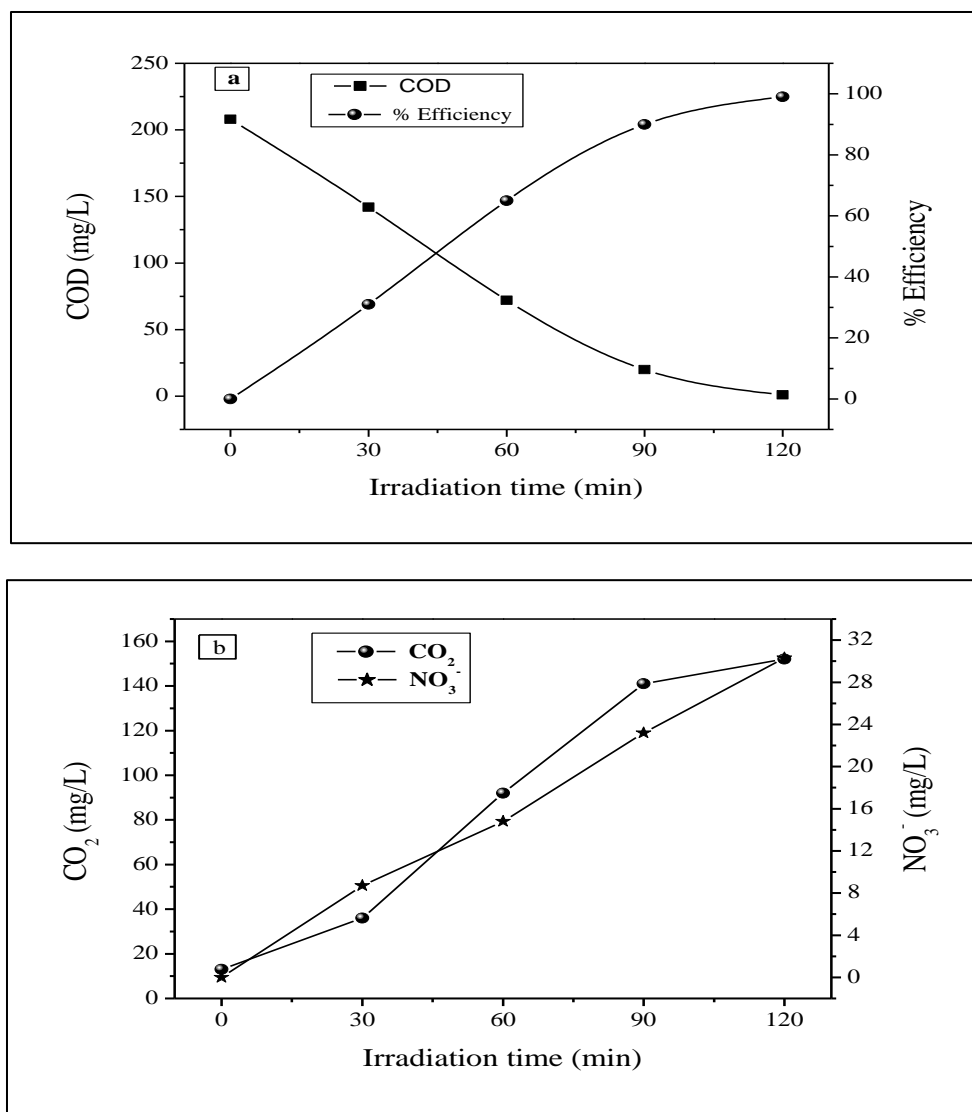


Fig. 4.81: (a) COD trend and % Efficiency (b) CO₂ trend and formation of NO₃⁻ during mineralization of NR: [NR] = 5.5 × 10⁻⁵ mol dm⁻³, ZnO NPs = 70 mg/100mL, pH = 9.2, Light intensity = 20 × 10³ Lux.

4.7.15: Mechanism of Neutral Red dye degradation:

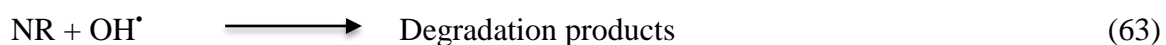
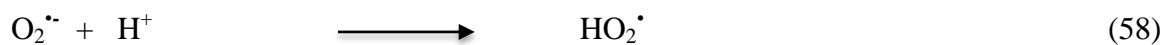
The photo-catalytic degradation of the NR dye was studied by the use of additives such as H₂O₂, K₂S₂O₈ etc. electron scavengers like H₂O₂ and K₂S₂O₈ accept a photo-generated electron from the conduction band (CB) and thus avoid electron-hole recombination producing OH[•] [61]. Valence band holes (h_{vb}⁺) and conduction band electrons (e_{cb}⁻) are

generated when aqueous ZnO NPs suspension is irradiated with visible light having more energy than (3.2 eV) band gap energy. These electron and hole pairs interacts with another molecules separately. Now valance band holes (h_{VB}^+) reacted with H_2O or OH^- radical's bonded on surface to procedure hydroxyl radical (OH^\bullet). And molecule oxygen generated superoxide radicals, as shown in Eq. (45) to Eq. (54) [62-64]. Such electron generated disrupted the conjugation system of dye and decomposition of dye and the hole so generated creates OH^\bullet from water which again leads to degradation of dye. The mechanism is as follows: [65, 66]

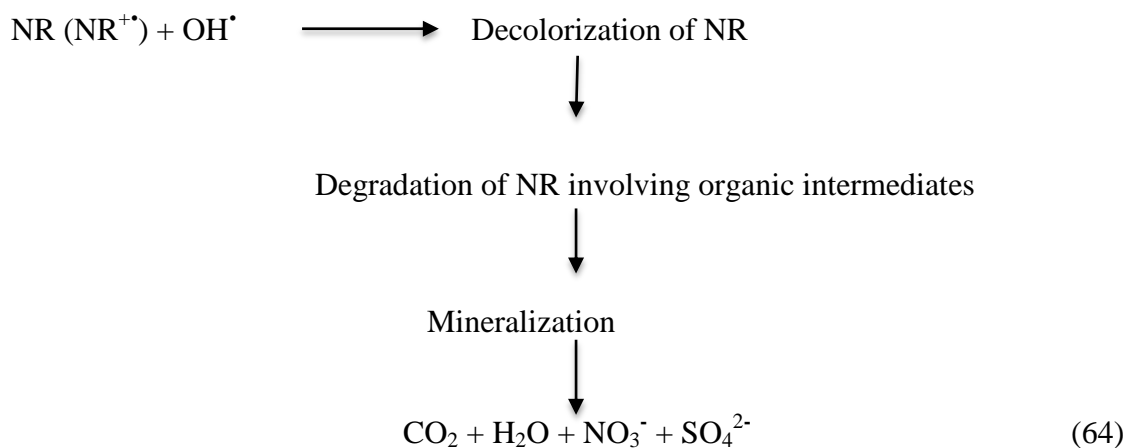


Secondly, sensitization of dye molecule by visible light leads to excitation of dye molecule in singlet or triplet state, subsequently followed by electron injection from excited dye molecule onto conduction band of semiconductor particles. The mechanism of dye sensitization is summarized in Eq. (55) to Eq. (64) [67-71].





The mechanism of semiconductor photo-catalysis is of very complex nature. Dye molecules interact with $\text{O}_2^{\bullet -}$, HO_2^{\bullet} , or OH^{\bullet} species to generate intermediates ultimately lead to degradation products. OH^{\bullet} radical being very strong oxidizing agent (oxidation potential 3.2 eV) mineralizes dye to various end products. The role of reductive pathways in heterogeneous photo-catalysis has been found to be in minor extent as compared to oxidation [72, 73].



NR = Neutral Red

References:

1. Zhi-gang J., Kuan-kuan P., Yan-hua L. and Rong-sun Z., *Trans. Nonferrous Met. Soc. China*, 22 (2012) 873.
2. Kuar J., Kumar P., Sathiaraj T. S. and Thangaraj R., *Int. Nano Lett.*, 3 (2013) 1.
3. Ansari M. A., Khan H. M., Khan A. A., Sultan A. and Azam A., *Appl Microbiol Biotechnol*, 94 (2012) 467.
4. Shah M. A., *Advanced Materials Research*, 67 (2009) 215.
5. Rao N. S. and Rao M. V. B., *American Journal of Materials Science*, 5 (2015) 66.
6. Anandraj L. F. A. and Jayalakshmy E., *Oriental Journal of Chemistry*, 31 (2015) 51.
7. Asad Y. and Hiraj T., *Journal of Colloid and Int. Science*, 284 (2005) 184.
8. Parvin T., Keerthiraj N., Ibrahim I. A., Phanichphant S. and Byrappa K., *Int. J. Photoenergy*, 2012 (2012) 1.
9. Suwanboon S., *Science Asia*, 34 (2008) 31.
10. Ibrahim, M., Nada A. and Kamal D. E., *Indian Journal of Pure & Applied Physics*, 43 (2005) 911.
11. Hoffmann M. R., Martin S. T., Choi W. and Bahermann D. W., *Chem. Rev.*, 95 (1995) 69.
12. Chatterjee D. and Dasgupta S., *J. Photochem. Photobiol. C Photochem.*, 6 (2005) 186.
13. Konstantinou I. K. and Albanis T. A., *Appl. Catal., Environ.*, 49 (2004) 1.
14. Gaya U. I. and Abdullah A. H., *J. Photochem. Photobiol. C Photochem.*, 9 (2008) 1.
15. Mahmad M. A., Poncheri A., Badr Y. And Abd EI Wahed M. G., *South African J. Sci.*, 105 (2009) 299.

16. Mashkour M. S., Al-Kaim A. F., Ahmed L. M. and Hussein F. H., *Int. J. Chem. Sci.*, 9 (2011) 969.
17. Pare B., Singh P. and Jonnalagadda S. B., *Indian J. of Chemistry*, 47 (2008) 830.
18. Al-kaim A. F., Aljeboree A. M., Alrazaq N. A., Baquir S. J., Hussein F. H. and Lilo A. J., *Asian J. of Chemistry*, 26 (2014) 8445.
19. Lee J. D., *Concise Inorganic Chemistry, 5th Edn*, (Blackwell Science, United Kingdom) (1999) 843.
20. Lu C. S., Chen C. C., Huang L. K., Tsai P. A and Lai H. F., *Catalysis*, 3, (2013) 501.
21. Behnajady M. A., Modirshahla N. and Hamzavi R., *J. Hazard. Mater. B*, 133 (2006) 226.
22. Rejani P., Radhakrishnan A. and Beena B., *Ironica Journal of Energy & Environment*, 5 (2014).
23. Chakrabarti S. and Dutta B. K., *J. Hazard. Mater.*, 112 (2004) 269.
24. Bauer C., Jacqueus P. and Kalt A., *J. Photochem. Photobiol. A Chem.*, 140 (2000) 87.
25. Gandhi J., Dangi R., Sharma J. C., Verma N. and Bhardwaj S., *Pelagia Res. Library, Der Chemica Sinca*, 1 (2010) 77.
26. Hussein A. S. and Fairouz N. Y., *J. of Babylon Uni./Pure and Applied Sci.*, 24 (2016) 2510.
27. Kumawat P., Joshi M., Ameta R. and Ameta S. C., *Ind. J. Sci. Res. And Tech.*, 3 (2015) 72.
28. Pawar M. J., Khanajone A. D., Gaoner M. D. and Chander P. S., *Int. J. of Adv. Sci. Res. And Tech.* 2 (2012) 471.
29. Pare B., Tomar H., Bhagwat V. W. and Foglaini C., *Aust. J. Ed. Chem.*, (2007) 30.

30. Giahi M., Taghavi H., Habibi S. and Sariri R., *Journal of Physical and Theoretical Chemistry*, 8 (2011) 251.
31. Pare B., Singh V., More P. and Thapak T. R., *Int J. Chem Sci*, 9 (2011) 537.
32. Tolia J. V., Chakraborty M. and Murthy Z. V. P., *Polish Journal of Chemical Technology*, 14 (2012) 16.
33. Chang M. W., Chung C. C., Chern J. M. and Chen T. S., *Chemical Engineering Science*, 65 (2010) 135.
34. Daneshvar N., Aber S., Seyed Dorraji M. S., Khataee A. R., and Rasoulifard M. H., *World Academy of Science, Engineering and Technology*, 29 (2007) 267.
35. Eslami A., Nasserli S., Yadollahi B., Mesdaghinia A., Vaezi F., Nabizadeh R. Mesdaghinia A. and Nazmara S., *J. Chem Technol Biotechnol*, 83 (2008) 1447.
36. Pare, B., Singh, P. and Bhagwat, V. W., *Chemenviron*, 4: (2008)12.
37. Seyed-Dorroji M. S., Daneshvar N. and Aber S., *Global NEST the Int. J.*, 4 (2009) 535.
38. Pare B., Singh P., and Jonnalagadda S. B., *Indian Journal of Chemistry*, 47 (2008) 830.
39. Pignatello J. Oliveros E. and Mackay A., *Crit. Rev. Environ. Sci. Tech.*, 36 (2006)1.
40. Pignatello J., *J. Environ. Sci. Tech.*, 26 (1992)944.
41. Pare B., Singh P. and Jonnalagadda S. B., *Journal of Scientific & Industrial Research*, 68 (2009) 724.
42. Chen C., Li X., Ma W., Zhao J., Hidaka H. and Serpone N., *J. Phys. Chem. B*, 106 (2002) 318.
43. Qu P., Zhao J., Shen T. and Hidaka H., *J. Mol. Catal. A Chem.*, 129 (1998) 127.
44. Baran W., Makowski A. and Waradas W., *Chemosphere*, 48 (2002) 78.

45. Baran W., Makowski A. and Waradas W., *Chemosphere*, 53 (2003) 87.
46. Dutta A., Banerjee P., Sarkar D., Bhattacharjee S. and Chakrabarti S., *Desalination and Water Treatment*, (2014) 1.
47. Wang S., *Dyes and Pigments*, 76 (2008) 714.
48. Ameta S. C., Kumar A., Paliwal M. and Ameta R., *J. Iran. Chem. Soc.*, 5 (2008) 346.
49. Pare B., Singh P. and Jonnalagadda S. B., *Indian Journal of Chemistry* 17 (2010) 391.
50. Xie Y., Chen F., He J., Zhao J. and Wang H., *J. Photochem. Photobiol. A Chem.*, 136 (2000) 235.
51. Ameta K. L., Papnani N. and Ameta R., *Journal of Materials*, (2014) 1.
52. Pare B., Solanki V. S., Gupta P. and Jonnalagadda S. B., *Indian Journal of Chemical Technology*, 23 (2016) 513.
53. Zhang D., Qiu R., Song L., Eric B., Mo Y. and Huang X., *J. Hazard. Mater.*, 163 (2009) 843.
54. Shivraju H. P., *Int J. Environ. Sci.*, 1 (2011) 5.
55. Kua W. S. and Ho P. H., *Chemosphere*, 45 (2001) 77.
56. Pare B., Singh P. and Jonnalagadda S. B., *Indian Journal of Chemistry*, (2008) 1364.
57. Patil N. and Shrivastava V. S., *Archives of Appld. Sci. Res.*, 3 (2011) 596.
58. Rawal S. B., *Sonsik Journal*, 3 (2011) 38.
59. Byrappa K., Subramani A. K., Ananda S, Lokanatha Rai K. M., Dinesh R. and Yoshimura M., *Bull. Mater. Sci*, 29 (2006) 433.
60. Abhilarasu A., Somanathan T., Saravanan A., Saravanan V. and Rajakumar P., *Int. J. Pharma Bio Sci.*, 7 (2016) 93.

61. Hoffmann M. R., Martin S. T., Choi W. and Bahnemann D. W., *Chem. Rev.*, 95 (1995) 69.
62. Abdel-Khalek A. A., Nassar H. F., Gawad F. Kh. A. and Hashem A., *Der Pharma Chemica*, 7 (2015) 264.
63. Pare B., Jonnalagadda S. B., Tomar H., Singh P. and Bhagwat V. W., *Desalination*, 232 (2008) 80.
64. Akyol A. and Bayramoglou M., *J. Hazard. Mater. B*, 124 (2005) 241.
65. Curri M. L., Comparelli R., Cozzoli P. D., Mascolo G. and Agostiano A., *Mater. Sci. Eng. C*, 23 (2003) 285.
66. Poullos I., Micropoulou E., Panou R. and Kostopoulou E., *Appl. Catal. B Environ*, 41 (2003) 345.
67. Epling G. A. and Lin C., *Chemosphere*, 46 (2002) 561.
68. Dhatshanamurthi P., Santhi M. and Swaminathan M., *Journal of Water Process Engineering*, 16 (2017) 28.
69. Galidino C., Jacqueus P. and Kalt A., *J. Photochem. Photobiol. A Chem.*, 141 (2001) 47.
70. Sarwan B., Pare B. and Acharya A. D., *Applied surface Science*, 301 (2014) 99.
71. Vinodgopal K., Bedja I. and Kamat P. V., *Chem. Mater.*, 8 (1996) 2180.
72. Alton I. A., Balciogolu I. A. and Bahnmen D., *Wat. Res.*, 31 (1997) 1728.
73. Feng W. Nansheng D. and Helin H., *Chemosphere*, 41 (2000) 1233.
74. Elmorsi T. M., Elsayed M. H. and bakr M. F., *American Journal of Chemistry*, 7 (2017) 48.
75. Abdollahi Y., Halim Abdullah A., Zainal Z. and Azah Yusof N., *Int J Mol Sci*, 13 (2012) 302.

76. Luo M., Bowden D. and Brimblecombe P., *Water Air Soil Pollut*, 198 (2009) 233.
77. Janani L., Henry K. and Enwine K., *Int Journal of Res. & Review*, 2 (2015) 343.
78. Gupata S., Tak P., Ameta R. & Benjamin S., *Journal of Adv. Chemical Science*, 1 (2015) 38.
79. Toor A. P., Verma A., Joshi C. K., Bajpai P. K. and Singh V., *Dyes Pigm.*, 68 (2006) 53.
80. Mohamed R. M., Mckinney D., Kadi M. W., MKhalid I. A. and Sigmund W., *Ceramics International*, (2016).
81. Bahnemann W., Muneer M. and Huque M. M., *Catalysis Today* 124 (2007) 133.
82. Nasser M., Behnajady, Ali B. M. and Reza M. J.O., *Iran. J. Chem. Chem. Eng.*, 28 (2009) 49.
83. Cheng M., Zeng G., Huang D., Lai C., Xu L., Zhang C. and Liu Y., *Chemical Engi. Journal*, (2015).
84. Kumawat R., Bhati and Ameta R., *Acta Chim. Pharm. Indica*, 2 (2012) 46.
85. Wang C. T., Chou W. L., Chung M. H. and Kuo Y. M., *Desalination*, 253 (2010) 129.
86. Alkaim A. F., Aljeboree A. M., Alrcozaq N. A., Baquir S. J., Hussein F. H. and Lilo A. J., *Asian Journal of Chemistry*, 26 (2014) 8445.
87. Gupta S., Tak P., Ameta R. and Benjamin S., *J. Adv. Chem. Sci.*, 1 (2015) 38.
88. Chang M. W., Chung C. C., Chern J. M. and Chen T. S., *Chemical Engi. Sci.*, 65 (2010) 135.
89. Pare B., Swami D., More P. and Qureshi T. Thapak T. R., *Int. J. Chem. Sci.*, 9 (2011) 1685.
90. Abo-Frah S. A., *J. American Sci.*, 6 (2010) 128.

91. Sakthivel S., Shankar M. V., Palanichamy M., Arabindoo B. and Murugesan V., *J. Photochem. Photobiol. A: Chem.*, 148 (2002) 153.
92. Papic S. Vujevic D., Koprivanac N. and Sinko D., *J. Hazardous Mater.*, 164 (2009) 1137.
93. Medien Hesham A. A. and Khalil S., *J. of King Saud University (Sci.)*, 22 (2010) 147.
94. Verma N. K., Gurjar L. and Bhardwaj S., *Der Chemica Sinca*, 2 (2011) 258.
95. Kumar P., Teng T. T., Chand S. and Wasewar K. L., *Desalination and Water Treatment*, 28 (2011) 260.
96. More P., Swami D., Pandey H. and Pare B., *Int. J. Chem. Sci.*: 10 (2012) 1549.
97. Pare B., Sarwan B. and Jonnalgadda S. B., *Appld. Surf. Sci.*, 258 (2011) 247.
98. Nadjia L., Abdelkader E. and Ahmed B., *J. Chem. Eng. Process Technol.*, 2 (2011) 108.
99. Sarwan B., Pare B. and Acharya A. D., *Particulate Science and Technology, An International Journal*, (2016) 1548.
100. Chen L. C. and Chou T. C., *J. Mol. Catal.*, 85 (1993) 201.
101. Subramani, A. K., Byrappa, K., Ananda, S. and Lokanatha Rai, M. K., *Bulletin Material Science*, 30 (2007) 37.
102. Pare B., Swami D., Thapak T. R. and Qureshi T., *Int J Chem Sci*, 9 (2011) 1183.
103. Kumar D. and Ameta R., *J. Chem. Pharm. Res.*, 5 (2013) 68.
104. Pare B., Singh D., Solanki V. S., Gupta P. and Jonnalgadda S.B., *Int J. Chem.3* (2014) 351.
105. Saquib M., Tariq M. A., Faisal M., and Muneer M., *Desalination*, 219 (2007) 301.
106. Xu X. R., Li H. B., Wang W. H. and Gu J. D., *Chemosphere*, 57 (2004) 595.

107. Pare B., Singh V. and Jonnalgadda S.B., *Indian J. Chem.*, A 50 (2011) 1061.
108. Lu C. S., Chen C. C., Huang L. K., Tsai P. A. and Lai H. F., *Catalysts*, 3 (2013) 501.
109. Vijay A., Nihalani S., Yadav I. and Bhardwaj S., *Res. J. of Chem. Sci.*, 3 (2013) 60.
110. Ghaly M. Y., Farah J. Y. and Fathy A. M., *Desalination*, 217 (2007) 74.
111. Teka T. and Reda A., *Int. J. Technol. Enhancements & emerging Engi. Res.*, 2 (2014) 2347.
112. Saien J. and Soleymani A. R., *J. Hazard. Mater.*, 144 (2007) 506.
113. Epling G. A. and Lin C., *Chemosphere*, 46 (2002) 561.
114. Pare B., Tomar H., Singh P. Ayachit M. and Bhagwat V. W., *Sci-fronts*, 1 (2007) 69.
115. Shankar M. V., Neppolian B., Sakthivel S., Arbindoo B., Palanichammy M. and Murugesan V., *Indian J. Eng. & Mat. Sci.*, 8 (2001) 104.
116. Kositzi M., Poullos I., Malato S., Caceres J. and Campos A., *Wat. Res.*, 38 (2004) 1147.

CHAPTER-V

Conclusion & Recommendations

CONCLUSION AND RECOMMENDATIONS:

The primary objective of the present study has been optimizing the photo-catalytic degradation of selected dyes using different experimental conditions. Heterogeneous photo-catalysis is a promising technique for the photo-catalytic degradation of organic pollutants present in industrial wastewater. It mineralizes the organic contaminants into harmless final end product(s). Nanostructured ZnO photo-catalyst is found to be most useful for photo-catalytic degradation of Malachite Green, Methylene Green, Direct Blue-1, Orange-II, Acridine Orange and Neutral Red dyes in the presence of visible light. ZnO NPs have been taken for present study and found that it is effective, low cost and non-toxic catalyst for degradation of dye it is synthesized by precipitation method. Visible light responsive photo-catalyst is obtained by employing a proper synthesis method. Characterization of ZnO NPs is done by various methods such as XRD, SEM and FTIR spectral studies. The purity of crystalline phase was confirmed by X-Ray Diffraction which showed no impurity peaks in XRD image.

The average particle size of ZnO NPs was found to be 30 nm by XRD and SEM studies. Zn-O vibration band is confirmed by FTIR spectra. The smaller particle size and low band gap let to the highest photo-catalytic property degradation of dye. Photo-catalysis using visible light responsive ZnO NPs emerged made it an attractive method for water treatments. The photo-catalytic activity of the ZnO NPs is attributed to their ability to absorb band gap photons under visible light. The changes in the absorption spectra of dye solution during the photo-catalytic degradation process at different irradiation times suggested the complete mineralization of dye along with color removal which was further supported by decrease in COD value and decrease in CO₂. ZnO NPs catalyst proved its versatile nature economically cheap and efficiently against photo-catalytic degradation

of textile dye. This technology is in its infancy and has a potential of being applied across the water treatment processes.

To set and optimize the reaction condition for the efficient degradation of dyes taken for investigation, the effect of various operational parameters investigated. The results obtained can be concluded as:

- ❖ No significant change in dye color was obtained in dark and during only photolysis. Photo-assisted mineralization of all the dyes effectively carried out utilizing ZnO NPs with visible light and the amount of synthesized nanoparticles required for complete degradation is found to be less in comparison to the amount required in case of commercially available bulk ZnO solid.
- ❖ Kinetic analysis indicated that the heterogeneous photo-catalytic degradation kinetics of all the selected six dyes followed the Langmuir-Hinshelwood (L-H) model.
- ❖ From the observation it clearly indicated that pH directly affected the heterogeneous photo-catalytic procedure. In all the cases, optimum photo-catalytic degradation was observed in alkaline medium.
- ❖ The addition of oxidants such as H_2O_2 and $\text{K}_2\text{S}_2\text{O}_8$ in the suspension of dye/ZnO improved significantly the photo-mineralization process of dye by enhancing the formation of hydroxyl radicals as well as by inhibiting the electron/hole pair recombination.
- ❖ Carbonate and chloride ions were found to have detrimental effect on the rate of degradation.
- ❖ Efficiency of photo-catalytic process has been found to be improved by FeCl_3 and Fenton's reagent mediated reaction.

- ❖ Increase in light intensity improved the degradation process.
- ❖ Dissolved oxygen regarded as conduction band electrons scavenger was found to inhibit fast carrier recombination and thereby increased the photo-catalytic efficiency in contrast to N₂ purging which reduced the efficiency by preventing O₂ radical anion generation.
- ❖ Reduced band gap and visible light response of synthesized ZnO NPs made it more efficient photo-catalyst than other photo-catalysts which absorb in UV region.
- ❖ Only a marginal changes in photo-catalytic efficiency after three batch reactions indicated cost effectiveness of ZnO NPs.

Finally, it is concluded from the present study that heterogeneous catalysis may be used as for the treatment of water released from industries as an efficient and environmental friendly procedure. The textile dye effluent was successfully degraded in large scale by the photo-catalytic oxidation process under visible light/ZnO NPs system. Based on this work, ZnO NPs promise to be one of the important materials in photo-catalytic applications.

Additionally, improvement in the whole photo-catalytic procedure will make it more sustainable towards practical application.

- ❖ To utilize pH range, some improvement in reaction process is required.
- ❖ Nano-composites with the coupling of more than one catalyst can effectively improve the photo-catalytic efficiency.
- ❖ Utilization of solar light should be preferred over artificial visible light.
- ❖ Effective design of photo-catalytic reactor system or parabolic solar collector for higher utilization of solar energy to reduce the electricity costs.

- ❖ The photo-catalyst in use should be doped in such a way that the efficiency be increased by several folds.

Hence for degradation of various organic dyes in visible light using ZnO NPs is recommended as a conclusion of the present study.

Summarized Tabulated Results

S. No.	Variation Studied	Malachite Green	Methylene Green	Direct Blue-1	Orange II	Acridine Orange	Neutral Red
1.	Effect of change in pH	Rate constant was maximal at pH 8.0.	Rate constant was maximal at pH 8.5.	Rate constant was maximal at pH 6.5.	Rate constant was maximal at pH 7.5.	Rate constant was maximal at pH 8.4.	Rate constant was maximal at pH 9.2.
2.	Effect of change in Catalyst amount	Rate constant was maximal at 60 mg/100mL.	Rate constant was maximal at 120 mg/100mL.	Rate constant was maximal at 160 mg/100mL.	Rate constant was maximal at 90 mg/100mL.	Rate constant was maximal at 80 mg/100mL.	Rate constant was maximal at 70mg/100mL.
3.	Effect of change in dye concentration	Rate constant was maximal at 4.0×10^{-5} mol dm^{-3} .	Rate constant was maximal at 4.5×10^{-5} mol dm^{-3} .	Rate constant was maximal at 2.0×10^{-5} mol dm^{-3} .	Rate constant was maximal at 5.2×10^{-5} mol dm^{-3} .	Rate constant was maximal at 2.5×10^{-5} mol dm^{-3} .	Rate constant was maximal at 5.5×10^{-5} mol dm^{-3} .
4.	Effect of change in H_2O_2 and $\text{K}_2\text{S}_2\text{O}_8$ concentration	Rate constant was maximal at 8.0×10^{-6} mol dm^{-3} of H_2O_2 and 8.0×10^{-6} mol dm^{-3} of $\text{K}_2\text{S}_2\text{O}_8$.	Rate constant was maximal at 8.0×10^{-6} mol dm^{-3} of H_2O_2 and 8.0×10^{-6} mol dm^{-3} of $\text{K}_2\text{S}_2\text{O}_8$.	Rate constant was maximal at 8.0×10^{-6} mol dm^{-3} of H_2O_2 and 8.0×10^{-6} mol dm^{-3} of $\text{K}_2\text{S}_2\text{O}_8$.	Rate constant was maximal at 8.0×10^{-6} mol dm^{-3} of H_2O_2 and 8.0×10^{-6} mol dm^{-3} of $\text{K}_2\text{S}_2\text{O}_8$.	Rate constant was maximal at 10.0×10^{-6} mol dm^{-3} of H_2O_2 and 8.0×10^{-6} mol dm^{-3} of $\text{K}_2\text{S}_2\text{O}_8$.	Rate constant was maximal at 6.0×10^{-6} mol dm^{-3} of H_2O_2 and 6.0×10^{-6} mol dm^{-3} of $\text{K}_2\text{S}_2\text{O}_8$.
5.	Effect of change in Na_2CO_3 and NaCl concentration	Rate constant decreased with increase in concentration of Na_2CO_3 and NaCl .	Rate constant decreased with increase in concentration of Na_2CO_3 and NaCl .	Rate constant decreased with increase in concentration of Na_2CO_3 and NaCl .	Rate constant decreased with increase in concentration of Na_2CO_3 and NaCl .	Rate constant decreased with increase in concentration of Na_2CO_3 and NaCl .	Rate constant decreased with increase in concentration of Na_2CO_3 and NaCl .

6.	Effect of change in FeCl₃	Rate constant was maximal at 8.0×10^{-5} mol dm ⁻³ of FeCl ₃ .	Rate constant was maximal at 8.0×10^{-5} mol dm ⁻³ of FeCl ₃ .	Rate constant was maximal at 8.0×10^{-5} mol dm ⁻³ of FeCl ₃ .	Rate constant was maximal at 8.0×10^{-5} mol dm ⁻³ of FeCl ₃ .	Rate constant was maximal at 8.0×10^{-5} mol dm ⁻³ of FeCl ₃ .	Rate constant was maximal at 6.0×10^{-5} mol dm ⁻³ of FeCl ₃ .
7.	Effect of change in Fenton's reagent	Rate constant was maximal at [1.4:1] of [Fe ³⁺ :H ₂ O ₂].	Rate constant was maximal at [1:4] of [Fe ³⁺ :H ₂ O ₂].	Rate constant was maximal at [3:4] of [Fe ³⁺ :H ₂ O ₂].	Rate constant was maximal at [1.4:1] of [Fe ³⁺ :H ₂ O ₂].	Rate constant was maximal at [1.4:1] of [Fe ³⁺ :H ₂ O ₂].	Rate constant was maximal at [1.4:1] of [Fe ³⁺ :H ₂ O ₂].
8.	Effect of change in light intensity	Rate constant increased with increase in light intensity.	Rate constant increased with increase in light intensity.	Rate constant increased with increase in light intensity.	Rate constant increased with increase in light intensity.	Rate constant increased with increase in light intensity.	Rate constant increased with increase in light intensity.
9.	Effect of bubbling of N₂ and O₂	Rate constant decreased on bubbling of N ₂ , but increased on bubbling of O ₂ .	Rate constant decreased on bubbling of N ₂ , but increased on bubbling of O ₂ .	Rate constant decreased on bubbling of N ₂ , but increased on bubbling of O ₂ .	Rate constant decreased on bubbling of N ₂ , but increased on bubbling of O ₂ .	Rate constant decreased on bubbling of N ₂ , but increased on bubbling of O ₂ .	Rate constant decreased on bubbling of N ₂ , but increased on bubbling of O ₂ .
10.	Effect of Solar light	Value of rate constant increased in the presence of solar light.	Value of rate constant increased in the presence of solar light.	Value of rate constant increased in the presence of solar light.	Value of rate constant increased in the presence of solar light.	Value of rate constant increased in the presence of solar light.	Value of rate constant increased in the presence of solar light.
11.	Effect of other catalyst	The order of photo-catalyst activity follows the order ZnO NPs > ZnO > BiOCl > TiO ₂ > BaCrO ₄ .	The order of photo-catalyst activity follows the order ZnO NPs > ZnO > BiOCl > TiO ₂ > BaCrO ₄ .	The order of photo-catalyst activity follows the order ZnO NPs > ZnO > BiOCl > TiO ₂ > BaCrO ₄ .	The order of photo-catalyst activity follows the order ZnO NPs > ZnO > BiOCl > TiO ₂ > BaCrO ₄ .	The order of photo-catalyst activity follows the order ZnO NPs > ZnO > BiOCl > TiO ₂ > BaCrO ₄ .	The order of photo-catalyst activity follows the order ZnO NPs > ZnO > BiOCl > TiO ₂ > BaCrO ₄ .

12.	Reusability of ZnO NPs	ZnO NPs can be used without any change up to three cycle of photo-catalysis.	ZnO NPs can be used without any change up to three cycle of photo-catalysis.	ZnO NPs can be used without any change up to three cycle of photo-catalysis.	ZnO NPs can be used without any change up to three cycle of photo-catalysis.	ZnO NPs can be used without any change up to three cycle of photo-catalysis.	ZnO NPs can be used without any change up to three cycle of photo-catalysis.
13.	Determination of COD and CO₂	COD decreased from 265 mg/L to 0 mg/L while CO ₂ increased from 41 mg/L to 236 mg/L in 115 min. of irradiation time.	COD decreased from 196 mg/L to 5 mg/L while CO ₂ increased from 24 mg/L to 158 mg/L in 150 min. of irradiation time.	COD decreased from 224 mg/L to 4 mg/L while CO ₂ increased from 24 mg/L to 175 mg/L in 180 min. of irradiation time.	COD decreased from 216 mg/L to 0 mg/L while CO ₂ increased from 32 mg/L to 232 mg/L in 4 h. of irradiation time.	COD decreased from 218 mg/L to 9 mg/L while CO ₂ increased from 21 mg/L to 192 mg/L in 60 min. of irradiation time.	COD decreased from 208 mg/L to 1 mg/L while CO ₂ increased from 13 mg/L to 115 mg/L in 120 min. of irradiation time.
14.	Identification of mineralized products	CO ₂ and NO ₃ ⁻ have been identification as mineralized products.	CO ₂ and NO ₃ ⁻ have been identification as mineralized products.	CO ₂ and NO ₃ ⁻ have been identification as mineralized products.	CO ₂ and NO ₃ ⁻ have been identification as mineralized products.	CO ₂ and NO ₃ ⁻ have been identification as mineralized products.	CO ₂ and NO ₃ ⁻ have been identification as mineralized products.

List of Publications

List of Publications:

1. Brijesh Pare and **Veer Singh Barde**, (2018) “Visible Light Induced Innovative Technique for the Remediation of Wastewater containing organic contaminants using ZnO Nano photocatalyst”, International Journal for Research in Applied Science and Engineering Technology (IJRASET), Vol. 6 (1), 3243-3248.
2. Sunaina Chouhan, Brijesh Pare and **Veer Singh Barde**, (2018) “Heterogeneous photocatalytic degradation of Azure-A dye by highly efficient ZnO-nano photocatalyst in presence of different operational parameters”, International Journal of Engineering Science Invention (IJESI), Vol. 7 (3), 49-54.
3. **Veer Singh Barde** and Brijesh Pare, (2018) “Enhanced Photocatalytic Degradation of Direct Blue-1 dye by ZnO Nanoparticles Using Visible Light” International Journal of Scientific Research in Science, Engineering and Technology (IJSRSET), Vol. 4 (1), 195-198.
4. **Veer Singh Barde**, Brijesh Pare, Shivpriya Pare and Satish Piplode, (2017) “Visible light irradiated photocatalytic degradation of Orange II dye in presence of ZnO nanoparticles” International Journal of Engineering Technologies and Management Research (IJETMR), Vol. 4 (12), 98-103.
5. **Veer Singh Barde** and Brijesh Pare, (2017) “Photocatalytic degradation of organic contamination by ZnO: A Review” Naveen Shodh Sansar (An International Refereed/Peer Review Research Journal) (NSS), Vol. 3, 34-37.
6. Brijesh Pare, Satish Piplode, Vaishali Joshi and **Veer Singh Barde**, (2016) “Application of solar light induced AOPs in detoxification of contaminated water”, Journal of Advance in science and Technology (JAST), Vol. 10 (21), 1-4.



Visible Light Induced Innovative Technique for the Remediation of Wastewater containing Organic Contaminants using ZnO Nano Photocatalyst

Brijesh Pare¹, Veer Singh Barde²

^{1,2}*Laboratory of Photocatalysis, Dept. of Chemistry, Govt. Madhav Science P G College,*

Abstract

Advanced oxidation processes (AOPs) have been found to be highly efficient in wastewater treatment specially containing hazardous organic pollutants such as dyes. In present study, we have carried out photo-catalytic degradation of Acridine Orange (AO) dye using ZnO NPs in presence of visible light. An effective and green reaction procedure has been established. ZnO as nanocatalyst has been found to be highly efficient for dye degradation particularly Acridine Orange. Several reaction parameters such as amount of catalyst, reaction pH, addition of H₂O₂ and K₂S₂O₈ and addition of Na₂CO₃, and NaCl have been studied.

Keywords: ZnO NPs, Acridine Orange dye, Photo-catalytic degradation, Visible light

Enhanced Photocatalytic Degradation of Direct Blue-1 Dye by ZnO Nanoparticles Using Visible Light

Veer Singh Barde*, Brijesh Pare

Laboratory of Photocatalysis, Department of Chemistry, Govt. Madhav Science P. G. College, (af. Vikram University), Ujjain, Madhya Pradesh, India

ABSTRACT

Photocatalytic degradation of Direct Blue-1 has been studied in ZnO nanoparticles dispersion medium under visible light. The absorbance of Direct Blue-1 dye under investigation has been found to be decreased in the presence of visible light and ZnO nanoparticles. The degradation studies have been carried out under various parameters such as catalyst loading, initial dye concentration, pH, effect of oxidant and effect of light intensity etc. The photocatalyst ZnO nanoparticles have been found to be more efficient for the degradation of Direct Blue-1 dye than other reported catalysts.

Keywords: ZnO NPs, Direct Blue-1 Dye, Photo-Catalytic Degradation, Visible Light

I. INTRODUCTION

The degradation of dyes and other organic contaminants of wastewater effluents has now become the matter of environmental concern. Dyes are carcinogenic and potential pollutants. Hence attention has been paid toward the removal of harmful and these wastewater contaminants [1, 2]. These pollutants are generated from paper; textile and leather industries etc. and when discharged to environment have crucial impact on the aquatic life and human health as well. Thus it resulted into serious consequences to the ecosystem. The main objective of this work is to study the degradation of Direct Blue-1 dye by using ZnO nanoparticles in the presence of visible light [3, 4].

Recently, the heterogeneous photocatalysis is emerging as an effective AOP. Particularly ZnO nanoparticles have been applied as effective, inexpensive and nontoxic photocatalyst for the degradation of a wide range of organic chemicals [5, 6]. In present work, visible light irradiate photo-catalytic degradation of dye wastewater has been investigated using ZnO nanoparticles as photocatalyst. We have investigated this degradation process under different reaction condition to assess the feasibility and optimization of process for industrial dyes effluents [7-10].

II. EXPERIMENTAL PROCEDURE

Materials

The dye used Direct Blue-1, was analytic grade reagent. $\text{Zn}(\text{NO}_3)_2$ and NaOH were obtained from Merck Co. (Germany). Ethanol (99%) was purchased from Aldrich Co. (England). The other chemicals used in present study like H_2O_2 , $\text{K}_2\text{S}_2\text{O}_8$, Na_2CO_3 , NaCl and FeCl_3 were of analytical grade and used as received. The double distilled water was used throughout to carry out experimental work.

Apparatus and experimental conditions

In a specially designed double-walled slurry type batch reactor vessel made up of Pyrex glass (7.5 cm height, 6 cm diameter) and water circulation arrangement was made to keep the temperature in the range of $30 \pm 0.5^\circ\text{C}$. Photocatalytic experiments were carried out with 100ml of dye solution using ZnO NPs as photocatalyst under exposure to visible irradiation. Light irradiation was carried out using 500 W halogen lamp surrounded by aluminum reflector to avoid irradiation loss.

During photocatalytic experiment, after stirring for 10 min. slurry composed of dye solution and catalyst was placed in dark for 30 min in order to establish equilibrium between adsorption and desorption phenomenon of dye molecule on photocatalyst surface. Then slurry containing aqueous dye solution and ZnO NPs were stirred magnetically to ensure complete

suspension of catalyst particle in visible light. At specific time intervals, aliquot (3 ml) was withdrawn and centrifuged for 2 min at 3500 rpm to remove ZnO nanoparticles to assess extent of decolorization spectrophotometrically. Absorption spectra were recorded with UV-Vis. Spectrophotometer (Systronic Model No.166). Intensity of visible radiation was measured by a digital Lux-meter (Lutron LX - 101). The desired pH of the solution was adjusted by the addition of previously standardized 0.050M H₂SO₄ and 1.0M NaOH solutions and measurement was done using digital pH meter. COD & CO₂ estimation were performed and studied by using standard procedure [11-13].

III. RESULTS AND DISCUSSION

a. Effect of ZnO nanophotocatalyst

The amount of catalyst is basic parameter to assess the degradation of Direct Blue-1 dye. It has been studied using 80mg/100 mL to 220mg/100 mL concentration keeping all other parameters constant. (Figure 1) Results showed that the rate increased with an increase in the amount of catalyst till 160mg/100mL and remained almost constant above this concentration. Optimum rate was found at 160mg/100mL and further increase in ZnO nanoparticles concentration increase the number of photons absorbed and consequently absorption of light of dye molecule increases. As the concentration of catalyst was further increased ZnO nanoparticles inhibited the direct contact of light with dye molecule and rate became almost constant [14, 15].

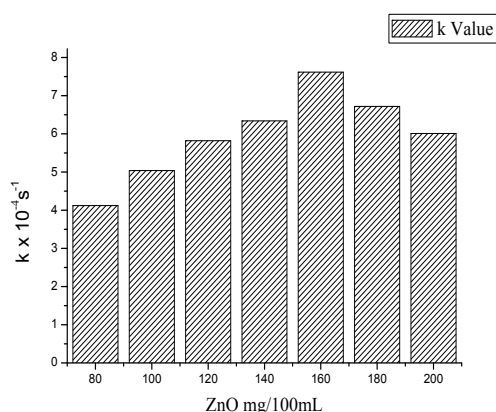


Figure 1. Effect of catalyst loading on photocatalytic degradation of DB-1

[DB-1 = 2.0 x 10⁻⁵ mole dm⁻³, pH = 6.5, light Intensity = 30 x 10³ Lux]

b. Effect of pH variation

The effect of pH on the rate of degradation needs to be studied since industrial effluents might not be at neutral pH. Experiments were carried out at pH values, ranging from 3.5 to 9.5 for constant dye concentration (2.0 x 10⁻⁵ mol dm⁻³) and catalyst loading (160mg/100ml). The reaction rate increased with increase in pH exhibiting optimum rate of degradation was found at pH 6.5 (figure 2) [16, 17].

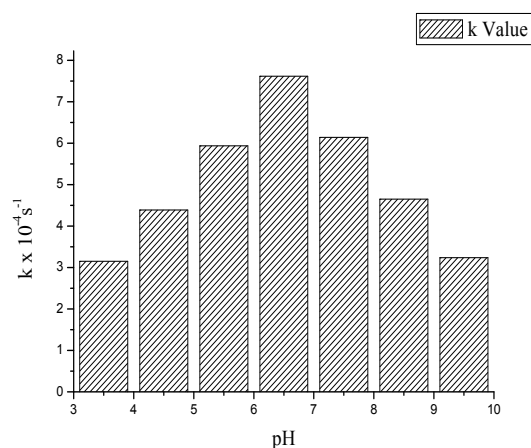


Figure 2. Effect of pH on photocatalytic degradation of DB-1

[DB-1 = 2.0 x 10⁻⁵ mole dm⁻³, ZnO NPs = 160mg/100ml, light Intensity = 30 x 10³ Lux]

c. Effect of initial dye concentration

It is also important to study the dependence of initial dye concentration for the degradation kinetics. The influence of initial dye concentration was studied in the range of 1.0 x 10⁻⁵ mol dm⁻³ to 3.5 x 10⁻⁵ mol dm⁻³. The photocatalytic degradation rate was found to increase from 3.08 x 10⁻⁴ s⁻¹ to 7.62 x 10⁻⁴ s⁻¹ with increase in concentration of dye up to 2.0 x 10⁻⁵ mol dm⁻³ and increase in dye concentration degradation rate again decreased as found in figure 3. It may be due to that initially as the concentration of dye was increased, more dye molecules were available for excitation and consecutive energy transfer. Since the illumination time and amount of catalyst were constant, therefore, further increase in dye concentration causes virtual masking of greater number of adsorbed dye molecules on the surface of catalyst particles. [18-20]

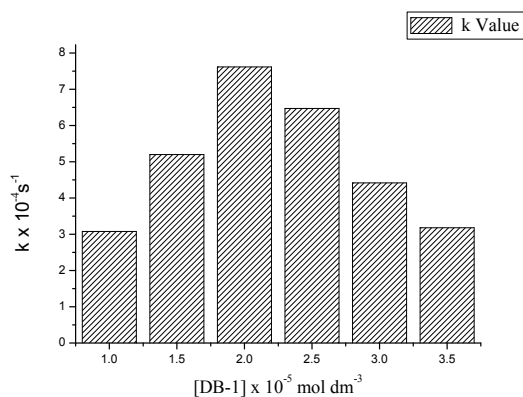


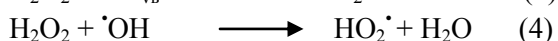
Figure 3. Effect of initial dye concentration on photocatalytic degradation of DB-1 [ZnO NPs = 160mg/100ml, pH =6.5, light Intensity = 30×10^3 Lux]

d. Effect of H₂O₂ and K₂S₂O₈

The degradation rate has been studied at different H₂O₂ and K₂S₂O₈ concentrations. The degradation rate increased with increasing H₂O₂ concentrations from 2.0×10^{-6} mol dm⁻³ to 8.0×10^{-6} mol dm⁻³. The reaction rate increased for H₂O₂ from 8.03×10^{-4} s⁻¹ to 11.23×10^{-4} s⁻¹ (Figure 4). This was because H₂O₂ inhibited the electron-hole recombination and hence, accelerated the reaction by producing an extremely strong and non-selective oxidant hydroxyl radical from scavenging the electrons and absorption of visible light by the following reactions: [21, 22]



Further increase in concentration of H₂O₂ beyond optimal concentration, resulted into the decrease in rate constant because at an excess H₂O₂ concentration, it might start acting as hydroxyl radical and hole scavenger [23, 24].



With increase in K₂S₂O₈ concentration from 2.0×10^{-6} mol dm⁻³ to 8.0×10^{-6} mol dm⁻³, rate constant increased from 8.12×10^{-4} s⁻¹ to 10.93×10^{-4} s⁻¹. At optimal amount of K₂S₂O₈, the rate of degradation has been found to be 10.93×10^{-4} s⁻¹. K₂S₂O₈ has always been found to be a beneficial oxidizing agent in

photocatalytic detoxification due to generation of SO₄^{•-} radicals [25, 26]

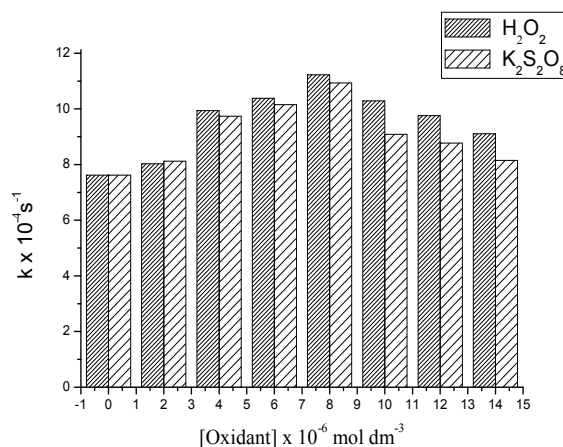


Figure 4. Effect of oxidants on photocatalytic degradation of DB-1 [DB-1 = 2.0×10^{-5} mole dm⁻³, ZnO NPs = 160 mg/100ml, light Intensity = 30×10^3 Lux, pH = 6.5]

e. Effect of light intensity

The effect of the variation of the light intensity on the rate of reaction has also been investigated. The data indicated that the degradation rate was accelerated as the intensity of light was increased because any increase in the light intensity increased the number of photons striking per unit time per unit area of the semiconductor powder resulted in more hydroxyl radicals (figure 5) [27].

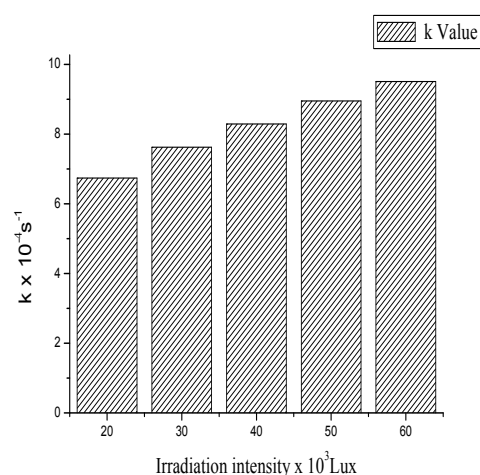


Figure 5. Effect of Light intensity on photocatalytic degradation of DB-1 [DB-1 = 2.0×10^{-5} mole dm⁻³, ZnO NPs = 160 mg/100ml, pH = 6.5]

IV. CONCLUSION

The detailed experimental findings suggest that the use of nano ZnO particles under visible light makes an efficient green degradation technique for complete mineralization of Direct Blue-1 dye.

V. ACKNOWLEDGEMENT

Authors acknowledged Head of Department of Chemistry and Principal, Govt. Madhav Science P.G. College, Ujjain (M.P.) for providing support and laboratory facilities to carry out the experimental work.

VI. REFERENCES

- [1]. He R., Hocking R. K., Tsuzuki T., Journal of the Australian Ceramic Society 49(1), (2013) 70-75.
- [2]. Sano T., Puzenat E., Guillard C., Geantet C., Journal of Physical Chemistry C, 113: (2009) 5535-5540.
- [3]. Akyol A., Bayramoglu M., Chemical Engineering and Processing, 47 (2008) 2150-2156.
- [4]. Mills A., Lee S. K., J. Photochem. Photobiol. A: Chem. 152 (2002) 233-247.
- [5]. Nageswara Rao A., Sivasankar B., Sadasivam V., J. Mol. Catalysis A: Chemical, 306 (2009) 77.
- [6]. Munter R., Proc. Estonian Acad Sci. Chem., 50, 2 (2001) 59-80.
- [7]. Tayade R. J., Surolia P. K., Kulkarni R. G., Jarsa R. V., Sci. Technol. Adv. Mater., 8 (2007) 455.
- [8]. Reife A., Fremann H. S., Environmental Chemistry of Dyes and Pigments, Wiley, New York 307-316.
- [9]. Cai X., Cai Y., Liu Y., Deng S., Wang Y., Wang Y., Djerdj I., Ceramics Int., 40 (2014)67-65.
- [10]. Pare B., Jonnalagadda S. B., Tomar H. S., Bhagwat V. W., Singh P., Desalination, 232 (2008) 80-90.
- [11]. Moghaddam A. B., Nazari T., Badraghi J., Kazemzad M., Int. J. Electrochem. Sci., 4 (2009) 247.
- [12]. Pare B., Sarwan B., Jonnalagadda S. B., Applied Surface Science, 258 (2011) 247-255.
- [13]. APHA, Standard Methods for Examination of Water and Wastewater 6th edition, American Water Workers Association, New York, 1985, p. 535.
- [14]. Pare B., Swami D., Thapak T. R., Qureshi T., Int J Chem Sci, 9 (2011) 1183.
- [15]. Lu C. S., Chen C. C., Huang L. K., Tsai P. A, Lai H. F., Catalysis, 3, (2013) 501-516.
- [16]. Tan T. K., Khiew P. S., Chiu W. S., Radiman S, Abd-Shukor R., Huang N. M., Lim H. N., World Academy of Sci., Engg. Tech., 79 (2011) 791.
- [17]. Luo M., Bowden D., Brimblecombe P., Water Air Soil Pollut, 198 (2009) 233.
- [18]. Mohamed R. M., M. khalid I. A., Baeissa E. S., Al-Rayyani M. A., Journal of Nanotech., (2012) 5.
- [19]. Sheikh M. A., Kumar A., Paliwal M., Ameta R., Khandelwal R. C., Ind. J. Chem., A, 47 (2008) 1681.
- [20]. Meena R. C., Pachwarya R. B., J. Scient. Ind. Res., 68 (2009) 730.
- [21]. Eslami A., Nasserli S., Yadollahi B., Mesdaghinia A., Vaezi F., Nabizadeh R. Mesdaghinia A., Nazmara S., J. Chem Technol Biotechnol, 83 (2008) 1447.
- [22]. Pare B., Singh P., Jonnalagadda S. B., Ind. J. Chem. Tech., 17 (2010) 391.
- [23]. Sarwan B., Pare B., Acharya A. D., Particulate Science and Technology: An International Journal, (2016) 1548-0046.
- [24]. Daneshvar N., Aber S., Seyed Dorraji M. S., Khataee A. R., Rasoulifard M. H., World Academy of Science, Engineering and Technology, 29 (2007) 267.
- [25]. Tang, W. Z., Zhang, Z., Quintana, M. O. and Torres, D. F., Environ. Technol., 18: (1997)1-12.
- [26]. Evgenidou E., Fytianos K., Poullos I., Appl. Catal. B, 59 (2005) 81.
- [27]. Kumawat R., Bhati I., Ameta R., Acta Chim. Pharm. Indica, 2 (2012) 46.

**Seminars, Conferences,
Workshops & Trainings**

Paper-Oral Presentation:

1. Participated in International conference on Science Technology and Society organized by Indore Christian College, Indore (M. P.) on 6th to 7th January 2018 and presented a scientific paper entitled “Semiconductor ZnO nanoparticles assisted photocatalytic degradation of Malachite Green dye under visible light”.
2. Participated in National conference on new frontiers in science: A paradigm shift to policy planning organized by Govt. Madhav Science P. G. College, Ujjain (M. P.) on 1st and 3rd December 2017 and presented a scientific paper entitled “Visible light irradiated photocatalytic degradation of Orange II dye in presence of ZnO nanoparticles”.
3. Participated in National consortium/science Festival from Photonics to Economic of Light organized by Govt. Madhav Science P. G. College, Ujjain (M. P.) on 3rd and 4th February 2016 and presented a review paper entitled “Application of solar light induced AOPs in detoxification of contaminated water”.
4. Participated in National seminar on Latest Trends in Analytical Instrumentation and Innovative Techniques organized by Govt. Madhav Science P. G. College, Ujjain (M. P.) on 19th to 20th March 2015 and presented a review paper entitled “Photocatalytic Degradation of Organic Contamination by ZnO: A Review”.

Participation in Seminars/Conference/Workshops/Trainings:

1. Participated in two days National workshop on Separation Techniques organized by School of Studies in Chemistry and Biochemistry, Vikram University, Ujjain (M. P.) on 23 to 24 February 2018.
2. Participated in two day workshop on “Latest Technologies in Synthesis with special reference to Microwave assisted Organic Reaction Enhancement (MORE)” organized by Govt. Madhav Science P. G. College, Ujjain (M. P.) on 3rd and 4th August 2017.
3. Participated in National seminar on Environmental Awareness Clean and Green Earth-Today, Tomorrow and forever organized by Bherulal Patidar Govt. P. G. College, MHOW on 2nd and 3rd December 2016.
4. Participated in National seminar on “Environmental and Socio-Economic Impact of Dams on River Narmada” organized by Pt. Jawahar Lal Nehru Govt. College, Barwaha on 17 to 18 November 2016.
5. Acted as mentor in three days Student Research Internship Programme in Chemistry organized as a cluster activity from 3rd to 5th November 2016 held at Govt. Madhav Science P. G. College, Ujjain (M. P.).
6. Participated in five days National workshop on “Drug Discovery Technology/Approach of Computational Chemistry in Drug Design a new era of Bioinformatics & Biotechnology” conducted by Bio Discover Group, India in collaboration with Govt. Madhav Science P. G. College, Ujjain (M. P.) on 8 to 12 September 2016.
7. Participated in National seminar on “Strategies for Sustainable use of Land, Water, Air, Agriculture and Energy Resources” organized by Govt. Kalidas Girls Lead College, Ujjain (M. P.) on 29 - 30 March 2016.

8. Participated in National workshop on “Basic of Bioinformatics” organized by Govt. Madhav Science P. G. College, Ujjain (M. P.) on 10 to 12 September 2015.
9. Participated in 2nd “International Virtual Congress” (IVC 2015) on 5th to 10th May 2015.
10. Participated in Pre-Congress workshop on Research Methodology and Scientific Paper Writing held at M. P. Council of Science and Technology, Bhopal during February 25-27, 2015.
11. Participated in National seminar on “Computational Biology” organized by Govt. Madhav Science P. G. College, Ujjain (M. P.) on 7th February 2015.
12. Participated in National seminar on “Current Ecological and Environmental Issues” organized by Govt. Madhav Science P. G. College, Ujjain (M. P.) on 29 January 2015.
13. Participated in workshop on “Working and Repairing of Scientific Instruments” organized by Govt. Madhav Science P. G. College, Ujjain (M. P.) on 19 to 27 January 2015.
14. Participated in workshop on “Computer in Chemistry: Tool and Innovative Techniques” organized by Govt. Madhav Science P. G. College, Ujjain (M. P.) on December 19, 2014.
15. Participated in training cum workshop program on “Water Quality Monitoring Methods” held at M. P. Council of Science and Technology, Bhopal on 18th to 21st November 2014.
16. Participated in workshop on “Chromatographic Separation Techniques Manual and Instruments” held at M. P. Council of Science and Technology, Bhopal on 15th to 17th October 2014.

17. Participated in seminar on “Crystallography and Its Applications” organized by Govt. Girls P. G. College, Ujjain on 25-26 September 2014.
18. Participated in National conference on Emerging Trends in physical and chemical Science held at Govt. (Autonomous) Holkar Science College, Indore during 15-16th March 2014.
19. Participated in National conference on Indian Environmentalism and Development Issues organized by Govt. Girls P. G. College, Ujjain on March 3rd and 4th, 2014.
20. Participated in Pre-Congress workshop on Research Methodology and Scientific Paper Writing held at M. P. Council of Science and Technology, Bhopal during February 25-27, 2014.
21. Participated in seminar on “Interdisciplinary Approach of Basic Science” organized by Govt. Girls P. G. College, Ujjain on February 21, 2014.
22. Participated in National Lecture cum Discussion series for Youth on Energy and Sustainability organized by Govt. Madhav Science P. G. College, Ujjain (M. P.) on February 11, 2014.